



MONASH University

**Advanced Studies in Gas Chromatography, Fourier
Transform Infrared Spectroscopy and Mass Spectrometry**

Junaida Shezmin Zavahir Ismail

BSc, MSc

**A thesis submitted for the degree of Doctor of Philosophy at
Monash University in April 2021**

School of Chemistry

Faculty of Science

Monash University

I dedicate this thesis to

My father (Dada) Zavahir and my mother (Mummy) Hazeera, for sharing this dream with me, instilling in me the love of learning from a tender age and for raising me to be the person I am today.

My precious daughters Aaliyah and Aleena – the lights of my life – for your endless love and making me more fulfilled than I could have ever imagined.

My husband Rumies – my gentle giant – for believing in me, standing by me and sharing the beauty of life with me. You never cease to amaze me with your unwavering love.

Copyright notice

© Junaida Shezmin Zavahir Ismail (2021)

I certify that I have made all reasonable efforts to secure copyright permission for third part content included in this thesis and have not knowingly added copyright content to my work without the owner's permission.

Signature

Junaida Shezmin Zavahir Ismail

Date 14th April 2021

Chapter 1 – Reprinted with permission from *TrAC Trends in Analytical Chemistry*, J.S. Zavahir, Y. Nolvachai, P.J. Marriott, Molecular spectroscopy – information rich detection for gas chromatography, *TrAC Trends Anal. Chem.* 99 (2018) 47-65. Copyright 2018 with permission from Elsevier.

Chapter 2 – Reprinted with permission from *Separations*, J.S. Zavahir, J.S.P. Smith, S. Blundell, H.D. Waktola, Y. Nolvachai, B.R. Wood, P.J. Marriott, Relationships in Gas Chromatography—Fourier Transform Infrared Spectroscopy—Comprehensive and Multilinear Analysis, *Separations* 7 (2020) 27. Copyright 2020 with permission from MDPI.

Chapter 3 – Reprinted with permission from *Analyst*, J.S. Zavahir, Y. Nolvachai, B.R. Wood, P.J. Marriott, Gas chromatography-Fourier transform infrared spectroscopy reveals dynamic molecular interconversion of oximes, *Analyst* 144 (2019) 4803-4812. Copyright 2019 with permission from Royal Society of Chemistry.

This page intentionally left blank

Table of Contents

Copyright notice	i
Abstract	vi
Declaration	viii
Research output during enrolment	ix
Thesis including published works declaration.....	xii
Acknowledgements	xv
Abbreviations and parameters	xvii
Synopsis of thesis investigation	xxi

Chapter 1

Background to gas chromatography, and spectroscopic and spectrometric detection1

1.1	Introduction to GC	3
1.1.1	Separation process in gas chromatography	3
1.1.2	Multidimensional gas chromatography	7
1.1.3	Comments on data handling	8
1.2	Detection criteria in gas chromatography	10
1.2.1	Classification of detectors	11
1.3	Flame ionisation detector	13
1.4	Mass measurement molecular ionisation detection	14
1.4.1	Components and types of mass spectrometers	15
1.4.2	High-resolution mass spectrometry (HRMS)	16
1.4.3	Mass analyser types	18
1.5	Molecular spectroscopic detection	19
1.5.1	GC–nuclear magnetic resonance	22
1.5.2	Detectors based on ultra-violet and visible absorption	24
1.5.3	Detectors based on molecular emission	26
1.5.4	Detectors based on molecular luminescence spectrometry	28
1.6	GC–Fourier transform infrared spectroscopy (GC–FTIR)	30
1.6.1	Background to Fourier transform infrared spectroscopy	31
1.6.2	Attenuated total reflectance (ATR) spectroscopy	34

1.6.3	Data processing in infrared spectroscopy	37
1.6.4	Background to GC-FTIR	38
1.6.5	Development of GC-FTIR hyphenation	39
1.6.6	Generation of chromatograms	42
1.6.7	Applications of GC-FTIR	42
1.7	Detector figures of merit	45
1.8	Multiple detector hyphenation	47
	References	52

Chapter 2

Materials, methods and preliminary validation using an in-house designed hyphenated gas chromatography-Fourier transform infrared instrument

2.1	Introduction	70
2.2	Design of in-house built hyphenated system of gas chromatography with Fourier transform infrared spectroscopy for GC-FTIR analysis	72
2.2.1	Gas chromatograph	72
2.2.2	Mass spectrometer	76
2.2.3	Fourier transform infrared (FTIR) spectroscopy	76
2.2.4	PIKE light-pipe interface	77
2.3	Other instrumentation	80
2.3.1	GC-MS analysis	81
2.3.2	GC×GC-TOFMS analysis	81
2.3.3	GC-FPD analysis	81
2.3.4	ATR-FTIR analysis	81
2.3.5	FTICR MS analysis	82
2.4	Software	82
2.5	Standards and sample preparation	85
2.6	Comparison of FTIR settings	90
2.6.1	Comparison of scan speed	91
2.7	Daily performance validation analysis	95
2.8	Establishment of a user-defined in-house spectral library	98
2.9	Conclusions	102
	References	102

Chapter 3

Relationships in gas chromatography–Fourier transform infrared spectroscopy — comprehensive and multilinear analysis

3.1	Chapter synopsis	105
3.2	Graphical abstract published in journal issue	108
3.3	Article	109
3.4	Published supplementary material	126
3.5	Invited cover page of the journal issue the article was published in	137

Chapter 4

Gas chromatography–Fourier transform infrared spectroscopy reveals dynamic molecular interconversion of oximes

4.1	Chapter synopsis	139
4.2	Graphical abstract published in journal issue	142
4.3	Article	143
4.4	Published supplementary material	154

Chapter 5

High resolution analysis of thermally oxidised aviation fuel — comprehensive two-dimensional gas chromatography vs high-resolution mass spectrometry

5.1	Chapter synopsis	161
5.2	Manuscript for submission to journal	164
5.3	Supporting information	197

Chapter 6

Conclusions and future prospects

6.1	Conclusions	209
6.2	Future prospects	211

Appendix	215
-----------------------	------------

Abstract

The accurate chemical identification of components is the main goal – or should be of primary concern – of analysts in various spheres. In many instances the necessity of identification at a sufficient level of precision is not achieved, mainly due to over reliance on analytical methods which fail to adequately identify components. Gas chromatography (GC) is a versatile technique for separating analytes in complex matrices and can be hyphenated to various purpose-suited detectors. Of these, mass spectrometry (MS) is a universal, sensitive and powerful tool with superior detection limits, having available standard protocols, and its provision of a mass spectrum of a molecule Identification using MS relies on spectrum libraries which is based on a probability factor, which places importance on the need for retention indices and authentic standards. Its incapability however, to differentiate certain isomers and closely related structures is limited, and the opportunity for GC–MS detection can be complemented with spectroscopic detectors such as Fourier transform infrared (FTIR) spectroscopy. FTIR provides specific and selective detection using molecular vibrational information. In this study we use the hyphenated GC–FTIR technique consisting of a light-pipe interface to identify chemical components based on the unique spectrum rendered by FTIR. The light-pipe interface allows on-line detection of GC separated components in real time and is well suited for GC detection.

This thesis explores the use of light-pipe GC–FTIR to analyse compounds of numerous chemical classes. Here we carry out preliminary validation studies using an interface transfer system devised in-house to carry out analysis, detailed in three chapters. We show the complementarity of MS and FTIR spectra and observe various relationships specific to the use of GC–FTIR. Of interest is the study of oxime species which undergo on-column isomerisation. Our analysis proved the ability of GC–FTIR to report pure individual isomer profiles within the characteristic oxime ‘dynamic reaction’ chromatogram using the simplest one-dimensional GC-FTIR approach. The novel approach of two-dimensional separation by GC×FTIR is employed for an alternative interpretation of this dynamic GC phenomenon. Various chemometric methods are employed to support extraction of qualitative and quantitative data from multivariate analysis using FTIR spectra.

Thermal oxidation of aviation fuels can lead to alterations in fuel composition which can have unfavourable effects on the fuel’s quality and performance in aircraft engines. The inability of

standalone FTIR systems to render the sensitivity required for such trace analysis makes it unsuitable for analysing minor changes in chemical composition. Thus, in the final part of the thesis we characterise components in thermally stressed aviation fuels using the techniques of high-resolution comprehensive two-dimensional GC hyphenated to time-of-flight mass spectrometry and high-resolution MS using Fourier transform ion cyclotron resonance. The former provides component separation, including some isomer separations, with different chemical classes located in separate regions of the 2D space. The latter is unable to uniquely identify isomers of the same mass, but can be interpreted by various data interpretation methods and plots to provide sensitive hetero atom compos. We draw comparisons between the two techniques to best identify the changes rendered by oxidation.

This significance of this study is that it informs our pragmatic understanding of integrating various GC separation approaches and detector technologies for precise molecular characterisation of chemical compounds.

Declaration

This thesis is an original work of my research and contains no material which has been accepted for the award of any other degree or diploma at any university or equivalent institution and that, to the best of my knowledge and belief, this thesis contains no material previously published or written by another person, except where due reference is made in the text of the thesis.

Signature:

Junaida Shezmin Zavahir Ismail

Date: 14th April 2021

Research output during enrolment

- * The publications below have been published under my previous (maiden) name Junaida Shezmin Zavahir (J. S. Zavahir), as a continuation of my publishing name since the commencement of my research journey.

Summary of outcomes during enrolment

- Published peer reviewed papers – 3
- Papers in preparation for submission – 2
- Conference presentations – 6
- Industry application notes – 1

Publications

- J.S. Zavahir, Y. Nolvachai, P.J. Marriott, Molecular spectroscopy – information rich detection for gas chromatography, *TrAC Trends Anal. Chem.* 99 (2018) 47–65.
- J.S. Zavahir, Y. Nolvachai, B.R. Wood, P.J. Marriott, Gas chromatography-Fourier transform infrared spectroscopy reveals dynamic molecular interconversion of oximes, *Analyst* 144 (2019) 4803–4812.
- J.S. Zavahir, J.S.P. Smith, S. Blundell, H.D. Waktola, Y. Nolvachai, B.R. Wood, P.J. Marriott, Relationships in Gas Chromatography—Fourier Transform Infrared Spectroscopy—Comprehensive and Multilinear Analysis, *Separations* 7 (2020) 27.

Industry application notes

- J. S. Zavahir, Y. Nolvachai, R. Herron, P. J. Marriott Z. Lawton (2020) On-site Analysis of VOCs Emitted from Plants Using Headspace SPME and Portable GC/MS. Application note authored for PerkinElmer Inc. Shelton, CT, USA.

Conference and research related presentations

- J. S. Zavahir Ismail, Y. Nolvachai, P. J. Marriott (2020) FTIR combined with MS provides additional characterisation of analytes in gas chromatography, Food, Nutrition & Analytical Chemistry (FNAC) Symposium, Melbourne, Australia. Awarded 1st place for presentation.
- J. S. Zavahir, P. J. Marriott (2019) Spectroscopic detection in gas chromatography – opportunities and advances. Graduate Research Industry Partnership internship presentation to BASF, Ludwigshafen, Germany
- J. S. Zavahir Ismail, S. P. Smith, S. Blundell, H. D. Waktola, Y. Nolvachai, B. R. Wood, P. J. Marriott (2018) An improved hyphenated GC–FTIR/MS design and preliminary results for integrated compound identification, 42nd International Symposium on Capillary Chromatography (ISCC) and 15th GC×GC Conference, Riva Del Garda, Italy.
- J. S. Zavahir Ismail, A. Lipphardt, L. S. Seyerlein, P. J. Marriott (2018) Use of headspace SPME and person-portable gas chromatography-mass spectrometry for rapid analysis of citrus volatiles, 2nd International Conference on Food Analysis, Melbourne, Australia.
- J. S. Zavahir Ismail, P. J. Marriott (2018) From cocktails to cockpits with separation science. Australian Centre for Research on Separation Science (ACROSS) Annual Winter Meeting, Melbourne, Australia.
- Annual 3-minute thesis competitions – School of Chemistry, Monash University.
*Awarded 1st place for presentation.

- J. S. Zavahir (9th January 2018) Hype of hyphenating gas chromatography with mass spectrometry and Fourier transform infrared spectroscopy. Special guest lecture presentation to National Institute of Fundamental Studies, Kandy, Sri Lanka
- J. S. Zavahir Ismail, S. P. Smith, A. Tipler, P. J. Marriott (2017) Exploration of Cresol isomers in a hyphenated light-pipe GC-FTIR/MS system, RACI 100-year Anniversary Conference and 8th International Conference on Green and Sustainable Chemistry, Melbourne, Australia.
- J. S. Zavahir Ismail, P. J. Marriott (2016) Column to Kiln - PCB Analysis in Waste Fuels, ASASS2 – ACROSS International Symposium on Advances in Separation Science, Hobart, Tasmania, Australia.

Thesis including published works declaration

I hereby declare that this thesis contains no material which has been accepted for the award of any other degree or diploma at any university or equivalent institution and that, to the best of my knowledge and belief, this thesis contains no material previously published or written by another person, except where due reference is made in the text of the thesis.

This thesis includes 3 original papers published in peer-reviewed journals and 1 publication in preparation for submission to the journal *Analytical Chemistry*. The core theme of the thesis is the development of advanced information strategies to characterise and identify chemical species using gas chromatography and highly informative detectors. The ideas, development and writing up of all the papers in the thesis were the principal responsibility of myself, the candidate, working with the School of Chemistry, Faculty of Science under the supervision of Prof. Philip J. Marriott and Prof. Bayden R. Wood, both of the School of Chemistry, Faculty of Science, Monash University.

The inclusion of co-authors reflects the fact that the work came from active collaboration between researchers and acknowledge input into team-based research.

In the case of Chapters 1, 3, 4 and 5 my contribution to the work involved the following:

Thesis chapter	Publication title	Status	Nature and % of student contribution	Co-author name(s) Nature and % of co-author's contribution	Co-author(s) Monash student Y/N
Chapter 1	Molecular spectroscopy – information rich detection for gas chromatography	Published	85% contribution. First author. Structured the idea, acquired and organised information, prepared entire manuscript.	1. Yada Nolvachai, editorial assistance; 5% 2. Philip J. Marriott, Supervision, proposed the review topic, assisted interpretation, editorial assistance 10%	1. No 2. No
Chapter 3	Relationships in gas chromatography–Fourier transform infrared spectroscopy — comprehensive and multilinear analysis	Published	70% contribution. First author. Prepared and analysed samples, developed and validated methods, analysed and interpreted data, prepared entire manuscript.	1. Jamieson S. P. Smith, assisted in instrumental analysis; 4% 2. Scott Blundell, instrument set up assistance; 4% 3. Habtewold D. Waktola, essential oil analysis; 4% 4. Yada Nolvachai, technical and editorial assistance; 4% 5. Bayden R. Wood, Co-supervision for IR analysis; 4% 6. Philip J. Marriott, Supervision, proposed instrument design, assisted in study design and interpretation of results, editorial assistance 10%	1. No 2. No 3. No 4. No 5. No 6. No
Chapter 4	Gas chromatography–Fourier transform infrared spectroscopy reveals dynamic molecular interconversion of oximes.	Published	80% contribution. First author. Prepared and analysed samples, developed and validated methods, analysed and interpreted data, prepared entire manuscript.	1. Yada Nolvachai, technical and editorial assistance; 5% 2. Bayden R. Wood, Co-supervision for IR analysis; 5% 3. Philip J. Marriott, Supervision, proposed study, assisted in study design and interpretation of results, editorial assistance 10%	1. No 2. No 3. No
Chapter 5	High Resolution Analysis of Thermally Oxidised Aviation Fuel — comprehensive two-dimensional gas chromatography vs High-Resolution Mass Spectrometry	Prepared for submission	75% contribution. First author. Prepared and analysed samples - IDGC and FTIR, analysed and interpreted data, prepared entire manuscript	1. Renee Webster, Sample analysis and GC×GC data acquisition; 5% 2. Federico Floris, HRMS Sample analysis; 5% 3. Mark Barrow, assisted interpretation of results; 5% 4. Philip J. Marriott, Supervision, proposed study design, assisted interpretation of results, editorial assistance; 10%	1. No 2. No 3. No 4. No

I have not renumbered sections of submitted or published papers in order to generate a consistent presentation within the thesis.

Student name: Junaida Shezmin Zavahir Ismail

Student signature:

Date: 14th April 2021

I hereby certify that the above declaration correctly reflects the nature and extent of the student's and co-authors' contributions to this work. In instances where I am not the responsible author I have consulted with the responsible author to agree on the respective contributions of the authors.

Main Supervisor name: Philip J. Marriott

Main Supervisor signature:

Date: 14th April 2021

Acknowledgements

All praise and thanks to Almighty Allah for granting me the sustenance, countless blessings, knowledge and opportunity to complete this mammoth task. I have immensely enjoyed every moment of this PhD journey.

Throughout the work contained in this thesis I have received assistance and immeasurable support from many to whom I render my heartfelt appreciation.

My deep gratitude to my supervisor Prof. Philip Marriott, who, with his amiability, expert mentorship and chromatographic genius continually conveyed a spirit of adventure to research and analytical chemistry. Phil, it has been a great privilege to work with you.

To Prof. Bayden Wood for his supervision on infrared aspects, and to everyone in the Chemicals and Plastics Graduate Research Industry Partnership (GRIP), especially Prof. Tony Patti for his insightful advice and encouragement.

To Dr. David Turner, Assoc. Prof. Kellie Tuck, Monash Graduate Education, The Faculty of Science, The School of Chemistry and Esolutions for their support. To Anna Severin, Sarah Williams and Dr. Kim Shepherd for administrative assistance, especially Anna for her moral support. To my research review panel members Prof. Mike Grace and Prof. Bart Folink, and to Dr. Scott Fraser for their guidance and expert advice.

To Dr. Yada Nolvachai and Dr. Habtewold Waktola for their friendship and help in navigating through the hardest stages of my research. To all the members of the Marriott group past and present for your camaraderie and eager help - Chadin, Jalal, Giselle, Sharif, Mala, Wong, Dandan, Aprilia, Jamieson, Adémario, Fabio, Michelle, Riley and Renee. To Finlay Shanks, Dr. David Perez-Guaita and everyone from the BioSpectroscopy group. To the ACROSS and analytical chemistry community for the inspiring science – all of you have my sincere appreciation.

I also acknowledge the financial support by the Monash University Faculty of Science Deans Research Scholarship and my GRIP industry partner PerkinElmer Inc.

A special thank you to all my friends for helping me survive these years. To Roshini, Susantha, Surangi, Savithri and Manisha – for the encouragement, countless meals and helping me with caring for my children. To my Awesome98 group Aminta, Damithri, Gayintha, Harshini, Mihiri, Milani, Romaine, Ruwanthika, Saluja, Susanne, Vishni, Yasanthi and Zana – for being there for me and the lifelong friendship.

This PhD journey has had its many interesting episodes. I have tempered the hard times through research catastrophes, a massive instrument lab flood and the global Covid-19 pandemic. And through it all I enjoyed life and research work, published an edited book, travelled widely and created many cherished memories with family and friends. I have the most heartfelt appreciation reserved for my family for standing by me and instilling a spirit of never giving up through the challenging times, and for sharing the good times.

Akki (Shirazi Jaleel-Khan) and Malli (Shamir Zavahir) – I am the luckiest sister in the world to have you both encourage and motivate me no matter where we are in this wide world. The cherished memories and our unbreakable unity will always stay strong.

Akke (Rizni) and Sinal (Rismiya) – I am sincerely grateful to you for being there for our family through the years and all you continue to do with love and generosity.

Thank you to all your four families for all you have done these past years.

My parents Dada (S. F. M. Zavahir) and mummy (Hazeera Zavahir) – I hope this achievement will complete the aspirations you had for me when you chose to give me the best all-round education and great childhood I had. You have been constant cheerleaders through every personal and academic endeavour in my life. I am forever indebted to you for making me who I am today and for teaching me the value of family ties, hard work, perseverance, faith and piety.

My wonderful daughters Aaliyah and Aleena – my treasures – who give me all the reasons to stand in the face of challenges and to conquer them all. I am amazed by your resilience, earnest support and encouragement through these years, despite your tender age. You are a pivotal part in all my goals and my motivation to see this thesis work through completion.

My amazing husband (Rumies Ismail) – words will never suffice to earnestly thank you for being by my side and supporting me with your wisdom, patience, unswerving encouragement and unconditional love. You never doubted my success and constantly shared the joys of caring for our beautiful family. You have my deepest gratitude for being my pillar of strength to conquer it all to make this thesis and my PhD dream a reality.

Abbreviations and parameters

β	Phase ratio $r=2d_f$ for the capillary column
ε	Molar absorptivity (or extinction coefficient)
λ	Wavelength
A	Absorbance
AED	Atomic emission detector
APPI	Atmospheric pressure photoionisation
ATR	Attenuated total reflectance
C_M	Concentration of analyte in the mobile phase
C_S	Concentration of analyte in the stationary phase
1D	Single dimension / one-dimensional
¹ D	First dimension column
2D	Two-dimensional
² D	Second dimension column
D	Minimum detectability or detectivity (also known as LOD or MDQ)
DBE	Double bond equivalence
DCM	Dichloromethane
DD	Direct deposition
d_f	stationary phase film thickness
DFS	Deactivated fused silica
DGC	Dynamic gas chromatography
DL	Detection limit
DS	Dean switch
ECD	Electron capture detector
FAME	Fatty acid methyl ester
FID	Flame ionisation detector
FPD	Flame photometric detector
FTICR	(also FT-ICR) Fourier transform ion cyclotron resonance

FTIR	Fourier transform infrared
GC	Gas chromatography
GC×GC	Comprehensive two-dimensional gas chromatography
GC–FID	Gas chromatography–flame ionisation detection
GC–FID	Gas chromatography–flame photometric detection
GC–FTIR	Gas chromatography–Fourier transform infrared spectroscopy detection
GC–MS	Gas chromatography–mass spectrometry
H/C	Heart-cut
<i>HETP</i>	(or <i>H</i>), Height equivalent to a theoretical plate
HRGC	High-resolution gas chromatography
HRMS	High resolution mass spectrometry
<i>I</i>	Retention index
¹ <i>I</i>	Retention index in ¹ D
² <i>I</i>	Retention index in ² D
ID	(also i.d.) Internal diameter
INJ	Injector
IR	Infrared
<i>k</i>	Retention factor (or partition ratio or capacity factor or capacity ratio)
<i>K</i>	Distribution (or equilibrium) constant or partition coefficient
KMD	Kendrick mass defect
<i>L</i>	Column length
LC	Liquid chromatography
LOD	Limit of detection
LP	Light-pipe
LRI	Linear retention index
<i>m/z</i>	Mass-to-charge ratio
MCR	Multivariate curve resolution
MCT	Mercury cadmium telluride (detector)
MD	Multidimensional
MDL	Minimum detection limit

MDQ	Minimum detectable quantity
MDGC	Multidimensional gas chromatography
MI	Matrix isolation
M_R	Modulation ratio
MS	Mass spectrometry
MS/MS	Tandem mass spectrometry
N	Theoretical plates
n_c	Peak capacity
NCD	Nitrogen chemiluminescence detector
NIST	National Institute of Standards and Technology
NMR	Nuclear magnetic resonance
NPD	Nitrogen-phosphorous detector
P/NP	Polar / non-polar
PAHs	Polycyclic aromatic hydrocarbons
PCA	Principal component analysis
PFPD	Pulsed flame photometric detector
PIONA	Paraffins, Isoparaffins, Olefins, Naphthenes, Aromatics
PLSR	Partial least square regression
P_M	Modulation period
PMT	Photomultiplier tube
qMS	Quadrupole mass spectrometer
qTOF	Quadrupole time of flight
r	Radius
RI	Retention index
RMS	Root mean square
RT	Retention time and Room temperature
RRT	relative retention time
SCD	Sulfur chemiluminescence detector
SIM	Selected ion monitoring
SNR	(also S/N) Signal-to-noise ratio

SSI	Split / splitless inlet
T	Temperature
TL	Transfer line
T_M	Modulation temperature
TOFMS	Time-of-flight mass spectrometry
1t_R	Retention time in 1D
2t_R	Retention time in 2D
UV	Ultraviolet
VOC	Volatile organic compounds
VUV	Vacuum ultraviolet
V_M	Volume of mobile phase
V_S	Volume of stationary phase
V_R	Retention volume
W	Wavenumber
w_B	Peak width at base
w_h	Peak width at half height

Units

Prefix

G	Giga ($\times 10^9$)	m	Milli ($\times 10^{-3}$)
k	Kilo ($\times 10^3$)	μ	Micro ($\times 10^{-6}$)
c	Centi ($\times 10^{-2}$)	n	Nano ($\times 10^{-9}$)

Suffix

$^\circ$	Degree	L	Litre
$^\circ C$	Degree Celsius	m	Metre
g	Gram	min	Minute
h	Hour	s	Second
Hz	Hertz (cycles per second)	V	Volts
cm^{-1}	Wavenumber		

Synopsis of thesis investigation

The separation of individual components from complex matrices and their subsequent identification demands reliable and robust techniques of chemical analysis. Gas chromatography (GC), a mature analytical technique, has attained its current status as a leading separation platform for analysing volatile and semi-volatile chemical components. This well understood method, capable of qualitative and quantitative analysis, further relies on the efficient detection of GC column effluent. With detectors varying in their specificity and sensitivity, they can often be chosen to suit the need of analysis. Such purpose-suited detectors often succeed in distinguishing and the subsequent identification of compounds which possess a high-degree of chemical similarity. This task is aided by (i) the reproducibility of capillary GC analysis, which provides precise retention times, to allow matching of a compound and an authentic standard; (ii) the use of retention indices that provides a comparison of compound retention vs an alkane standard mix to contrast with literature data; (iii) the use of a spectroscopic detector to provide some measure of molecular specificity for structural analysis.

The most widely used detector in GC is the FID, but it merely provides retention and response/quantitative data. Of the spectroscopic/spectrometric detectors, the most extensively used has been the mass spectrometer (MS), which is a universal detector giving fundamental information about a molecule based on its mass-to-charge ratio (m/z) of analytes and fragment ions, and importantly the use of a library database that compares an acquired mass spectrum with those of stored spectra. Despite this powerful tool's successes and advantages, MS-based approaches have limitations in carrying out key identification tasks which include the inability to differentiate structural isomers and other compounds that incidentally have very similar fragmentation patterns. The overreliance of analysts to accept a library match identification without question can lead to incorrectly attributed identities. Thus, there still remains the importance of spectroscopic (i.e. relying on interaction between a molecule and incident light/radiation) techniques which can render an accurate identification even in the simplest form of one-dimensional GC. They succeed in this task due to the production of characteristic spectra resulting from rotational and vibrational energies, which in turn can be employed to support the identification of compounds or determination of their structure. This can also be used to confirm the presence of certain functional groups based on their characteristic absorbance at definite frequencies.

Amongst the various spectroscopic detectors, Fourier transform infrared (FTIR) yields a wealth of unique structural information obtained from discriminating spectral patterns based on a molecule's structure. This acts as a unique 'fingerprint' for each individual compound, subject to the magnitude of differences between the FTIR results for each compound. Information offered by such FTIR spectra in identifying functional groups, discriminating specific isomers and elucidating structures supported by MS results can be used to correctly identify each individual isomer. The hyphenation of GC to FTIR resulting in GC-FTIR systems by using a variety of interfaces, have gained usefulness for routine analyses and applications through various instrument design modifications. Of the various FTIR interfacing options, the light-pipe facilitates real-time analysis when hyphenated to a GC, thus identifying analytes in the GC effluent on the fly.

Whilst GC-FTIR instrumentation have been available for many years, it is most probable that advancements in MS technologies saw a decline in the use of FTIR. This was largely due to FTIR systems having a considerable lack of sensitivity and difficulty of maintenance compared to MS systems. However, the need for the extra discrimination of detection beyond that available from MS alone still remains a topic of interest. Hence a renewed interest in GC-FTIR has emerged as a result of technological advances in the detector and associated interfaces. The role of incorporating MS and FTIR detection into single or multidimensional systems assists in eliminating false positive results and deliver a more accurate and reliable identification of compounds in matrices through enhanced physical separation of analytes. This research project focuses on exploring the combination of a GC-FTIR system for accurate component identification, especially in circumstances where MS cannot deliver incontrovertible identity.

The Chapters in the thesis systematically develop methods using GC-FTIR to analyse various compound classes which can be present in diverse matrices. One main drawback of this technique is the lack of sufficient sensitivity to detect components in trace quantities or the detection of homologous series in complex matrices such as petroleum samples, in which *n*-alkanes are of high abundance. The challenges faced in using this technique for extremely complex media, such as aviation fuels studied in this thesis, must be augmented by the investigation of high-resolution analytical techniques to answer questions based on chemical components within these samples. This thesis thus aims to develop integrated detection approaches to achieve an accurate identification of components belonging to various chemical classes.

The thesis is structured based on a 'Thesis including published works' and consists of six chapters. Of these three Chapters are based on published articles and one Chapter has been prepared for submission shortly. Journal formatting has been maintained for published papers. The thesis concludes with a general discussion.

Chapter 1, the introductory chapter, presents a systematic overview of the various instrumentation, principles and techniques used in the completion of this thesis as well as a comprehensive background to the various approaches and methods contained within the remaining experimental chapters of the thesis. The theoretical concepts are established together with a substantial literature review. Together with an overview of MS detection and different molecular spectroscopic detector technologies, this Section expounds on the need for various GC detectors for compound identification. Here, FTIR detection is highlighted due to its application in a majority of the experiments in the thesis. Further, the recent developments of the field are explored together with a comparison of the figures of merit of the various detectors highlighted. Finally, the ability to hyphenate multiple detectors is discussed, followed by a summary of the typical GC–molecular spectroscopic detection applications. Parts of this Chapter have been based on and adapted from the review paper entitled *Molecular Spectroscopy – Information Rich Detection in Gas Chromatography* (2018) published in Trends in Analytical Chemistry.

At the commencement of this project the main aim was to develop an in-house designed system consisting of a gas chromatograph hyphenated to a MS and a FTIR spectroscopy instrument with the use of a light-pipe interface. Of the available interface designs, light-pipes present as the best option for real time GC effluent analysis. **Chapter 2** is presented as a methodology Chapter which and gives an overview of the instrumentation, methods and experimental approaches used in the Chapters which follow. It also presents a detailed explanation of the design and implementation of the hyphenated GC–FTIR system (with GC–MS and GC–FID capabilities) configured in-house using a custom-built transfer line set up. Preliminary validation studies were conducted on this flow through system, which consists of a gold-coated light-pipe interface, whilst assessing the most suitable settings for various FTIR parameters. This Chapter also includes an overview of the in-house developed IR spectrum library with an appendix consisting of an example collection of the spectra included to date in the in-house library.

Chapter 3 is based on the article *Relationships in Gas Chromatography—Fourier Transform Infrared Spectroscopy—Comprehensive and Multilinear Analysis* published in 2020. This Chapter explores the various relationships pertaining to the hyphenated GC–FTIR system set out in Chapter 2. Components of a multitude of compound classes are analysed to demonstrate both the specificity of infrared spectra as well as the system’s capability to carry out quantitative and qualitative analysis. This Chapter also explores GC×FTIR, a ‘comprehensive’ style two-dimensional separation approach which combines GC and FTIR data. Finally, the use of the multivariate quantitative analysis method partial least square regression (PLSR) is applied to co-eluting isomers having similar mass spectra but differing FTIR spectra. The superiority of such multivariate analyses over univariate analyses in predicting a response or change in a chemical system is discussed.

Chapter 4 is based on the published article *Gas chromatography–Fourier transform infrared spectroscopy reveals dynamic molecular interconversion of oximes* (2019). This Chapter focusses on the ability of FTIR spectra to give precise identification of oxime isomers which undergo characteristic interconversion (dynamic chromatography) when analysed with GC. The studies use the GC–FTIR system outlined in Chapter 2 which enables the online acquisition of FTIR spectra of GC separated oxime components. Their elution behaviour under varying temperature and carrier gas flow velocities are assessed and compared for acetaldehyde and propionaldehyde oxime isomers. Characteristic single isomer profiles for the *E* and *Z* isomers are retraced using selective wavenumbers of individual FTIR spectra specific for each isomer. Such detection specificity is not possible using other GC detectors such as FID or MS. The only alternative technique capable of reporting the individual oxime isomers relies on GC×GC approaches – i.e. physical separation. The chemometric technique of multivariate curve resolution is applied to confirm the elution profiles of isomers, with elution order confirmed using molecular simulations of the IR spectra. The effect on interconversion rates and changes in FTIR spectra brought about by changing chromatographic parameters is assessed. Concurrent acquisition of GC–FID and GC–FTIR data is used to ratify chromatographic profiles during isomerisation.

The final stage of this study, **Chapter 5**, is based on the manuscript prepared for submission which compares the use of high-resolution multidimensional GC (HRMDGC) and high-resolution MS (HRMS) in the study of accelerated aviation fuel oxidation. Although GC-FTIR was initially proposed to aid identification of the biofuel oxidation products, this technique was not sufficiently selective or sensitive, and so HRMDGC and HRMS were then employed for the analysis of the fuel samples. This Chapter presents a background to these high-resolution techniques and their capabilities. It compares and contrasts the power of HRMDGC and HRMS as well as evaluates the boundaries of the two approaches in achieving molecular specificity. The two highly informative methods are then applied in petroleomics to achieve a detailed molecular characterisation of jet fuel samples using various data interpretation approaches, thus aligning with the thesis' aim of achieving precise and unmistakable identification of components in complex matrices.

Chapter 6 is the concluding Chapter. This Chapter collates the individual Chapters with a general discussion whilst summarising and reflecting on the research contained within the thesis. This reiterates the key points of the thesis while drawing conclusions to the work presented. Possible avenues leading to the future of accurate chemical component characterisation will be looked delved into. The contribution this study makes to the field of unambiguous compound identification, the limitations faced and the future prospects and further research will be laid out.

Chapter 1

Background to gas chromatography, and spectroscopic and spectrometric detection

1.1	Introduction to GC.....	2
1.2	Detection criteria in gas chromatography	9
1.3	Flame ionisation detector.....	12
1.4	Mass measurement molecular ionisation detection	13
1.5	Molecular spectroscopic detection.....	19
1.6	GC–Fourier transform infrared spectroscopy (GC–FTIR)	29
1.7	Detector figures of merit	44
1.8	Multiple detector hyphenation.....	46
	References	51

Select parts of this chapter have been reproduced from the review paper J. Shezmin Zavahir et al. “Molecular spectroscopy – Information rich detection in gas chromatography”, published in the journal Trends in Analytical Chemistry Vol 99 (2018) pp 47–65 [1]. This is included at the end of this Thesis as Appendix A. A detailed scope of the thesis is presented in the preliminary pages.

1.1 Introduction to GC

Since its very inception in 1952 [2], gas chromatography (GC) has proved to be an immensely valuable technique in the analytical separation of organic and inorganic compounds with volatile or semi volatile properties. In GC, the sample partitions between two phases – the first a stationary phase consisting of a column with a large surface area and the second, the mobile phase, a gas which percolates through the stationary phase. Whilst early columns were of the packed column format, surface coated capillary columns are now the routine technology. The chromatographic separation is thus enabled by the transportation of gaseous analytes through the column by the continuously flowing mobile phase referred to as the *carrier gas*.

This dynamic tool has gained importance in an extraordinarily wide range of fields and for a broad range of chemical compound classes, and has boosted application areas such as biochemistry, pharmacology, natural products chemistry, toxicology, petrochemistry, forensic investigations, chemical weapons research, food and agriculture etc.

1.1.1 Separation process in gas chromatography

During the GC process, the volatile sample is injected using a micro-syringe through a rubber disk known as the *septum*, into a heated injection port, where the sample is rapidly vaporised and swept into the chromatographic column by He, H₂ or N₂ carrier gas. Here it partitions between the mobile and stationary phases, is separated into individual components and subsequently passed on to the *detector*, a device which measures a generated signal proportional to the sample quantity. The resulting signal, with the help of a data analysis system, generates a *chromatogram* – a plot of the effluent concentration or response versus effluent retention times denoted by a row of peaks corresponding to the separated components – which is displayed on a computer.

The GC column, the site where separation occurs, may be *open tubular* or *packed*. Today the most commonly used are the *fused silica open tubular* columns, made of fused silica (SiO₂) and coated with the stationary phase, which despite having a lower sample capacity than their packed column counterparts, have greater sensitivity per unit mass, higher resolution and shorter analysis times [3]. The stationary phase thickness (d_f) of

such capillary columns vary typically from 0.1 to 5 μm with internal diameters of 0.05–0.53 mm and lengths of 5–100 m.

The *retention time* (t_R or RT) for each component separated on a column calculated as the time elapsed for an analyte (sometimes referred to as ‘solute’ in literature) from sample injection into a chromatography column to its maximum detected response upon arrival at the detector. Its *retention volume* (V_R) is the volume of mobile phase needed to elute the component from the column. The minimal possible time for the mobile phase or unretained analyte to travel through the column is called *unretained time of the column* (t_M) also called the *void time*, *dead time*. The *adjusted retention time* (t'_R) is the additional time required by an analyte beyond its t_M to travel the column’s length. This can be given by Equation 1.1.

$$t'_R = t_R - t_M \quad \text{Eq. (1.1)}$$

The *retention factor*, k , also known as *partition ratio*, *capacity factor* and *capacity ratio*, describes the migration of an analyte on a column. This is a variable which indicates how much time an analyte spends in the stationary phase compared to an inert non-retained component. The longer an analyte is retained on a column, the larger its k value is, and this can be expressed as Equations 1.2 and 1.3.

$$k = \frac{\text{time analyte spends in the stationary phase}}{\text{time analyte spends in the mobile phase}} \quad \text{Eq. (1.2)}$$

$$k = \frac{t_R - t_M}{t_M} \quad \text{Eq. (1.3)}$$

Equation 1.2 is directly proportional to the ratio of the number of moles of the analyte in the stationary and mobile phases. Thus Equation 1.2 can be given as Equation 1.4.

$$k = \frac{\text{time analyte spends in the stationary phase}}{\text{time analyte spends in the mobile phase}} = \frac{\text{moles of analyte in stationary phase}}{\text{moles of analyte in mobile phase}} \quad \text{Eq. (1.4)}$$

This is equivalent to Equation 1.5 where C_s and C_m are the concentration of analyte in the stationary and mobile phases respectively, and V_s and V_m are the volumes of the stationary and mobile phases respectively, and can be expressed as Equation 1.5.

$$k = \frac{C_s V_s}{C_m V_m} \quad \text{Eq. (1.5)}$$

The ratio of analyte concentrations in the stationary and mobile phases C_s/C_m describes the distribution equilibrium of sample components and is known as the *partition coefficient* or *distribution constant*, K , and can be cast as Equation 1.6. Due to having different polarities, boiling points and adsorption properties, components are separated within the column based on the differences in their distribution constants [4].

$$K = \frac{C_s}{C_m} \quad \text{Eq. (1.6)}$$

Equations 1.5 and 1.6 can be related to Equation 1.7 as follows.

$$k = K \frac{V_s}{V_m} \quad \text{Eq. (1.7)}$$

For capillary GC columns, the *phase ratio*, β , represents the ratio between V_m and V_s as follows.

$$\beta = \frac{V_m}{V_s} \quad \text{Eq. (1.8)}$$

For typical columns the β can be given as Equation 1.9 in relation to the column radius r and film thickness d_f ,

$$\beta = \frac{r}{2d_f} \quad \text{Eq. (1.9)}$$

and thus, increasing the thickness of the stationary phase decreases β .

Therefore, for a wall-coated GC capillary column the retention factor, distribution constant and phase ratio can be given by the relationship expressed in Equation 1.10.

$$k = \frac{K}{\beta} \quad \text{Eq. (1.10)}$$

The selectivity of components (α) can be given as the ratio of their retention factors e.g. k_1/k_2 , where component 1 is the later eluting compound. The selectivity alone does not

guarantee the separation of components since the narrowness of their peaks needs to be taken into consideration.

A column's ability to produce narrow peaks is called its *efficiency*, thus denoting that all molecules of the same compound elute within a narrow time window; due to various diffusion and equilibrium effects the compound generates a defined peak width, which is essentially the standard deviation or variance of this time window. This efficiency is gauged by the *number of theoretical plates*, N , or sometimes by the *height equivalent to a theoretical plate* (HETP or H). HETP can be calculated using the column's length L and theoretical plates N as Equation 1.11.

$$HETP = \frac{L}{N} \quad \text{Eq. (1.11)}$$

Thus, higher the N and lower the HETP, the chromatographic peaks that a column generates will be narrower, contributing to a greater efficiency of the system [5].

The entire GC process is based on three fundamental theories; the (1) thermodynamics theory – which studies the interaction between the stationary phase and analytes, (2) kinetic theory - which studies the effects of the separation parameters, and (3) separation theory – which studies the optimisation of the various operating conditions [4].

Much has transpired since GC's early days of packed columns to its current status of being considered a 'mature' technique, which has evolved to have high performance and efficient inlets, ovens and detectors [6, 7]. Other recent developments in GC include retention time stability achieved with electronic pressure and flow control, column flow splitting using capillary flow technology (CFT) micro-machined devices, column back-flushing, fast oven heating and cooling, resistive heating of columns, simpler column installations and flow chip technologies amongst other innovations which continually enter the market [8, 9]. This includes recent interest in portable GC instrumentation – with ease of analysis and sample accessibility, microfabrication technology using microchip GCs with shorter non-cylindrical columns etc. [10, 11]. Another factor which is to be considered in temperature gradient elution is *peak capacity*, n_c , the maximum number of peaks that can be resolved within a retention window of a chromatogram (over a baseline during the total analysis time) [12, 13], which is a measure of the

performance in chromatographic separation. Peak capacity values or informing power of nearly 1000 have been noted with some gradient elution approaches [12]. Modern single- or multidimensional GC configurations yield enhanced separation efficiency where the n_c of a single GC column can be 500–600, and this number can be raised to a 6.6×10^9 with GC-MS/MS approaches [14].

With the main aim being effective resolution (separation) of sample components, use of GC has proved to be one of the most powerful analytical tools with capabilities extending to a wide array of qualitative and quantitative analysis with adaptations to suit the need.

1.1.2 Multidimensional gas chromatography

Inadequate chromatographic separation, which may result by the conventional single capillary column (one dimensional; 1D GC) approach, may be overcome by multidimensional GC (MDGC). In 2005 Marriott defined MDGC as, “the process of selecting a (limited) region or zone of eluted compounds issuing from the end of one GC column, and subsequently subjecting the zone to a further displacement” [15]. Since its initiation in 1958 [16], this technique has developed into an established technique with advances in separation-phase choice, automation and data analysis. The n_c obtainable using a single column is often inadequate to resolve complex samples. Hence, a well-constructed system of two or more GC columns, which inherently has a greater n_c , renders the ability to resolve a larger number of analytes from the sample [17]. With the final desired outcome of an increased separation power and thereby an improved resolution, the arrangement of columns plays a crucial role. MDGC conventionally employs (at least) two columns of different selectivity (different stationary phases) [18], connected sequentially via a sampling device positioned between the two columns. This increased resolution also effectively delivers fewer overlapping compounds to the detector, which consequently means a significant improvement in the identification, quantification and quality of analysis.

The two approaches of MDGC are (i) the conventional heart-cut (H/C) method of subjecting a target portion of the first (¹D) column to the second (²D), or (ii) comprehensive two-dimensional GC (GC×GC) where the entire sample is subjected to two

column separation, according to the criteria Giddings espoused [19]. A well-detailed series of reviews by Adahchour et. al. delves into the significance as well as the various instrumental, developmental and application aspects of GC×GC [20-24]. Figure 1.1 illustrates various options from 1D GC to MDGC arrangements. MDGC has greater resolving power and may improve detection limits, removing underlying chemical interferences, with larger analyte peak capacity than 1D GC [25, 26]. The development of new hardware such as micro-fluidic switches [27] and cryogenic modulators render MDGC distinct advantages over 1D GC towards both quantitative and qualitative analysis [28]. MDGC has been used in conjunction with a variety of detectors in many applications, generally with excellent quantitative and qualitative results [29, 30].

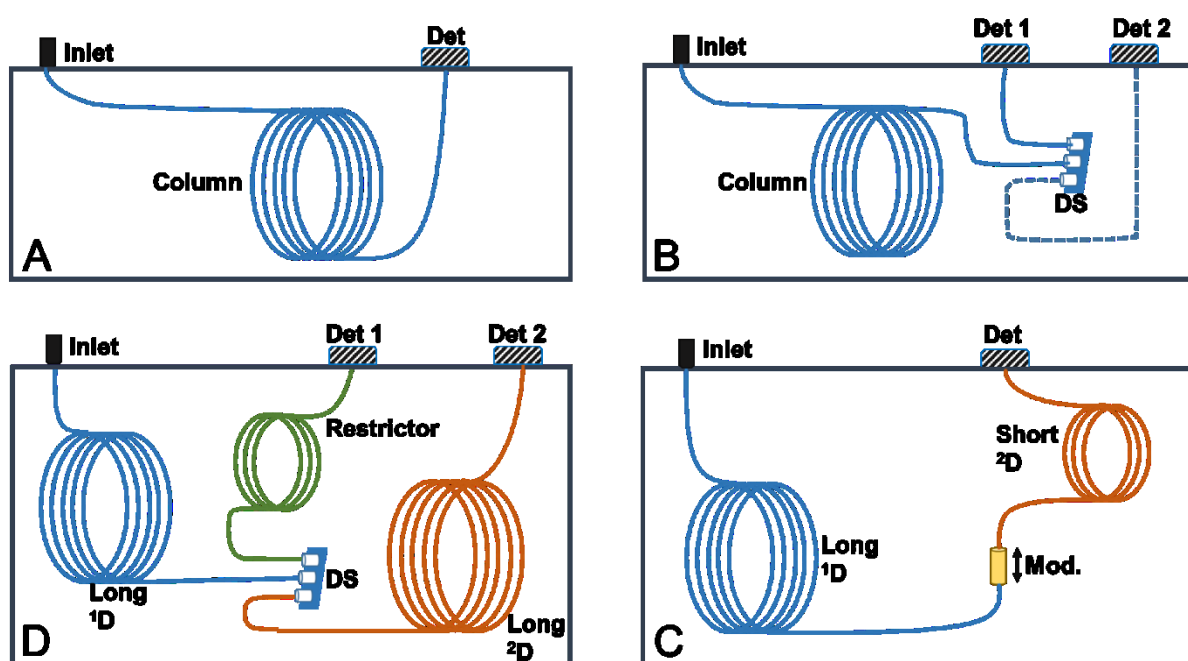


Figure 1.1. Diagrams illustrating example experimental setups in (A) GC with single detector, (B) GC with DS enabling switching between two detectors, (C) GC×GC and (D) Heart cut (H/C) MDGC. ¹D, first column; ²D, second column; Det, detector; Mod., modulator; DS, Deans Switch.

1.1.3 Comments on data handling

The analysis of chromatographic detection results is continually improving with the development of various software to suit the detection method and criteria. Conversion of the analog signal originating from the detector to a computer-compatible digital signal, enables convenient data handling by the analyst [31]. Digitised time and signal magnitude are generated by sampling the detector output at the required frequency (data points per s). The rate of data acquisition of chromatographic data affects precision of factors such as peak retention times, area repeatability, peak resolution of closely eluting compounds, etc. [32]. In the move to faster GC analysis, detector acquisition rate is a critical need. Very 'fast' GC peaks may have a width at half peak height of < 0.5 s, so an acquisition rate of about 50 Hz is appropriate for adequate quantitative analysis (i.e. a minimum of about 10 data points per peak). However, influencing factors such as detector electronics and extended path length flow cells or larger internal volume of some detectors may not be suited to such speed. Treating large quantities of data thus generated by complex matrices, benefit greatly from the use of chemometric techniques [33]. Use of multivariate data analysis in both 1D GC and MDGC can provide information otherwise inaccessible [34]. The problem of deconvolution of co-eluting peaks can be solved by dedicated software which deconvolute spectra results to render better identification of compounds [35].

Data presentation of both 1D and MDGC methods rely on the fundamental property of retention time (RT), which depends on many factors such as analysis conditions, type/dimensions of column, column degradation, gas flow rate, etc. Qualitative analysis normally compares RTs of a peaks in an unknown sample with those of known standards, where these are available. Here, the relative RT (RRT), which expresses the sample's RT relative to a pure standard's RT, is a useful tool in identification. RT may be transformed to retention index data (*I*) based on comparative RT data of, for instance, alkane homologues [36], and peak detection – the ability to distinguish an analyte signal from the background noise and other analyte signals [29]. Where confirmation of molecular structure based on spectroscopic detection is required, it is preferable that the molecule be detected as a unique species in the detector. This requires either adequate separation from other matrix material (best achieved with MDGC), or an effective deconvolution

procedure which is able to spectroscopically isolate and attribute just the response of the target molecule.

The versatility of modern systems thus allows many parameter alterations to suit the analysis need. With its high analyte detectability, linear range, exceptional resolving power, relatively good precision, repeatability, fast analysis and comparatively low cost, GC surpasses most other techniques in its ability to monitor volatile components. This excellent technique often accompanies simultaneous qualitative and/or quantitative information which makes reliable, efficient and sensitive detection possible, often with potential identification capabilities.

1.2 Detection criteria in gas chromatography

The hyphenation of GC systems to purpose-suited detectors enables the detection of separated components in which a main role is played by ‘chemical identification’ – where an analyte or analytical signal is assigned to one of the sets of chemical compounds or to a class/group of compounds. A fundamental part of chromatographic systems, this can be any physical technique which offers a real-time, on-line or quasi-on-line dynamic response to the change in composition of the components being analysed. Exploiting both the GCs separation power and detection method’s physical process converge for the detector response to reproduce a compound’s elution profile. Characterisation of an ideal detector is based on several pivotal features which are to be considered in its choice for hyphenation to the GC.

It is vital to have a *detectability* sufficient to yield a signal at the desired concentration level for the component(s) in a sample, and is referred to as the *analyte detectability* which is the response per unit mass or concentration of sample. Sometimes referred to in literature as ‘*sensitivity*’ (S), detectabilities can be in the range of 10^{-8} to 10^{-15} g of analyte per second. The lowest limit that can be detected is referred to by the terms *limit of detection* (LOD), *minimum detectable quantity* (MDQ), *detectivity* or by IUPAC as *minimum detectability* (D) [37]. D is given by Equation (1.12) where N is the noise level and S is the sensitivity.

$$D = 2N/S \quad (\text{Eq. 1.12})$$

Following the discussion on various GC detectors in this Chapter, Table 1.2 compares the analytical figures of merit of the various spectroscopic and mass spectrometric detectors and is presented in Section 1.7.

Sensitivity vs selectivity (normally, the ability to distinguish a certain functional group or element within the molecule or matrix without interferences from other components) [38] is also to be considered. Selectivity may be *element-selective* towards a defined element's identity (e.g. carbon being the responsive element for the FID) or *structure-selective* towards a defined arrangement of atoms in a molecule's portion [39]. Although it may be beneficial to have the response factor (a measure of the response of a detector per mass of compound) of the detector be similar for all analytes, it is not a pre-requisite for effective detection.

1.2.1 Classification of detectors

GC detectors are generally classified under five main classification systems [40] and as a result enable identifying the detector most appropriate for the task at hand.

(1) Universal vs selective – This is based on the mechanism by which response to analytes occur and the percentage or number of analytes a given system can detect. (i) *universal* detectors –respond to all analytes and (ii) *selective* detectors –respond to a particular class of compounds – this is usually not towards carbon or hydrogen but rather towards a hetero-element in the compound. This classification which is based on the nature of the response is also called *specific* and *non-specific* detectors, although *selective* detector usage is preferred.

(2) Concentration vs mass flow rate - Based on their response to analytes, chromatographic detectors are classified as (i) *concentration sensitive* – those which respond to changes in mass per unit volume (g mL^{-1}) or as (ii) *mass sensitive* – those which respond to changes in mass per unit time (g s^{-1}) [41]. Decrease of flow rate has an effect on the peaks for these two categories where the area increases with height

unchanged in the concentration type, and the peak height decreases with the area unchanged in the mass flow rate type [40].

(3) Destructive vs non-destructive - A detector gives its response when an analyte reaches it and is possible irrespective of whether the compound retains its identity or gets destroyed during detection. *Non-destructive* detectors directly measure the analytes enabling it to be further analysed using other detectors or instruments. This however can also be achieved using *destructive* (such as mass sensitive) detectors with the splitting of the GC effluent to release only part of it to the detector.

(4) Bulk property vs analyte property - This classification is based on the type of property which is being measured. *Bulk property* detectors measure a bulk physical property of the mobile phase and hence are sensitive to changes in pressure and flow rate. Therefore, GC operating conditions need to be carefully controlled. *Analyte property* detectors measure some property of the analyte which is not possessed (or has a reduced extent) by the mobile phase. This classification of detectors can be confusing and not clearly divisible since a given detector may show both characteristics based on the GC operating conditions [42].

(5) Analog vs digital - This is based on the feature of the GC output to the data handling device, the signal. Whilst analog signals signify a continuous signal that keeps changing with a time period, digital signals present a signal with discrete values. Analog signals are easily susceptible to many types of interferences so conversion to a digital signal at the earliest increases the signal-to-noise ratio. The latter are used in many detectors in the current era.

Other properties when choosing suitable detectors include stability, having a wide dynamic linear range, suitable detection limit, ease of use, repeatability of response, base line stability, inexpensive cost and maintenance, predictability and reliability [43]. A detector's efficacy in producing its output or signal is also based on three factors *viz* (i) noise (*N*) or background – random signals produced in the absence of sample, (ii) time constant – which measures the detector's speed of response, and (iii) cell volume.

Tracing the progress in the first detector's invention in 1952 [2] to the present date has seen a broad range of inventions and innovations leading to the introduction of detectors with a vast variety of design, function and selectivity [44]. Despite the recent past (<5 years) seeing little revolutionary innovation in this field, there is a constant attempt to improve detector designs. This is mainly through attempts to modify detector cell volume, miniaturisation, developments in microelectronics for data control, acquisition, analysis, display and storage [45]. One such attempt has led to the recent innovation of the vacuum ultraviolet (VUV) detector.

Complex sample analysis continues to be a hurdle in some fields despite the great strides made in GC instrumentation. Yet it is a gentle balance to achieve the best separation and detection of such samples. For example, higher flow rates in GC (e.g. with make-up gas) may have the negative effect of dilution and decreased detectability. Delivering of discrete and chosen fractions of the sample into the GC achieved by sample pre-treatment to bring the molecules into a form applicable to GC, such as derivatisation, pyrolysis and thermochemolysis [46], can be beneficial when separation of the entire sample can cause difficulty [47]. Such sample preparation can also be used to suit the detector's need by simplifying the total sample response by selective detection. For example, in using the electron capture detector (ECD), halogen-containing derivatives render an increased sensitivity and selectivity by facilitating the detection of compounds with weak electron capture properties [48]. Selective detection may be considered one way to simplify a total sample response; sample preparation may be targeted to suit the detector used.

1.3 Flame ionisation detector

A wide range of GC detectors exist which adapt various principles of detection. Of these, ionisation detectors – those which detect gas phase ionised molecules – have been used with increased popularity over the years. They have been reviewed for their detailed structure, modes and principles [30, 39, 42]. The most commonly used gas phase ionisation detectors are the flame ionisation detector (FID), photoionisation detector (PID), electron capture detector (ECD), thermionic detector (TID), helium ionisation detector (HID) and pulsed discharge detector (PDD).

Of these, the FID, without doubt is the most popular and is used across many disciplines providing a near universal, mass-dependent response. Since its introduction in 1958 by two independent groups it has proved successful in its hyphenation to GC (GC-FID) [49]. It is considered a 'workhorse detector' which responds well to a wide range of chemical moieties with reliability, linearity in the 10^6 – 10^7 range, low noise of 10^{-12} – 10^{-14} A, stability, predictability, fast response and operational simplicity.

The FID works by burning carbon (C) compounds in a H_2 rich flame with the response proportional to the number of C atoms. It is thus carbon selective with a near equal molar response to hydrocarbons and has a minimum detectable level of 2×10^{-12} g C s^{-1} . It can however be operated as an element-selective detector with minor modifications. Attempts have also been made to miniaturise it with designs such as the counter-current FID and a folded flame design [39]. In a typical FID, the H_2 combustion gas and make up gas mix with the carrier gas from the GC column entering from the bottom. This is burned at the jet with air which is added to establish a flame. Positively charged combustion product particles are accelerated towards the negatively biased collector electrode (-200 – -300 V) positioned above the flame. This is then electronically amplified and digitised where the current is directly proportional to the number of ions collected [50]. The powerful attributes of the FID maintain its position as a widely used and reliable detector.

1.4 Mass measurement molecular ionisation detection

Of the molecular ionisation detectors, the most widely adopted and used is the mass spectrometer (MS), which is capable of yielding molecular structure information with reliable qualitative and quantitative analysis. Although the MS also detects gas phase ionised entities its instrumental and functional complexities differ from other spectroscopic detectors. Since its origin in the early 20th century and its subsequent hyphenation to GC in the 1950s [51, 52] the mass spectrometer has proved to be a 'gold standard' detector in GC to support identification.

Over 85% of GC analyses [53] are, or can be carried out using an MS, which also provides a benchmark in universal detection. MS is one of the most powerful tools for identification of chemical components, based on mass-to-charge (m/z) ratios of analytes and their

fragment ions. Of all 'molecular structural' detectors, MS – despite the complexity and the management and maintenance requirements of its instrumentation [54] – is readily hyphenated with the GC experiment by simply attaching the column to the MS interface. This is universally referred to as *GC-MS* or *GC/MS* in literature. It gives a very high 'production rate' of valuable information enhanced by the availability of sophisticated and comprehensive databases with well-developed strategies for comparison of spectra. The detection limit of this technique is about 0.25 pg [25]. MS has become one of the most information-rich tools for volatile chemical analysis and essentially produces a beam of gas phase ions from analytes, sorts these ion mixtures based on their m/z ratio and provides an analog or digital output. The resulting signals can be plotted as a histogram of intensity (relative abundance) vs. m/z of detected ionic species, representing the distribution of ions by mass in a sample, known as a *mass spectrum*.

In untargeted GC-MS analysis, compound identification is based on the possibility of comparing the measured spectra to matching library spectra. Additional scan information can assist in reducing false positives in targeted analysis which can occur as a result of matrix or component interferences and/or co-elution. *Linear retention indices* (LRI) provide additional compound identification and is a reliable tool for routine analysis using GC-MS, whether it be targeted or untargeted analysis. Using both LRI and MS matching improves identification.

1.4.1 Components and types of mass spectrometers

Development of MS systems have seen magnetic sector analysers, as well as the currently widely used quadrupole mass analysers which has made it a routine analytical tool. Despite dramatic evolution of the MS that have made the systems smaller, faster, more robust and more sensitive, the single quadrupole (SQ) remains the routine workhorse [9].

Major components contributing to ionisation, mass separation and detection in a MS include (1) sample introduction system, (2) ion source for analyte vaporisation and ion production, (3) mass analyser where ions are separated based on m/z ratio, (4) ion detector for determining the signal intensities of each separated m/z value, (5) vacuum

system which prevents loss of ions through collision with gas ions or MS components, and (6) computer(s) for instrument control and data processing. Figure 1.2 depicts a schematic of a quadrupole mass spectrometer.

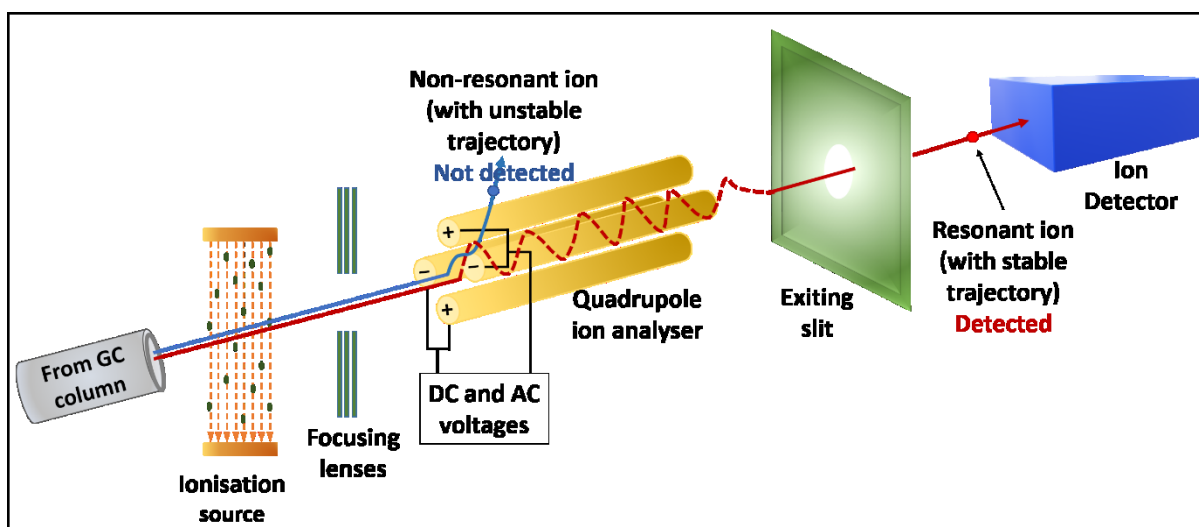


Figure 1.2. Schematic of a quadrupole mass spectrometer. The path of a non-resonant ion which is not detected and resonant ion which is detected has been depicted.

Of the ionisation sources, electron ionisation (EI) was the first and most widely used method usually based on a standard 70 eV ionisation energy obtained from a heated filament inside the ionisation vacuum chamber. Resulting EI mass spectra are very stable and reproducible – and relatively consistent for different design sources – and make comparison with reference library spectra straightforward. Other less frequently used techniques include (1) *soft ionisation techniques* such as chemical ionisation (CI), field ionisation (FI), single- or multi-photon photo-ionisation (PI), use of supersonic molecular beams (SMB), and (2) *atmospheric ionisation techniques* such as atmospheric pressure photo-ionisation (APPI), atmospheric pressure chemical ionisation (APCI), electrospray ionisation (ESI) and matrix-assisted laser desorption/ionisation (MALDI) – although the latter two are not used with GC [55].

1.4.2 High-resolution mass spectrometry (HRMS)

The ability of a mass spectrometer to discriminate ions of similar m/z values is known as its *resolution*. It determines the mass spectrometer's resolving power and is calculated as $m/\Delta m$, where m is the ion's mass (read as m/z) and Δm the peak width (mostly measured by the full-width at half-maximum, FWHM approach) or spacing between two equal intensity peaks with a valley [56]. Mass spectrometers can thus be categorised as *unit-mass-resolution* (capable of measuring mass to single-digit units; nominal mass) and *high-resolution* (mass can be measured to several decimal places; accurate mass) instruments.

High-resolution mass spectrometry (HRMS) instruments belong to either time-of-flight (TOF) or Fourier transform (FT) analyser types, where the FT instruments include the FT ion cyclotron resonance (FTICR) and orbitrap instruments. The FTICR MS instruments are based on the cyclotron frequency of ions in a fixed magnetic field and offer the highest mass resolution and mass accuracy. The large volume of data generated are interpreted with methods including double bond equivalence (DBE), Kendrick mass defect (KMD), van Krevelen diagrams, aromaticity index (AI) divisions, CHO index etc. [57]. The Orbitrap analysers employ trapping ions in electrostatic fields, with the development of numerous Orbitrap-based instrumentation incorporating various ionisation and separation techniques to accommodate its breadth of applications with high selectivity and sensitivity [58, 59]. Of the various HRMS platforms currently available for coupling to GC, magnetic sectors are most frequently used which offer a resolution exceeding 60,000. They can work in either full-scan or selected ion monitoring (SIM) modes, with the latter enabling ultra-trace detection limits as low as femto or attogram levels. The mass spectra acquisition rate of magnetic sectors is limited to a maximum of 20 spectra per s, diminishing their usefulness in fast GC and GC×GC measurements. In contrast, the TOFMS instruments can record up to 500 spectra per s making them suitable for GC×GC analysis, though are of low resolution. Slower acquisition HR TOFMS, has a maximum of 50 Hz cycle time, and can achieve resolutions of 10,000–50,000 [56]. HRMS instruments measure the exact mass without analyte fragmentation but can also be combined to quadrupoles which allow fragmentation and enhance its selectivity e.g. QTOF MS instruments.

Currently commercially available GC–HRMS instruments have a linear dynamic range of $>10^3$ – 10^6 and use electron-, chemical-, positive chemical- or negative chemical ionisation techniques. The high acquisition rates and high resolution of HRMS generates an enormous amount of data which can be further used for target or non-target analysis. This constantly calls for data evaluation processes and algorithm developments to process data under different conditions [60]. The latest major progress in HRMS instrumentation for GC includes the development of the quadrupole-orbitrap MS which can provide resolutions up to 120,000 [61]. Recent reviews expound the instrumentation and recent advances in HRMS [57, 62].

1.4.3 Mass analyser types

The value of MS is heightened by the availability of standard database libraries which have >240,000 mass spectra (though not all unique), plus a collection of specialist libraries related to specific applications; library spectrum entries are relatively independent of instrumental design [25, 63, 64]. However, for compound identification, a GC–MS spectrum alone may be insufficient for adequate characterisation, especially for untargeted analysis in complex matrix samples, primarily due to the similarity of spectra for closely related compounds. Assignment of molecular identity to peaks in GC–MS may lead to erroneous results, especially if authentic standards are not available to compare exact retentions and confirm mass spectra.

MS proves superior to most other identification techniques due to its multi-analytical property, selectivity, sensitivity and component characterisation. Various aspects of chemical identification using MS and chromatography have been amply expounded by Milman [65, 66]. MS together with nuclear magnetic resonance spectroscopy (NMR) have currently been used as the main analytical tools for *metabolomics*, the comprehensive study of small molecules known as metabolites within biological systems and their interactions within such systems known as the metabolome [67]. HRMS methods have seen a growing trend in of being used in *petroleomics*, the detailed characterisation of petroleum-related samples [68-71].

Multidimensional MS (MS/MS) can be performed in order to improve selectivity and also signal-to-noise (S/N) ratio. This approach involves further fragmentation of the primary ion(s) and selective monitoring of product ions by using different MS scanning routines, such as ion ratios of precursor and product ions. A variety of ion source and analyser combinations exist with the further possibility of combining analysers into sophisticated *tandem* instruments such as triple quadrupole (QqQ) or quadrupole time-of-flight (qTOF) with MS/MS capability, or with MSⁿ capability by using an ion trap MS (ITMS), although the latter is limited by the (currently) reduced size of their databases. Mass spectrum deconvolution software plays a further role in identification of co-eluting peaks. Recent advances in MS includes application of GC×GC–TOFMS for non-target compound analysis in saffron [72], food safety and quality analysis using MS [73], GC×GC with TOFMS in environmental analysis [74], QqTOF and QqQ-MS/MS for nutraceuticals analysis [75], multiple reaction monitoring (MRM) analysis with GC×GC–QqQMS for essential oil [76], combining MS/MS and exact mass analysis in shale oil analysis [77] etc. Such methods allow high confidence in compound analysis based on ¹I, ²I retention index values, accurate mass MS, and MS fingerprint data.

GC and MS coupling is recognised as the most popular analytical technique for targeted and untargeted analysis of studying volatile organic compounds (VOCs) and semi volatile organic compounds (SVOCs). Although this hyphenation provides useful information such as specific *m/z* of precursor/product ions of analytes, it has limitations in differentiating isomers or compounds with very similar fragmentation patterns, and analysing thermally labile, highly polar and very high/low mass compounds. MS may fail to provide absolute identification of compounds, which may further demand functional group identification, proton structural environment, electronic transitions or 3D structures. Some of these challenges may be overcome by approaches such as chemical modification of samples by derivatization techniques and modification of chromatographic components. This emphasises the need for detectors which may provide alternate or complementary information to MS. The hyphenation of spectroscopic detectors may thus offer atomic and molecular information which can very often complement information derived from other sources, for improved compound identification.

1.5 Molecular spectroscopic detection

Spectroscopy may be broadly defined as the study of the interactions between electromagnetic radiation and matter. Electromagnetic radiation is composed of electric and magnetic waves travelling perpendicular to each other in repetitive cycles. The *wavelength* (λ) is the distance travelled by a wave during a cycle and the *wavenumber* (W) is the number of cycles a wave undergoes per unit length. These are the reciprocal of each other as presented in Equation 1.13.

$$W = 1/\lambda \quad \text{Eq. (1.13)}$$

Whilst atomic spectroscopy relates mainly to transitions which take place when changes to atomic electronic configurations occur, molecular spectroscopy considers the energy states corresponding to nuclei and/or functional group vibrations and rotations within a molecule, or molecular electronic transitions. According to the Born-Oppenheimer approximation the energy of a molecule as presented in Equation 1.14 is given as the sum of electronic energy (E_{el}), vibrational energy (E_{vib}) and rotational energy (E_{rot}).

$$E = E_{el} + E_{vib} + E_{rot} \quad \text{Eq. (1.14)}$$

Here, the energy difference corresponding to the excitation of electrons $\Delta E_{el} = h\nu_{el}$ is larger than that corresponding to molecular vibrations $\Delta E_{vib} = h\nu_{vib}$ which is in turn larger than the energy difference of molecular rotations $\Delta E_{rot} = h\nu_{rot}$ and can be presented as Equation 1.15.

$$h\nu_{el} \gg h\nu_{vib} \gg h\nu_{rot} \quad \text{Eq. (1.15)}$$

It is this energy change which takes place by the absorption, emission, resonance or scattering by functional groups, bonds, vibrations, or atoms within the molecules that leads to specific patterns in the molecular spectrum, which is more complex than atomic spectra and also contain additional information on bond strength and molecular structure. The absorbance-based methods within the electromagnetic spectrum rely on the ratio of radiation power measurements; one before a beam has passed through an analyte medium (P_0) and the other after (P), leading to *transmittance* (T) and *absorbance*

(A) measurements, which are related by the relationship $A = -\log T$ and $T = \log P_0/P$. For monochromatic radiation, absorbance follows the *Beer-Lambert law*; $A \propto c$, where c = the absorbing species concentration. Also $A = \epsilon cL$, where L = path length through the sample, whose *molar absorptivity* (referred to as *extinction coefficient* in older literature) = ϵ [78].

Thus, molecular spectroscopy, with its potential complexity and fine structure, provides useful information on molecular properties. For instance, the relatively simple UV-vis band spectrum of molecules with low resolution spectrometers, contrasts with the infrared spectrum with its high degree of detail of the very same molecule. Needless to say, the MS offers a further contrast to these spectroscopies, and dual detection where MS occupies one detection dimension, and molecular spectroscopy the other, is of obvious interest. Molecular spectroscopy offers information quite distinct to MS, and is of importance in chromatographic analysis in order to improve compound identification, and to further understand the chemical construction of compounds eluted from the column, leading to the development of hyphenation with spectroscopic detectors in GC.

Depending on need, spectroscopic GC detectors can be chosen for detection of either atomic or molecular species. Although spectroscopic detectors in GC have been reviewed previously [79, 80] there has been a dearth of recent reviews. GC detectors based on atomic spectroscopy provide atomic or elemental selective detection. Of these, the atomic emission detector (AED), a highly selective detector based on atomic emission, is the most prominent and widely hyphenated atomic detector to GC (GC-AED); it has been the focus of many reviews and chapters [81-84]. Atomic spectrometric detectors for GC, including the GC-AED, were reviewed extensively by Li et. al. in 2016 [43]. In contrast a broad view of the various molecular spectroscopic detectors used in GC, with highlights of a few emerging detectors in this area, were presented in the review by us [1]. Due to superior detection limits, many available standard protocols, and widely established databases, MS technologies have overwhelmed less popular molecular spectroscopic methods, for hyphenation with GC. But the latter have their specific niche applications, and need to be considered.

Based on their interaction between matter, energy, sensing principle and hyphenation with different operations, molecular spectroscopic detectors in GC can be classified as shown in Figure 1.3.

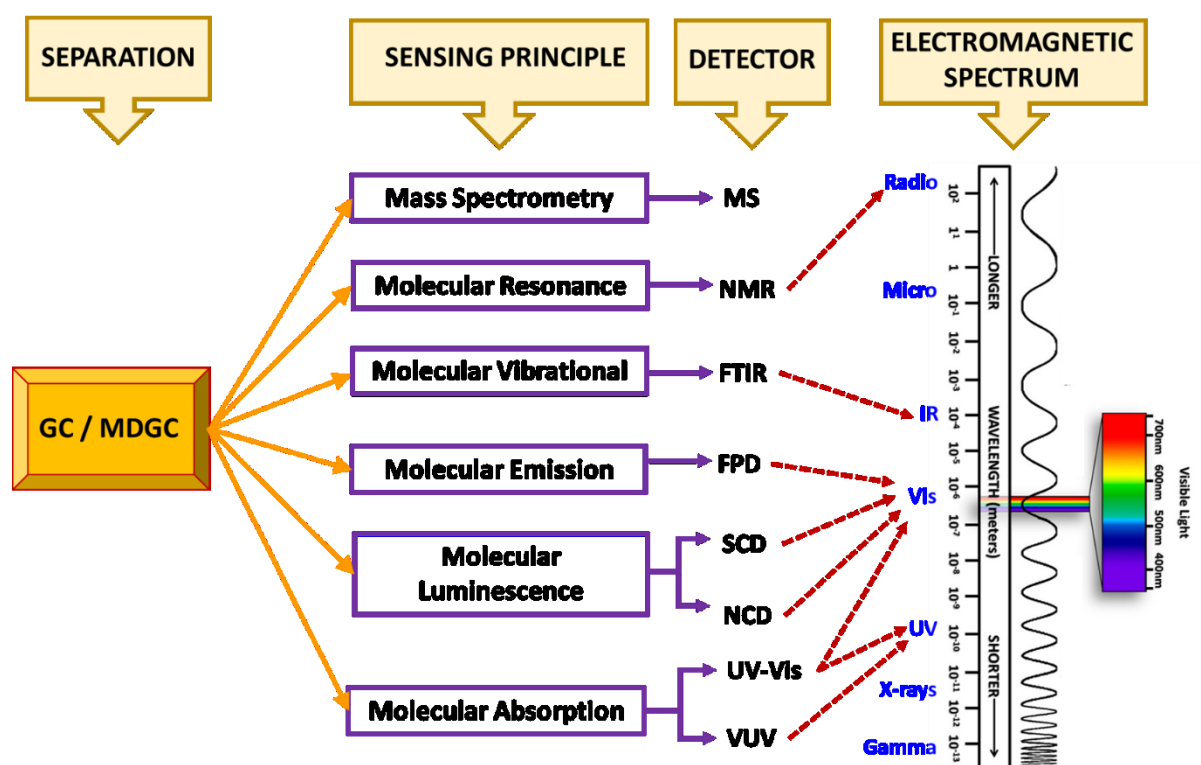


Figure 1.3. Diagram illustrating hyphenations of GC and MDGC with different spectroscopic detectors (MDGC is intended to also imply GC×GC). Source: J. S. Zavahir et al. (2018).

A majority of the studies in this thesis have been based on using the advantages of infrared spectroscopy with gas chromatographic analysis, mainly through the use of a GC–Fourier transform infrared spectroscopy (GC–FTIR) system. To fully appreciate FTIR’s place amongst other molecular spectroscopic detectors used in GC, a brief overview of each of the other molecular spectroscopic detectors are given below, followed by an expanded discussion on GC–FTIR in the next Section. In each instance the detector’s use in both one dimensional and multidimensional GC (MDGC) is presented as applicable.

1.5.1 GC–nuclear magnetic resonance

Of all spectroscopic tools, nuclear magnetic resonance (NMR) has the highest capability of distinguishing diastereomers and enantiomers (constitutional and configurational

isomers; enantiomers when shift reagents are used), and bond connectivities, providing a most robust interpretation of the entire spectrum [85]. Upon absorbing radio frequency energy, electrons around nuclei create strong and homogenous magnetic fields. The resulting characteristic chemical shifts provide information on the dynamics, reaction states, chemical environments and structure of molecules [86]. NMR thus assigns structures based on molecular connectivity, for the arrangement of carbons and protons in a molecule. Off-line NMR is relatively widely reported for GC separations, usually for preparative scale collection where individual resolved compounds are separately collected for transfer to NMR [87]. Depending on the amount of material collected, NMR techniques vary, including ^1H , ^{13}C , and multidimensional NMR methods. Absorption of electromagnetic radiation is measured in the 4–900 MHz radio-frequency region. The most useful isotopes used in NMR are those with a spin value of $I = \frac{1}{2}$. This is most commonly seen for the relevant element isotopes ^1H , ^{13}C , ^{19}F , and ^{31}P , enabling the analysis of many organic compounds of relevance to GC.

Although implementation is considerably more technically demanding since the NMR flow cell must be located in a strong magnetic field, hyphenating GC to capillary NMR should give the best spectroscopic elucidation of structures of unknown compounds [88]. NMR spectroscopy shows a relatively poorer analyte detectability and higher limits of detection in comparison to other spectroscopic detection techniques [89]. Detection limits in the low-nanogram range have been provided by modern solenoidal microprobes [90], whilst one study using microscale-preparative MDGC with NMR reported resolution of 1- and 2-methylnaphthalenes in crude oil at a natural abundance of ca. 0.2% [87].

1.5.1.1 Applications of GC–NMR

Molecular stereo-chemical interpretation from GC–NMR provides complementary information to MS [91]. On-line coupling of GC to NMR has been problematic as continuous recording of NMR spectra was not possible. Capillary-NMR applications have included structure analysis for volatile model compounds [90], separation of stereoisomers and enantiomers of *cis*- and *trans*-1,2-dimethylcyclohexane [92] and enantioselective GC separation of racemic mixtures [93]. Off-line NMR analysis applications include preparative MDGC of geraniol and crude oil [87, 94] and

polyaromatic catalyst products [95], with the latter study also reporting X-ray crystallography structures of the collected fractions.

The greatest advantages of NMR as a GC detector lie in its structural elucidation possibilities from a small amount of sample and its non-destructive nature, although its routine on-line hyphenation is unlikely in the near future.

1.5.2 Detectors based on ultra-violet and visible absorption

Absorption spectroscopy in the UV/vis and vacuum UV (VUV) region add value to molecular analysis, and have been used to develop absorption-based instrumentation for GC detection.

1.5.2.1 Gas chromatography-ultraviolet-visible spectroscopy (GC-UV)

The UV and vis regions span 10–400 nm and 400–700 nm wavelength regions respectively. This Section on UV will exclude the VUV region. When polychromatic UV/vis radiation passes through a medium, bonding electrons are excited enabling correlation of absorption bands to bonds of the molecules it passes through, although is lacking in detailed structural elucidation. Functional groups have different absorptivities, producing different sensitivities and absorption maxima. The wavelength is hence tuned to suit the compound of interest's molecular structure with use of a variable wavelength, diode-array type detector. They generally use a deuterium, xenon or tungsten, lamp and a monochromator.

Due to difficulties in interfacing the GC experiment, flow cell, and passage of light, GC separation with UV-vis has been modest. GC-UV-vis has been a niche area of limited acceptance within the GC-detection sphere. The recently developed vacuum UV detection may reverse this trend.

1.5.2.2 Gas chromatography-vacuum ultraviolet spectroscopy (GC-VUV)

Most compounds have limited absorption sensitivity in UV-vis, but strong absorption in the VUV region; the VUV absorption cross-section is much stronger and corresponds to light absorption in the 120–240 nm region by high energy electronic transition of bonded and non-bonded electrons. VUV is a mass-sensitive, non-destructive, universal detector for GC analytes (GC-VUV) with good general analyte detectability. It has applicability to differentiating *cis*-/*trans*-isomers, deconvoluting co-eluting molecules and performing pseudo-absolute quantification. It may provide information in areas where MS may fail with some maintenance advantages over MS. Limits of earlier studies on VUV detector has been overcome by a recent commercial benchtop VUV detector which successfully addresses many shortcomings posed by earlier spectroscopic detector technologies [53, 96, 97]. Similar to earlier instruments, this has a D₂ light source, heated GC transfer line, makeup gas, flow cell and grating. Coated reflective optics and back-thinned charge-coupled device (CCD) enable simultaneous collection of high-quality VUV absorption data over 115–240 nm for GC peaks. VUV offers predictability of class-response, data acquisition rates as high as 100 Hz, good repeatability of spectra allowing software deconvolution of overlapping spectra to provide analyte differentiation, [98, 99] and selective identification of classes of molecules using digitally created ‘spectral filters’.

1.5.2.3 Applications of GC-UV and GC-VUV

Both the UV and VUV detectors enable qualitative and quantitative analysis and are non-destructive towards analytes, making sequential detection possible e.g. VUV/MS. Quantitative analysis is based on the Beer-Lambert law. As with GC-FTIR and GC-MS, they fall into the same category of full scan analysis.

Being broad band absorptions, there is limited scope for structural identification by use of UV-vis spectroscopy. It is a routine analytical tool for many organic, inorganic and biological species, in environmental, chemical and forensic laboratories [100]. Applications have included structural isomer differentiation [101], analysis of aromatic and conjugated compounds [102-105], alcohols and phenols [106], wine [107], indoor dust [108], biomass ash [109], coal tar pitch [110], nitro organic explosives using

pyrolysis [111], simultaneous analyte and decomposition product detection [112] and elemental mercury in natural gas or light hydrocarbons [113]. Analyte detectability of GC–UV has LODs in the nanogram range. Resulting well-defined vapour phase UV spectra, unaffected by solvent effects or the detector's temperature [109], enable compound classification and library-based searches.

In practice, GC–VUV produces more detail-featured absorption spectra than that of UV and can be applied to analysing complex sample matrices in areas including petrochemicals, environmental science, agrochemicals, forensics, food technology and flavour analysis - probably as broad as GC-MS, with successful analysis of a myriad of compounds. Applications include analysis of pesticides [114], essential oils [115], vanilla extracts [116], fatty acid methyl esters [117-119], hydrocarbon and fuels [120-123], PCB congeners [124], various drug isomers [125-129], ink photoinitiators in food packaging [130], carbohydrates identification [131], benzene isotopologues [132], nitrate ester explosives [133], chemical warfare simulants [134], phenylethylamines [135], blood plasma [136, 137] etc.

Improvements over conventional methods include time interval deconvolution (TID) [138], pseudo-absolute quantification, spectral filters for LOD enhancement [98], theoretical simulation and quantum mechanics calculations [139] and GC×VUV separation [140]. This detector is suitable for fast GC, MDGC and GC×GC due to its fast acquisition rates and signal averaging ability [53]. GC–VUV has been proven to be a complementary technique to MS able to offer good selectivity in complex mixture analysis [98, 141].

1.5.3 Detectors based on molecular emission

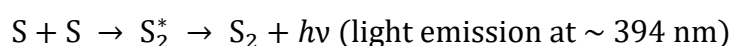
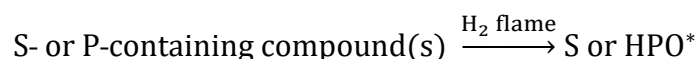
An upper energy state atom or molecule transition to a lower energy state emits electromagnetic radiation, where the energy state of the emitted photon is equal to the energy difference between the two states. Differences in electron transitions and radiated energy render an emission spectrum. Molecular emission GC detectors normally correspond to element species in a molecule, which produce small-molecule excited state

species as a result of a flame or chemical reaction, with corresponding characteristic radiation useful for element-specific detection.

1.5.3.3 GC-flame photometric detection (GC-FPD)

Based upon photometric detection by flame emission in a hydrogen-air flame, the flame photometric detector (FPD) has been used as a GC detector since its inception in the late 1960s [142]. Used mainly for the sensitive and selective detection of organic compounds containing sulfur (S) and phosphorus (P), it responds well to other elements including iron group metals, lead, tin, boron, antimony, arsenic, selenium, germanium, etc. [143-145]. It has been reviewed previously [146, 147]. In the FPD, GC effluent burns in a H₂-rich flame where combustion products lead to some specific excited state small molecules which subsequently decay and emit light. This chemiluminescent reaction generates a band emission, usually with multiple emission maxima. The emitted light passes through a filter which selects light unique to the desired species. A photomultiplier tube (PMT) records and amplifies the signal response.

Selectivity towards S and P compounds – the two most commonly measured by FPD – arise from selected optical filters which isolate the respective emission bands for passage to the PMT; S compounds produce excited S₂* with a S selective filter transmitting ~ 394 nm or at other maxima. P compounds produce excited HPO*, with a P selective filter usually transmitting at ~ 526 nm. Scheme 1 is a representative description of this process.



Scheme 1.1. Production of light emission with S and P selective filters for FPD

Generally, the FPD has high analyte detectability, simplicity, comparatively low price, stability, ease of use and good selectivity, and detects very low quantities of sulfur and/or

phosphorus compounds. It has a non-linear, often quadratic, amount-dependent response, due to atomic S recombination to produce S_2^* [146], and a variable, non-uniform response factor over a broad range of analytes due to the variation in S_2^* emission intensity [148, 149] and analyte response quenching by even moderate amounts of co-eluting hydrocarbons [150].

Proposed modified systems of the FPD to overcome some limitations include dual detection burners [151], dual-channels [152], dual flames [153], geometric modifications and flame doping with S compounds [154], pulsed-FPD [155], reactive flow detectors, pulsed flame photometric ionisation detector (PFPID) [156], counter-current FPD (μ FPD) [157, 158], multiple microflame (mFPD) formats [159] and dual wavelength FPDs [160].

1.5.3.4 Applications of GC-FPD

GC-FPD is used largely for studies on pesticides [161-163], and also used routinely for e.g. studies in environmental emissions [164-166], petroleum products [167, 168], food production [169, 170], human health risk [171, 172], and Chinese medicinal wine [173]. Techniques such as purge and trap (PT) can be linked to GC-FPD. This much used spectroscopic detector can be used in conjunction with the MS for compound identification in matrices [174] and its quantification ability can yield LODs in the 0.0005–0.004 mg kg⁻¹ range [169]. With data acquisition rates of >100 Hz, FPDs can be used in fast GC [175] and has been hyphenated to GC×GC [30] for analysing pesticides in soil and food matrices [176-178], petroleum [160, 179], and shale oil [180]. LODs for such GC×GC-FPD systems were 45 pg s⁻¹ in the P-mode and 617 pg s⁻¹ in the S-mode [160].

1.5.4 Detectors based on molecular luminescence spectrometry

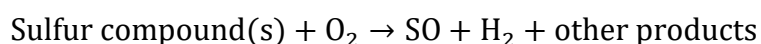
GC-chemiluminescence detectors

Chemiluminescent detectors were developed mainly with ozone as reactant [181]. The sensing region is preceded by a conversion step, usually via high-temperature pyrolysis, of analytes to sulfur monoxide (SO) or nitric oxide (NO), enabling downstream S- and N-

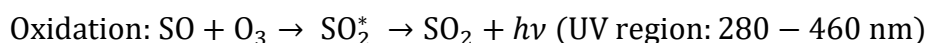
detection using a PMT with desired chemiluminescence signal achieved by an optical filter.

Chemiluminescent detectors show many advantageous features over other element-selective methods [182]. The high response factor to the analyte of interest (S or N) over other substances leads to excellent selectivity; values of 107 for flame-based SCD and NCD and 108 for non-flame SCDs over carbon [183]. SCD and NCD have negligible background interference, and hence very high analyte detectability to their respective elements, with better detectability than FPD towards S but are somewhat less robust than the FPD. Both SCD and NCD exhibit a linear response, proportional to the heteroatom concentration. The SCD has been reviewed previously [184]. Early commercial SCDs employed fluorine-induced detection [185-187] and have been improved by ozone-induction [188], flameless designs [189], dual detection systems [190] and dual plasma systems [191], and cryotrapping sample preparation steps [192]. Scheme 1.2 sets out the reduction and oxidation combustion.

Reduction then oxidative combustion in the SCD is as follows [188]

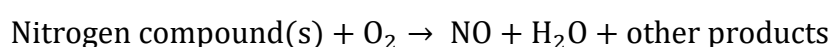


Reduced pressure oxidation with O₃ in the ozone reactor [193]:



Scheme 1.2 Reductive and oxidative combustion in SCD.

The NCD and SCD are analogous technologies in respect of their design and implementation, and are conceptually similar in their underlying chemical processes and performance. Coupling the redox chemistry of NO₂ with chemiluminescence produced the NCD as the redox chemiluminescence detector (RCD; 1985) following the SCD [194]. Universal reduction then oxidative combustion in the NCD is as presented in Scheme 1.3;



followed by the chemiluminescent reaction generating near-infrared emission

Oxidation: $\text{NO} + \text{O}_3 \rightarrow \text{NO}_2^* \rightarrow \text{NO}_2 + h\nu$ (Near infrared region: 800 – 3200 nm)

Scheme 1.3 Reduction and oxidative combustion in the NCD

The NCD has exceptional N selectivity over C. Like the SCD, it has very little or no quenching. Its response is linear and equimolar towards various N-compounds.

1.5.4.1 Applications of GC–SCD and GC–NCD

Applications of SCD include trace S analysis [195], S selectivity [189, 193], dual plasma SCD [196], petrochemical and energy studies [197], analysing photo-degradation [198], alcoholic beverages [199-201], flavours [202], sewer waters [203], volatile organic S compounds (VOSCs) [204], and pyrolysis oil [205]. MDGC with SCD has been used for petroleum products [206, 207] as well as process water studies [208]. The SCD preceded use of the FPD to determine S compounds by GC×GC. Of main interest is the detector acquisition rate, expected to be > 50 Hz for GC×GC applications. The separation, identification and quantification of S compounds in petroleum and pyrolysis products was reported [206].

The SCD and NCD have little mutual interference of their spectra, so provide good selectivity towards their respective element. Applications of NCD include petrochemicals [209, 210], environmental samples [211], spices [212] and explosives [213].

GC×GC–NCD applications have been used in feedstock [214], meat products [215], starchy food [216] urban air samples [217] pyrolysis oil [205] and shale oil [218]. NCD was reported to have improved equimolar response than NPD, FID and MS [219], and lower LOD and better repeatability than MS [220] LODs reported in the 1.66–3.86 $\mu\text{g L}^{-1}$ range [215].

1.6 GC–Fourier transform infrared spectroscopy (GC–FTIR)

A major part of the work in this thesis has been carried out using a hyphenated GC–FTIR system explicitly described in Chapter 2. Hence, the following Section has been discussed

in detail as a background to placing the importance of GC-FTIR in compound identification.

1.6.1 Background to Fourier transform infrared spectroscopy

Infrared (IR) spectroscopy has aided material analysis of any physical/chemical state – subject to a choice of suitable sampling technique – as a workhorse technique for decades, with advantages of being universal, relatively fast, easy and inexpensive as well as rendering information rich spectra. However, they are accompanied by a few disadvantages such as the inability to measure individual atoms (e.g. He, Ar), monoatomic ions, homonuclear diatomic molecules (e.g. O₂, N₂) and the masking of analyte spectra by water molecules due to its broad intense peaks.

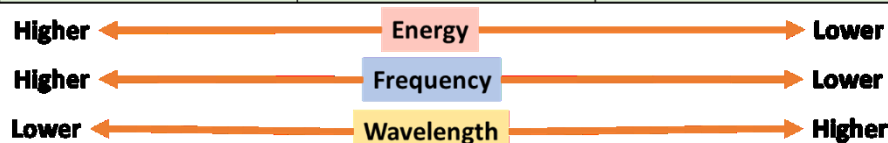
The infrared spectrum refers to the plot of measured infrared intensity absorption/transmission on the *y*-axis versus the variation in frequency or wavelength on the *x*-axis. The frequency is typically measured as wavenumber (measured in cm⁻¹), with the higher wavenumber generally plotted to the left and the lower on the right. Units of IR wavelength is given in micrometres (μm) which relates to wavenumber in a reciprocal way. Such IR spectra are used for a variety of purposes including unknown analysis by correlating peak positions of the spectrum and molecular structure, identity testing, quantitative analysis etc. The absorbance spectrum of a sample is calculated using the Equation 1.16.

$$A = \log(I_0/I) \quad (\text{Eq. 1.16})$$

The IR region of the electromagnetic spectrum is divided into three zones as seen in Table 1.1.

Table 1.1. IR regions with their corresponding wavenumbers and wavelengths

IR Region name	Near Infrared (Near-IR)	Mid Infrared (Mid-IR)	Far Infrared (Far-IR)
Wavenumber (cm ⁻¹)	13,500–4000	4000–400	400–10
Wavelength (nm)	780–2500	2,500–25,000	25,000–1,000,000



Many IR applications employ the mid IR region although the far IR and near-IR regions can also yield information regarding certain material [221]. General band assignments of mid-IR region aid spectroscopists in assigning an identification to the compound of interest.

Molecules are made of atoms connected by a bond. A diatomic molecule is considered as two spherical masses (m_1 and m_2) connected with a 'spring' to give a force constant f and can be represented by Equation 1.17.

$$\bar{\nu} = \frac{1}{2\pi c} \sqrt{\frac{f}{\mu}} \quad (\text{Eq. 1.17})$$

The absorption of infrared radiation leads to molecular vibrations within molecules. Due to the varied bond lengths and strengths between atoms in a molecule, the frequency of radiation absorption varies with molecular bonds and vibration modes. Since IR absorbances are very specific to stretches/wagging/rocking etc. vibrations of molecules, the IR signal fingerprint can be directly predicted based on quantum chemistry. The prediction is especially useful when approximate confirmation of functional groups, isomer structures or closely related structures of a compound is required [222]. This further extends to the use of FTIR to differentiate geometric (*cis/trans* or *E/Z*) isomers [223]. The unique spectrum obtained for each molecule also encapsulates information from the intact molecule, as opposed to molecular fragments seen in MS.

Early instruments were of the *dispersive* type which used prisms and gratings to separate individual frequencies from the IR source. However, the development of Fourier transform IR (FTIR) instrumentation, which exploits the mathematical process of Fourier transformation with an interferometer's use, has greatly enhanced IR data quality and reduced spectrum acquisition time. FTIR spectroscopy is considered an extremely accurate, reproducible and reliable technique for positive identification and is enabled by FTIR software which converts the discrete signals of the detector into an interpretable spectrum. [221].

FTIR instruments are preferred over dispersive counterparts due to their advantages which include (i) higher optical throughput as they have no prisms, gratings or slits which attenuate light; Jaquinot's advantage, (ii) all frequencies being measured simultaneously to give a spectrum quickly; Fellgett's advantage, (iii) highly accurate frequencies in spectrum enabling processing techniques; Connes advantage, (iv) precise measurements with no external calibration needed, (iv) speed increasing ability with per second scans, (v) little chance of mechanical breakdown as the moving mirror is the only continuously moving part, and (vi) increased sensitivity with scan co-adding ability to ratio out random noise.

FTIR instruments use a Michelson interferometer to generate Fourier transformation of light beams. A beam splitter splits the incoming light into two optical beams; one reflects off a fixed mirror and the other off a reciprocating mirror. These two beams then recombine at the beam splitter constructively and destructively and then presented as a function of the two beams travelled and their wavelengths. These two "interfering" beams result in an interferogram $I(\delta)$ which is a function of the optical path difference (δ) between the fixed and moving mirrors. Since all frequencies are measured simultaneously the interferometer renders very fast measurements. The "decoding" of these frequencies by Fourier transformation renders the spectrum analysis as a frequency spectrum. Figure 1.4 depicts the Fourier transform process. As depicted in Figure 1.4(B) the interferogram displays a strong peak at the zero mirror path difference due to constructively interference of all wavelengths of light.

The ability to measure spectra with high signal-to-noise ratios (SNRs) is a major advantage of FTIRs over other IR spectrometers. SNR is a measure of a peak's quality and

higher SNRs increase the instrument's sensitivity and quantitative accuracy. SNRs of 100 or over can be measured by FTIRs due to their various advantages.

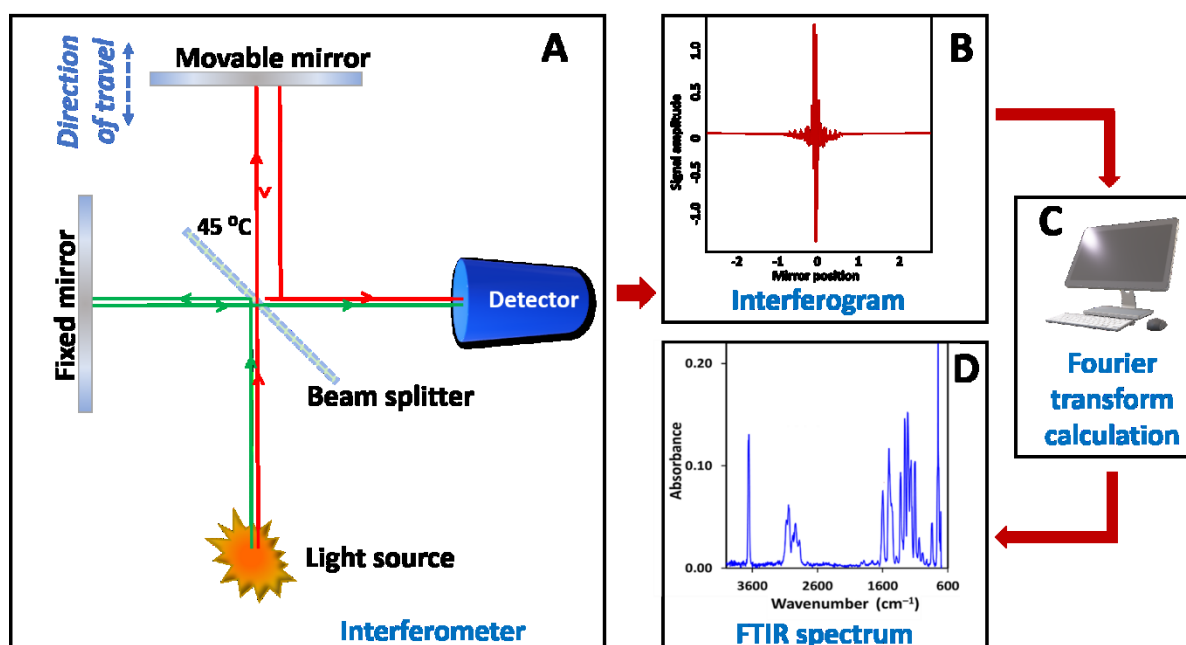


Figure 1.4. Schematic of the Fourier transform process to obtain FTIR spectra. (A) Michelson's interferometer, which produces an interferogram (B) which upon Fourier transformation (C) renders an FTIR spectrum (D).

1.6.2 Attenuated total reflectance (ATR) spectroscopy

The superseding of dispersive spectrometers by the more powerful FTIR instruments expanded the versatility of IR spectroscopy being used as an analytical tool for solids, liquids and gaseous samples [224]. Standalone FTIR instrumentation has been used in conjunction with GC–MS in the study of various material to gain a better understanding of the samples being analysed [225, 226]. Since the sample is analysed in its gas phase upon vaporisation at the GC injection port, GC–FTIR analysis often needs none or the usual GC sample preparation prior to analysis to extract samples and remove interferences. However, other standalone FTIR instrumentation may often require sample preparation to suit the instrumental technique being used.

To enable measuring IR spectra in transmission mode, samples have to be prepared as thin films or non-absorbing matrices. This is not a limitation to measure spectra in the reflectance mode – whose spectra appear different to those of transmission modes, but nevertheless can be a versatile tool providing useful information. Radiation can be reflected, transmitted or absorbed when it strikes a surface. The refractive indices of the two media and angle of incidence determine the relative amounts of reflection and transmission. Reflectance measurements can be categorised as *external* or *internal* (total) reflectance based on their sampling methods. The main forms of *external reflections* include (1) specular reflection (SR); where radiation is reflected and collected from the front surface of a bulk sample, and (2) diffuse reflectance (DR); where the incident ray is scattered at many angles from the surface (rather than one angle as in SR) – a sensitive tool when combined to IR Fourier transform (FT) spectrometers, (DRIFT) [227].

Simultaneously introduced by Harrik and Fahrenfort[224], *attenuated total reflection* (ATR) uses the property of *total internal reflection*. An IR light beam passes through the ATR crystal and reflects off its internal surface which is in contact with the sample, and creates an evanescent wave perpendicular to the surface of the crystal (up to $\sim 1\text{--}2\ \mu\text{m}$) at the point(s) of reflection. Whilst the sample absorbs some energy of the evanescent wave, the internally reflected radiation is returned in an attenuated manner to the detector. The infrared-transparent high refractive index crystal (mostly >2), called the *internal reflection element* (IRE), is made of diamond, ZnSe Ge or Si. A schematic of an ATR system is depicted in Figure 1.5.

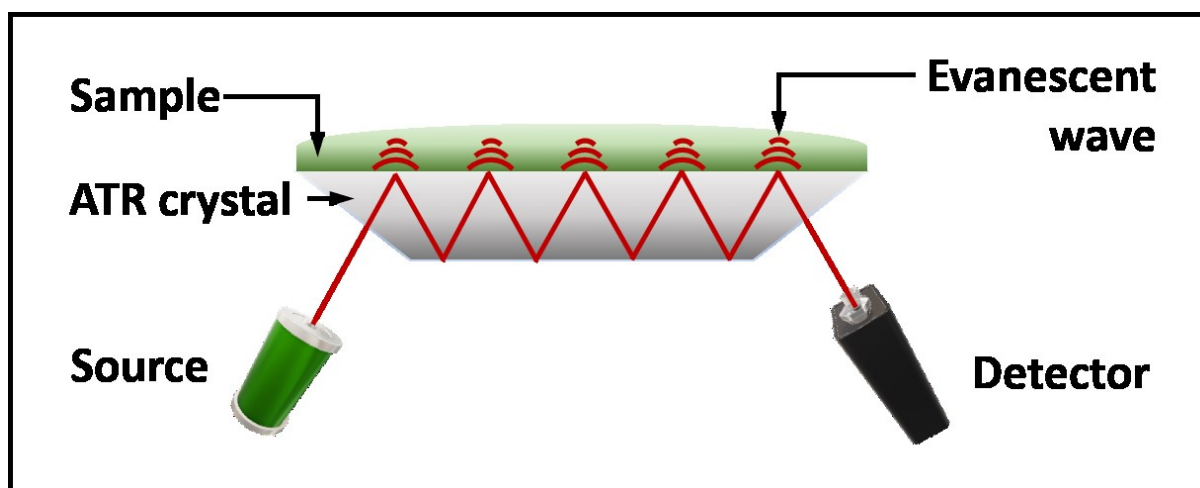


Figure 1.5. Schematic representation of instrumentation in ATR-FTIR.

ATR-FTIR can measure samples at a penetration depth of 0.5–5 μm from the crystal's surface. The IRE often has a higher refractive index (n_1) than the sample (n_2), and these can be related to the angle of IR incidence as 1.18.

$$\theta = \sin^{-1}\left(\frac{n_2}{n_1}\right) \quad \text{Eq. (1.18)}$$

The majority of ATR applications are seen in the mid-IR region but have lately been expanded in to the near-IR, far-IR, UV and visible regions as well. Although ATR has not been directly hyphenated to GC instrumentation, in recent years ATR methods have seen strides in development to achieve versatility in obtaining IR spectra and supporting information gained from GC-MS analysis [228].

The advantages of ATR-FTIR spectroscopy include (i) requiring a small amount of material (1–100 μg), (ii) ability to reduce or eliminate the liquid water signal in the spectrum, (iii) short time (few minutes) to record spectra, (iv) is non-destructive, (v) is able to modulate the environment of the molecule, (vi) often an ability to directly measure with very little/no sample preparation and (vii) can benefit a wide array of biological, chemical and environmental applications [229, 230].

1.6.3 Data processing in infrared spectroscopy

Infrared spectra once measured using a spectrometer often need to be converted to a more useful form to obtain its full value [231]. In current times, most spectra measured are on Fourier transform IR spectrometers. The following techniques are the most commonly used and have been used at various points during the experiments included in this thesis.

- (1) Band intensity and concentration proportionality — A single beam FTIR spectrum is derived by the calculation of the ratio of the sample and background interferogram. Whilst transmission spectra use the Beer-Lambert law, reflectance (ATR, specular or diffuse) spectra use various equations and corrections as set out by Griffith [231].
- (2) Apodization — Although theoretical integration of Fourier transformation ranges from positive to negative infinity, this is not the case in physical settings. The discontinuity of data caused by the finite range produces undesirable ripples on either side of the interferogram's large central peak. Literally meaning "removing the feet or podes", the apodization function reduces the ripples in the FT integration by multiplying the interferogram by a weighting function. Various apodization functions used in spectroscopy to suit the need include Box-car, Triangular, Happ-Genzel, Cosine, Lorentzian, Blackman-Harris, Norton-Beer and Gaussian etc. [232].
- (3) Smoothing — This is used with the goal of reducing the noise with a minimal reduction in the resolution. This is most effective with spectra whose bands are wider than the resolution they are measured at. Popular smoothing technique include Savitzky-Golay and moving average algorithm [232].
- (4) Derivative spectra calculation — IR spectra can be differentiated and overlapping bands can be resolved by mathematical derivatization of their bands which thereby decrease the band's width. First or higher order derivatives can be used as needed with the second derivative being the most commonly used [233].
- (5) Baseline Correction — Although an ideal IR spectrum should have a flat baseline at zero absorbance, it can be offset due to sample preparation, instrument problems, environmental fluctuations etc. Spectrum processing of baseline correction techniques are undertaken to remove the slope and curvature of a spectrum [234].

- (6) Deconvolution — When two or more spectrum peaks overlap deconvolution can enhance the resolution by pulling apart overlapped peaks. This yields spectra with narrower bands enabling closely spaced features to be distinguished [235].

Other spectrum data processing techniques include peak picking, curve fitting, interpolation etc. which can be used as per the nature of the actual measures spectra and need of analysis [231]. Infrared spectra have also benefited greatly from the advances in computer-based procedures and statistical procedures since the 1980s [236]. The above-mentioned data processing techniques together with univariate and multivariate chemometric methods have greatly enhanced analytical powers of FTIR as a detector in GC.

1.6.4 Background to GC-FTIR

IR spectroscopy can be hyphenated to various chromatographic techniques such as liquid chromatography, GC, thin layer chromatography, supercritical fluid chromatography etc., of which GC is most widely used and developed in many aspects [221, 237]. GC-FTIR had many devotees 40+ years ago, mainly stemming from its greater probability to correctly identify each peak in a chromatogram in comparison to that of GC-MS. This however was impeded by detection limits of GC-FTIR being two to three orders of magnitude higher than GC-MS, and hence over the years method difficulties, poor reliability, and lack of support for system maintenance and upgrades saw many abandon the technique which is once again gaining momentum in use as a technique for reliable compound analysis [238]. With its ability to provide a wealth of molecular vibrational (and fine-structure) information, related to molecular functionalities and structures, FTIR spectroscopy is recognised as a detector which can be a universal and yet molecular qualitative detection method, providing complementary information to mass-based ionisation detectors in GC. These reasons, together with the various software algorithms developed and improvements in interface designs to obtain a better sensitivity and reliability, has increased FTIR's practical use for qualitative and quantitative analysis.

Common FTIR spectrometers (Figure 1.4) consist of an infrared source, an interferometer, sample compartment, detector, amplifier and a computer for Fourier

transformation. The hyphenated GC–FTIR instrument ‘simply’ requires replacement of the sample compartment, and design of the light source/detector arrangement. The mercury cadmium telluride (MCT) detector, the most used detector in GC–FTIR instrumentation, allows rapid data acquisition. Various reviews have explored GC–FTIR as a source of spectroscopic detection [239, 240]. Why did FTIR lose most of its allure? The emergence of MS, with its many options, keen marketing, reliability, plethora of available methods, and immediate access to a ‘molecular answer’ has a powerful reinforcement effect in GC–MS. The FTIR, by contrast, which generally is more difficult to maintain, has a lower detectability for analytes [238]. With FTIR’s main attribute being its molecular selectivity and identification — which is more-or-less also provided by MS — consigning FTIR to a historical curiosity might be understood. It is necessary to directly confront this perception. However, recent instrumental advances have rekindled the interest in this technique [241].

1.6.5 Development of GC–FTIR hyphenation

GC–IR was introduced in the 1960s [242], initially using packed columns. The 1980s saw capillary column GC hyphenation with spectroscopic methods for molecular detection, to improve analytical identification through improved peak separation and purity [243, 244] with interface improvements between GC and IR. Such interfacing enables GC effluent detection by either an on-line approach using flow-through cells, or quasi-on-line methods where the effluent is concentrated and immobilised on a trapping medium [245]. The interface should address the challenge of retaining GC resolution as well as improve interaction of the IR beam with eluted analytes.

1.6.5.1 Types of interfaces

Three main interface types are available for GC–FTIR [246] of which one type is based on flow-through cells (light-pipes) and the others on the elimination of the mobile phase.

a) Light-pipe (LP) interface — The light-pipe interface is the most commonly used interface [245] in which GC effluent passes into the LP through which IR radiation

transits, for collection of gas phase spectra. Introduced in 1964 [247], and re-designed by Azaragga [248], a heated gas phase IR flow cell with high reflectivity gold-coated internal surface. Input and exit ports for GC effluent and IR-transparent windows at either end facilitate reflection of the IR beam through the cell. Detectability is improved by using a longer light-pipe; this can reduce GC resolution. Design compromises analyte detectability and resolution, with purging He or N₂ gas to tune IR sensitivity and GC resolution. The internal diameter (I.D.) and length of the cell are typically 0.3–1.0 mm and 50–100 mm, respectively, rendering a volume of about 80 μ L and so is compatible with the average peak volume for 0.25 mm or 0.32 mm I.D. GC capillaries [249]. The flow-through design offers real-time analysis, which other interface types may not. Although common, the LP is least sensitive (ng range). The drawback of pyroelectric detectors such as deuterated triglycine sulfate (DTGS) not being able to acquire low-noise spectra in 1–2 s has been overcome by the more sensitive mercury cadmium telluride (MCT) detectors. The MCT detector however has the drawback of interferogram amplitude drop when temperatures are raised above 250 °C.

b) Matrix isolation (MI) interface — In MI-FTIR, GC effluent in a matrix of cold inert gas (argon) is directed under vacuum for cryogenic trapping onto the surface of a gold-plated collection disc. The helium carrier gas is pumped away and the GC eluates freeze within a solid argon matrix. Trapped analytes undergo interrogation via an IR beam which is directed onto the disc through beam condensing optics and then analysed by the detector. Costly and complex, MI-FTIR provides high sensitivities, and low detection limits to 100s of pg [250], a sensitivity comparable to some MS methods. Low temperature trapping in GC-MI-FTIR renders sharp, intense and narrow IR peaks due to minimal thermal band broadening making higher sensitivities achievable. This however has disadvantages of complex experimental apparatus and non-real-time spectrum acquisition.

c) Direct deposition (DD) interface — DD-FTIR positions an IR microscope very close to the deposition site of GC analytes. Effluent is directed in vacuo onto a cooled (liquid N₂) moving zinc selenide (ZnSe) infrared substrate. With high sensitivity and a lower detection limit than the LP design, DD can detect at sub-ng levels of analyte with no pre-concentration. In a study of FAMES, DD-FTIR had better capacity than the LP to

characterise complex mixtures of variable concentration [251]. This has advantages over MI-FTIR with near-real-time spectral acquisition since the beam focus is immediately next to the deposition site and the similarity to condensed phase spectra acquisition enabling condensed phase IR libraries' use.

d) Cryotrapping matrix isolation interface — A separate GC-FTIR interface has been reported in which both MI and cryotrapping (Xe matrix gas; liquid N₂ coolant) occurs [252] where a study reported sub-ng detection limits [246].

MI- and DD-FTIR systems share some common advantages over LP systems such as increased sensitivity, possibility of post-run signal averaging performed (due to analytes remaining condensed on the window until it warms up) thus improving the signal-to-noise ratio over those attained by GC-LP-FTIR, and the upper temperature being decided by the GC experiment (not being limited by the IR interface) [238].

Figure 1.6 represents a GC-FTIR setup with various interface types indicated. GC-FTIR scanning is generally carried out over 4000–600 cm⁻¹; a background scan may precede the sample scan. Derivatisation of compounds benefits FTIR detection by either improving the detectability by an increased IR response [253], or by enabling identification of compounds inaccurately identified by MS [254].

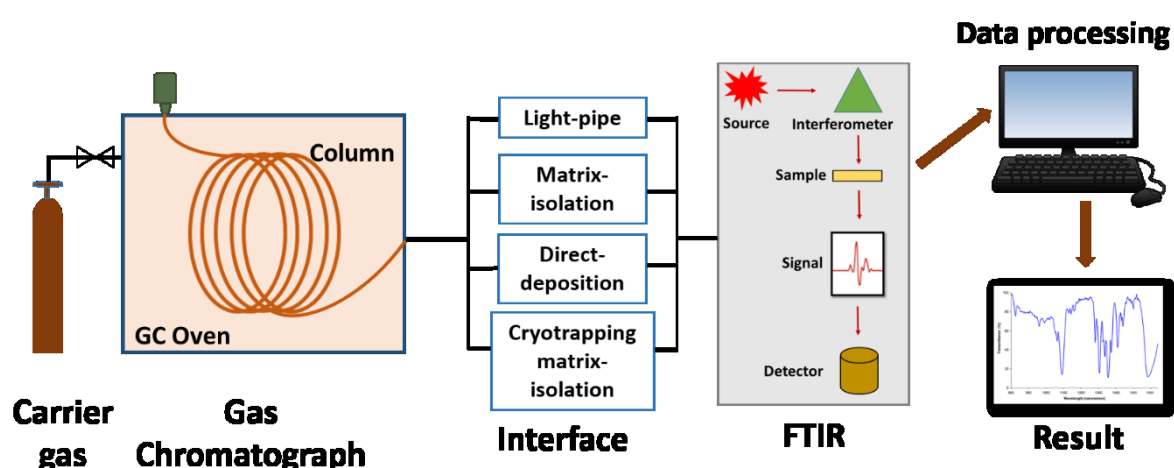


Figure 1.6. Schematic diagram illustrating the GC-FTIR set up with various interfaces and data processing.

1.6.6 Generation of chromatograms

Irrespective of the chromatographic method hyphenated to the FTIR instrument or the interface used, the result is always represented by a plot of the detector's response vs retention time. Structure-specific IR spectroscopic information is converted into chromatogram plots using one of two main methods - the Gram-Schmidt (GS) vector orthogonalisation method and the functional group-specific chromatogram method.

The GS method is a direct, simple to implement yet computationally efficient approach which has been well documented [255]. Its intensity measures the difference of the interferogram vectors from the background subspace. The functional group-specific method on the other hand is more information regarding requiring more calculations to create. Here the integrated IR absorbance within specific wavelength regions are plotted against the chromatography elution time [256].

1.6.7 Applications of GC-FTIR

GC-FTIR enables the unambiguous structural elucidation of structures as well as confirmation of an unknown based on spectroscopic identification and chromatographic retention time (t_R). Retention index (I) data in GC or MDGC allows a preliminary screen of possible compound identity. FTIR allows functional group analysis to detect hydroxyl, aromatic, aliphatic, amine, nitrile etc. groups [100], since each functional group has a characteristic vibrational absorption, which can be used for qualitative, or quantitative purposes.

GC-FTIR spectra can be searched against available reference spectra in digital spectral database libraries for individualised compound identity, and potentially class identity [257] based on the matches between experimental spectra and database spectra. Since homologues show similar, but not identical, IR spectra, library searches of unknown compounds will often match the homologue, which may assist structural elucidation. Reliance on MS spectra and GC retention index data alone does not *per se* provide the absolute structure identification which is the main aim in most analyses. FTIR spectra give a comparatively higher level of confidence than MS data. This level of confidence can be greatly enhanced by using approaches of molecular simulation of IR spectra. Such

modelling methods rapidly improve with the advances in high-performance computing, algorithm efficiencies, theoretical methods, computational chemistry etc. and offers a way of drawing meaningful conclusions to questions raised in an experiment. This is a tool which saves time in predicting the structure of a molecule as well as structure-activity relationships, especially in instances where suitable experimental designs cannot be applied [258]. FTIR spectra and molecular structures can be simulated by the application of different levels of theory and by calculating the relative energy at different levels [259] and is of interest in differentiating isomers, especially in instances where mass spectra fail to distinguish them [260]. Thus, the confirmation of component structure using a combination of molecular simulation approaches, FTIR experimental spectra, MS library hits and GC retention index data can greatly widen the scope of GC-FTIR as a tool of unambiguous chemical identification.

With one of GC-FTIR's greatest successes residing in its ability to differentiate between geometric isomers, it finds application as a complementary or 'orthogonal' method to GC-MS [245, 261] with applications covering several disciplines [237] outlined below.

As novel substances increasingly appear in psychoactive substances and illegal drugs, there is a need to identify substances whose isomers very often have different biological activities. The sensitivity of FTIR spectra towards even minor changes in a molecule's structure to provide "fingerprinting" of molecules and the complementarity of GC-FTIR to GC-MS detection is an asset in drug analysis. This has been applied to structural elucidation of designer drug studies [262], forensic and clinical studies [263, 264] and modelling classes of compounds [239]. This isomer differentiation ability is especially of use in food adulteration and essential oil studies [240] and increasing awareness in food and dietary supplement adulteration. Target components include geometric isomers in complex mixtures such as fatty acid methyl esters, essential oils, edible fats and oils, often with increased probability matches as compared to MS searches [265]. The *cis/trans* geometry of double bonds in the natural oil conjugated linoleic acid, often used in dietary supplements, was confirmed in GC-FTIR by differentiation in the 3000 cm⁻¹ region of the spectrum [266] as seen in Figure 1.7.

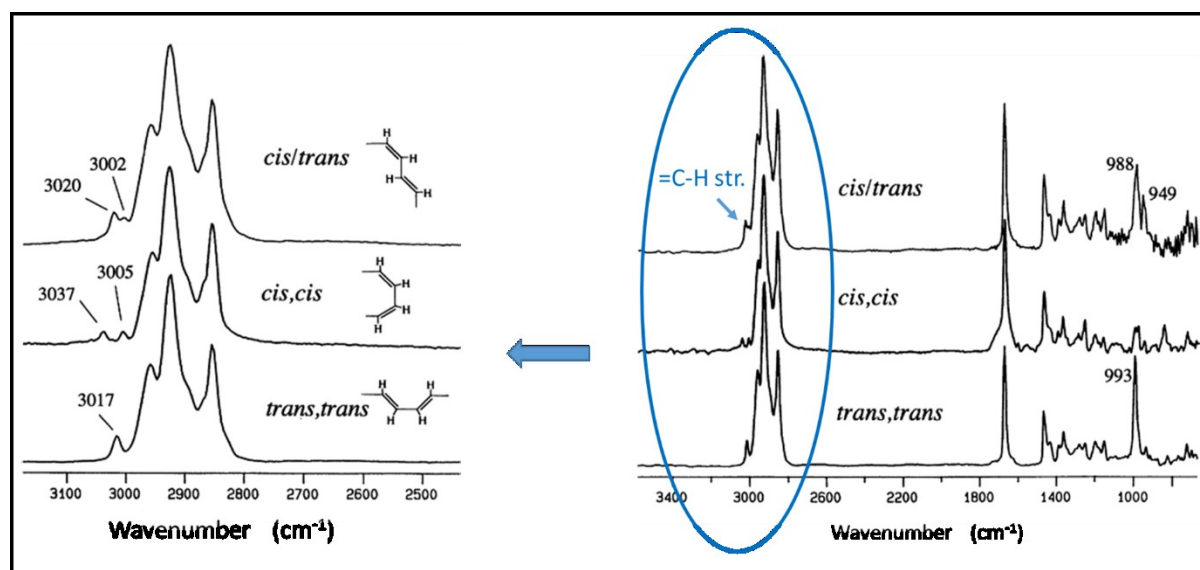


Figure 1.7. GC-DD-FTIR spectra observed at 8 cm^{-1} resolution discriminated between CLA geometric isomers as shown for DMOX derivatives. Adapted from Roach et. al. 2002 with permission.

Interfacing FTIR to MDGC systems incorporating cryogenic trapping was introduced in the early 1990s [267] and used for qualitative analysis of complex mixtures [268]. Quantitative analysis of GC-FTIR can be obtained using univariate and multivariate approaches by one of four methods; chromatographic peak height, chromatographic peak area, absorbance value of the spectrum peak or integrated area of spectrum peak [269, 270]. Analyte detectability can be increased with techniques such as large volume injections and solid phase extraction [271]. LODs of $0.1\text{--}1\ \mu\text{gL}^{-1}$ were achieved using pre-selected wavenumber regions ($2820\text{--}2980\ \text{cm}^{-1}$, $1640\text{--}1670\ \text{cm}^{-1}$, $1520\text{--}1580\ \text{cm}^{-1}$ and $1000\text{--}1050\ \text{cm}^{-1}$) in a study to determine micro-contaminants in water [272].

Further identification and/or quantification applications of GC-FTIR include structural elucidation of natural saccharides [273], marine origin complexes [274], toxicological compounds [275], insect pheromones and volatiles [276, 277], pinene degradation studies [278], pharmaceutical analysis [279], isomeric studies on drugs of abuse [280], chemical weapons [253], petroleum hydrocarbon characterisation [281], compound identification in fentanyl metabolites [282] and essential oil adulteration studies [283]. In some instances the assigning of structures based on FTIR and MS data helps in investigating biological significance of animals and plant components [276]. The development of a two-dimensional separation approach, defined as GC \times FTIR, presents

GC capillary column separation as the first dimension and spectroscopic separation as the second dimension [270, 284]. The large amount of data produced in a single GC-FTIR run calls for appropriate hardware and software. High scan speeds of 1–10 scans per s suffice for this need [269].

1.7 Detector figures of merit

Figures of merit are numerical parameters usually employed to characterise and compare the performance capability of an analytical method, system or device, relative to its alternatives [285]. The focus of the maintenance or improvement of figures of merit stems from the intention of reducing the detrimental effect of the analytical method or technique. This simultaneously improves the selectivity, accuracy and sensitivity of the analytical approach's determinations [286]. Table 1.2 presents a summary of various analytical figures of merit for a variety of spectroscopic detectors in comparison to mass spectrometric detection based on recent literature.

Table 1.2 Classification of detectors and relative analytical figures of merit for spectroscopic detectors and mass spectrometry detection

Detector	Response classification	Mass/ concentration sensitive	Linear range	Limit of detection (LOD)	Reference
FTIR	Spectrum of intact molecule	Concentration	10^3	$10^{-9} \text{ g mL}^{-1}$	[272]
NMR	Spectrum of intact molecule	Concentration	10^1	$10^{-4} \text{ g mL}^{-1}$	[89]
UV	Spectrum of intact molecule	Concentration	10^2	$10^{-6} \text{ g mL}^{-1}$	[106]
VUV	Spectrum of intact molecule	Concentration	10^3	$10^{-6} \text{ g mL}^{-1}$	[96]
FPD (S)	S ₂ emission	Mass	10^4	$10^{-11} \text{ g s}^{-1}$	[43]
FPD (P)	HPO emission	Mass	10^4	$10^{-12} \text{ g s}^{-1}$	[43]
SCD	SO ₂ emission	Mass	$>10^4$	$10^{-12} \text{ g s}^{-1}$	[31]
NCD	NO ₂ emission	Mass	$>10^4$	$10^{-12} \text{ g s}^{-1}$	[31]
MS	m/z ratio of ion fragments	Mass	10^6	$10^{-12} \text{ g s}^{-1}$	[66]

1.8 Multiple detector hyphenation

Multiple detectors hyphenated with GC provide additional information over and above that of a single detector [287, 288]. Figure 1.1 (Section 1.1.1) illustrates some experimental setups of GC systems containing one or more detectors.

Multiple detector hyphenations to GC experiments often allow monitoring and confirmation of compound identities with greater confidence. With their inherent ability to provide structural information on a molecule's intact structure compared to the molecular fragments obtained in MS, as well as complementary information provided by isomer identification, molecular spectroscopic detectors are often hyphenated with MS. A non-destructive detector (e.g. FTIR, UV, VUV) may be serially hyphenated before another detector, either in parallel or sequentially [53]. Hyphenation should produce better – qualitative and/or quantitative – results, such as spectroscopic detection using both MS and FTIR where the latter has capabilities for detailed isomer information [80]. The practice of multiple hyphenation and the ability of molecular spectroscopic methods such as UV-vis, FTIR, and NMR to provide complementary information to MS have been reviewed [288].

Of the molecular spectroscopic techniques, GC-FTIR/MS has been of especial interest. The first capillary GC-FTIR/MS arrangement was reported in 1982 [243], achieved by a variety of approaches such as tunable ratio post-column splitting with time-synchronised detection [245]. This can also be achieved by using two identical columns, switching between two detectors with an open cross splitter, or running the effluent stream through serially linked detectors [289]. Employing cryogenic IR methods is useful to minimise analyte detectability differences between the two detectors, but is not amenable to on-line methods. The diverse applications of GC-FTIR/MS include amino acid pyrolysis products [223], polymer pyrolysis studies [290], and flavour analysis [291]. In the latter study [291], a multidimensional approach was used to isolate a specific region from a first column, then expand its retention on one of 2 second dimension columns. Each could then be recorded by using MS, FTIR or FID detection. Figure 1.8 exemplifies a study using a parallel GC-FTIR/MS system to identify lithium battery degradation products in which FTIR show spectra different to each other, whilst MS displays similar spectra for ethylene oxide and acetaldehyde [292].

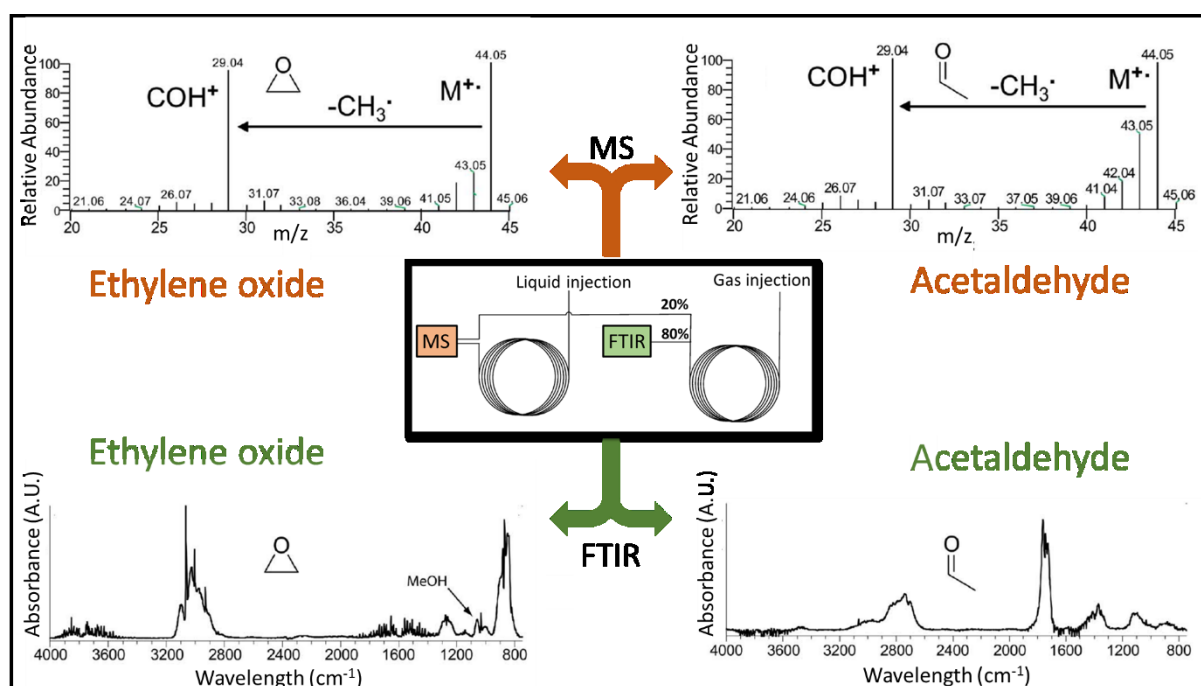


Figure 1.8 Parallel GC-FTIR/MS system showing MS and FTIR spectra for ethylene and acetaldehyde. Adapted from Gachot, Grugeon et al. (2014) with permission.

The complementarity of information gained through parallel spectroscopic and spectrometric detection has been highlighted in the use of MS with other spectroscopic detectors such as PFPD(S) to analyse aging of *Shochu* (Japanese beverage) [293], SCD and NCD for S compounds in aging whisky [199] and with AED for wastewater [294] and petrochemicals [295]. Unambiguous elucidation of structures in unknown substances thus calls for spectroscopic tools, such as FTIR, to complement MS detection.

Table 1.3 reports example applications of GC with various spectroscopic detectors, including instances of multiple detector techniques with focus on GC-FTIR.

Table 1.3 Selective summary of typical applications of GC–molecular spectroscopic detector applications published since 2007.

Detection technique	Sample source	Comments/ application	Reference
GC–FTIR	Alcoholic beverages	Methanol and ethanol identification and quantitation using library spectra	[257]
GC–FTIR	Chemical weapons	Trace analysis of convention related chemicals	[253]
GC–FTIR	Insect pheromones and volatiles	Structure assigning and isomer identification	[276, 277, 296-298]
GC–FTIR	Side chain substituted regioisomers	Differentiation of regioisomers	[280]
GC–FTIR	Petroleum products	Petroleum product characterisation	[281, 299]
GC–FTIR	Essential oil	Structure elucidation and quantitative studies	[270, 300-302]
GC–FTIR	Recycled tire rubber	Volatile component identification during emissions testing	[303]
GC–FTIR	Designer drugs, forensic compounds	Complementary structural elucidation to GC-MS analysis	[262, 264, 304-307]
GC–FTIR	Oxime	Dynamic molecular interconversion studies	[260, 270]
MDGC–FTIR–MS	Fragrances	Irritant identification using spectral library identification	[289]

GC- ¹ H NMR (Off line)	Mix of diethyl ether, dichloromethane, tetrahydrofuran	Use of solenoid type micro coil for volatiles detection	[90]
GC- ¹ H NMR (On-line)	1,2-dimethylcyclohexane	Identification of volatile <i>cis-/trans</i> -stereoisomers	[92]
GC- ¹ H NMR (On-line)	Unfunctionalised racemic chiral alkane	Separation and identification of enantiomers	[93]
MDGC- ¹ H NMR (Off line)	Crude oil	Methylnaphthalene isomer identification in offline NMR mode	[87]
MDGC-2D NMR (Off-line)	Essential oils	Volatile component identity confirmation	[94]
GC-UV	Biomass ash	PAHs and other organic compounds	[105]
GC-UV	Explosives	Enables simultaneous detection of target analyte and decomposition product	[112]
GC-VUV	Turpentine mixtures	Co-eluting peaks deconvoluted, quantitative analysis of terpenes	[115]
GC-VUV	FAME mix and food oils	Co-eluting peaks deconvoluted, <i>cis-/trans</i> -isomeric differentiation of FAMES, fatty acid profiling of food oil	[117]
GC-VUV	Jet and diesel fuel	Computational deconvolution, speciation of dimethylnaphthalene in fuel	[98]
GC-VUV	Petroleum products	Timed interval deconvolution applied, hydrocarbon speciation	[138]
GC-VUV	Water	Natural and toxic gas analysis in Li battery run off	[99]

GC-VUV	Pesticide	Multiclass pesticide identification, isomer differentiation	[114]
GC×GC-VUV	Breath gas	Analysis of VOCs	[54]
PT-GC-pFPD	Seawater	Trace-level dimethylsulfide analysis	[308]
GC-FPD/P	Pepper	Analysis of toxic metabolites	[169]
GC-FPD	Sea water	Butyltin hydride extraction using quartz surface-induced tin emission FPD	[309]
GC×GC-FPD	Pesticides and Kerosene	S and P containing compounds identified. Higher detection limits than 1D GC-FPD seen.	[160]
GC×GC-FPD(S)	Shale oil	Sulfur speciation and quantification	[180]
GC×GC-FPD(P)	Spiked Diesel matrix	OP pesticides & esters	[176]
GC-SCD	Crude oil	Sulfur compound speciation	[197]
GC-NCD	Petrochemicals	Nitrogen compounds speciation and quantitation	[209]
GC×GC-NCD GC×GC-SCD	Plastic waste pyrolysis oil	S- and N- containing groups identified	[205]
GC-MS-FTIR	Li battery degradation	Identification of electrolyte degradation products	[292]
GC-SCD/NCD/MS	Whisky	Simultaneous detection of S and N compounds	[199]

References

- [1] J.S. Zavahir, Y. Nolvachai, P.J. Marriott, Molecular spectroscopy – information rich detection for gas chromatography, *TrAC Trends Anal. Chem.* 99 (2018) 47–65.
- [2] A. James, A. Martin, Gas-liquid partition chromatography: the separation and micro-estimation of volatile fatty acids from formic acid to dodecanoic acid, *Biochem J.* 50 (1952) 679–690.
- [3] D.C. Harris, *Gas Chromatography, Quantitative Chemical Analysis*, W. H. Freeman & Co., New York, 2016, pp. 633–666.
- [4] Y. Han, Y. Zhang, H. Liu, *Gas Chromatography | Principles*, in: P. Worsfold, C. Poole, A. Townshend and M. Miró (Eds.), *Encyclopedia of Analytical Science*, third ed., Academic Press, Oxford, 2019, pp. 237–244.
- [5] E. Stauffer, J.A. Dolan, R. Newman, *Gas Chromatography and Gas Chromatography—Mass Spectrometry*, in: E. Stauffer, J.A. Dolan and R. Newman (Eds.), *Fire Debris Analysis*, Academic Press, Burlington, 2008, pp. 235–293.
- [6] H.M. McNair, J.M. Miller, N.H. Snow, *Introduction in: Basic Gas Chromatography*, third ed., John Wiley & Sons, Inc., 2019, pp. 1–14.
- [7] H.M. McNair, J.M. Miller, N.H. Snow, *Introduction in: Basic Gas Chromatography*, third E ed., John Wiley & Sons, Inc., 2019, pp. 37–50.
- [8] V. D’Atri, S. Fekete, A. Clarke, J.-L. Veuthey, D. Guillarme, Recent advances in chromatography for pharmaceutical analysis, *Anal. Chem.* 91 (2018) 210–239.
- [9] B. Gruber, F. David, P. Sandra, Capillary gas chromatography-mass spectrometry: Current trends and perspectives, *TrAC Trends Anal. Chem.* 124 (2020) 115475.
- [10] A. Ghosh, C.R. Vilorio, A.R. Hawkins, M.L. Lee, Microchip gas chromatography columns, interfacing and performance, *Talanta* 188 (2018) 463–492.
- [11] R. Gras, J. Luong, R.A. Shellie, Miniaturized micromachined gas chromatography with universal and selective detectors for targeted volatile compounds analysis, *J. Chromatogr. A.* 1573 (2018) 151–155.
- [12] U.D. Neue, Theory of peak capacity in gradient elution, *J. Chromatogr. A.* 1079 (2005) 153–161.
- [13] J.C. Giddings, Generation of variance, “theoretical plates,” resolution, and peak capacity in electrophoresis and sedimentation, *Sep. Sci.* 4 (1969) 181–189.
- [14] D.A. Kidwell, L.A. Riggs, Comparing two analytical methods: minimal standards in forensic toxicology derived from information theory, *Forensic Sci. Int.* 145 (2004) 85–96.
- [15] P.J. Marriott, *Gas chromatography | Multidimensional techniques*, in: P. Worsfold, A. Townshend and C. Poole (Eds.), *Encyclopedia of Analytical Science*, second ed., Elsevier. Oxford, 2005, pp. 39–47.
- [16] M.C. Simmons, L.R. Snyder, Two-Stage Gas-Liquid Chromatography, *Anal. Chem.* 30 (1958) 32–35.
- [17] P.J. Marriott, S.-T. Chin, Y. Nolvachai, Techniques and application in comprehensive multidimensional gas chromatography – mass spectrometry, *J. Chromatogr. A.* 1636 (2021) 461788.
- [18] J. de Zeeuw, J. Luong, Developments in stationary phase technology for gas chromatography, *TrAC Trends Anal. Chem.* 21 (2002) 594–607.
- [19] J.C. Giddings, *Dynamics of Chromatography: Principles and Theory*, CRC Press, 2002.

- [20] M. Adahchour, J. Beens, R.J.J. Vreuls, U.A.T. Brinkman, Recent developments in comprehensive two-dimensional gas chromatography (GC × GC): I. Introduction and instrumental set-up, *TrAC Trends Anal. Chem.* 25 (2006) 438–454.
- [21] M. Adahchour, J. Beens, R.J.J. Vreuls, U.A.T. Brinkman, Recent developments in comprehensive two-dimensional gas chromatography (GC×GC), *TrAC Trends Anal. Chem.* 25 (2006) 821–840.
- [22] M. Adahchour, J. Beens, R.J.J. Vreuls, U.A.T. Brinkman, Recent developments in comprehensive two-dimensional gas chromatography (GC × GC). IV. Further applications, conclusions and perspectives, *TrAC Trends Anal. Chem.* 25 (2006) 821–840.
- [23] M. Adahchour, J. Beens, R.J.J. Vreuls, U.A.T. Brinkman, Recent developments in comprehensive two-dimensional gas chromatography (GC × GC). III. Applications for petrochemicals and organohalogens, *TrAC Trends Anal. Chem.* 25 (2006) 726–741.
- [24] M. Adahchour, J. Beens, R.J.J. Vreuls, U.A.T. Brinkman, Recent developments in comprehensive two-dimensional gas chromatography (GC × GC). II. Modulation and detection, *TrAC Trends Anal. Chem.* 25 (2006) 540–553.
- [25] Y. Nolvachai, C. Kulsing, P.J. Marriott, Pesticides analysis: Advantages of increased dimensionality in gas chromatography and mass spectrometry, *Crit. Rev. Env. Sci. Technol.* 45 (2015) 2135–2173.
- [26] S.T. Chin, P.J. Marriott, Multidimensional gas chromatography beyond simple volatiles separation, *Chem. Commun.* 50 (2014) 8819–8833.
- [27] K.M. Sharif, S.-T. Chin, C. Kulsing, P.J. Marriott, The microfluidic Deans switch: 50 years of progress, innovation and application, *TrAC Trends Anal. Chem.* 82 (2016) 35–54.
- [28] J.A. Murray, Qualitative and quantitative approaches in comprehensive two-dimensional gas chromatography, *J. Chromatogr. A* 1261 (2012) 58–68.
- [29] L.L.P. van Stee, U.T. Brinkman, Peak detection methods for GC× GC: An overview, *TrAC Trends Anal. Chem.* 83 (2016) 1–13.
- [30] P.J. Marriott, Detector technologies and applications in comprehensive two-dimensional gas chromatography, in: L. Mondello (Ed.), *Comprehensive Chromatography in Combination with Mass Spectrometry*, John Wiley & Sons, Inc., Hoboken, N.J., 2011, pp. 243–280.
- [31] J.T. Andersson, Detectors, in: K. Dettmer-Wilde and W. Engewald (Eds.), *Practical Gas Chromatography: A Comprehensive Reference*, Springer, Berlin, Heidelberg, 2014, pp. 205–248.
- [32] R.C. Blase, K. Llera, A. Luspai-Kuti, M. Libardoni, The importance of detector acquisition rate in comprehensive two-dimensional gas chromatography (GC×GC), *Sep. Sci. Technol.* 49 (2014) 847–853.
- [33] K.M. Pierce, J.L. Hope, J.C. Hoggard, R.E. Synovec, A principal component analysis based method to discover chemical differences in comprehensive two-dimensional gas chromatography with time-of-flight mass spectrometry (GC×GC-TOFMS) separations of metabolites in plant samples, *Talanta* 70 (2006) 797–804.
- [34] K. Héberger, M. Görgényi, Principal component analysis of Kováts indices for carbonyl compounds in capillary gas chromatography, *J. Chromatogr. A* 845 (1999) 21–31.
- [35] S. Dagan, Comparison of gas chromatography–pulsed flame photometric detection–mass spectrometry, automated mass spectral deconvolution and identification system and gas chromatography–tandem mass spectrometry as tools for trace level detection and identification, *J. Chromatogr. A* 868 (2000) 229–247.
- [36] V.I. Babushok, Chromatographic retention indices in identification of chemical compounds, *TrAC Trends Anal. Chem.* 69 (2015) 98–104.

- [37] L.S. Ettre, Nomenclature for chromatography (IUPAC recommendations 1993), *Pure Appl. Chem.* 65 (1993) 819–872.
- [38] B. Domon, R. Aebersold, Options and considerations when selecting a quantitative proteomics strategy, *Nat. Biotechnol.* 28 (2010) 710–721.
- [39] C.F. Poole, Ionization-based detectors for gas chromatography, *J. Chromatogr. A.* 1421 (2015) 137–153.
- [40] H.M. McNair, J.M. Miller, Detector, in: *Basic Gas Chromatography*, second ed., John Wiley & Sons, Inc., pp. 104–128.
- [41] C.F. Poole, *The Essence of Chromatography*, Elsevier, Amsterdam, 2003.
- [42] R.P. Scott, *Chromatographic Detectors: Design: Function, and Operation*, CRC Press, 1996.
- [43] C. Li, Z. Long, X. Jiang, P. Wu, X. Hou, Atomic spectrometric detectors for gas chromatography, *TrAC Trends Anal. Chem.* 77 (2016) 139–155.
- [44] K.D. Wilde, W. Engewald, *Practical Gas Chromatography: A Comprehensive Reference*, Springer-Verlag, Berlin, 2014.
- [45] J.M. Miller, *Chromatography: Concepts and Contrasts*, second ed., John Wiley & Sons Inc., Hoboken, N.J., 2005.
- [46] E. Kaal, H.-G. Janssen, Extending the molecular application range of gas chromatography, *J. Chromatogr. A.* 1184 (2008) 43–60.
- [47] B.H. Fumes, M.R. Silva, F.N. Andrade, C.E.D. Nazario, F.M. Lanças, Recent advances and future trends in new materials for sample preparation, *TrAC Trends Anal. Chem.* 71 (2015) 9–25.
- [48] C.F. Poole, Derivatization reactions for use with the electron-capture detector, *J. Chromatogr. A.* 1296 (2013) 15–24.
- [49] T. Holm, Aspects of the mechanism of the flame ionization detector, *J. Chromatogr. A.* 842 (1999) 221–227.
- [50] M.S. Klee, Detectors, in: C.F. Poole (Ed.) *Gas Chromatography*, Elsevier, Amsterdam, 2012, pp. 307–347.
- [51] J. Holmes, F. Morrell, Oscillographic mass spectrometric monitoring of gas chromatography, *Appl. Spectrosc.* 11 (1957) 86–87.
- [52] R.S. Gohlke, Time-of-Flight Mass Spectrometry and Gas-Liquid Partition Chromatography, *Anal. Chem.* 31 (1959) 535–541.
- [53] I.C. Santos, K.A. Schug, Recent advances and applications of gas chromatography vacuum ultraviolet spectroscopy, *J. Sep. Sci.* 40 (2017) 138–151.
- [54] B. Gruber, T. Groeger, D. Harrison, R. Zimmermann, Vacuum ultraviolet absorption spectroscopy in combination with comprehensive two-dimensional gas chromatography for the monitoring of volatile organic compounds in breath gas: A feasibility study, *J. Chromatogr. A.* 1464 (2016) 141–146.
- [55] J. Greaves, J. Roboz, *Mass spectrometry for the novice*, CRC Press, Boca Raton, FL, 2014.
- [56] I. Špánik, A. Machyňáková, Recent applications of gas chromatography with high-resolution mass spectrometry, *J. Sep. Sci.* 41 (2018) 163–179.
- [57] D. Nolting, R. Malek, A. Makarov, Ion traps in modern mass spectrometry, *Mass Spectrom. Rev.* 38 (2019) 150–168.
- [58] S. Eliuk, A. Makarov, Evolution of Orbitrap mass spectrometry instrumentation, *Annu. Rev. Anal. Chem.* 8 (2015) 61–80.
- [59] A. Makarov, D. Grinfeld, K. Ayzikov, Fundamentals of Orbitrap analyzer, in: B. Kanawati and P. Schmitt-Kopplin (Eds.), *Fundamentals and Applications of Fourier Transform Mass Spectrometry*, Elsevier, 2019, pp. 37–61.

- [60] X. Wei, X. Shi, M. Merrick, P. Willis, D. Alonso, X. Zhang, A method of aligning peak lists generated by gas chromatography high-resolution mass spectrometry, *Analyst* 138 (2013) 5453–5460.
- [61] A.C. Peterson, J.-P. Hauschild, S.T. Quarmby, D. Krumwiede, O. Lange, R.A. Lemke, F. Grosse-Coosmann, S. Horning, T.J. Donohue, M.S. Westphall, Development of a GC/Quadrupole-Orbitrap mass spectrometer, part I: design and characterization, *Anal. Chem.* 86 (2014) 10036–10043.
- [62] F. Xian, C.L. Hendrickson, A.G. Marshall, High resolution mass spectrometry, *Anal. Chem.* 84 (2012) 708–719.
- [63] S. Stein, Mass spectral reference libraries: An ever-expanding resource for chemical identification, *Anal. Chem.* 84 (2012) 7274–7282.
- [64] B.L. Milman, I.K. Zhurkovich, Mass spectral libraries: A statistical review of the visible use, *TrAC Trends Anal. Chem.* 80 (2016) 636–640.
- [65] B.L. Milman, Identification of chemical compounds, *TrAC Trends Anal. Chem.* 24 (2005) 493–508.
- [66] B.L. Milman, General principles of identification by mass spectrometry, *TrAC Trends Anal. Chem.* 69 (2015) 24–33.
- [67] X. Liu, L. Zhou, X. Shi, G. Xu, New advances in analytical methods for mass spectrometry-based large-scale metabolomics study, *TrAC Trends Anal. Chem.* 121 (2019) 115665.
- [68] A.G. Marshall, R.P. Rodgers, Petroleomics: The next grand challenge for chemical analysis, *Accounts of Chemical Research* 37 (2004) 53–59.
- [69] T.M.S. Ryan P. Rodgers, and Alan G. Marshall, Petroleomics: MS returns to its roots, *Anal. Chem.* 77 (2005) 20 A–27 A.
- [70] M.P. Barrow, Petroleomics: study of the old and the new, *Biofuels* 1 (2010) 651–655.
- [71] D.C.P. Lozano, M.J. Thomas, H.E. Jones, M.P. Barrow, Petroleomics: Tools, challenges, and developments, *Annual Review of Analytical Chemistry* 13 (2020) 405–430.
- [72] M. Jiang, C. Kulsing, Y. Nolvachai, P.J. Marriott, Two-dimensional retention indices improve component identification in comprehensive two-dimensional gas chromatography of Saffron, *Anal. Chem.* 87 (2015) 5753–5761.
- [73] X. Wang, S. Wang, Z. Cai, The latest developments and applications of mass spectrometry in food-safety and quality analysis, *TrAC Trends Anal. Chem.* 52 (2013) 170–185.
- [74] M.S. Alam, R.M. Harrison, Recent advances in the application of 2-dimensional gas chromatography with soft and hard ionisation time-of-flight mass spectrometry in environmental analysis, *Chem. Sci.* 7 (2016) 3968–3977.
- [75] G. Martínez-Domínguez, P. Plaza-Bolaños, R. Romero-González, A. Garrido-Frenich, Analytical approaches for the determination of pesticide residues in nutraceutical products and related matrices by chromatographic techniques coupled to mass spectrometry, *Talanta* 118 (2014) 277–291.
- [76] P.Q. Tranchida, F.A. Franchina, M. Zoccali, S. Pantò, D. Sciarrone, P. Dugo, L. Mondello, Untargeted and targeted comprehensive two-dimensional GC analysis using a novel unified high-speed triple quadrupole mass spectrometer, *J. Chromatogr. A.* 1278 (2013) 153–159.
- [77] B. Mitrevski, P.J. Marriott, Evaluation of quadrupole-time-of-flight mass spectrometry in comprehensive two-dimensional gas chromatography, *J. Chromatogr. A.* 1362 (2014) 262–269.
- [78] D.C. Harris, *Quantitative Chemical Analysis*, ninth ed., W.H. Freeman & Co., New York, 2016.
- [79] C.L. Wilkins, Hyphenated spectroscopic detectors for gas chromatography, in: C.F. Poole (Ed.), *Gas Chromatography*, Elsevier. Amsterdam, 2012, pp. 349–354.

- [80] N. Ragunathan, K.A. Krock, C. Klawun, T.A. Sasaki, C.L. Wilkins, Gas chromatography with spectroscopic detectors, *J. Chromatogr. A.* 856 (1999) 349–397.
- [81] L.L.P. van Stee, U.A.T. Brinkman, H. Bagheri, Gas chromatography with atomic emission detection: a powerful technique, *TrAC Trends Anal. Chem.* 21 (2002) 618–626.
- [82] J.T. Andersson, Some unique properties of gas chromatography coupled with atomic-emission detection, *Anal. Bioanal. Chem.* 373 (2002) 344–355.
- [83] L.L.P. van Stee, U.A.T. Brinkman, Developments in the application of gas chromatography with atomic emission (plus mass spectrometric) detection, *J. Chromatogr. A.* 1186 (2008) 109–122.
- [84] H. Bagheri, M. Saraji, U.A.T. Brinkman, Environmental applications of gas chromatography-atomic emission detection, *Tech. Instrum. Anal. Chem.* 21 (2000) 211–238.
- [85] E. Becker, A brief history of nuclear magnetic resonance, *Anal. Chem.* 65 (1993) 295A–302A.
- [86] C.F. Poole, Spectroscopic Detectors for Identification and Quantification, *The Essence of Chromatography*, Elsevier Science. Amsterdam, 2003, pp. 719–792.
- [87] G.T. Eyres, S. Urban, P.D. Morrison, P.J. Marriott, Application of microscale-preparative multidimensional gas chromatography with nuclear magnetic resonance spectroscopy for identification of pure methylnaphthalenes from crude oils, *J. Chromatogr. A.* 1215 (2008) 168–176.
- [88] K. Patel, J. Patel, M. Patel, G. Rajput, H. Patel, Introduction to hyphenated techniques and their applications in pharmacy, *Pharm. Methods* 1 (2010) 2–13.
- [89] M. Kühnle, K. Holtin, K. Albert, Capillary NMR detection in separation science, *J. Sep. Sci.* 32 (2009) 719–726.
- [90] M.D. Grynbaum, D. Kreidler, J. Rehbein, A. Porea, P. Schuler, W. Schaal, H. Czesla, A. Webb, V. Schurig, K. Albert, Hyphenation of gas chromatography to microcoil ¹H nuclear magnetic resonance spectroscopy, *Anal. Chem.* 79 (2007) 2708–2713.
- [91] C. Paiva, A. Amaral, M. Rodriguez, N. Canyellas, X. Correig, J. Ballescà, J. Ramalho-Santos, R. Oliva, Identification of endogenous metabolites in human sperm cells using proton nuclear magnetic resonance (¹H-NMR) spectroscopy and gas chromatography-mass spectrometry (GC-MS), *Andrology* 3 (2015) 496–505.
- [92] M. Kühnle, D. Kreidler, K. Holtin, H. Czesla, P. Schuler, W. Schaal, V. Schurig, K. Albert, Online coupling of gas chromatography to nuclear magnetic resonance spectroscopy: Method for the analysis of volatile stereoisomers, *Anal. Chem.* 80 (2008) 5481–5486.
- [93] M. Kühnle, D. Kreidler, K. Holtin, H. Czesla, P. Schuler, V. Schurig, K. Albert, Online coupling of enantioselective capillary gas chromatography with proton nuclear magnetic resonance spectroscopy, *Chirality* 22 (2010) 808–812.
- [94] G.T. Eyres, S. Urban, P.D. Morrison, J.-P. Dufour, P.J. Marriott, Method for small-molecule discovery based on microscale-preparative multidimensional gas chromatography isolation with nuclear magnetic resonance spectroscopy, *Anal. Chem.* 80 (2008) 6293–6299.
- [95] C.P. Rühle, J. Niere, P.D. Morrison, R.C. Jones, T. Caradoc-Davies, A.J. Canty, M.G. Gardiner, V.-A. Tolhurst, P.J. Marriott, Characterization of tetra-aryl benzene isomers by using preparative gas chromatography with mass spectrometry, nuclear magnetic resonance spectroscopy, and X-ray crystallographic methods, *Anal. Chem.* 82 (2010) 4501–4509.
- [96] K.A. Schug, I. Sawicki, D.D. Carlton, Jr., F. Hui, H.M. McNair, J.P. Nimmo, P. Kroll, J. Smuts, P. Walsh, D. Harrison, Vacuum ultraviolet detector for gas chromatography.(Report), *Anal. Chem.* 86 (2014) 8329–8335.

- [97] A. Lelevic, V. Souchon, M. Moreaud, C. Lorentz, C. Geantet, Gas chromatography vacuum ultraviolet spectroscopy: A review, *J. Sep. Sci.* 43 (2020) 150–173.
- [98] J. Schenk, J.X. Mao, J. Smuts, P. Walsh, P. Kroll, K.A. Schug, Analysis and deconvolution of dimethylnaphthalene isomers using gas chromatography vacuum ultraviolet spectroscopy and theoretical computations, *Anal. Chim. Acta.* 945 (2016) 1–8.
- [99] L. Bai, J. Smuts, P. Walsh, H. Fan, Z. Hildenbrand, D. Wong, D. Wetz, K.A. Schug, Permanent gas analysis using gas chromatography with vacuum ultraviolet detection, *J. Chromatogr. A.* 1388 (2015) 244–250.
- [100] D.A. Skoog, *Principles of Instrumental Analysis*, sixth ed., Thomson, Brooks/Cole, Belmont, CA, 2007.
- [101] L. Lagesson-Andrasko, V. Legesson, J. Andrasko, The use of gas-phase UV spectra in the 168–330-nm wavelength region for analytical purposes. 1. Qualitative measurements, *Anal. Chem.* 70 (1998) 819–826.
- [102] T.D. Searl, F.J. Cassidy, W.H. King, R.A. Brown, An analytical method for polynuclear aromatic compounds in coke oven effluents by combined use of gas chromatography and ultraviolet absorption spectrometry, *Anal. Chem.* 42 (1970) 954–958.
- [103] E. Sawicki, Tentative method of analysis for polynuclear aromatic hydrocarbons in automobile exhaust, *Health Lab. Sci.* 11 (1974) 228–239.
- [104] M. Novotny, F.J. Schwende, M.J. Hartigan, J.E. Purcell, Capillary gas chromatography with ultraviolet spectrometric detection, *Anal. Chem.* 52 (1980) 736–740.
- [105] H. Lagesson, A. Nilsson, C. Tagesson, Qualitative determination of compounds adsorbed on indoor dust particles using GC-UV and GC-MS after thermal desorption, *Chromatographia* 52 (2000) 621–630.
- [106] I. Sanz-Vicente, S. Cabredo, J. Galban, Gas chromatography with UV-vis molecular absorption spectrometry detection: Increasing sensitivity of the determination of alcohols and phenols by derivatization, *Chromatographia* 48 (1998) 542–547.
- [107] T. Cedrón-Fernández, C. Sáenz-Barrio, S. Cabredo-Pinillos, I. Sanz-Vicente, Separation and determination of volatile compounds in synthetic wine samples by gas chromatography using UV-visible molecular absorption spectrometry as detector, *Talanta* 57 (2002) 555–563.
- [108] A. Nilsson, E. Kihlström, V. Lagesson, B. Wessén, B. Szponar, L. Larsson, C. Tagesson, Microorganisms and volatile organic compounds in airborne dust from damp residences, *Indoor Air* 14 (2004) 74–82.
- [109] P. Straka, M. Havelcova, Polycyclic aromatic hydrocarbons and other organic compounds in ashes from biomass combustion, *Acta Geodyn. Geomater.* 9 (2012) 481–490.
- [110] R.A. Greinke, I.C. Lewis, Development of a gas chromatographic-ultraviolet absorption spectrometric method for monitoring petroleum pitch volatiles in the environment, *Anal. Chem.* 47 (1975) 2151–2155.
- [111] R. Hodyss, J.L. Beauchamp, Multidimensional detection of nitroorganic explosives by gas chromatography-pyrolysis-ultraviolet detection, *Anal. Chem.* 77 (2005) 3607–3610.
- [112] J. Andrasko, L. Lagesson-Andrasko, J. Dahlén, B.H. Jonsson, Analysis of Explosives by GC-UV, *J. Forensic Sci.* 62 (2017) 1022–1027.
- [113] R. Gras, J. Luong, R.A. Shellie, Direct measurement of trace elemental mercury in hydrocarbon matrices by gas chromatography with ultraviolet photometric detection.(Report), *Anal. Chem.* 87 (2015) 11429–11432.
- [114] H. Fan, J. Smuts, P. Walsh, D. Harrison, K.A. Schug, Gas chromatography-vacuum ultraviolet spectroscopy for multiclass pesticide identification, *J. Chromatogr. A.* 1389 (2015) 120–127.

- [115] C. Qiu, J. Smuts, K.A. Schug, Analysis of terpenes and turpentines using gas chromatography with vacuum ultraviolet detection, *J. Sep. Sci.* 40 (2017) 869–877.
- [116] I.C. Santos, J. Smuts, K.A. Schug, Rapid profiling and authentication of Vanilla extracts using gas chromatography-vacuum ultraviolet spectroscopy, *Food Anal. Methods* 10 (2017) 4068–4078.
- [117] H. Fan, J. Smuts, L. Bai, P. Walsh, D.W. Armstrong, K.A. Schug, Gas chromatography–vacuum ultraviolet spectroscopy for analysis of fatty acid methyl esters, *Food Chem.* 194 (2016) 265–271.
- [118] C.A. Weatherly, Y. Zhang, J.P. Smuts, H. Fan, C. Xu, K.A. Schug, J.C. Lang, D.W. Armstrong, Analysis of long-chain unsaturated fatty acids by ionic liquid gas chromatography, *J. Agric. Food Chem.* 64 (2016) 1422–1432.
- [119] I.C. Santos, J. Smuts, W.-S. Choi, Y. Kim, S.B. Kim, K.A. Schug, Analysis of bacterial FAMES using gas chromatography – vacuum ultraviolet spectroscopy for the identification and discrimination of bacteria, *Talanta* 182 (2018) 536–543.
- [120] B.M. Weber, P. Walsh, J.J. Harynuk, Determination of hydrocarbon group-type of diesel fuels by gas chromatography with vacuum ultraviolet detection, *Anal. Chem.* 88 (2016) 5809–5817.
- [121] M. Zoccali, K.A. Schug, P. Walsh, J. Smuts, L. Mondello, Flow-modulated comprehensive two-dimensional gas chromatography combined with a vacuum ultraviolet detector for the analysis of complex mixtures, *J. Chromatogr. A* 1497 (2017) 135–143.
- [122] H. Liu, G. Raffin, G. Trutt, V. Dugas, C. Demesmay, J. Randon, Hyphenation of short monolithic silica capillary column with vacuum ultraviolet spectroscopy detector for light hydrocarbons separation, *J. Chromatogr. A* 1595 (2019) 174–179.
- [123] A.R. García-Cicourel, B. van de Velde, J. Verduin, H.-G. Janssen, Comprehensive off-line silver phase liquid chromatography × gas chromatography with flame ionization and vacuum ultraviolet detection for the detailed characterization of mineral oil aromatic hydrocarbons, *J. Chromatogr. A* 1607 (2019) 460391.
- [124] C. Qiu, J. Cochran, J. Smuts, P. Walsh, K.A. Schug, Gas chromatography-vacuum ultraviolet detection for classification and speciation of polychlorinated biphenyls in industrial mixtures, *J. Chromatogr. A* 1490 (2017) 191–200.
- [125] L. Skultety, P. Frycak, C. Qiu, J. Smuts, L. Shear-Laude, K. Lemr, J.X. Mao, P. Kroll, K.A. Schug, A. Szewczak, C. Vaught, I. Lurie, V. Havlicek, Resolution of isomeric new designer stimulants using gas chromatography – vacuum ultraviolet spectroscopy and theoretical computations, *Anal. Chim. Acta.* 971 (2017) 55–67.
- [126] R.F. Kranenburg, A.R. García-Cicourel, C. Kukurin, H.-G. Janssen, P.J. Schoenmakers, A.C. van Asten, Distinguishing drug isomers in the forensic laboratory: GC–VUV in addition to GC–MS for orthogonal selectivity and the use of library match scores as a new source of information, *Forensic Sci. Int.* 302 (2019) 109900.
- [127] S. Buchalter, I. Marginean, J. Yohannan, I.S. Lurie, Gas chromatography with tandem cold electron ionization mass spectrometric detection and vacuum ultraviolet detection for the comprehensive analysis of fentanyl analogues, *J. Chromatogr. A* 1596 (2019) 183–193.
- [128] A. Leghissa, J. Smuts, C. Qiu, Z.L. Hildenbrand, K.A. Schug, Detection of cannabinoids and cannabinoid metabolites using gas chromatography with vacuum ultraviolet spectroscopy, *Sep. Sci. Plus* 1 (2018) 37–42.
- [129] Z.R. Roberson, H.C. Gordon, J.V. Goodpaster, Instrumental and chemometric analysis of opiates via gas chromatography–vacuum ultraviolet spectrophotometry (GC–VUV), *Anal. Bioanal. Chem.* 412 (2020) 1123–1128.

- [130] R. Pechancová, C. Qiu, J. Smuts, K. Lemr, K.A. Schug, Comparative study of ink photoinitiators in food packages using gas chromatography with vacuum ultraviolet detection and gas chromatography with mass spectrometry, *J. Sep. Sci.* 42 (2019) 556–565.
- [131] J. Schenk, G. Nagy, N.L.B. Pohl, A. Leghissa, J. Smuts, K.A. Schug, Identification and deconvolution of carbohydrates with gas chromatography-vacuum ultraviolet spectroscopy, *J. Chromatogr. A* 1513 (2017) 210–221.
- [132] C. Weston, J. Smuts, J.X. Mao, K.A. Schug, Investigation of gas phase absorption spectral similarity for stable-isotopically labeled compounds in the 125–240nm wavelength range, *Talanta* 177 (2018) 41–46.
- [133] C.A. Cruse, J.V. Goodpaster, Generating highly specific spectra and identifying thermal decomposition products via gas chromatography / vacuum ultraviolet spectroscopy (GC/VUV): Application to nitrate ester explosives, *Talanta* 195 (2019) 580–586.
- [134] R. Reiss, B. Gruber, S. Klingbeil, T. Gröger, S. Ehlert, R. Zimmermann, Evaluation and application of gas chromatography - vacuum ultraviolet spectroscopy for drug- and explosive precursors and examination of non-negative matrix factorization for deconvolution, *Spectrochim. Acta, Part A* 219 (2019) 129–134.
- [135] Z.R. Roberson, J.V. Goodpaster, Differentiation of structurally similar phenethylamines via gas chromatography-vacuum ultraviolet spectroscopy (GC-VUV), *Forensic Chem.* 15 (2019) 100712.
- [136] I.C. Santos, J. Smuts, M.L. Crawford, R.P. Grant, K.A. Schug, Large-volume injection gas chromatography-vacuum ultraviolet spectroscopy for the qualitative and quantitative analysis of fatty acids in blood plasma, *Anal. Chim. Acta* 1053 (2019) 169–177.
- [137] J.A. Diekmann, J. Cochran, J.A. Hodgson, D.J. Smuts, Quantitation and identification of ethanol and inhalant compounds in whole blood using static headspace gas chromatography vacuum ultraviolet spectroscopy, *J. Chromatogr. A* 1611 (2020) 460607.
- [138] P. Walsh, M. Garbalena, K.A. Schug, Rapid analysis and time interval deconvolution for comprehensive fuel compound group classification and speciation using gas chromatography-vacuum ultraviolet spectroscopy, *Anal. Chem.* 88 (2016) 11130–11138.
- [139] J.X. Mao, P. Walsh, P. Kroll, K.A. Schug, Simulation of vacuum ultraviolet absorption spectra: paraffin, isoparaffin, olefin, naphthene, and aromatic hydrocarbon class compounds, *Appl. Spectrosc.* 74 (2020) 72–80.
- [140] F.C.-Y. Wang, GC × VUV study of diesel: A two-dimensional separation approach, *Energy Fuels* 34 (2020) 1432–1437.
- [141] R. Gras, J. Luong, P.R. Haddad, R.A. Shellie, Gas chromatography with simultaneous detection: Ultraviolet spectroscopy, flame ionization, and mass spectrometry, *J. Chromatogr. A* 1563 (2018) 171–179.
- [142] S. Brody, J. Chaney, Flame photometric detector: The application of a specific detector for phosphorus and for sulfur compounds - sensitive to subnanogram quantities, *J. Chromatogr. Sci.* 4 (1966) 42–46.
- [143] W.A. Aue, X.Y. Sun, B. Millier, Inter-elemental selectivity, spectra and computer-generated specificity of some main-group elements in the flame photometric detector, *J. Chromatogr. A* 606 (1992) 73–86.
- [144] X.-Y. Sun, W.A. Aue, Selective detection of volatile iron compounds by flame photometry, *J. Chromatogr. A* 467 (1989) 75–84.
- [145] G.-B. Jiang, Q.-F. Zhou, B. He, Speciation of organotin compounds, total tin, and major trace metal elements in poisoned human organs by gas chromatography-flame photometric detector and inductively coupled plasma-mass spectrometry, *Environ. Sci. Technol.* 34 (2000) 2697–2702.

- [146] S.O. Farwell, C.J. Barinaga, Sulfur-selective detection with the FPD: Current enigmas, practical usage, and future directions, *J. Chromatogr. Sci.* 24 (1986) 483–494.
- [147] W. Wardencki, B. Zygmunt, Gas chromatographic sulphur-sensitive detectors in environmental analysis, *Anal. Chim. Acta.* 255 (1991) 1–13.
- [148] C.H. Burnett, D.F. Adams, S.O. Farwell, Relative FPD responses for a systematic group of sulfur-containing compounds, *J. Chromatogr. Sci.* 16 (1978) 68–73.
- [149] T. Sugiyama, Y. Suzuki, T. Takeuchi, Characteristics of S₂ emission intensity with a flame photometric detector, *J. Chromatogr. A.* 77 (1973) 309–316.
- [150] M. Dressler, *Selective Gas Chromatographic Detectors*, Elsevier, New York, 1986.
- [151] S. Kapila, C.R. Vogt, FPD: Burner configurations and the response to hetero-organics, *J. Chromatogr. Sci.* 17 (1979) 327–332.
- [152] M.C. Bowman, M. Beroza, Gas chromatographie detector for simultaneous sensing of phosphorus- and sulfur-containing compounds by flame photometry, *Anal. Chem.* 40 (1968) 1448–1452.
- [153] P.L. Patterson, Dual-flame photometric detector for sulfur and phosphorus compounds in gas chromatograph effluents, *Anal. Chem.* 50 (1978) 339–344.
- [154] C.G. Flinn, W.A. Aue, Geometric and chemical discrimination in a non-dispersive flame photometric detector, *J. Chromatogr. Sci.* 18 (1980) 136–138.
- [155] L. Kalontarov, H. Jing, A. Amirav, S. Cheskis, Mechanism of sulfur emission quenching in flame photometric detectors, *J. Chromatogr. A.* 696 (1995) 245–256.
- [156] N. Tzanani, A. Amirav, Combined pulsed flame photometric ionization detector, *Anal. Chem.* 67 (1995) 167–173.
- [157] K.B. Thurbide, C.D. Anderson, Flame photometric detection inside of a capillary gas chromatography column, *Analyst* 128 (2003) 616–622.
- [158] T.C. Hayward, K.B. Thurbide, Characteristics of sulfur response in a micro-flame photometric detector, *J. Chromatogr. A.* 1105 (2006) 66–70.
- [159] A.G. Clark, K.B. Thurbide, An improved multiple flame photometric detector for gas chromatography, *J. Chromatogr. A.* 1421 (2015) 154–161.
- [160] S.T. Chin, Z.Y. Wu, P.D. Morrison, P.J. Marriott, Observations on comprehensive two dimensional gas chromatography coupled with flame photometric detection for sulfur- and phosphorus-containing compounds, *Anal. Methods* 2 (2010) 243–253.
- [161] X. Du, Y.L. Ren, S.J. Beckett, An Innovative rapid method for analysis of 10 organophosphorus pesticide residues in wheat by HS-SPME-GC-FPD/MSD, *J. AOAC Int.* 99 (2016) 520–526.
- [162] X. Zhao, W. Kong, J. Wei, M. Yang, Gas chromatography with flame photometric detection of 31 organophosphorus pesticide residues in *Alpinia oxyphylla* dried fruits, *Food Chem.* 162 (2014) 270–276.
- [163] S. Berijani, Y. Assadi, M. Anbia, M.-R. Milani Hosseini, E. Aghaee, Dispersive liquid–liquid microextraction combined with gas chromatography-flame photometric detection: Very simple, rapid and sensitive method for the determination of organophosphorus pesticides in water, *J. Chromatogr. A.* 1123 (2006) 1–9.
- [164] T. Otake, J. Yoshinaga, Y. Yanagisawa, Analysis of organic esters of plasticizer in indoor air by GC–MS and GC–FPD, *Environ. Sci. Technol.* 35 (2001) 3099–3102.
- [165] H. Singh, B. Millier, W. Aue, Time-integrated spectra from a flame photometric detector, *J. Chromatogr. A.* 724 (1996) 255–264.

- [166] V.P. Campos, A.S. Oliveira, L.P. Cruz, J. Borges, T.M. Tavares, Optimization of parameters of sampling and determination of reduced sulfur compounds using cryogenic capture and gas chromatography in tropical urban atmosphere, *Microchem. J.* 96 (2010) 283–289.
- [167] C.T. Yue, S.Y. Li, H. Song, Simulation experiments on the generation of organic sulfide in the Shengli crude oil, *Geochem. Int.* 53 (2015) 1052–1063.
- [168] N. Jantaraksa, P. Prasassarakich, P. Reubroycharoen, N. Hinchiranan, Cleaner alternative liquid fuels derived from the hydrodesulfurization of waste tire pyrolysis oil, *Energy Convers. Manage.* 95 (2015) 424–434.
- [169] M.M. Rahman, J.-H. Choi, A.A. El-Aty, M.D. Abid, J.-H. Park, T.W. Na, Y.-D. Kim, J.-H. Shim, Pepper leaf matrix as a promising analyte protectant prior to the analysis of thermolabile terbufos and its metabolites in pepper using GC-FPD, *Food Chem.* 133 (2012) 604–610.
- [170] D.-Q. Ye, X.-T. Zheng, X.-Q. Xu, Y.-H. Wang, C.-Q. Duan, Y.-L. Liu, Evolutions of volatile sulfur compounds of Cabernet Sauvignon wines during aging in different oak barrels, *Food Chem.* 202 (2016) 236–246.
- [171] R. Yu, Q. Liu, J. Liu, Q. Wang, Y. Wang, Concentrations of organophosphorus pesticides in fresh vegetables and related human health risk assessment in Changchun, Northeast China, *Food Control* 60 (2016) 353–360.
- [172] W. Naksen, T. Prapamontol, A. Mangklabruks, S. Chantara, P. Thavornnyutikarn, M.G. Robson, P.B. Ryan, D.B. Barr, P. Panuwet, A single method for detecting 11 organophosphate pesticides in human plasma and breastmilk using GC-FPD, *J. Chromatogr. B.* 1025 (2016) 92–104.
- [173] Q. Liu, W. Kong, F. Qiu, J. Wei, S. Yang, Y. Zheng, M. Yang, One-step extraction for gas chromatography with flame photometric detection of 18 organophosphorus pesticides in Chinese medicine health wines, *J. Chromatogr. B.* 885–886 (2012) 90–96.
- [174] J.P. Cao, Z.M. Zong, X.Y. Zhao, M. Zhou, X.X. Ma, G.J. Zhou, P. Wu, W. Zhao, B.M. Li, X.Y. Wei, Identification of octathiocane, organonitrogens, and organosulfurs in Tongchuan shale, *Energy Fuels* 21 (2007) 1193–1194.
- [175] P. Korytár, H.-G. Janssen, E. Matisová, U.A.T. Brinkman, Practical fast gas chromatography: methods, instrumentation and applications, *TrAC Trends Anal. Chem.* 21 (2002) 558–572.
- [176] X. Liu, D. Li, J. Li, G. Rose, P.J. Marriott, Organophosphorus pesticide and ester analysis by using comprehensive two-dimensional gas chromatography with flame photometric detection, *J. Hazard. Mater.* 263, Part 2 (2013) 761–767.
- [177] X. Liu, B. Mitrevski, D. Li, J. Li, P.J. Marriott, Comprehensive two-dimensional gas chromatography with flame photometric detection applied to organophosphorus pesticides in food matrices, *Microchem. J.* 111 (2013) 25–31.
- [178] E. Engel, J. Ratel, P. Blinet, S.T. Chin, G. Rose, P.J. Marriott, Benchmarking of candidate detectors for multiresidue analysis of pesticides by comprehensive two-dimensional gas chromatography, *J. Chromatogr. A.* 1311 (2013) 140–148.
- [179] C. Kulsing, P. Rawson, R.L. Webster, D.J. Evans, P.J. Marriott, Group-type analysis of hydrocarbons and sulfur compounds in thermally stressed Merox jet fuel samples, *Energy Fuels* 31 (2017) 8978–8984.
- [180] B. Mitrevski, M.W. Amer, A.L. Chaffee, P.J. Marriott, Evaluation of comprehensive two-dimensional gas chromatography with flame photometric detection: Potential application for sulfur speciation in shale oil, *Anal. Chim. Acta.* 803 (2013) 174–180.
- [181] X. Yan, Detection by ozone-induced chemiluminescence in chromatography, *J. Chromatogr. A.* 842 (1999) 267–308.
- [182] X. Yan, Unique selective detectors for gas chromatography: Nitrogen and sulfur chemiluminescence detectors, *J. Sep. Sci.* 29 (2006) 1931–1945.

- [183] R.L. Shearer, E.B. Poole, J.B. Nowalk, Application of gas chromatography and flameless sulfur chemiluminescence detection to the analysis of petroleum products, *J. Chromatogr. Sci.* 31 (1993) 82–87.
- [184] S. Pandey, K.-H. Kim, A Review of Methods for the Determination of Reduced Sulfur Compounds (RSCs) in Air, *Environ. Sci. Technol.* 43 (2009) 3020–3029.
- [185] J.K. Nelson, R.H. Getty, J.W. Birks, Fluorine induced chemiluminescence detector for reduced sulfur compounds, *Anal. Chem.* 55 (1983) 1767–1770.
- [186] R.J. Glinski, E.A. Mishalanie, J.W. Birks, Molecular emission spectra in the visible and near IR produced in the chemiluminescent reactions of molecular fluorine with organosulfur compounds, *J. Photochem.* 37 (1987) 217–231.
- [187] A.J. Hills, D.H. Lenschow, J.W. Birks, Dimethyl Sulfide Measurement by Fluorine-Induced Chemiluminescence, *Anal. Chem.* 70 (1998) 1735–742.
- [188] R.L. Benner, D.H. Stedman, Universal sulfur detection by chemiluminescence, *Anal. Chem.* 61 (1989) 1268–1271.
- [189] R.L. Shearer, Development of flameless sulfur chemiluminescence detection: application to gas chromatography, *Anal. Chem.* 64 (1992) 2192–2196.
- [190] T.B. Ryerson, R.M. Barkley, R.E. Sievers, Selective chemiluminescence detection of sulfur-containing compounds coupled with nitrogen—phosphorus detection for gas chromatography, *J. Chromatogr. A* 670 (1994) 117–126.
- [191] R. Gras, J. Luong, R. Mustacich, R. Shearer, DP-SCD and LTMGC for determination of low sulfur levels in hydrocarbons, *J. ASTM Int.* 2 (2005) 1–15.
- [192] M.A.H. Khan, M.E. Whelan, R.C. Rhew, Analysis of low concentration reduced sulfur compounds (RSCs) in air: Storage issues and measurement by gas chromatography with sulfur chemiluminescence detection, *Talanta* 88 (2012) 581–586.
- [193] H.R. Martin, R.J. Glinski, Chemiluminescence from sulfur compounds in novel flame and discharge systems: proof of sulfur dioxide as the emitter in the new sulfur chemiluminescence detector, *Appl. Spectrosc.* 46 (1992) 948–952.
- [194] S.A. Nyarady, R.M. Barkley, R.E. Sievers, Redox chemiluminescence detector: application to gas chromatography, *Anal. Chem.* 57 (1985) 2074–2079.
- [195] H.P. Tuan, H.-G.M. Janssen, C.A. Cramers, E.M. Kuiper-van Loo, H. Vlap, Evaluation of the performance of various universal and selective detectors for sulfur determination in natural gas, *J. High Resol. Chromatogr.* 18 (1995) 333–342.
- [196] R. Gras, J. Luong, R. Shearer, A unified approach for the measurement of individual or total volatile organic sulfur compounds in hydrocarbon matrices by dual-plasma chemiluminescence detector and low thermal mass gas chromatography, *J. Chromatogr. Sci.* 45 (2007) 671–676.
- [197] D. Singh, A. Chopra, P.K. Mahendra, V. Kagdiyal, D. Saxena, Sulfur compounds in the fuel range fractions from different crude oils, *Petr. Sci. Technol.* 34 (2016) 1248–1254.
- [198] S. Tsuge, H. Yokoi, Y. Ishida, H. Ohtani, M.A. Becker, Photodegradative changes in chemical structures of silk studied by pyrolysis–gas chromatography with sulfur chemiluminescence detection, *Polym. Degrad. Stab.* 69 (2000) 223–227.
- [199] N. Ochiai, K. Sasamoto, K. MacNamara, Characterization of sulfur compounds in whisky by full evaporation dynamic headspace and selectable one-dimensional/two-dimensional retention time locked gas chromatography-mass spectrometry with simultaneous element-specific detection, *J. Chromatogr. A* 1270 (2012) 296–304.
- [200] D. Rauhut, H. Kürbel, K. MacNamara, M. Grossmann, Headspace GC-SCD monitoring of low volatile sulfur compounds during fermentation and in wine, *Analisis* 26 (1998) 142–145.

- [201] M. Burmeister, C. Drummond, E. Pfisterer, D. Hysert, Y. Sin, K. Sime, D. Hawthorne, Measurement of volatile sulfur compounds in beer using gas chromatography with a sulfur chemiluminescence detector, *J. Am. Soc. Brew. Chem.* 50 (1992) 53–58.
- [202] J. Steely, K. Zeller, Molasses Flavor Investigations with Sulfur chemiluminescence detection, in: T.H. Parliament, M.J. Morello and R.J. McGorin (Eds.), *Thermally Generated Flavours: Maillard, Microwave, and Extrusion Processes*, ACS Symp. Ser. Am. Chem. Soc. 543 (1994) 80–94.
- [203] B. Wang, E.C. Sivret, G. Parcsi, R.M. Stuetz, Determination of VOSCs in sewer headspace air using TD-GC-SCD, *Talanta* 137 (2015) 71–79.
- [204] J. Sun, S. Hu, K.R. Sharma, B. Keller-Lehmann, Z. Yuan, An efficient method for measuring dissolved VOSCs in wastewater using GC-SCD with static headspace technique, *Water Res.* 52 (2014) 208–217.
- [205] H.E. Toraman, T. Dijkmans, M.R. Djokic, K.M. Van Geem, G.B. Marin, Detailed compositional characterization of plastic waste pyrolysis oil by comprehensive two-dimensional gas-chromatography coupled to multiple detectors, *J. Chromatogr. A.* 1359 (2014) 237–246.
- [206] R. Hua, Y. Li, W. Liu, J. Zheng, H. Wei, J. Wang, X. Lu, H. Kong, G. Xu, Determination of sulfur-containing compounds in diesel oils by comprehensive two-dimensional gas chromatography with a sulfur chemiluminescence detector, *J. Chromatogr. A.* 1019 (2003) 101–109.
- [207] V.V. Lobodin, W.K. Robbins, J. Lu, R.P. Rodgers, Separation and characterization of reactive and non-reactive sulfur in petroleum and its fractions, *Energy Fuels* 29 (2015) 6177–6186.
- [208] C.E. West, A.G. Scarlett, A. Tonkin, D. O'Carroll-Fitzpatrick, J. Pureveen, E. Tegelaar, R. Gieleciak, D. Hager, K. Petersen, K.-E. Tollefsen, Diaromatic sulphur-containing 'naphthenic' acids in process waters, *Water Res.* 51 (2014) 206–215.
- [209] M. Navas, A. Jiménez, Chemiluminescent methods in petroleum products analysis, *Crit. Rev. Anal. Chem.* 30 (2000) 153–162.
- [210] K.E. Edwards, K. Qian, F.C. Wang, M. Siskin, Quantitative analysis of conjugated dienes in hydrocarbon feeds and products, *Energy Fuels* 19 (2005) 2034–2040.
- [211] B.A. Tomkins, W.H. Griest, C.E. Higgins, Determination of N-nitrosodimethylamine at part-per-trillion levels in drinking waters and contaminated groundwaters, *Anal. Chem.* 67 (1995) 4387–4395.
- [212] E.M. Fujinari, Pungent flavor profiles and components of spices by chromatography and chemiluminescent nitrogen detection, in: S.J. Risch and C.-T. Ho (Eds.), *Spices*, ACS Publications. Washington, DC, 1997, pp. 98–112.
- [213] C.R. Bowerbank, P.A. Smith, D.D. Fetterolf, M.L. Lee, Solvating gas chromatography with chemiluminescence detection of nitroglycerine and other explosives, *J. Chromatogr. A.* 902 (2000) 413–419.
- [214] F. Adam, F. Bertoncini, C. Dartiguelongue, K. Marchand, D. Thiébaud, M.C. Hennion, Comprehensive two-dimensional gas chromatography for basic and neutral nitrogen speciation in middle distillates, *Fuel* 88 (2009) 938–946.
- [215] M.Z. Ozel, F. Gogus, S. Yagci, J.F. Hamilton, A.C. Lewis, Determination of volatile nitrosamines in various meat products using comprehensive gas chromatography–nitrogen chemiluminescence detection, *Food Chem. Toxicol.* 48 (2010) 3268–3273.
- [216] Y. Weijun, Direct determination of acrylamide in food by gas chromatography with nitrogen chemiluminescence detection, *J. Sep. Sci.* 38 (2015) 2272–2277.
- [217] M.Z. Özel, J.F. Hamilton, A.C. Lewis, New sensitive and quantitative analysis method for organic nitrogen compounds in urban aerosol samples, *Environ. Sci. Technol.* 45 (2011) 1497–1505.

- [218] T. Dijkmans, M.R. Djokic, K.M. Van Geem, G.B. Marin, Comprehensive compositional analysis of sulfur and nitrogen containing compounds in shale oil using GC× GC–FID/SCD/NCD/TOF-MS, *Fuel* 140 (2015) 398–406.
- [219] K. Cai, Z. Xiang, J. Zhang, S. Zhou, Y. Feng, Z. Geng, Determination of eight tobacco alkaloids in flue-cured tobacco samples by gas chromatography with nitrogen chemiluminescence detection (NCD), *Anal. Methods* 4 (2012) 2095–2100.
- [220] N. Ramírez, L. Vallecillos, A.C. Lewis, F. Borrull, R.M. Marcé, J.F. Hamilton, Comparative study of comprehensive gas chromatography-nitrogen chemiluminescence detection and gas chromatography-ion trap-tandem mass spectrometry for determining nicotine and carcinogen organic nitrogen compounds in thirdhand tobacco smoke, *J. Chromatogr. A* 1426 (2015) 191–200.
- [221] B. Stuart, Experimental Methods, in: *Infrared Spectroscopy: Fundamentals and applications*, John Wiley & Sons Ltd. West Sussex, 2004, pp. 15–44.
- [222] V.A. Basiuk, R. Navarro-González, Identification of hexahydroimidazo[1,2-a]pyrazine-3,6-diones and hexahydroimidazo[1,2-a]imidazo[1,2-d]pyrazine-3,8-diones, unusual products of silica-catalyzed amino acid thermal condensation and products of their thermal decomposition using coupled high-performance liquid chromatography–particle beam mass spectrometry and gas chromatography–Fourier transform infrared spectroscopy–mass spectrometry, *J. Chromatogr. A* 776 (1997) 255–273.
- [223] V.A. Basiuk, R. Navarro-González, E.V. Basiuk, Pyrolysis of alanine and α -aminoisobutyric acid: identification of less-volatile products using gas chromatography/Fourier transform infrared spectroscopy/mass spectrometry, *J. Anal. Appl. Pyrolysis* 45 (1998) 89–102.
- [224] M.F. Atitar, H. Belhadj, R. Dillert, D.W. Bahnemann, The relevance of ATR-FTIR spectroscopy in semiconductor photocatalysis, in: M.L. Larramendy, S. Soloneski (Eds.) *Emerging Pollutants in the Environment: Current and Further Implications*, InTech, Rijeka, Croatia, 2015, pp. 201–227.
- [225] A.C. Scott, R.F. Young, P.M. Fedorak, Comparison of GC–MS and FTIR methods for quantifying naphthenic acids in water samples, *Chemosphere* 73 (2008) 1258–1264.
- [226] Y.-Q. Li, D.-X. Kong, H. Wu, Analysis and evaluation of essential oil components of cinnamon barks using GC–MS and FTIR spectroscopy, *Ind. Crops. Prod.* 41 (2013) 269–278.
- [227] U.P. Fringeli, ATR and Reflectance IR Spectroscopy, Applications, in: J.C. Lindon (Ed.), *Encyclopedia of Spectroscopy and Spectrometry*, second ed., Academic Press. Oxford, 1999, pp. 94–109.
- [228] R.A. Spragg, IR spectroscopy sample preparation methods, in: J.C. Lindon (Ed.), *Encyclopedia of Spectroscopy and Spectrometry*, second ed., Academic Press. Oxford, 1999, pp. 1210–1217.
- [229] J.-M. Ruysschaert, V. Raussens, ATR-FTIR analysis of amyloid proteins, in: B.L. Nilsson and T.M. Doran (Eds.), *Peptide Self-Assembly: Methods and Protocols*, Springer New York. New York, NY, 2018, pp. 69–81.
- [230] C. Lindenberg, J. Cornel, J. Schöll, M. Mazzotti, ATR-FTIR Spectroscopy, in: C. Lindenberg, J. Cornel, J. Schöll and M. Mazzotti (Eds.) *Industrial Crystallization Process Monitoring and Control*, Wiley-VCH Verlag GmbH & Co. KGaA, 2012, pp. 81–91.
- [231] P.R. Griffiths, IR spectroscopic data processing, in: J.C. Lindon, G.E. Tranter and D.W. Koppenaal (Eds.), *Encyclopedia of Spectroscopy and Spectrometry*, third ed., Academic Press. Oxford, 2017, pp. 428–436.

- [232] V.c.A. Lórenz-Fonfría, E. Padrós, Curve-fitting of Fourier manipulated spectra comprising apodization, smoothing, derivation and deconvolution, *Spectrochim. Acta, Part A*. 60 (2004) 2703–2710.
- [233] W.-J. Yang, P. Griffiths, Second derivative and Fourier self-deconvolution approaches to resolution enhancement of Fourier transform infrared (FTIR) spectra, *Proc. SPIE, Intl. Conf. on Fourier Transform Infrared Spectroscopy*, 1981.
- [234] B.C. Smith, *Fundamentals of Fourier Transform Infrared Spectroscopy*, second ed., CRC press, 2011.
- [235] B.H. Stuart, *Infrared Spectroscopy: Fundamentals and Applications*, John Wiley & Sons Ltd., West Sussex, 2005.
- [236] J. Seil, I. Köhler, C.W. v.d. Lieth, H.J. Opferkuch, Interpretation of infrared spectra based on statistical approaches, *Anal. Chim. Acta*. 188 (1986) 219–227.
- [237] G. Jalsovszky, *Chromatography-IR, Applications*, in: J.C. Lindon, G.E. Tranter and D.W. Koppenaal (Eds.), *Encyclopedia of Spectroscopy and Spectrometry*, third ed., Academic Press. Oxford, 2017, pp. 246–250.
- [238] P.R. Griffiths, D.A. Heaps, P.R. Brejna, The gas chromatography/infrared interface: past, present, and future, *Appl. Spectrosc.* 62 (2008) 259A–270A.
- [239] S. Gosav, R. Dinica, M. Praisler, Choosing between GC–FTIR and GC–MS spectra for an efficient intelligent identification of illicit amphetamines, *J. Mol. Struct.* 887 (2008) 269–278.
- [240] C. Cordella, I. Moussa, A.C. Martel, N. Sbirrazzouli, L. Lizzani-Cuvelier, Recent developments in food characterization and adulteration detection: Technique-oriented perspectives, *J. Agric. Food Chem.* 50 (2002) 1751–1764.
- [241] P.Q. Tranchida, L. Mondello, Detectors and basic data analysis, in: N. Snow (Ed.), *Basic Multidimensional Gas Chromatography*, Elsevier, 2020, pp. 205–227.
- [242] M.J.D. Low, Rapid infrared analysis of gas-chromatography peaks, *Chem. Commun.*, (1966) 371–372.
- [243] R.W. Crawford, T. Hirschfeld, R.H. Sanborn, C.M. Wong, Organic analysis with a combined capillary gas chromatograph/mass spectrometer/Fourier transform infrared spectrometer, *Anal. Chem.* 54 (1982) 817–820.
- [244] T. Hirschfeld, The hy-phen-ated methods, *Anal. Chem.* 52 (1980) 226–232.
- [245] T. Visser, FT-IR detection in gas chromatography, *TrAC Trends Anal. Chem.* 21 (2002) 627–636.
- [246] C.J. Wurrey, Applications of gas chromatography-Fourier transform IR spectrometry in environmental analyses, *TrAC Trends Anal. Chem.* 8 (1989) 52–58.
- [247] P.A. Wilks, R.A. Brown, Construction and performance of an infrared chromatographic fraction analyzer, *Anal. Chem.* 36 (1964) 1896–1899.
- [248] L.V. Azarraga, Construction and performance of an infrared chromatographic fraction analyzer, *Appl. Spectrosc.* 34 (1980) 224–225.
- [249] N. Ragunathan, K.A. Krock, C. Klawun, T.A. Sasaki, C.L. Wilkins, Multispectral detection for gas chromatography, *J. Chromatogr. A*. 703 (1995) 335–382.
- [250] M.M. Mossoba, R.A. Niemann, J.Y.T. Chen, Picogram level quantitation of 2,3,7,8-tetrachlorodibenzo-p-dioxin in fish extracts by capillary gas chromatography/matrix isolation/Fourier transform infrared spectrometry, *Anal. Chem.* 61 (1989) 1678–1685.
- [251] E. Sémon, S. Ferary, J. Auger, J.L. Le Quéré, Gas chromatography-Fourier transform infrared spectrometry of fatty acids: New applications with a direct deposition interface, *J. Am. Oil Chem. Soc.* 75 (1998) 101–105.

- [252] R.S. Brown, C.L. Wilkins, Cryogenically cooled interface for gas chromatography Fourier-transform infrared spectrometry, *Anal. Chem.* 60 (1988) 1483–1488.
- [253] P. Garg, A. Purohit, V.K. Tak, D. Dubey, Enhanced detectability of fluorinated derivatives of N, N-dialkylamino alcohols and precursors of nitrogen mustards by gas chromatography coupled to Fourier transform infrared spectroscopy analysis for verification of chemical weapons convention, *J. Chromatogr. A* 1216 (2009) 7906–7914.
- [254] S.D. Richardson, A.D. Thruston, T.V. Caughran, P.H. Chen, T.W. Collette, T.L. Floyd, K.M. Schenck, B.W. Lykins, G.-r. Sun, G. Majetich, Identification of new ozone disinfection byproducts in drinking water, *Environ. Sci. Technol.* 33 (1999) 3368–3377.
- [255] R. Bhargava, I.W. Levin, Gram-Schmidt orthogonalization for rapid reconstructions of Fourier transform infrared spectroscopic imaging data, *Appl. Spectrosc.* 58 (2004) 995–1000.
- [256] R.L. White, Chromatography-IR, methods and instrumentation, in: G.E. Tranter and D.W. Koppenaal (Eds.), *Encyclopedia of Spectroscopy and Spectrometry*, Academic Press. Oxford, 2017, pp. 251–255.
- [257] K. Sharma, S.P. Sharma, S. Lahiri, Novel method for identification and quantification of methanol and ethanol in alcoholic beverages by gas chromatography-Fourier transform infrared spectroscopy and horizontal attenuated total reflectance-Fourier transform infrared spectroscopy, *J. AOAC Int.* 92 (2009) 518–526.
- [258] L. Zhao, D. Zhai, H. Zheng, J. Ji, L. Wang, S. Li, Q. Yang, C. Xu, Molecular modeling for petroleum-related applications, in: C. Xu and Q. Shi (Eds.), *Structure and Modeling of Complex Petroleum Mixtures*, Springer International Publishing. Cham, 2016, pp. 121–177.
- [259] A. Andrzejewska, L. Lapinski, I. Reva, R. Fausto, Matrix isolation FTIR and molecular orbital study of E and Z acetaldoxime monomers, *Phys. Chem. Chem. Phys.* 4 (2002) 3289–3296.
- [260] J.S. Zavahir, Y. Nolvachai, B.R. Wood, P.J. Marriott, Gas chromatography-Fourier transform infrared spectroscopy reveals dynamic molecular interconversion of oximes, *Analyst* 144 (2019) 4803–4812.
- [261] T.A. Sasaki, C.L. Wilkins, Gas chromatography with Fourier transform infrared and mass spectral detection, *J. Chromatogr. A* 842 (1999) 341–349.
- [262] A. Carlsson, S. Lindberg, X. Wu, S. Dunne, M. Josefsson, C. Åstot, J. Dahlén, Prediction of designer drugs: synthesis and spectroscopic analysis of synthetic cannabinoid analogues of 1H-indol-3-yl(2,2,3,3-tetramethylcyclopropyl)methanone and 1H-indol-3-yl(adamantan-1-yl)methanone, *Drug Test. Anal.* 8 (2016) 1015–1029.
- [263] B. Mile, Chemistry in court, *Chromatographia* 62 (2005) 3–9.
- [264] T.M.G. Salerno, P. Donato, G. Frison, L. Zamengo, L. Mondello, Gas chromatography—Fourier transform infrared spectroscopy for unambiguous determination of illicit drugs: A proof of concept, *Front. Chem.* 8 (2020).
- [265] J. Cai, P. Lin, X.L. Zhu, Q. Su, Comparative analysis of clary sage (*S. sclarea* L.) oil volatiles by GC-FTIR and GC-MS, *Food Chem.* 99 (2006) 401–407.
- [266] J.A. Roach, M.M. Mossoba, M.P. Yurawecz, J.K. Kramer, Chromatographic separation and identification of conjugated linoleic acid isomers, *Anal. Chim. Acta.* 465 (2002) 207–226.
- [267] P.A. Rodriguez, C.L. Eddy, C. Marcott, M.L. Fey, J.M. Anast, Combined two-dimensional GC/MS/matrix isolation FT-IR with a versatile sample introduction system, *J. Microcolumn Sep.* 3 (1991) 289–301.
- [268] C.L. Wilkins, Multidimensional GC for qualitative IR and MS of mixtures, *Anal. Chem.* 66 (1994) 295A–301A.

- [269] T. Visser, Gas Chromatography/Fourier Transform Infrared Spectroscopy, in: P.R. Griffiths and J.M. Chalmers (Eds.), Handbook of Vibrational Spectroscopy, John Wiley & Sons, Ltd. Chichester, 2006, pp. 1605–1626.
- [270] J.S. Zavahir, J.S.P. Smith, S. Blundell, H.D. Waktola, Y. Nolvachai, B.R. Wood, P.J. Marriott, Relationships in Gas Chromatography—Fourier Transform Infrared Spectroscopy—Comprehensive and Multilinear Analysis, Separations 7 (2020) 27.
- [271] T. Visser, M.J. Vredenburg, A.P.J.M. de Jong, G.W. Somsen, T. Hankemeier, N.H. Velthorst, C. Gooijer, U.A.T. Brinkman, Improvements in environmental trace analysis by GC-IR and LC-IR, J. Mol. Struct. 408 (1997) 97–103.
- [272] T. Hankemeier, E. Hooijschuur, R.J.J. Vreuls, U.A.T. Brinkman, T. Visser, On-line solid phase extraction-gas chromatography-cryotrapping-infrared spectrometry for the trace-level determination of microcontaminants in aqueous samples, J. High Resol. Chromatogr. 21 (1998) 341–346.
- [273] R. Veness, C. Evans, Identification of monosaccharides and related compounds by gas chromatography-Fourier transform infrared spectroscopy of their trimethylsilyl ethers, J. Chromatogr. A. 721 (1996) 165–172.
- [274] P. Doumenq, M. Guiliano, G. Mille, GC/FTIR potential for structural analysis of marine origin complex mixtures, Int. J. Environ. Anal. Chem. 37 (1989) 235–244.
- [275] J.C. Young, D.E. Games, Analysis of Fusarium mycotoxins by gas chromatography-Fourier transform infrared spectroscopy, J. Chromatogr. A. 663 (1994) 211–218.
- [276] A. Machara, J. Křivánek, K. Dolejšová, J. Havlíčková, L. Bednářová, R. Hanus, P. Majer, P. Kyjaková, Identification and enantiodivergent synthesis of (5*z*,9*s*)-tetradec-5-en-9-olide, a queen-specific volatile of the termite *Silvestritermes minutus*, J. Nat. Prod. 81 (2018) 2266–2274.
- [277] D.M. Vidal, C.F. Fávaro, M.M. Guimarães, P.H.G. Zarbin, Identification and synthesis of the male-produced sex pheromone of the soldier beetle *Chauliognathus fallax* (Coleoptera: Cantharidae), J. Braz. Chem. Soc. 27 (2016) 1506–1511.
- [278] W. Schrader, J. Geiger, D. Klockow, E.-H. Korte, Degradation of α -pinene on Tenax during sample storage: effects of daylight radiation and temperature, Environ. Sci. Technol. 35 (2001) 2717–2720.
- [279] K. Łaniewski, T. Wännman, G. Hagman, Gas chromatography with mass spectrometric, atomic emission and Fourier transform infrared spectroscopic detection as complementary analytical techniques for the identification of unknown impurities in pharmaceutical analysis, J. Chromatogr. A. 985 (2003) 275–282.
- [280] T. Belal, T. Awad, J. DeRuiter, C.R. Clark, GC-IRD methods for the identification of isomeric ethoxyphenethylamines and methoxymethcathinones, Forensic Sci. Int. 184 (2009) 54–63.
- [281] K. Sharma, S. Sharma, S. Lahiri, Characterization and identification of petroleum hydrocarbons and biomarkers by GC-FTIR and GC-MS, Petr. Sci. Technol. 27 (2009) 1209–1226.
- [282] J. Guitton, M. Desage, S. Alamercury, L. Dutruch, S. Dautraix, J. Perdrix, J. Brazier, Gas chromatographic-mass spectrometry and gas chromatographic-Fourier transform infrared spectroscopy assay for the simultaneous identification of fentanyl metabolites, J. Chromatogr. B. 693 (1997) 59–70.
- [283] K.A. Krock, N. Ragunathan, C.L. Wilkins, Multidimensional gas chromatography coupled with infrared and mass spectrometry for analysis of Eucalyptus essential oils, Anal. Chem. 66 (1994) 425–430.
- [284] F.C.-Y. Wang, K.E. Edwards, Separation of C2-naphthalenes by gas chromatography \times Fourier transform infrared spectroscopy (GC \times FT-IR): Two-dimensional separation approach, Anal. Chem. 79 (2007) 106–112.

- [285] A.C. Olivieri, G.M. Escandar, Analytical figures of merit, in: A.C. Olivieri and G.M. Escandar (Eds.), *Practical Three-Way Calibration*, Elsevier, Boston, 2014, pp. 93–107.
- [286] S. Armenta, M. de la Guardia, Green chromatography for the analysis of foods of animal origin, *TrAC Trends Anal. Chem.* 80 (2016) 517–530.
- [287] O.Y. Al-Dirbashi, K. Nakashima, Hyphenated chromatographic methods for biomaterials, *Biomed. J. Chromatogr.* 2000, pp. 406–421.
- [288] I.D. Wilson, U.A.T. Brinkman, Hyphenation and hypernation: The practice and prospects of multiple hyphenation, *J. Chromatogr. A* 1000 (2003) 325–356.
- [289] M.J. Tomlinson, C.L. Wilkins, Evaluation of a semi-automated multidimensional gas chromatography-infrared-mass spectrometry system for irritant analysis, *J. High Resol. Chromatogr.* 21 (1998) 347–354.
- [290] R. Navarro-González, P. Coll, R. Aliev, Pyrolysis of γ -irradiated bisphenol-A polycarbonate, *Polym. Bull.* 48 (2002) 43–51.
- [291] K.A. Krock, N. Ragunathan, C. Klawun, T. Sasaki, C.L. Wilkins, Multidimensional gas chromatography-infrared spectrometry-mass spectrometry. Plenary lecture, *Analyst* 119 (1994) 483–489.
- [292] G. Gachot, S. Grugeon, I. Jimenez-Gordon, G.G. Eshetu, S. Boyanov, A. Lecocq, G. Marlair, S. Pilard, S. Laruelle, Gas chromatography/Fourier transform infrared/mass spectrometry coupling: a tool for Li-ion battery safety field investigation, *Anal. Methods* 6 (2014) 6120–6124.
- [293] J. Taira, A. Tsuchiya, H. Furudate, Initial Volatile Aroma Profiles of Young and Aged Awamori *Shochu* Determined by GC/MS/Pulsed FPD, *Food Sci. Technol. Res.* 18 (2012) 177–181.
- [294] L. L. P. Van Stee, P. E. G. Leonards, R. J. J. Vreuls, U. A. T. Brinkman, Identification of non-target compounds using gas chromatography with simultaneous atomic emission and mass spectrometric detection (GC-AED/MS): analysis of municipal wastewater, *Analyst* 124 (1999) 1547–1552.
- [295] L.L.P. van Stee, J. Beens, R.J.J. Vreuls, U.A.T. Brinkman, Comprehensive two-dimensional gas chromatography with atomic emission detection and correlation with mass spectrometric detection: principles and application in petrochemical analysis, *J. Chromatogr. A* 1019 (2003) 89–99.
- [296] R.A. Soldi, M.A.C.M. Rodrigues, J.R. Aldrich, P.H.G. Zarbin, The male-produced sex pheromone of the true bug, *Phthia picta*, is an unusual hydrocarbon, *J. Chem. Ecol.* 38 (2012) 814–824.
- [297] P.E.A. Teal, D. Jones, G. Jones, B. Torto, V. Nyasembe, C. Borgemeister, H.T. Alborn, F. Kaplan, D. Boucias, V.U. Lietze, Identification of methyl farnesoate from the hemolymph of insects, *J. Nat. Prod.* 77 (2014) 402–405.
- [298] E. Hedenström, F. Andersson, N. Sjöberg, T. Eltz, 6-(4-Methylpent-3-en-1-yl)naphthalene-1,4-dione, a behaviorally active semivolatile in tibial perfumes of orchid bees, *Chemoecology* 28 (2018) 131–135.
- [299] J. Kempe, C. Bellmann, D. Meyer, F. Windrich, GC-IR based two-dimensional structural group analysis of petroleum products, *Anal. Bioanal. Chem.* 382 (2005) 186–191.
- [300] A. Prashar, P. Hili, R.G. Veness, C.S. Evans, Antimicrobial action of palmarosa oil (*Cymbopogon martinii*) on *Saccharomyces cerevisiae*, *Phytochemistry* 63 (2003) 569–575.
- [301] D. Sciarrone, A. Schepis, G. De Grazia, A. Rotondo, F. Alibrando, R.R. Cipriano, H. Bizzo, C. Deschamps, L.M. Sidisky, L. Mondello, Collection and identification of an unknown component from: *Eugenia uniflora* essential oil exploiting a multidimensional preparative three-GC system employing apolar, mid-polar and ionic liquid stationary phases, *Faraday Discussions* 218 (2019) 101–114.

- [302] S.A. Emami, S. Afsharypuor, J. Asili, M. Sairafianpour, chemical composition of the essential oils from Iranian conifers. Part I: Aroma profiles of leaves and fruits of *Juniperus polycarpus* var. *polycarpus* (Cupressaceae), *J. Essent. Oil Res.* 22 (2010) 103–106.
- [303] X. Yang, Z. You, D. Perram, D. Hand, Z. Ahmed, W. Wei, S. Luo, Emission analysis of recycled tire rubber modified asphalt in hot and warm mix conditions, *J. Hazard. Mater.* 365 (2019) 942–951.
- [304] M. Praisler, J. Van Bocxlaer, A. De Leenheer, D.L. Massart, Chemometric detection of thermally degraded samples in the analysis of drugs of abuse with gas chromatography–Fourier-transform infrared spectroscopy, *J. Chromatogr. A* 962 (2002) 161–173.
- [305] M. Praisler, I. Dirinck, J.F. Van Bocxlaer, A.P. De Leenheer, D.L. Massart, Computer-Aided Screening for Hallucinogenic and Stimulant Amphetamines with Gas Chromatography–Fourier Transform Infrared Spectroscopy (GC-FTIR), *J. Anal. Toxicol.* 25 (2001) 45–56.
- [306] A. Carlsson, V. Sandgren, S. Svensson, P. Konradsson, S. Dunne, M. Josefsson, J. Dahlén, Prediction of designer drugs: Synthesis and spectroscopic analysis of synthetic cathinone analogs that may appear on the Swedish drug market, *Drug Test. Anal.* 10 (2018) 1076–1098.
- [307] S. Gosav, M. Praisler, J. Van Bocxlaer, A.P. De Leenheer, D.L. Massart, Class identity assignment for amphetamines using neural networks and GC–FTIR data, *Spectrochim. Acta, Part A* 64 (2006) 1110–1117.
- [308] M. Zhang, L. Chen, Continuous underway measurements of dimethyl sulfide in seawater by purge and trap gas chromatography coupled with pulsed flame photometric detection, *Mar. Chem.* 174 (2015) 67–72.
- [309] G.-B. Jiang, J.-Y. Liu, K.-W. Yang, Speciation analysis of butyltin compounds in Chinese seawater by capillary gas chromatography with flame photometric detection using in-situ hydride derivatization followed by headspace solid-phase microextraction, *Anal. Chim. Acta* 421 (2000) 67–74.

Chapter 2

Materials, methods and preliminary validation using an in-house designed hyphenated gas chromatography–Fourier transform infrared instrument

Contents

2.1	Introduction.....	70
2.2	Design of in-house built hyphenated system of gas chromatography with Fourier transform infrared spectroscopy for GC–FTIR analysis	72
2.2.1	Gas chromatograph.....	72
2.2.2	Mass spectrometer	76
2.2.3	Fourier transform infrared (FTIR) spectroscopy	76
2.2.4	PIKE light-pipe interface.....	77
2.3	Other instrumentation.....	80
2.3.1	GC–MS analysis	81
2.3.2	GC×GC–TOFMS analysis.....	81
2.3.3	GC–FPD analysis	81
2.3.4	ATR–FTIR analysis.....	81
2.3.5	FTICR MS analysis	82
2.4	Software.....	82
2.5	Standards and sample preparation.....	85
2.6	Comparison of FTIR settings	90

2.6.1	Comparison of scan speed	91
2.7	Daily performance validation analysis	95
2.8	Establishment of a user-defined in-house spectral library	97
2.9	Conclusions	102
	References	102

2.1 Introduction

Separation of volatile and semi volatile chemical components in complex mixtures can be successfully carried out using gas chromatography (GC). Here, retention time (RT), the time taken for an analyte to reach a detector after its injection, can be used in component identification when compared to the RT of a known standard. RT is not fixed for a chromatography column as it is influenced by various factors and RT information alone cannot support identification of all major and minor components. Therefore, structural elucidation of GC separated analytes is supported by various detector technologies, of which mass spectrometry (MS) is the most commonly applied technique. Its hyphenation to GC (GC–MS) has today become the most widely adopted approach for component detection.

The MS however is limited in its ability to give an accurate identification for reasons which include; (i) the inability to distinguish closely related isomers due to their similar mass spectra, (ii) identification being dependent on the presence of the mass spectrum in a library, and (iii) the result being based on the computer's ability to find a similar mass fragmentation match value based on usually a proprietary metric of m/z and intensity values [1]. Thus, in GC analysis, detectors which provide information on the intact molecule have greater discriminatory power than the knowledge gained using fragments created by MS. Various spectroscopic detectors have proved to be successful in this task as set out in Chapter 1. Of these, Fourier transform infrared (FTIR) spectroscopy, has established itself as a molecular spectroscopic detection technique which has the potential to identify molecules without ambiguity [2-3].

FTIR spectroscopy can benefit component identification through its information-rich FTIR spectra which complement the ability of GC–MS [4] and has therefore become one of the foremost spectroscopy techniques for problem solving and analysing chemical structures associated with a wide variety of matrices. It is universal and relatively inexpensive, fast and easy to operate compared to most other analytical techniques. With its many advances and developments, it has the potential to be utilised in many spheres such as in industry, research and fundamental studies.

The generation of an infrared spectrum – a profile of absorption characteristics plotted against the wavenumber – is generated when infrared radiation interacts with molecular moieties. The result is a distinctive and unique ‘fingerprint’ – the corner stone of FTIR based identification. The hyphenation of GC to FTIR, abbreviated as GC–FTIR, marries the separation power of GC and the identification power of FTIR. This main benefit of component identification can also be coupled to quantification. GC–FTIR has been established via a variety of instrumental designs in which the successful interfacing of the GC and FTIR play a pivotal role. This has been achieved through light-pipes (LP), direct-deposition systems (DD) and matrix-isolation (MI) systems as detailed in Chapter 1. Of these, the LP enables real-time spectroscopic detection of the GC eluates in a flow-through arrangement unlike its DD and MI counterparts. A majority of the studies conducted in this thesis have been based on this GC–FTIR hyphenation achieved through an in-house designed heated flow transfer system consisting of a light-pipe interface in which we devised the transfer of GC effluent from the oven to the light-pipe interface using a custom-built transfer line.

This Chapter explicates the various instrumentation, materials, methods and software used in carrying out the experimental sections of this Chapter and the two Chapters which follow in the thesis. Details of the in-house design and implementation of the hyphenated GC–FTIR system together with the preliminary validation studies conducted to confirm its suitability in further studies is also detailed. This Chapter also explores various FTIR parameters to choose the best setting for the tasks at hand. A brief daily performance validation of the system is also mentioned followed by details of establishing of a user-defined in-house library.

2.2 Design of in-house built hyphenated system of gas chromatography with Fourier transform infrared spectroscopy for GC–FTIR analysis

GC–FTIR experiments in this Chapter and the Chapters which follow were carried out using an in-house designed hyphenated system as detailed in Section 2.2.1. The experiments conducted in Chapters 2, 3 and 4 were conducted using this light-pipe GC–FTIR system with GC–MS and GC–FID capability as well as sequential GC–FTIR–FID ability as depicted in Figure 2.4. Two computers were required for control and parameter set-up of the system, one for GC–MS and GC–FID control and the other for GC–FTIR control. The details of the system are presented as follows.

2.2.1 Gas chromatograph

The GC used in this system is a PerkinElmer Clarus 600 (PerkinElmer Inc., Shelton, CT, USA). This is a dual-channel temperature programmable system with an 82 vial autosampler attached which is fitted with a 10 μ L syringe. The front and rear injection ports together allow more than one column to be installed for individual sample injection as depicted in Figure 2.1, to enable analysis using different columns to be conducted without the need of column change. The installation of two injectors – a capillary column injector (CAP) and temperature-programmed split/splitless injector (PSS) – enables injection to the columns connected to suit the need. The ability to install gas sampling valves enables pneumatic pressure control (PPC) in which the carrier gas and detector gases can be monitored and controlled to manage pneumatic functions in the GC.

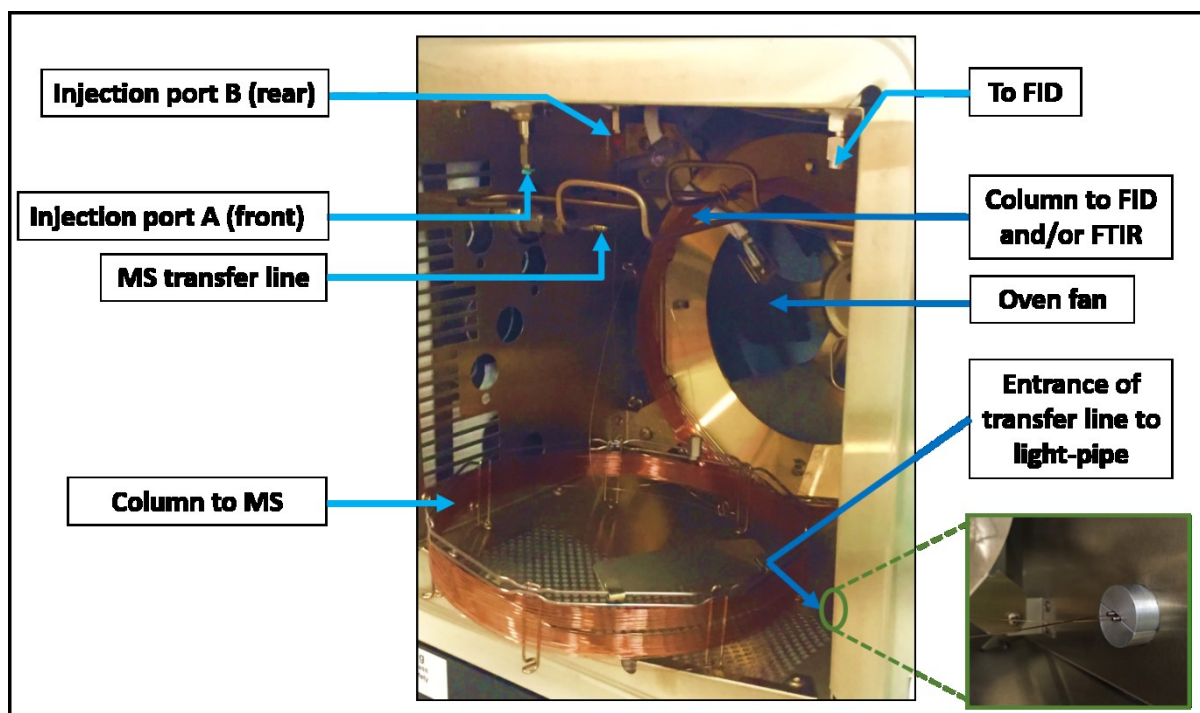


Figure 2.1. Interior of GC oven showing the setup of two columns, each connected to a separate injection port. The opening of the transfer line protruding into the oven is inset, showing the columns which connect to the light-pipe inlet and outlet.

The inbuilt FID of the GC facilitates simultaneous and sequential FID results benefitting the confirmation and validation studies of GC–FTIR analysis. Figure 2.2 depicts a representative diagram of the FID installed in the GC. The H_2 combustion gas and make up gas mix with the carrier gas from the GC column entering from the bottom. This is burned at the jet, with air which is added to establish a flame. Positively charged combustion product particles are accelerated towards the negatively biased collector electrode (-200–300 V) positioned above the flame. This is then electronically amplified and digitised where the current is directly proportional to the number of ions collected.

The inbuilt flame ionisation detector (FID) enables both pre- and post-light-pipe analysis. A dual-hole graphite ferrule as shown in Figure 2.2 is used in place of the single hole ferrule, using which, two restrictor columns are installed into the FID. This is done so that GC–FID (when the analytical column is connected to the FID directly) and GC–FTIR–FID (when the light-pipe outlet is connected to the FID) experiments can be alternated as needed by using universal Press-Tight connectors (Restec Corporation, Bellefonte, PA) to

connect to the column of need. This enables exchange of columns and changing the GC effluent path without the need of having to cool the FID or reinstall ferrules.

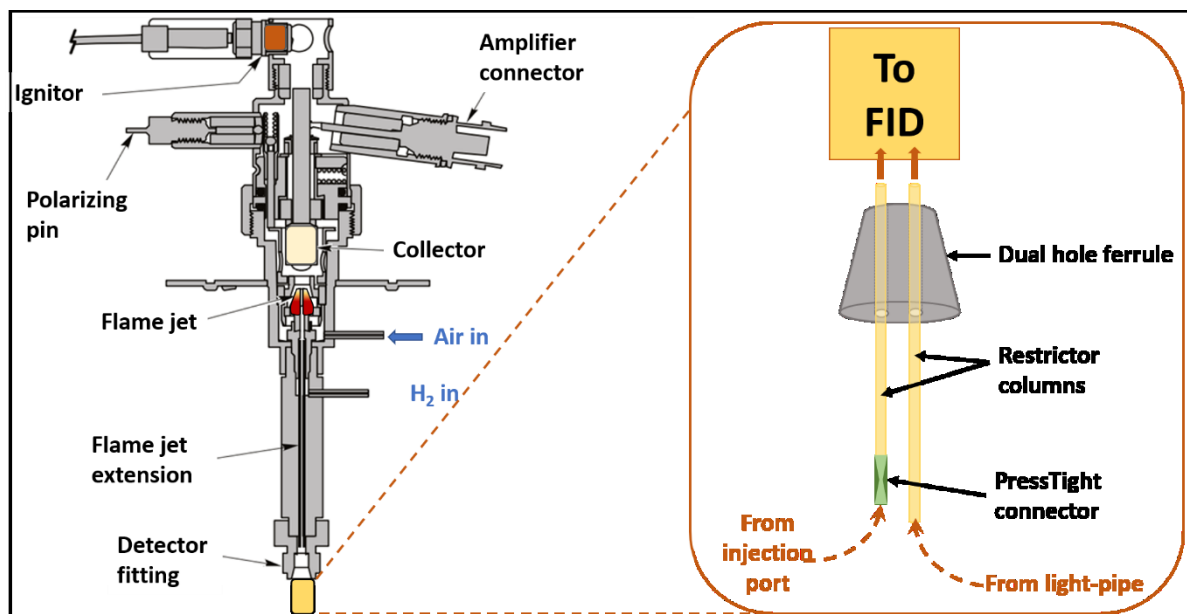


Figure 2.2. Schematic of FID installed in the system; the H₂ enters at the bottom of the jet with the GC effluent. Combustion products accelerate towards the collector electrode after which the signal is amplified. Inset, a schematic of double-hole ferrule enabling the use of the system in either the GC–FID or the GC–FTIR–FID configuration.

A range of columns were used for the various experiments as set out in Table 2.1.

Table 2.1 Names, dimensions and manufacturers of columns used

Column name	Specifications	Manufacturer	Experiment
BPX5	30 m × 0.25 mm I.D. × 0.25 µm d_f	SGE Trajan, Ringwood, Australia	GC–FTIR
Elite-5MS	30 m × 0.25 mm I.D. × 0.25 µm d_f	PerkinElmer, Shelton, CT, USA	GC–MS
DB-5 MS	30 m × 0.25 mm I.D. × 0.25 µm d_f	Agilent Technologies Mulgrave, Australia	GC–FTIR
HP-Innowax	30 m × 0.32 mm I.D. × 0.5 µm d_f	Agilent Technologies Mulgrave, Australia	GC–FTIR oxime analysis
	30 m × 0.25 mm I.D. × 0.25 µm d_f	SGE Trajan, Ringwood, Australia	¹ D column in GC×GC for jet fuel analysis
BPX5 column	1 m × 0.1 mm I.D. × 0.1 µm d_f	SGE Trajan, Ringwood, Australia	² D column in GC×GC for jet fuel analysis
Deactivated fused silica (DFS) transfer line column	0.5–1.0 m × 0.25 mm I.D.	Agilent Technologies Mulgrave, Australia	Light-pipe inlet and outlet connections

2.2.2 Mass spectrometer

The system used in this study also consists of a Clarus SQ 8 quadrupole mass spectrometer (MS) (PerkinElmer Inc., Waltham, MA, USA) attached to the left-hand side panel of the GC. This MS carries out electron ionisation (EI) with a 650:1 signal-to-noise ratio with a turbomolecular pump capacity of 75 L/sec. The posterior end of the capillary column connected to the GC injection port delivers effluent to the MS via a heated transfer line (TL). The TL is generally maintained at 250 °C.

Before use, the GC–MS system is checked for air leaks. Here it is ensured that the mass 4 (helium) is larger than mass 18 (water), which should be larger than mass 28 (nitrogen), which in turn should be approximately 4 times larger than the mass 32 (oxygen). The tuning of masses 69, 131, 219 and 502 using the custom tune option for the EI ion source and the Heptacosyl (also called FC-43, PTA, PFTBA and perfluorotributylamine) standard solution was carried out on a regular basis.

2.2.3 Fourier transform infrared (FTIR) spectroscopy

The GC connects to a Frontier™ Fourier transform infrared (FTIR) spectrometer (PerkinElmer Inc., Bucks, UK) via a light-pipe interface. This was achieved by drilling of the right-hand side panel of the GC and directly connecting the interface to the GC using a heated and insulated TL. Mid infrared radiation is emitted through the source which enters the PIKE light-pipe interface accessory for detection of GC effluent components. The TimeBase software (details in Section 2.3) which enables the trigger mechanism and time-resolved IR data collection, is used to choose FTIR data collection parameters. Of these, the most commonly used FTIR settings for the experiments in this thesis are 100 background scans, weak apodisation function, an optical resolution of 4 cm⁻¹ or 8 cm⁻¹, scan speed of 1 cm s⁻¹, ‘self’ phase correction and a wavenumber range of 4000–700 cm⁻¹ to suit the inbuilt mercury cadmium telluride (MCT) detector’s capability.

2.2.4 PIKE light-pipe interface

The light-pipe interface accessory (PIKE Technologies, Madison, WI, USA) is positioned between the GC and FTIR and contains a collection of mirrors, a mercury cadmium telluride (MCT) detector and a light-pipe (LP). This ensures the sample effluent from the end of the GC column is diverted into the LP where it interacts with the IR beam and is redirected to the GC oven (shown in Figure 2.4 inset) through a temperature-controlled and glass-lined stainless-steel TL.

The most important component of these, the LP, is a 120 mm × 1 mm internal diameter glass tube with a LP volume of 78.5 µL, which acts as a gas cell through which the GC effluent flows. It is gold-coated internally to maximise the reflections of the IR beam and thus maximise sensitivity. A 13 mm × 2 mm diameter KBr window acts as the IR transparent window at with end. The temperature of the LP plays a pivotal role in the signal-to-noise ratio (SNR) of the FTIR spectrum [5, 8]. This is achieved using the temperature controls for the LP and TL at the rear of the instrument which is settable up to 300 °C +/- 1.0 °C. The LP is insulated to minimise incidental heating of the FTIR spectrometer. It is advised to increase the temperature in increments of 50 °C to prevent damage to the glass LP. The LP and TL temperatures are maintained above the maximum temperature of the GC oven program to prevent condensation of GC eluents within the LP. Detection is achieved using a liquid nitrogen cooled mercury-cadmium-telluride (MCT) detector. Figure 2.3 depicts a schematic of this interface.

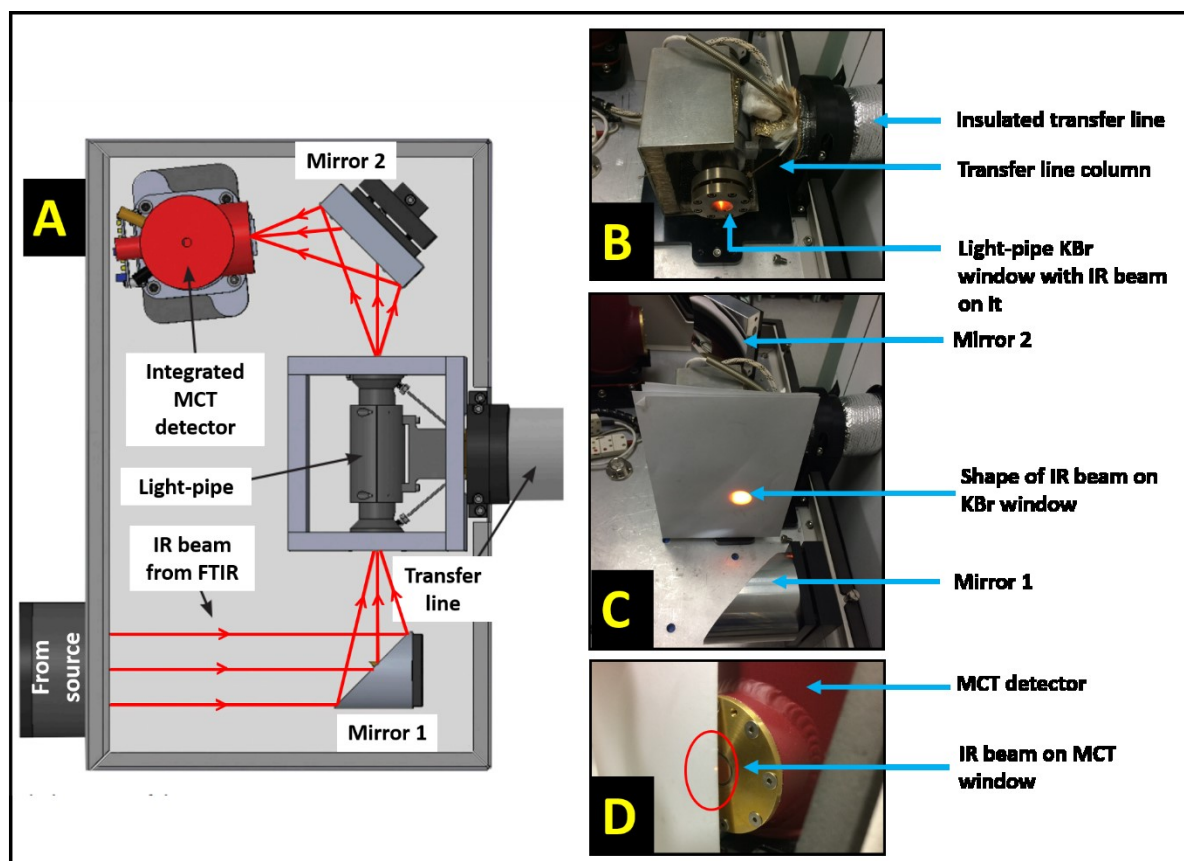


Figure 2.3. Schematic of the PIKE light-pipe interface accessory (A) with a view of the IR beam impinging on the light-pipe window (B), the technique used to focus the IR beam on the light-pipe holder (C), and a view of the IR beam when focused on the centre of the MCT detector window.

The PIKE interface accessory's two concave mirrors can be adjusted to ensure that the IR beam emitted by the spectrophotometer reaches the MCT detector. Here, the modulated IR beam which is collimated through the interferometer's external port is focused on the IR-transparent window at the entrance of the LP by adjustment of the first mirror (Figure 2.3 B and C). Adjusting the second mirror helps in focusing the IR beam exiting the LP (which contains the information of absorbing material in the LP) onto the centre of the MCT detector (Figure 2.3 D). This ensures a maximum sensitivity when recording the IR spectrum. A background scan is collected before collecting time-resolved data, the latter of which is ratioed against the background spectrum.

In the completely assembled hyphenated GC–FTIR system, both inlet and outlet TL columns are housed within the TL. In some previous models the TL was significantly longer and exited the GC from one of the top compartments, sometimes presented as a

‘snorkel’ over the GC, as opposed to the direct 20 cm path length achieved here using the custom-built TL. The TL connection between the GC and light-pipe interface was achieved by drilling a suitably sized hole on the right-hand side panel of the GC thus allowing the TL to pass unobstructed. Inlet and outlet TL capillary columns were contained within stainless steel tubes enclosed within the heated and insulated TL. This enabled a direct connection of the posterior end of the GC column to the inlet of the heated LP. Maintaining the TL and LP temperatures at a minimum of 10 °C higher than the maximum temperature of the GC oven program precludes condensation of semi-volatile components present in the GC effluent. The GC and the FTIR interface accessory are integrated through an external trigger box which facilitates the starting and stopping of the FTIR signal collection to align with the GC sample injection. Figure 2.4 illustrates the completely assembled instrument together with a schematic of the system.

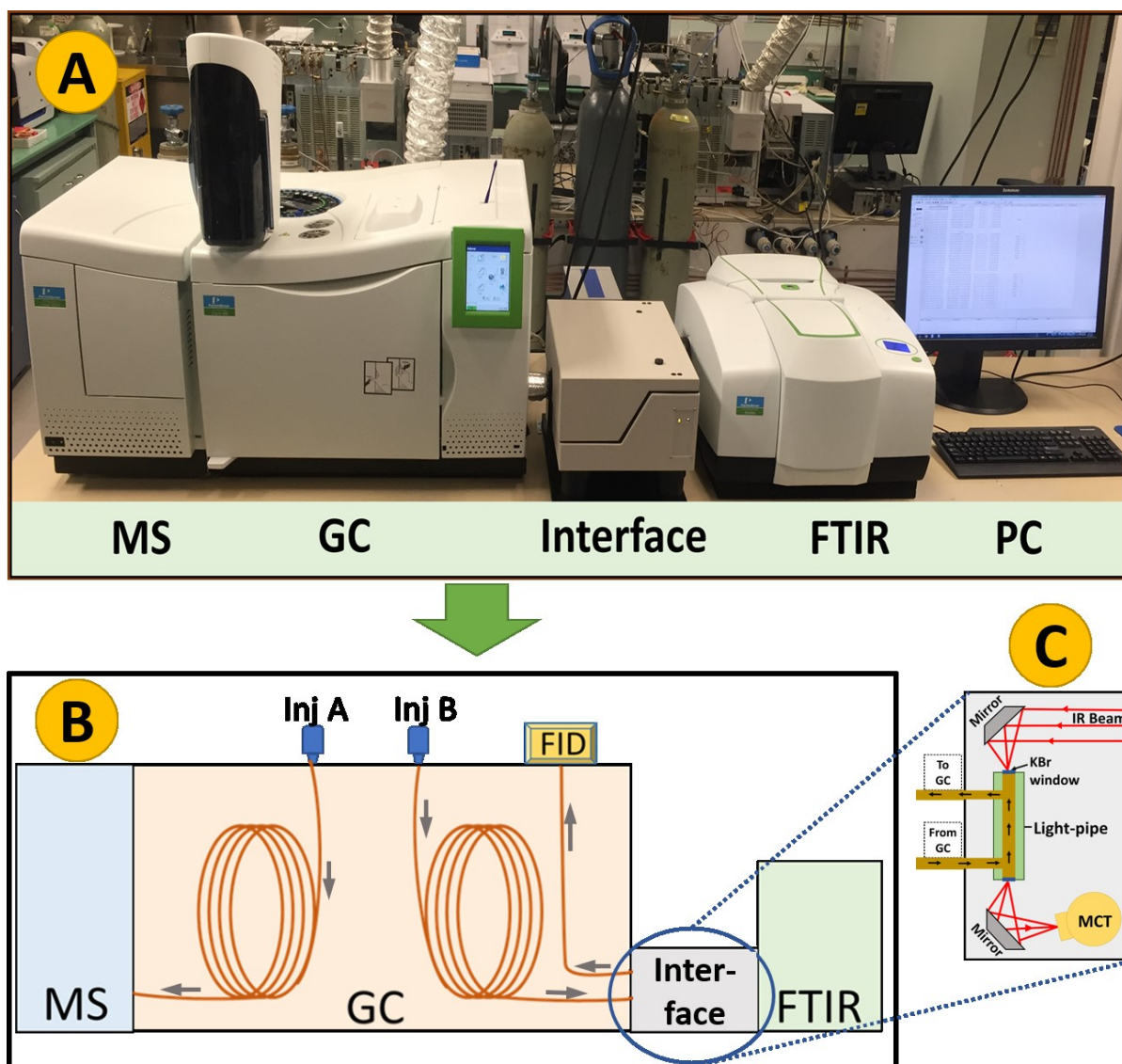


Figure 2.4. Complete assembled hyphenated instrument unit enabling GC–MS and GC–FTIR analysis (A) with a schematic of the unit depicted in (B). The GC is hyphenated with the FTIR via the PIKE interface accessory which is inset in (C) to illustrate the effluent flow and interaction with the IR beam within the light pipe. The GC effluent flows into the light-pipe via the heated and insulated transfer line between the GC and the interface.

2.3 Other instrumentation

A selection of additional laboratory instruments was used in Chapter 5 for the various analyses approaches in the study of biofuels, and are outlined as follows.

2.3.1 GC–MS analysis

One dimensional GC–MS of biofuels in Chapter 5 was carried out using an Agilent 7890A GC with a model 7000 triple quadrupole mass spectrometer (Agilent Technologies, Santa Clara, CA). Separation was achieved with a DB-5 MS column (30 m × 0.25 mm I.D. × 0.25 µm d_f) from Agilent Technologies Mulgrave, Australia.

2.3.2 GC×GC–TOFMS analysis

An Agilent 7890A GC (Agilent Technologies, Mulgrave, Australia) hyphenated to a Model 7200 accurate mass quadrupole time-of-flight mass spectrometer (accTOFMS; Agilent Technologies, Santa Clara, CA) was used for GC×GC–TOFMS experiments of aviation fuel samples as laid out in Chapter 5. A polar/nonpolar column arrangement was used for separation with a SolGel-WAX (SGE Trajan Scientific, Ringwood, Australia) column in the first dimension (¹D; 30 m × 0.25 mm I.D. × 0.25 µm d_f) and BPX5 column (SGE Trajan Scientific, Ringwood, Australia) in the second dimension (²D; 1 m × 0.1 mm I.D. × 0.1 µm d_f) connected by a deactivated Press-Tight connector (Restec Corporation, Bellefonte, PA). An Everest model longitudinally modulated cryogenic system (LMCS; Chromatography Concepts, Doncaster, Australia) was used as the system's modulator with carbon dioxide as the cryogen coolant.

2.3.3 GC–FPD analysis

For sulfur compound analysis an Agilent 7890A GC system fitted with a flame photometric detector (FPD) was used. Separation in the 1DGC–FPD system was achieved with a Supelcowax-10 column (

2.3.4 ATR–FTIR analysis

For aviation fuel analysis the ATR–FTIR spectra were collected using a Bruker Equinox 55 fitted with an MCT detector and single bounce diamond crystal as the internal

reflection element (Bruker Optik, Ettlingen Germany) The fuel sample to be analysed was placed on the platform bearing the crystal as depicted in Figure 2.5.

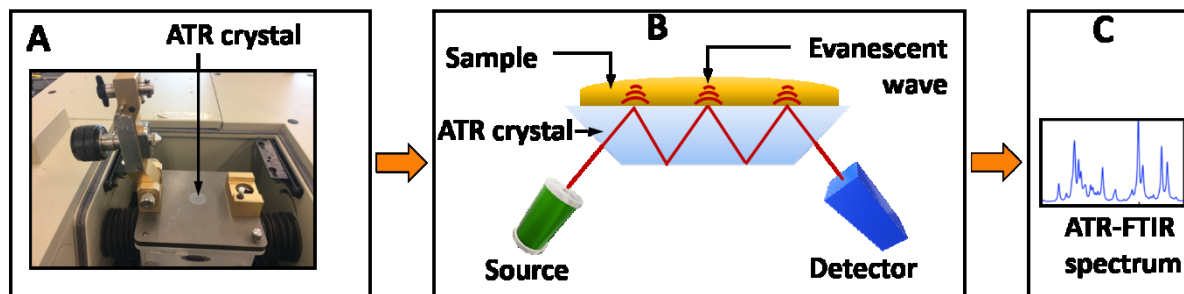


Figure 2.5. Platform of the Bruker ATR instrument used with the ATR crystal (A) upon which the sample is placed. IR radiation from the source travels through the crystal, interacts with the sample and reflects internally. This creates an evanescent wave which extends into the sample. This results in a slightly attenuated internal reflection (B) rendering an FTIR spectrum (C).

2.3.5 FTICR MS analysis

High resolution mass spectrometry analysis was conducted using a 12 Tesla solarix Fourier transform ion cyclotron resonance mass spectrometer (FTICR; Bruker Daltonik GmbH, Bremen, Germany). This was coupled to an Apollo II atmospheric pressure photoionisation (APPI) ion source operating in positive-ion mode operated with Nitrogen at a pressure of 1.0 bar. Ions were collected in the collision cell followed by detection and analysis.

2.4 Software

A range of software to suit the task at hand was used for the various experimental sections. These are tabulated as follows in Table 2.2.

Table 2.2 Software used in various experimental sections of the thesis together with the respective developer and experimental application

Software name	Software developer	Experimental application
TimeBase version 6.1.0.1963	PerkinElmer, Inc., Bucks, UK	Time resolved GC–FTIR data acquisition and manipulation using the PerkinElmer GC–FTIR system and PC-2
Spectrum version 10.4.2.27	PerkinElmer, Inc., Bucks, UK	FTIR spectra data processing using the PerkinElmer GC–FTIR system and PC-2
TurboMass version 6.1.0.1963	PerkinElmer, Inc., Shelton, CT, USA	GC and MS data acquisition and manipulation using the PerkinElmer GC–MS system and PC-1
MassHunter Workstation version 10.0	Agilent Technologies, Inc.	GC and MS data acquisition and processing for 1DGC–MS on Agilent instrumentation
MassHunter Workstation version 6.0	Agilent Technologies, Inc.	GC and MS data acquisition and processing for GC×GC–TOFMS on Agilent instrumentation
Agilent OpenLab CDS Chemstation version 2.3.54	Agilent Technologies, Inc.	GC–FPD data acquisition and processing on Agilent instrumentation
Canvas version W1.0.13.2	J&X Technologies Co., Ltd., Shanghai, China	GC×GC data processing
Opus version 6.0	Bruker Optik GmbH, Germany	ATR–FTIR data acquisition on Bruker ATR instrument
NIST 2011	National Institute of Standards and Technology	MS and FTIR library searching

Fluka IR library	Supplied by PerkinElmer Inc.	FTIR library searching using FTIR spectra collected on GC–FTIR
Nicolet™ FT-IR vapour phase spectral library	ThermoFisher Scientific	FTIR library searching using FTIR spectra collected on GC–FTIR
Matlab R2019a version 9.6.0.1072779	The Mathworks, Inc., Natick, MA, USA	Data processing of FTIR spectra
Partial Least Square (PLS) Toolbox	Eigenvector Research Inc., Wenatchee, WA, USA	Chemometric data processing of FTIR spectra
Quasar - Orange data mining toolbox version 3.0	University of Ljubljana, Slovenia	Principal component analysis (PCA) for ATR–FTIR data
KairosMS	University of Warwick, UK	FTICR MS data analysis and visualisation
Bruker DataAnalysis software version 5.0	Bruker Daltonik GmbH, Bremen, Germany	Calibration of mass spectra obtained from FTICR MS
Composer software version 1.5.6	Sierra Analytics, Modesto, CA, USA	Assigning FTICR MS data molecular compositions

2.5 Standards and sample preparation

A wide variety of standards were used for the various experimental sections of Chapters 2–5. Due to the extensive nature of this list, which also includes standards used for development of an in-house library, the standards and their manufacturers have been tabulated in Table 2.3.

Solvents used in various analyses were dichloromethane (DCM) ($\geq 99.8\%$ purity), *n*-hexane ($\geq 98.0\%$ purity) and acetone (99.8% purity) purchased from Merck KGaA, Darmstadt, Germany and methanol (99.9% purity) purchased from Scharlab S.L., Spain. Stock solutions were prepared from standard solutions and further diluted to obtain working solutions as per the requirement.

Biofuel samples used in the analyses contained in Chapter 5 were chosen to cover a range of sources and processing techniques.

Table 2.3 List of confirmed standards, molecular formula and their respective manufacturers, used in various analyses and addition in the in-house spectral library

Compound name	Molecular formula	Manufacturer
<i>E</i> -acetaldehyde oxime	C ₂ H ₅ NO	Sigma-Aldrich Co., St. Louis, MO, USA
<i>Z</i> -acetaldehyde oxime	C ₂ H ₅ NO	Sigma-Aldrich Co., St. Louis, MO, USA
acetic anhydride	C ₄ H ₆ O ₃	Sigma-Aldrich Co., St. Louis, MO, USA
acetic acid	C ₂ H ₄ O ₂	Sigma-Aldrich Co., St. Louis, MO, USA
acetonitrile	C ₂ H ₃ N	Sigma-Aldrich Co., St. Louis, MO, USA
acetone	C ₃ H ₆ O	Merck KGaA, Darmstadt, Germany
benzene-1,2-diol (catechol)	C ₆ H ₆ O ₂	Tokyo Chemical Industries Co. Ltd., Tokyo, Japan
benzene-1,3-diol (resorcinol)	C ₆ H ₆ O ₂	Tokyo Chemical Industries Co. Ltd., Tokyo, Japan
benzene-1,4-diol (hydroquinone)	C ₆ H ₆ O ₂	Tokyo Chemical Industries Co. Ltd., Tokyo, Japan
butanone	C ₄ H ₈ O	Sigma-Aldrich Co., St. Louis, MO, USA
1-butanol	C ₄ H ₁₀ O	Merck, Kilsyth, Australia
2-butanol	C ₄ H ₁₀ O	Sigma-Aldrich Co., St. Louis, MO, USA
chlorobenzene	C ₆ H ₅ Cl	Sigma-Aldrich Co., St. Louis, MO, USA
chloro-3-nitrobenzene	C ₆ H ₄ ClNO ₂	Tokyo Chemical Industries Co. Ltd., Tokyo, Japan
chloroform	CHCl ₃	Honeywell Burdick & Jackson, Muskegon, MI, USA
<i>o</i> -cresol	C ₇ H ₈ O	Tokyo Chemical Industries Co. Ltd., Tokyo, Japan
<i>m</i> -cresol	C ₇ H ₈ O	Tokyo Chemical Industries Co. Ltd., Tokyo, Japan

<i>p</i> -cresol	C ₇ H ₈ O	Tokyo Chemical Industries Co. Ltd., Tokyo, Japan
cyclohexane	C ₆ H ₁₂	Ajax Finechem Pty., Ltd., Sydney, Australia
<i>p</i> -cymene	C ₁₀ H ₁₄	Australian Botanical Products Pty. Ltd., Hallam, Australia
1,2-dichlorobenzene	C ₆ H ₄ Cl ₂	Tokyo Chemical Industries Co. Ltd., Tokyo, Japan
dichloroethane	C ₂ H ₄ Cl ₂	Tokyo Chemical Industries Co. Ltd., Tokyo, Japan
dichloromethane	CH ₂ Cl ₂	Merck KGaA, Darmstadt, Germany
1,4-dimethoxybenzene	C ₈ H ₁₀ O ₂	Sigma-Aldrich Co., St. Louis, MO, USA
2,3-dimethylpentane	C ₇ H ₁₆	Sigma-Aldrich Co., St. Louis, MO, USA
2,4-dimethylpentane	C ₇ H ₁₆	Sigma-Aldrich Co., St. Louis, MO, USA
ethanol	C ₂ H ₆ O	Sigma-Aldrich Co., St. Louis, MO, USA
ethylacetate	C ₄ H ₈ O ₂	Sigma-Aldrich Co., St. Louis, MO, USA
ethylbenzene	C ₈ H ₁₀	Tokyo Chemical Industries Co. Ltd., Tokyo, Japan
ethyldisulfide	C ₄ H ₁₀ S ₂	Eastman Kodak Co., Rochester, NY, USA
ethylene glycol	C ₂ H ₆ O ₂	Sigma-Aldrich Co., St. Louis, MO, USA
eugenol	C ₁₀ H ₁₂ O ₂	Australian Botanical Products Pty. Ltd., Hallam, Australia
formic acid	CH ₂ O ₂	Sigma-Aldrich Co., St. Louis, MO, USA
2-furaldehyde; 2-furancarbaldehyde	C ₅ H ₄ O ₂	Fluka Chemie GmbH, Buchs, Switzerland
geraniol	C ₁₀ H ₁₈ O	Australian Botanical Products Pty. Ltd., Hallam, Australia
<i>n</i> -hexane	C ₆ H ₁₄	Merck KGaA, Darmstadt, Germany
1-hexene	C ₆ H ₁₂	Sigma-Aldrich Co., St. Louis, MO, USA

limonene	C ₁₀ H ₁₆	Australian Botanical Products Pty. Ltd., Hallam, Australia
methanol	CH ₄ O	Scharlab S. L., Barcelona, Spain
Methylacetoacetate (methyl-3-oxobutanoate)	C ₅ H ₈ O ₃	Sigma-Aldrich Co., St. Louis, MO, USA
n-methylaniline	C ₇ H ₉ N	Sigma-Aldrich Co., St. Louis, MO, USA
2-methylbutane	C ₅ H ₁₂	Tokyo Chemical Industries Co. Ltd., Tokyo, Japan
2,2-dimethylbutane	C ₆ H ₁₄	Tokyo Chemical Industries Co. Ltd., Tokyo, Japan
methyl-dl-2-methylbutyrate	C ₆ H ₁₂ O ₂	Tokyo Chemical Industries Co. Ltd., Tokyo, Japan
methyl disulfide	C ₂ H ₆ S ₂	Sigma-Aldrich Co., St. Louis, MO, USA
methyl lactate; methyl-2-hydroxy propanoate	C ₄ H ₈ O ₃	Tokyo Chemical Industries Co. Ltd., Tokyo, Japan
2-methylpentane	C ₆ H ₁₄	Tokyo Chemical Industries Co. Ltd., Tokyo, Japan
naphthalene	C ₁₀ H ₈	Sigma-Aldrich Co., St. Louis, MO, USA
1-nitropropane	C ₃ H ₇ NO ₂	Sigma-Aldrich Co., St. Louis, MO, USA
2-nitrotoluene	C ₇ H ₇ NO ₂	Tokyo Chemical Industries Co. Ltd., Tokyo, Japan
3-nitrotoluene	C ₇ H ₇ NO ₂	Tokyo Chemical Industries Co. Ltd., Tokyo, Japan
4-nitrotoluene	C ₇ H ₇ NO ₂	Tokyo Chemical Industries Co. Ltd., Tokyo, Japan
nonane	C ₉ H ₂₀	Sigma-Aldrich Co., St. Louis, MO, USA
n-octane	C ₈ H ₁₈	Ajax Chemicals, Sydney, Australia
2-pentanone	C ₅ H ₁₀ O	Tokyo Chemical Industries Co. Ltd., Tokyo, Japan

2-phenylethanol; phenethylalcohol	C ₈ H ₁₀ O	Sigma-Aldrich Co., St. Louis, MO, USA
pentane	C ₅ H ₁₂	Sigma-Aldrich Co., St. Louis, MO, USA
phenol (carbolic acid)	C ₆ H ₆ O	Sigma-Aldrich Co., St. Louis, MO, USA
α -pinene	C ₁₀ H ₁₆	Australian Botanical Products Pty. Ltd., Hallam, Australia
β -pinene	C ₁₀ H ₁₆	Australian Botanical Products Pty. Ltd., Hallam, Australia
piperidine	C ₅ H ₁₁ N	Sigma-Aldrich Co., St. Louis, MO, USA
<i>E</i> -propionaldehyde oxime	C ₃ H ₇ NO	Sigma-Aldrich Co., St. Louis, MO, USA
<i>Z</i> -propionaldehyde oxime	C ₃ H ₇ NO	Sigma-Aldrich Co., St. Louis, MO, USA
2-propanol	C ₃ H ₈ O	Tokyo Chemical Industries Co. Ltd., Tokyo, Japan
pyridine	C ₅ H ₅ N	Sigma-Aldrich Co., St. Louis, MO, USA
γ -terpinene	C ₁₀ H ₁₆	Australian Botanical Products Pty. Ltd., Hallam, Australia
tetrachloroethylene	C ₂ Cl ₄	Sigma-Aldrich Co., St. Louis, MO, USA
tetrahydrofuran	C ₄ H ₈ O	Merck KGaA, Darmstadt, Germany
toluene	C ₇ H ₈	Sigma-Aldrich Co., St. Louis, MO, USA
2,2,4-trimethylpentane	C ₈ H ₁₈	Tokyo Chemical Industries Co. Ltd., Tokyo, Japan
undecane	C ₁₁ H ₂₄	Sigma-Aldrich Co., St. Louis, MO, USA
<i>o</i> -xylene	C ₈ H ₁₀	Sigma-Aldrich Co., St. Louis, MO, USA
<i>m</i> -xylene	C ₈ H ₁₀	Sigma-Aldrich Co., St. Louis, MO, USA
<i>p</i> -xylene	C ₈ H ₁₀	Sigma-Aldrich Co., St. Louis, MO, USA

2.6 Comparison of FTIR settings

In order to obtain the best spectrum results from the GC–FTIR experiments a range of FTIR operating conditions and parameters play a crucial role. This ensures reliability of results as well as maximum efficiency of resource use.

Since the acquisition of FTIR data is non-destructive the GC carrier flow can be directed to other detectors for post-LP analysis of the sample constituents. As depicted in Figure 2.4, the GC–FTIR system used in majority of the Chapters enables FID analysis of the GC effluent after being subjected to FTIR analysis. The sensitivity of the LP is maximised by the multiple internal reflections which increases the practical cell length which is enabled by the LP's reflective gold coating [6]. The resolution achieved by the component separation within the GC column can degrade within the mixing volume of the LP and connecting tubes - i.e. just-resolved peaks may travel through the light pipe simultaneously (the trailing edge of the first peak and the leading edge of the second peak) so a broadened apparent peak may result. the relatively large internal volume of the light pipe can degrade the chromatographic efficiency of the peak. It is imperative that the system design allows for minimal loss of efficiency of experimental results; in this instance the minimal reduction of chromatographic peak distortion and chromatographic resolution [7].

The current system was assessed for the effect of the LP on chromatographic peak shape by comparing the variation on the chromatographic FID peak between direct FID (GC–FID) and post-light-pipe FID (GC–FTIR–FID) configurations under various split ratios and temperature ramp combinations. The results of the same were reported in Zavahir et al 2020 which has been included in Chapter 3 [8].

The *signal-to-noise ratio* (SNR) in a FTIR spectrophotometer is a good indication of its sensitivity and in simple terms is the relative magnitude of the detector signal. SNR is calculated as a ratio of a spectrum peak's height to the noise in an adjacent baseline region. This is usually done in a region with the strongest response of the optical system and is quoted for a particular resolution. A good SNR thus increases the dominance of the detector signal and optimises the sensitivity of optical instruments and therefore should not be overlooked. SNR, a measure which compares the level of signal noise to that of the

background noise, relates to the measurement precision of the instrument and also relates to analytical figures of merit such as the limit of detection [9].

SNR in LP GC–FTIR systems have been improved from previous models by approaches which include minimising chromatographic peak broadening by optimising the LP's volume/length ratios [10], introducing rapid scan interferometers [11], optimisation of the LP interface's optical configuration [12] and employing suitable low-noise detectors [13]. Although the LP and TL need to be maintained at a T sufficiently higher than the GC oven to prevent condensation of GC solutes, this higher T has its disadvantages in causing the LP to act as an IR source [14]. This contributes to an increased intensity of unmodulated radiation which in turn may affect both the SNR as well as the linear response of the MCT detector [5]. This system was hence tested for its ability to carry out measurements with good SNR under varying crucial operational parameters. Thus, the effect on the SNR with increasing the LP and TL T as well as varying the FTIR spectral resolution and carrier gas flow was assessed, the results and discussions of which are reported in Zavahir et al 2020 which has been included in Chapter 3 [8]. The system was also assessed for the best scan speed setting to analyse components contained in this thesis as reported below.

2.6.1 Comparison of scan speed

A spectrum which includes characteristics of both the atmosphere and instrument and has not been ratioed against a background is referred to as a *single beam spectrum*. For a defined region noise is calculated either as p–p (peak-to-peak) or RMS (Root Mean Square) from a defined region. The 2200–2100 cm^{-1} is often chosen to measure the noise as it is the region with the greatest single beam intensity (with the least signal) whilst the poorest SNR seen is in the 600–400 cm^{-1} region) [9].

A spectrum's SNR depends on the time taken to scan as follows in Equation 2.1.

$$SNR \propto \sqrt{\text{Scanning time}} \quad (\text{Eq 2.1})$$

An increase in scanning time inevitably increases the number of scans, hence for a given scan speed, SNR and number of scans consist of the relationship seen in Equation 2.2.

$$SNR \propto \sqrt{\text{number of scans}} \quad (\text{Eq 2.2})$$

However, an increase in both scan speed and correspondingly increasing the number of scans does not necessarily improve the SNR. A real peak will always have the same point on the abscissa making it additive as scans accumulate as opposed to noise which occurs randomly and is hence not additive. Thus, there is an increase in SNR when more scans are added to the spectrum.

For an interferogram, its scan speed or scanning velocity (measured in cm/s or cm s⁻¹) is the rate at which the optical path difference (OPD) is varied. The moving mirror's velocity needs to stay constant to ensure the wavenumbers and Fourier frequencies measured are correct [15]. SNR of interferometers have been known to be inversely proportional to the square root of the *scanning velocity* (*v*) or speed [16] as shows in Equation 2.3.

$$SNR \propto v^{1/2} \quad (\text{Eq. 2.3})$$

A 20% solution of 2,3-dimethylpentane and 2,4-dimethylpentane prepared in dichloromethane was used to compare the scan speed settings on the in-house designed GC–FTIR instrument and choose the most appropriate setting for subsequent analysis. The sample was analysed on the GC–FTIR instrument using the settings outlined in Table 2.4 under various scan speed settings.

The resulting root mean square intensity profile chromatograms for the respective analyses are depicted in Figure 2.6A with the FTIR spectrum of the 2,3-dimethylpentane peak depicted in Figure 2.6B.

Signal to noise ratio calculations were carried out using Equation 2.4 as defined in [15].

$$\text{Signal to noise ratio (SNR)} = \text{Signal} / \text{Noise} \quad (\text{Eq. 2.4})$$

Here *signal* is considered as the intensity of the FTIR peak in absorbance units and the *noise* is measured as the *peak-to-peak noise* where the lowest noise point is subtracted from the highest noise point in absorbance units a peak-free region of the baseline spectrum.

Table 2.4 GC and FTIR settings for comparing scan speed of FTIR instrument

GC	
Temperature program	50 °C, rate 5 °C/min, up to 200 °C
Carrier gas flow	1.0 mL/min
Split	20:1
Injection volume	1.5 µL
Injector temperature	250 °C
Inlet line temperature	250 °C
Source temperature	200 °C
MS electron energy	70 eV
FID temperature	250 °C
FID Offset	5.0 mV
H ₂	45.0 mL/min
Air	450.0 mL/min
FTIR	
Resolution	8 cm ⁻¹
Number of background scans	100
Varying scan speed	0.2 cm s ⁻¹ , 0.5 cm s ⁻¹ , 1.0 cm s ⁻¹ , 2.0 cm s ⁻¹ , 4.0 cm s ⁻¹
Scan range	4000 – 700 cm ⁻¹
Phase correction	self
Apodisation	weak
Light pipe temperature	250 °C
Transfer line temperature	250 °C

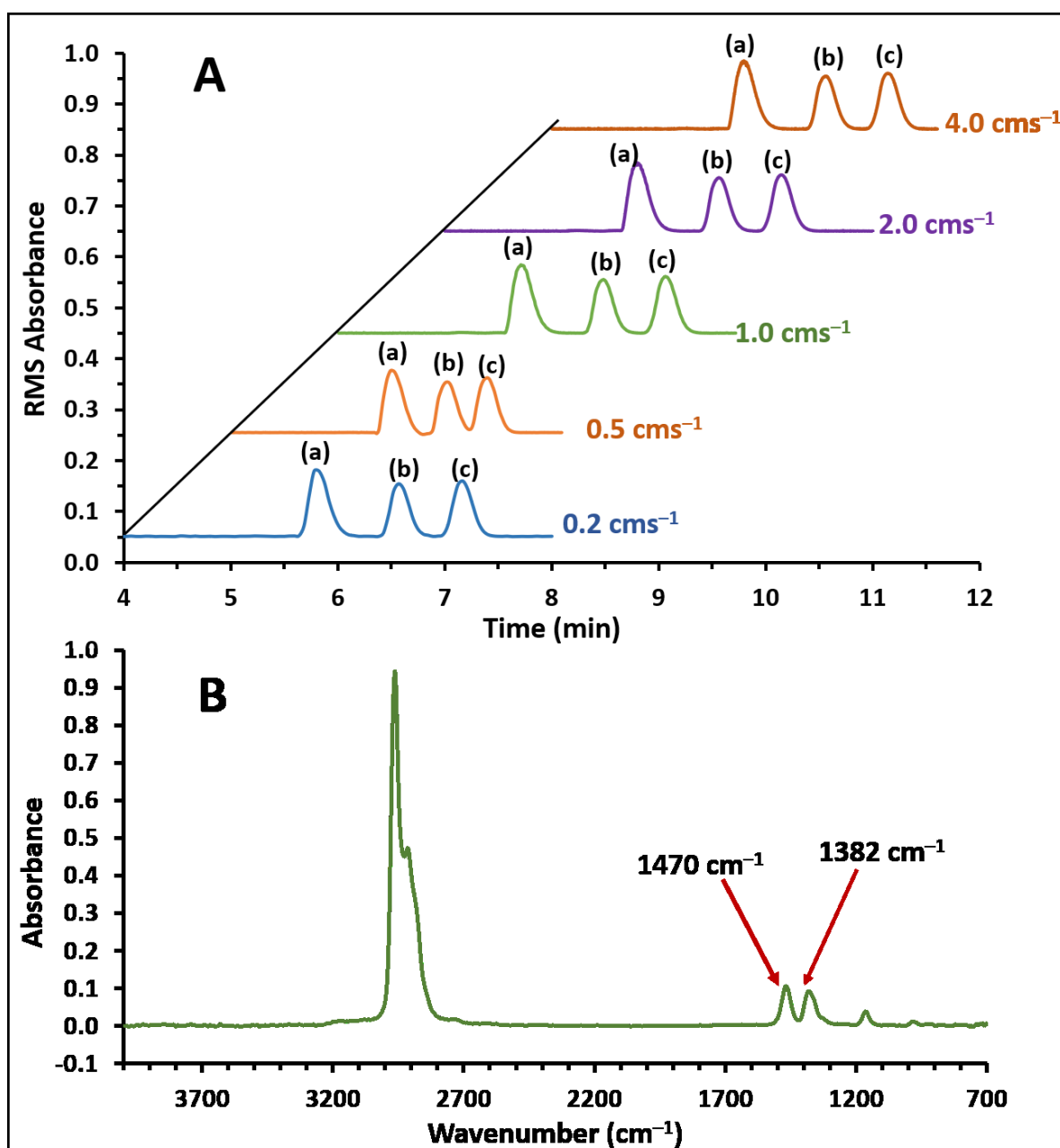


Figure 2.6. Root mean square intensity profiles (A) of the analyses using varying FTIR scan speeds of 0.2 cm s^{-1} , 0.5 cm s^{-1} , 1.0 cm s^{-1} , 2.0 cm s^{-1} and 4.0 cm s^{-1} . Peaks (a), (b) and (c) correspond to dichloromethane, 2,3-dimethylpentane and 2,4-dimethylpentane respectively. The FTIR spectrum of peak (b) is depicted in (B) with the FTIR peaks corresponding to wavenumbers 1470 cm^{-1} and 1382 cm^{-1} pointed out for which the SNR is calculated in Table 2.5.

Table 2.5 SNR calculations for peaks at 1470 cm⁻¹ and 1382 cm⁻¹ of 2,3-dimethylpentane peak obtained at varying scan speed settings.

Scan speed	Average peak to peak noise 2200–2000 cm ⁻¹	Peak height at 1470 cm ⁻¹	Peak height at 1382 cm ⁻¹	SNR of peak at 1470 cm ⁻¹	SNR of peak at 1382 cm ⁻¹
0.2	0.0026	0.1039	0.0916	39.96	35.23
0.5	0.0024	0.1049	0.0928	43.70	38.67
1	0.0011	0.1060	0.093	96.36	84.55
2	0.0019	0.1046	0.092	55.05	48.42
4	0.0012	0.1014	0.090	84.5	75.00

As confirmed in Table 2.5, the highest SNR was observed for a scan speed of 1 cm s⁻¹ and hence was chosen for analyses using the GC–FTIR system as this was also consistent with the scan speed value most commonly used in literature.

2.7 Daily performance validation analysis

A mixture of six standards with varying functional groups was prepared in dichloromethane as a standards mixture sample for regular validation of the in-house designed GC–FTIR system's performance. The components of this includes a 1% standards mixture of 1-nitropropane, 2-butanol, *m*-xylene and undecane from Sigma-Aldrich Co., (St. Louis, MO) and 2-pentanone and 3-nitrotoluene from Tokyo Chemicals Industry Co., Ltd., (Tokyo, Japan) diluted in dichloromethane. The samples mixture is analysed on the GC–FTIR system at the beginning of each day using the settings outlined in Table 2.6 (also used for accumulation of library spectra) prior to samples for the day being analysed on the system.

Table 2.6 GC and FTIR settings for collection of FTIR spectra for addition to the in-house FTIR spectral library

GC	
Temperature program	50 °C, rate 5 °C/min, up to 240 °C
Carrier gas flow	1.0 mL/min
Split	10:1
Injection volume	1.5 µL
Injector temperature	250 °C
Inlet line temperature	250 °C
Source temperature	200 °C
MS electron energy	70 eV
FID temperature	250 °C
FID Offset	5.0 mV
H ₂	45.0 mL/min
Air	450.0 mL/min
FTIR	
Resolution	4 cm ⁻¹
Number of background scans	100
Scan speed	1 cm s ⁻¹
Scan range	4000 – 700 cm ⁻¹
Phase correction	self
Apodisation	weak
Light pipe temperature	250 °C
Transfer line temperature	250 °C

The chromatographic results of this are then compared to a saved chromatogram of the same standard sample mixture analysis. This is maintained as a means of ensuring the system's stability and consistency of performance.

Figure 2.7 depicts the chromatogram resulting from this analysis together with the respective peaks and their retention times set out in Table 2.7.

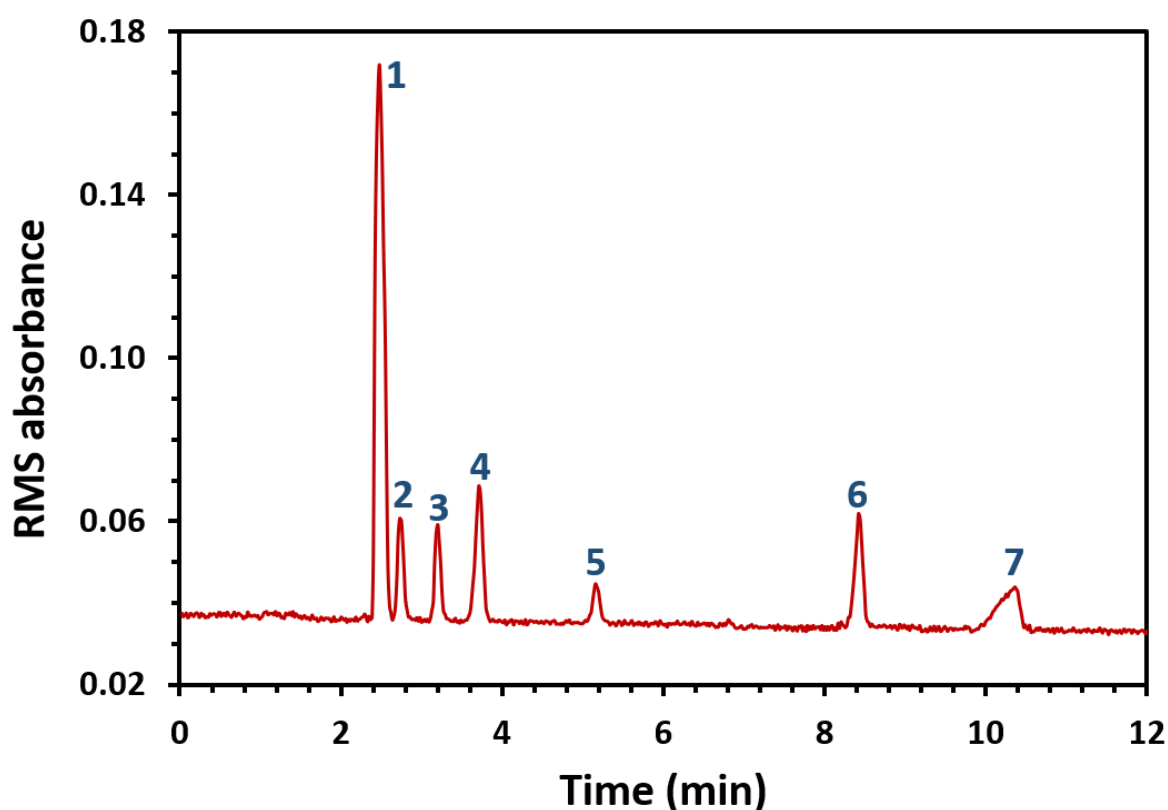


Figure 2.7. Chromatogram of standards sample mixture used for daily performance validation of GC–FTIR system with numbered peak descriptions included in Table 2.7.

Table 2.7 Compound names and retention times of the respective peaks numbered in the chromatogram depicted in Figure 2.7

Peak number	Compound name	Retention time (min)
1	Dichloromethane	2.48
2	2-butanol	2.73
3	2-pentanone	3.21
4	1-nitropropane	3.75
5	<i>m</i> -xylene	5.16
6	undecane	8.43
7	3-nitrotoluene	10.36

2.8 Establishment of a user-defined in-house spectral library

Although FTIR spectroscopic techniques yield an excellent source of identification and characterisation of chemicals, the complexity of spectra rendered by this method makes

the interpretation both a time-consuming and difficult task for spectroscopists. The development of advanced multi-component computer systems and software to suit the purpose has interested both spectroscopists and chemometricians alike in untangling the information contained in the spectra. Of these, the most common techniques to be used include library searches and pattern recognition techniques [17], which together with knowledge-based approaches, aid in structural elucidation of compounds [18].

The powerful technique of FTIR spectroscopy helps in the identification of a broad range of organic and inorganic compounds; with the main identification based on the type of chemical bond which is determined through the characteristic peak location on the spectrum (its wavenumber), its width (narrow or broad) and its intensity (weak or strong). Appendix B consists of a set of tables used to thus carry out preliminary elucidation of the structure of compounds using FTIR spectra. Table B–1 presents the main wavelength regions of the mid IR spectra which can be used for preliminary analysis of the presence of major functional groups. This table can also be used to determine the absence of such functional groups and thus eliminate the presence of compounds. Table B–2 consists of the broad absorption bands commonly seen in mid IR spectra which can further assist in assigning a possible compound identification. In addition, Table B–3, consisting of the absorption bands characteristic of benzene ring substitution, has been included due to the abundant analysis of aromatic isomers in the experiments contained in this thesis. Tables similar to these and a more extensive list of specific wavenumber ranges for functional groups and compound classes which absorb in the mid- and far-infrared regions can be found in the book chapter based on Spectra-Structure Correlations by Shurvell [19].

With the availability of spectrum libraries, the task of compound identification has become a less time-consuming task for spectroscopists. The identification of spectra based on library compounds is largely performed on the basis of comparing the spectrum similarities between the spectrum of the unknown (query) compound and the entire spectra collection to get a suitable reference compound (hit) from the library [20]. Such library searches are based on the representation of data, similarity measures and the search algorithm used [18]. Kuentzel (in 1951) is credited with the initial attempts of automated retrieval of reference spectra using Hollerith-Type punched cards and an IBM

electric sorting machine which was used as a sorting, indexing and correlating system for generated IR absorption data [21].

Any library search is originated by the construction of a set of reference spectra with individual spectra including additional information such as compound structure, name, connection data and molecular mass. These spectra together with the library search approach influence the comparison process, speed of data retrieval and amount of data storage space required for the reference library. Such spectrum collections as well as the growing trend of hyphenated and multidimensional techniques generate a vast volume of chemical and experimental data. This can be remediated through the compression of signals and data which in turn reduces the size of the database and increases the speed of spectrum searching. This is commonly done by wavelet transform (WT), a mathematical process which aids in signal processing, and has been applied in many fields including chromatography, mass spectrometry, IR and NMR spectroscopy electrochemical signals [17, 22]. WT is widely and successfully used as a signal processing tool due to its efficiency, abundance of basic functions and high data treatment speed [23].

IR library search systems are available at most instrument manufacturers as well as many commercial IR libraries which consist of several thousands of spectra which may be of a particular class of compounds or with varying compound types. This however is a relatively small number compared to the vast number of currently known compounds. FTIR spectrum libraries lack the widespread availability of MS spectrum libraries and the number of spectra in such FTIR libraries are lower than their MS counterparts.

Although such libraries can be purchased from instrument manufacturers and other commercial sources as spectrum libraries specific for certain classes of compounds, these may be at times limited to certain groups of chemicals. Hence, confidence in identification can also be achieved by using in-house spectrum libraries which have spectra specific for the analysis purpose saved for easy reference [24].

Thus, the creation of a user-defined in-house library was seen as apt as it would enable the confident identification of components commonly encountered in the research group. This will also enable the precise identification of components in sample matrices by

matching FTIR spectra of unknown components to those of known standards saved in the in-house library database.

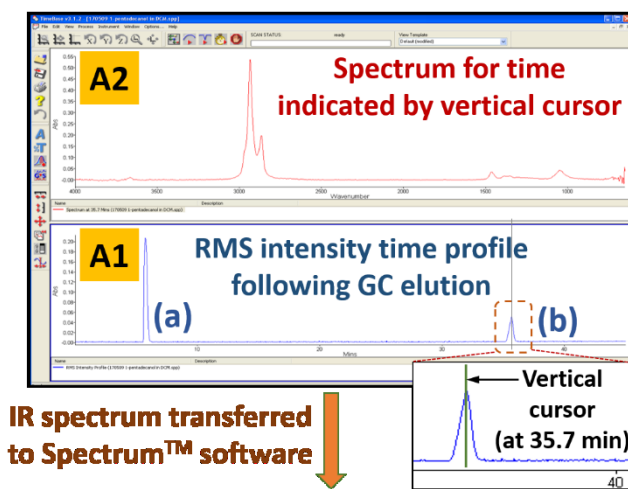
Addition of spectra was carried out by diluting the standard in a suitable solvent (dichloromethane or hexane) to prepare samples to be analysed by GC–FTIR. Parameters for GC (on the TurboMass™ software) and for FTIR (on the TimeBase™ software) data acquisition and processing are tabulated in Table 2.6 set out in Section 2.7. Data obtained as a result of time-resolved experiments in GC–FTIR analysis was viewed on the TimeBase™ software which presents the root mean square (RMS) absorbance intensity profile as depicted in Figure 2.8 A1. Here we use the example of 1-pentadecanol diluted in DCM. The peak profile is examined to obtain the peak of interest; in this instance 1-pentadecanol. The vertical cursor is then placed on the peak (Figure 2.8 A1 inset) which yields the FTIR spectrum at that particular retention time; in this example at 35.7 min. Figure 2.8 A2 depicts the respective spectrum. This spectrum is then transferred to the Spectrum™ software by dragging it across using the mouse cursor and saved as a file in the Spectrum™ software.

A suitable library from the *library* folder is now opened in the Spectrum™ software by clicking on the relevant *user-defined spectrum library* icon as seen in Figure 2.8 C. The in-house spectrum library has been named “Monash Uni in-house library”. The integrity of commercial spectrum libraries is maintained as they are locked and cannot be tampered with. Each individual FTIR spectrum obtained through the GC–FTIR experiment is saved in the library. This can also include the peak list containing wavenumbers of peak positions with their absorption intensities (Figure 2.8 D), CAS numbers for standard compounds as well as other relevant information for the individual compounds. It should be noted that these are gas-phase spectrum library data.

Appendix C sets out a list of selected spectra as example of those included in the user-defined Monash Uni in-house library.

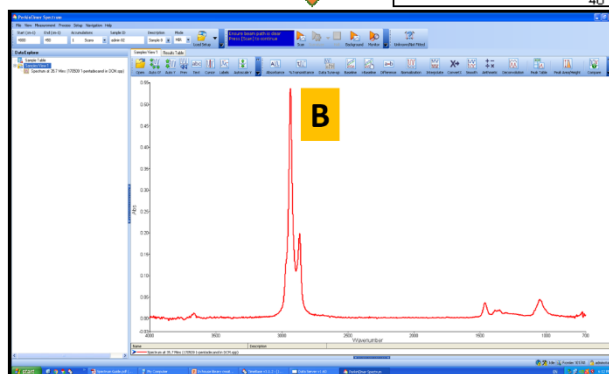
TimeBase™ software

Root mean square (RMS) intensity profile (A1) and IR spectrum (A2) at selected retention time
(a) Dichloromethane
(b) 1-pentadecanol



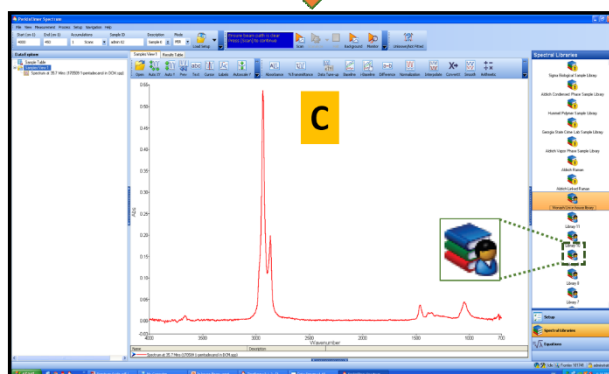
Spectrum™ software

FTIR spectrum view



Spectrum™ software

Choosing spectral library to save spectrum



Spectrum™ software

FTIR spectrum added to library content together with peak position table

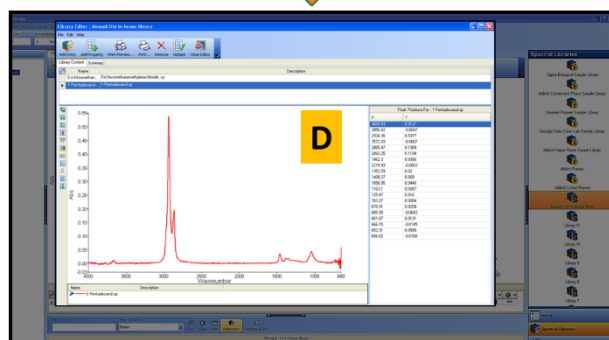


Figure 2.8. Process followed for adding FTIR spectra to the user-defined in-house spectrum library. RMS intensity profile obtained with the TimeBase software (A1) is used to extract the FTIR spectrum at a specific elution time (A2). This spectrum is transferred to the Spectrum software (B), the specific library to input the spectrum is chosen (C) and the spectrum together with its peak position table is added to the library content (D).

2.9 Conclusions

The methods and materials described in the sections above were used in various sections of the thesis to suit the experimental analysis at hand. The GC–FTIR system detailed in the preliminary parts of this Chapter are used extensively in Chapters 3 and 4 for a wide range of analyses. Here, each chapter will highlight any specific variations to the methods or sample preparation as needed to answer the research question at hand. The in-house user-defined spectrum library can be maintained for future FTIR analysis purposes with the ability to include additional spectra as required by the user. This will also facilitate ease and reliability of identification when analysing GC separated chemical components commonly encountered in various sample matrices.

References

- [1] J. Cai, P. Lin, X.L. Zhu, Q. Su, Comparative analysis of clary sage (*S. sclarea* L.) oil volatiles by GC-FTIR and GC-MS, *Food Chem.* 99 (2006) 401–407.
- [2] P.R. Griffiths, D.A. Heaps, P.R. Brejna, The gas chromatography/infrared interface: past, present, and future, *Appl. Spectrosc.* 62 (2008) 259A–270A.
- [3] T. Visser, Gas chromatography/Fourier Transform infrared spectroscopy, in: P.R. Griffiths and J.M. Chalmers (Eds.), *Handbook of Vibrational Spectroscopy*, John Wiley & Sons, Ltd. Chichester, 2006, pp. 1605–1626.
- [4] Y.-Q. Li, D.-X. Kong, H. Wu, Analysis and evaluation of essential oil components of cinnamon barks using GC–MS and FTIR spectroscopy, *Ind. Crops. Prod.* 41 (2013) 269–278.
- [5] R.S. Brown, J.R. Cooper, C.L. Wilkins, Lightpipe temperature and other factors affecting signal in gas chromatography/Fourier transform infrared spectrometry, *Anal. Chem.* 57 (1985) 2275–2279.
- [6] L.V. Azarraga, Gold coating of glass tubes for gas Chromatography/Fourier transform infrared spectroscopy "light-pipe" gas cells, *Appl. Spectrosc.* 34 (1980) 224–225.
- [7] H. Mark, J. Workman Jr, *Experimental designs: Part 1, Chemometrics in Spectroscopy*, Academic Press. Amsterdam, 2007, pp. 51–55.
- [8] J.S. Zavahir, J.S.P. Smith, S. Blundell, H.D. Waktola, Y. Nolvachai, B.R. Wood, P.J. Marriott, Relationships in gas chromatography—Fourier transform infrared spectroscopy—Comprehensive and multilinear analysis, *Separations* 7 (2020) 27.
- [9] J.P. Blitz, D.G. Klarup, Signal-to-noise ratio, signal processing, and spectral information in the instrumental analysis laboratory, *J. Chem. Educ.* 79 (2002) 1358–1360.
- [10] G.N. Giss, C.L. Wilkins, Effects of lightpipe dimensions on gas chromatography/Fourier transform infrared sensitivity, *Appl. Spectrosc.* 38 (1984) 17–20.
- [11] G.M. Brissey, D.E. Henry, G.N. Giss, P.W. Yang, P.R. Griffiths, C.L. Wilkins, Comparison of gas chromatography/Fourier transform infrared spectrometric Gram-Schmidt reconstructions from different interferometers, *Anal. Chem.* 56 (1984) 2002–2006.
- [12] D.E. Henry, A. Giorgetti, A.M. Haefner, P.R. Griffiths, D.F. Gurka, Optimizing the optical configuration for light-pipe gas chromatography/Fourier transform infrared spectrometry interfaces, *Anal. Chem.* 59 (1987) 2356–2361.

- [13] E. Theodorou, J.R. Birch, Detectors for mid- and far-infrared spectrometry: selection and use, in: P.R. Griffiths and J.M. Chalmers (Eds.), *Handbook of Vibrational Spectroscopy*, John Wiley & Sons, Ltd. Chichester, 2006, pp. 349–367.
- [14] P.R. Griffiths, J.A. de Haseth, Coupled techniques, in: P.R. Griffiths and J.A. de Haseth (Eds.), *Fourier Transform Infrared Spectrometry*, second ed., John Wiley & Sons, Inc., 2006, pp. 481–507.
- [15] B.C. Smith, *Fundamentals of Fourier Transform Infrared Spectroscopy*, second edition, CRC press, 2011.
- [16] R.L. White, Gas chromatography-Fourier transform infrared spectrometry, *Appl. Spectrosc. Rev.* 23 (1987) 165–245.
- [17] F. Tan, X. Feng, M. Li, Z. Wang, L. Yang, Y. Li, Y. Feng, F. Nie, Construction and application of a novel library: Fourier transform infrared wavelet coefficients library, *Anal. Chim. Acta.* 629 (2008) 38–46.
- [18] H.J. Luinge, Automated interpretation of vibrational spectra, *Vib. Spectrosc.* 1 (1990) 3–18.
- [19] H.F. Shurvell, Spectra-structure correlations in the mid- and far-infrared, *Handbook of Vibrational Spectroscopy* 3 (2002) 1783–1816.
- [20] H. Hobert, Library search — Principles and applications, in: J. Einax (Ed.), *Chemometrics in Environmental Chemistry - Applications*, Springer, Berlin Heidelberg. 1995, pp. 1–24.
- [21] L. Kuentzel, New codes for Hollerith-type punched cards, *Anal. Chem.* 23 (1951) 1413–1418.
- [22] A. Kai-Man Leung, F.T. Chau, J.B. Gao, T.M. Shih, Application of wavelet transform in infrared spectrometry: Spectral compression and library search, *Chemom. Intell. Lab. Sys.* 43 (1998) 69–88.
- [23] Z.N. Wen, K.L. Wang, M.L. Li, F.S. Nie, Y. Yang, Analyzing functional similarity of protein sequences with discrete wavelet transform, *Comput. Biol. Chem.* 29 (2005) 220–228.
- [24] M. Goldthorp, P. Lambert, Development of FTIR as a field technology for chemical spills, in: *Proceedings of The 27th Arctic and Marine Oilspill Program (AMOP) Technical Seminar*, Ottawa, Ontario, Canada, Jul. 2004, pp. 551–558.

Chapter 3

Relationships in Gas Chromatography–Fourier Transform Infrared Spectroscopy — Comprehensive and Multilinear Analysis

Junaida Shezmin Zavahir, Jamieson S. P. Smith, Scott Blundell, Habtewold D. Waktola, Yada Nolvachai, Bayden R. Wood and Philip J. Marriott

Published in: *Separations* Volume 7 – Issue 2, June 2020

Contents

3.1	Chapter synopsis.....	105
3.2	Graphical abstract published in journal issue	108
3.3	Article	109
3.4	Published supplementary material.....	126
3.5	Invited cover page of the journal issue the article was published in	137

3.1 Chapter synopsis

The work presented in this Chapter explores the various functional relationships in gas chromatography–Fourier transform infrared spectroscopy (GC–FTIR), using the in-house designed hyphenated GC–FTIR flow transfer system consisting of a light-pipe interface explained in Chapter 2. As amply highlighted in Chapter 1 and Chapter 2, FTIR spectroscopy complements mass spectrometry (MS) in the task of compound identification with the ability of FTIR to confirm functional groups as well as distinguish structural isomers which have identical or indistinguishable mass spectra. This instrumental arrangement, which also has GC–MS (as well as GC–FID) capabilities, is used to exemplify both the qualitative as well as quantitative abilities of the light-pipe GC–FTIR technique to give a higher confidence in analytical results. Thus, the specificity of FTIR spectra and their aptitude to aid in the precise identification of GC separated components is demonstrated using various compound classes. These include aromatics, essential oils, oximes etc., some of which are used to compare and distinguish isomers with similar mass spectra and their unique FTIR spectra.

The system's capability to conduct flame ionisation detection either directly (GC–FID) or sequentially (GC–FTIR–FID) is taken advantage of to assess the influence of varying chromatographic parameters on the chromatographic peak profile of GC effluents, which allows direct comparison of the arrangements with regard to peak widths and heights; this provides a measure of added peak broadening in the light-pipe interface, and by implication, a measure of reduced resolution. By injecting a standards mixture, the identities of GC peaks are confirmed by gas phase IR library matching, or by adding spectra of authentic compounds to the library. FTIR spectra present a 'molecular fingerprinting' feature as a result of the complex yet unique spectral band pattern they present – a result of discrete vibrational and rotational absorption bands. This feature is employed in the GC–FTIR system to study co-eluting essential oil isomers which have similar MS spectra, which would therefore render mismatches in MS library searches in GC–MS analysis. Although multidimensional GC methods have been amply used to study such essential oil isomers, one-dimensional GC separation of such isomer entities, when they co-elute on a GC column, remains a challenge. The light-pipe GC–FTIR system successfully overcomes this challenge by recording the distinctive FTIR spectra on either

side of the apex of a deliberately co-eluted single unresolved chromatographic peak consisting of two essential oil isomers using the example of *p*-cymene and limonene.

The early historical enthusiasm surrounding GC–FTIR of perhaps 30+ years ago lead to a dwindle with the more fast-paced development of MS techniques, which in turn led to a decline in the adoption of FTIR as a GC detector; the clear need for additional confirmation of chemical compounds in GC was apparent. But this trend appears to be reversing with the recognition of the identification power of FTIR as well as the on-going improvements in system sensitivities, interface techniques and data processing capabilities. An example of such an improvement is set forth in this Chapter where we explore the ability of combining GC and FTIR data to present a ‘comprehensive’ style analysis procedure referred to as the ‘GC×FTIR’ approach. This recent development in exploiting the value of the hyphenated GC–FTIR technique is used to observe on-column interconverting oxime species with the ability to view the peak profiles of individual oxime entities within its characteristic peak envelope. The resulting two-dimensional colour contour plot presentation of spectrum intensity is achieved by plotting the whole spectrum for each retention data point, aligning results along the retention time axis with the respective spectrum intensities on the *z* axis to obtain a comprehensive overview of the spectroscopic/separation information. This to the best of our knowledge is the first time multidimensional separation using the GC×FTIR approach has been used with one-dimensional GC–FTIR for studying interconverting oxime isomer species. The value and novelty of using GC–FTIR in analysing such oxime species is delved into deeper in Chapter 4.

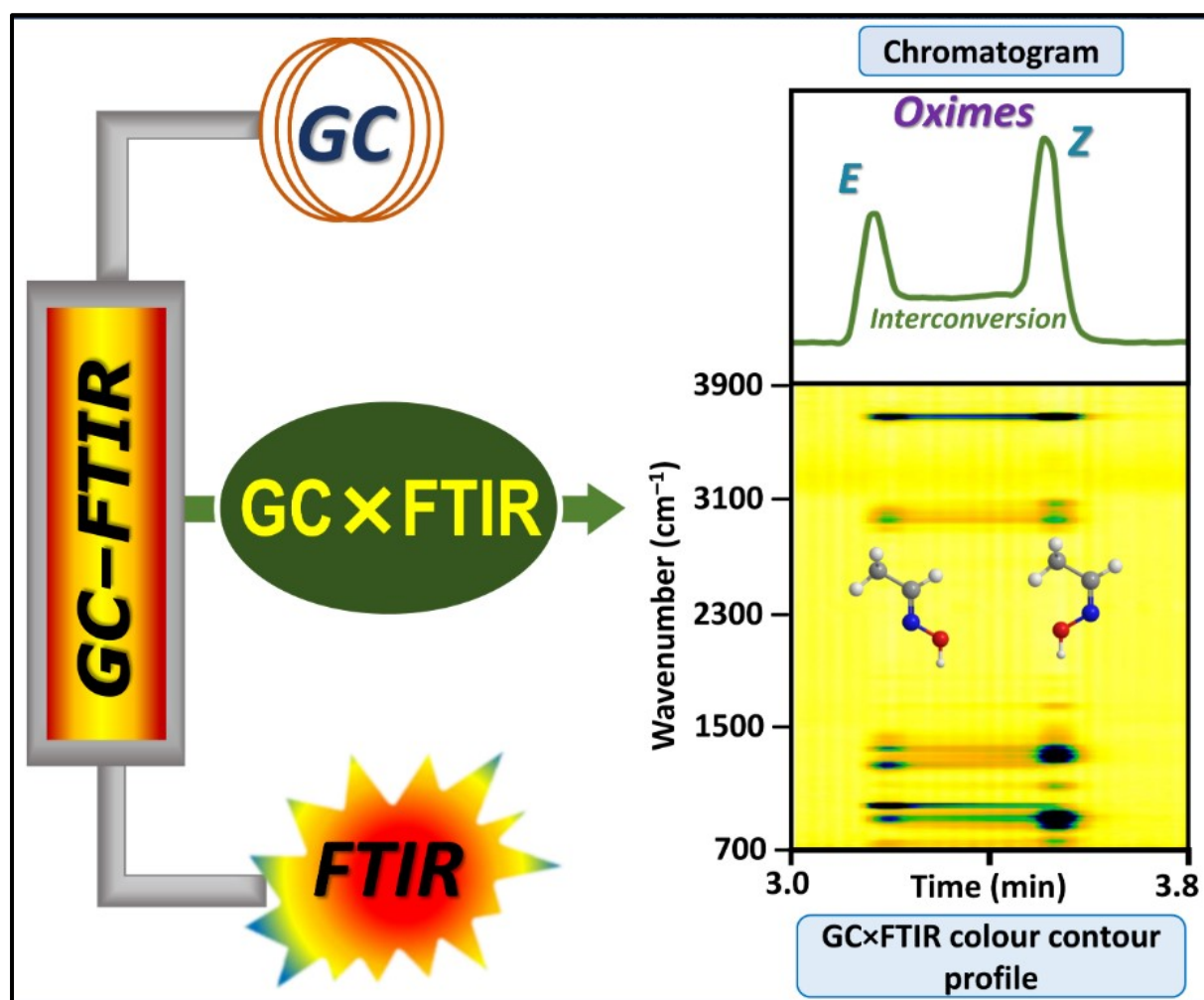
The Chapter also confirms the quantitative analysis capability of light-pipe GC–FTIR systems and goes beyond the conventional approach of univariate quantitation to adapt a multivariate analysis of co-eluting isomers. The system is validated for univariate quantitation using peak area and peak absorption maxima. This is followed by the development of a multivariate model using the partial least square regression (PLSR) technique to assess multiple variables of the FTIR spectrum, which is then used to predict the response to varying analyte concentrations as exemplified with co-eluting *m*- and *p*-cresol isomers.

This Chapter thus helps to reiterate the power of the hyphenation of GC and FTIR using a light-pipe interface system to yield reliable results in a wide range of samples. This has

been published in the form of an article in the peer-reviewed journal *Separations*. The graphical abstract of this published article, the published article and the published supplementary material together with the invited cover page for the respective journal issue, is presented as follows.

3.2 Graphical abstract published in journal issue

Separations Volume 7 – Issue 2, June 2020



3.3 Article

Relationships in Gas Chromatography—Fourier Transform Infrared Spectroscopy—Comprehensive and Multilinear Analysis

Junaida Shezmin Zavahir, Jamieson S. P. Smith, Scott Blundell, Habtewold D. Waktola, Yada Nolvachai, Bayden R. Wood and Philip J. Marriott

Published in *Separations* Volume 7 – Issue 2, June 2020



Article

Relationships in Gas Chromatography—Fourier Transform Infrared Spectroscopy—Comprehensive and Multilinear Analysis

Junaida Shezmin Zavahir ¹, Jamieson S. P. Smith ¹, Scott Blundell ², Habtewold D. Waktola ¹, Yada Nolvachai ¹, Bayden R. Wood ³ and Philip J. Marriott ^{1,*}

¹ Australian Centre for Research on Separation Science, School of Chemistry, Monash University, Wellington Road, Clayton, Melbourne, VIC 3800, Australia; junaida.ismail@monash.edu (J.S.Z.); jamiesonspsmith@gmail.com (J.S.P.S.); habtewold.waktola@monash.edu (H.D.W.); yada.nolvachai@monash.edu (Y.N.)

² Monash Analytical Platform, School of Chemistry, Monash University, Wellington Road, Clayton, Melbourne, VIC 3800, Australia; scott.blundell@monash.edu

³ Centre for Biospectroscopy, School of Chemistry, Monash University, Wellington Road, Clayton, Melbourne, VIC 3800, Australia; Bayden.Wood@monash.edu

* Correspondence: Philip.Marriott@monash.edu; Tel.: +61-3-9905-9630; Fax: +61-3-9905-8501

Received: 13 April 2020; Accepted: 8 May 2020; Published: 13 May 2020



Abstract: Molecular spectroscopic detection techniques, such as Fourier transform infrared spectroscopy (FTIR), provides additional specificity for isomers where often mass spectrometry (MS) fails, due to similar fragmentation patterns. A hyphenated system of gas chromatography (GC) with FTIR via a light-pipe interface is reported in this study to explore a number of GC–FTIR analytical capabilities. Various compound classes were analyzed—aromatics, essential oils and oximes. Variation in chromatographic peak parameters due to the light-pipe was observed via sequentially-located flame ionization detection data. Unique FTIR spectra were observed for separated mixtures of essential oil isomers having similar mass spectra. Presentation of GC×FTIR allows a ‘comprehensive’-style experiment to be developed. This was used to obtain spectroscopic/separation profiles for interconverting oxime species with their individual spectra in the overlap region being displayed on a color contour plot. Partial least square regression provides multivariate quantitative analysis of co-eluting cresol isomers derived from GC–FTIR data. The model resulted in an R^2 of 0.99. Prediction was obtained with R^2 prediction value of 0.88 and RMSEP of 0.57, confirming the method’s suitability. This study explores the potential of GC–FTIR hyphenation and re-iterates its value to derive unambiguous and detailed molecular information which is complementary to MS.

Keywords: GC–FTIR; light-pipe interface; isomers; GC×FTIR; oximes; PLSR; spectroscopic detector

1. Introduction

The separation and precise identification of components in complex samples is a desirable goal of many analytical chemists. Capillary gas chromatography (GC) supports this goal through high separation efficiency and is capable of both quantitative and qualitative analysis of volatile and semivolatile compounds. Confirmation of identity of GC-separated components rely largely upon the use of suitable detection technologies, although retention time invariance compared with authentic standards and use of retention indices also support identification. Amongst various detection technologies used are a range of ionization-based detectors [1], of which the flame ionisation detector (FID) is the most popular (but does not, *per se* provide identification) and spectroscopic technique-based detectors. The latter includes infrared (IR), nuclear magnetic resonance (NMR; off-line), flame

photometry, chemiluminescence and the recent commercially-developed vacuum ultraviolet (VUV) detector [2]. The online combination or hyphenation, of suitable detectors to GC has over the years brought new dimensions of identification to separation science [3].

The hyphenation of mass spectrometry (MS) to GC (GC–MS), has superseded many other detection techniques, due to its use of the highly ‘informing’ MS detector [4]. MS detection is based on the mass-to-charge ratio (m/z) of molecular and fragment ions of compounds, which can operate as a universal (in its total ion mode) or selective (in its single-ion mode) detector. This makes the MS a powerful tool with excellent selectivity and sensitivity, supported by the widespread availability of MS spectrum reference libraries [5]. These characteristics, however, conceal some erroneous measurements and interpretations arising from MS detection [6]. One main shortfall of MS is poor differentiation of molecules with similar fragmentation patterns [7], the reduced ability of MS to distinguish between, for example, diastereomers and positional isomers and information on functional groups and their position(s) within a molecule. This might be expressed as a need for caution of over-reliance on MS for molecular identification. These limitations suggest other detection techniques, such as spectroscopic tools, may play a support role for correct interpretation of compound identity. This has been re-confirmed recently by various studies conducted using GC–vacuum ultraviolet systems on a range of samples which have exemplified its capabilities to boost confidence in results [4], especially in instances where GC–MS is challenged by isomer differentiation. A recent review article amply demonstrates the complementary nature of molecular spectroscopic detection techniques to MS detection in GC to yield information-rich results [2].

Hyphenation of Fourier transform infrared (FTIR) spectroscopic detection to GC (GC–FTIR), provides unique spectra of eluted GC compounds based on the molecule’s various rotational and vibrational energy states [8]. These molecular absorbances have distinct IR frequencies, so GC–FTIR instruments impart information related to the functional groups and arrangement of atoms in molecules. Thus, FTIR detection boasts a molecular ‘fingerprinting’ ability, not available to MS, despite the relatively lower sensitivity of FTIR compared to MS. This places FTIR at an advantage in structural elucidation studies. FTIR detection is also non-destructive and universal, can be operated in series with other detectors and can be used for both selective and specific detection [9,10]. Its obedience to the Beer-Lambert law allows for quantitative analysis of data.

GC–FTIR is commonly implemented via one of three interface types. Two types – matrix-isolation and direct-deposition interfaces – use a trapping medium to concentrate and immobilise the GC effluent. The condensed phase GC–FTIR system has gained popularity in recent years for structural elucidation studies [11], with reportedly improved detection limits. The third, a light-pipe (LP) interface, offers on-line real-time detection. The characteristic IR absorption of GC eluted analytes is obtained by separation of sample components, with ideally sufficient resolution to obtain single compounds in the LP. Here, the GC column effluent passes into a heated gold-coated borosilicate glass flow cell into which the FTIR instrument’s light passes through KBr windows at either end of the cell, to provide complete vapour phase IR spectra.

IR spectroscopy can distinguish functional groups but may fail to adequately differentiate homologous series; MS may distinguish homologues and molecular masses, yet may be unable to adequately differentiate isomers. Use of MS with FTIR, with complementary detection capabilities, may be used simultaneously or sequentially for significantly improved identification of components in GC effluents. FTIR’s competence in hyphenation with other detectors in GC [3], allows integration of MS and FTIR for assignment of analyte structures and benefits complex mixture analysis [12]. These techniques can be applied by use of separate GC–MS and GC–FTIR instruments or as a hyphenated GC–FTIR/MS system [13–16]. However, GC–FTIR has not attained the same level of adoption as GC–MS due to performance criteria which include; (1) lower sensitivity compared to MS, (2) inferior dynamic detection range compared to MS, (3) relatively difficult quantification and (4) extensive MS databases available for component identification [17]. Limited access to libraries may also reduce GC–FTIR’s attraction. Yet the value of complementarity of GC–MS and GC–FTIR data

must be emphasised; comprehensive identification applications include pharmaceuticals, petroleum hydrocarbons, fatty acids, essential oils, Li-ion battery degradation, polymers and plastics [2].

The value of GC–FTIR as a useful technique was further validated in recent studies that investigated elution profiles of individual isomers of oximes that undergo characteristic on-column interconversion in GC (dynamic GC). Unambiguous identification and elution order of *E* and *Z* isomers were obtained [18].

In this study, an integrated light-pipe GC–FTIR for real-time spectroscopic detection of compounds, together with GC–FID and GC–MS capability for comparative interpretation, was developed. A variety of analyses were conducted, in general to establish qualitative and quantitative relationships of retention, concentration and response using the FTIR detector. The ability of GC–FTIR to differentiate chemical structures for resolved compounds was contrasted with GC–MS data and was also extended to unresolved compounds. The extra peak dispersion of the chromatographic peak arising from the LP interface was estimated by using the response of sequential FID detection. The system was tested for identification, quantification and peak deconvolution by using FTIR of different compounds and classes, such as aromatic essential oils and positional isomers, as detailed in the materials and methods section. Novel applicability of GC–FTIR for two-dimensional separation approaches presented as GC×FTIR retention/response data allowed clear display of the overlapping molecular interconversion isomers of oximes. Finally, multivariate analysis of overlapping *m*- and *p*-cresol isomer analysis permitted reliable identification and quantification of *m*-cresol.

2. Materials and Methods

2.1. Instrumentation

A PerkinElmer Clarus 680 GC with a flame ionisation detector (FID) hyphenated to a SQ 8T mass spectrometer (PerkinElmer Inc., Shelton, CT, USA) controlled by a PC (PC–1) was used for chromatographic analysis. For FTIR, a PIKE interface accessory (PIKE Technologies, Madison, WI, USA) consisting of a temperature (*T*) controllable gold coated 120 mm path-length × 1 mm I.D. heated gas cell (light-pipe; LP) and 13 mm diameter × 2 mm thick KBr windows at either end, with a narrow band mercury-cadmium-telluride (MCT) detector cooled to −196 °C by liquid N₂, was used. The PIKE accessory was located a few cm from the right hand side panel of the Clarus 680 GC, which was customised by drilling of an opening into the side of the GC shroud and oven and installation of a short length of stainless-steel transfer sleeve (tubing) of 300 mm length × 1.59 mm I.D. through which the transfer column passes. The insulated transfer line (TL) is ca. 5.7 cm cross-section, with a controllable *T* heating element. The accuracy of *T* control was ±1 °C for the TL and LP. A PerkinElmer Frontier SP8000 Fourier transform IR (PerkinElmer Inc., Bucks, UK) with a mid-infrared source, connected to the LP interface, was used as the IR source. FTIR data acquisition was controlled by a separate PC (PC–2) which was connected to a trigger mechanism for timing purposes initiated by the GC injection.

2.2. Standards and Sample Preparation

Standards of *ortho*-, *meta*- and *para*-cresol (*o*-, *m*-, *p*-; >99.9% purity) and ethylbenzene (>99.9% purity) were purchased from Tokyo Chemicals Industry Co., Ltd., (Tokyo, Japan). Nonane, acetaldehyde oxime (acetaldoxime; 99%) and propionaldehyde oxime (≥96%) were purchased from Sigma-Aldrich Co., (St. Louis, MO, USA). Essential oil standards (~95%) of α -pinene, β -pinene, γ -terpinene, limonene, *para*-cymene (*p*-cymene), geraniol and eugenol were gratefully provided by Australian Botanical Products Pty. Ltd. (Hallam, Australia). Solvents used were dichloromethane (DCM) (≥99.8% purity), *n*-hexane (≥98.0% purity) and acetone (99.8% purity) purchased from Merck KGaA, Darmstadt, Germany and methanol (99.9% purity) purchased from Scharlab S.L., Spain. Stock solutions were prepared from the above standards and further diluted to obtain working solutions. *n*-hexane was used for ethylbenzene and essential oils and DCM was used for cresols, nonane and oximes. For oxime analysis a 20% (v/v) sample of acetaldehyde oxime and propionaldehyde oxime was prepared in acetone with 250 μ L of 20% (v/v) butan-1-ol (99.5%, Merck, Kilsyth, Australia) as an internal standard.

2.3. Conditions

A PerkinElmer Elite-5MS column (30 m \times 0.25 mm I.D. \times 0.25 μ m d_f ; Shelton, CT, USA) connected injection port A to the MS. An SGE BPX5 column (30 m \times 0.25 mm I.D. \times 0.25 μ m d_f ; Ringwood, Australia) connected injection port B, with the column outlet joined to a deactivated fused silica (DFS) transfer line column (1 m \times 0.25 mm I.D., Agilent Technologies, Mulgrave, Australia) using a universal Press-Tight connector (Restek, Bellefonte, PA, USA), which in turn was connected to the LP inlet. Another DFS transfer line column (1 m \times 0.25 mm I.D., Agilent Technologies, Mulgrave, Australia) connected the LP outlet to the FID. Both inlet and outlet transfer line columns were housed within the insulated TL. A separate configuration connected the analytical column outlet to the FID using a DFS transfer line ensuring the total column length of both configurations remained the same. For oxime analysis a HP-INNOWax (30 m \times 0.32 mm I.D. \times 0.5 μ m d_f ; Agilent Technologies) column consisting of a polyethylene glycol (PEG) stationary phase was connected to injection port B, through the LP as above.

Experiments were carried out using the following operational conditions (unless stated otherwise). Injection volumes were 1 μ L for essential oils and 1.5 μ L for cresol isomer comparison, signal-to-noise ratio (SNR) observations and ethylbenzene calibration. Injections (2 μ L) were made for GC \times FTIR analysis and cresol calibration. Injections were made at 250 $^{\circ}$ C with split ratios of 2:1 for essential oil analysis, 20:1 for SNR observations and 10:1 for all other GC analyses. The carrier gas was He (99.999%) in constant flow mode with 2.0 mL min $^{-1}$ column flow rate for essential oil analysis, 3.0 mL min $^{-1}$ for oxime analysis and 1.0 mL min $^{-1}$ for all other analyses. T programs for the oven had an initial T of 100 $^{\circ}$ C for essential oil analyses and 50 $^{\circ}$ C for all other analyses, with T ramps of 5 $^{\circ}$ C min $^{-1}$ or 10 $^{\circ}$ C min $^{-1}$ as specified in each section. Oximes were analysed at an isothermal temperature of 110 $^{\circ}$ C. MS parameters were electron ionisation (EI) mode with 70 eV ionisation energy, 200 $^{\circ}$ C source T and 20–500 u mass range.

The TL and LP T s were thermostated between 100 $^{\circ}$ C and 300 $^{\circ}$ C (to prevent condensation of semi-volatile compounds within the LP flow cell interface) whilst ensuring these T s were maintained at least 10 $^{\circ}$ C more than the maximum T of the GC oven program. Real time spectra were recorded in the wavelength range of 4000–700 cm $^{-1}$ with weak apodization and 100 background scans. Optical resolutions of either 4 or 8 cm $^{-1}$ were used. Scan speed was 1 cm s $^{-1}$, which corresponds to data acquisition rates of 0.92 spectra s $^{-1}$ (0.92 Hz) at 4 cm $^{-1}$ and 1.68 spectra s $^{-1}$ (1.68 Hz) at 8 cm $^{-1}$.

2.4. Software

PerkinElmer TurboMass v6.1.0.1963 (PerkinElmer, Inc., Shelton, CT, USA) on PC–1 was used for GC and MS data. PerkinElmer Timebase v6.1.0.1963 (PerkinElmer, Inc., Bucks, UK) was used for FTIR data acquisition and PerkinElmer Spectrum v10.4.2.27 (PerkinElmer, Inc., Bucks, UK) for FTIR spectrum processing, both using PC–2. MS and FTIR library searching was conducted using National Institute of Standards and Technology (NIST) 2011, the Fluka IR library (library supplied by PerkinElmer Inc.) and the IR vapour phase library by Nicolet Corp. Matlab R2019a v9.6.0.1072779 (The Mathworks, Inc., Natick, MA, USA) and Partial Least Square Toolbox (Eigenvector Research Inc., Wenatchee, WA, USA) were used for chemometric data processing.

3. Results and discussion

3.1. Chromatographic Peak Variations

The instrument used in this study couples the GC and FTIR instruments via a light-pipe interface where IR radiation from the source is focussed onto the LP/carrier stream and the emerging beam is refocused onto the detector. Supplementary information Figure S1 shows a schematic of the GC/PIKE interface/FTIR source instrumental setup and an enlarged view of the effluent flow path and IR beam path within the LP interface. Being non-destructive, after acquisition of FTIR data, carrier flow can be directed to other detectors such as FID or MS. The reflective gold coating of the heated flow-through LP confers multiple internal reflection thereby increasing the practical cell length, which in turn maximises sensitivity (and also minimises reactivity). Use of a LP offers real-time analysis of GC

effluent, simple design and least complexity of operation compared to other interfaces [19] as well as spectrum matching to vapour-phase IR libraries. Minimal solute–solute interference (i.e., by ensuring adequate resolution) in the LP results in vapour phase IR spectra with sharp spectral features [20].

Resolution of components achieved on the GC column can be degraded due to the re-combination of the FTIR response of closely separated components, within the mixing volume of the LP and connecting tube(s) [21]. The flow cell volume of 120 mm length with 1 mm I.D. may be comparable to the average peak volume of capillary GC columns [9]. These dimensions are critical so as not to excessively reduce chromatographic resolution without compromising chromatographic peak distortion and maximising IR sensitivity [10]. A key consideration to designing the system was to use a short TL to minimise dead volume.

The current in-house designed system which allows post-light-pipe FID analysis was used to determine the influence of the LP on peak shape and width. A standard test mixture of 2-butanol, 2-pentanone, 1-nitropropane and *m*-xylene in DCM solvent was injected into the GC with two configurations and were chosen for their good chromatographic peak shape. Individual compound injection confirmed their elution order, further checked by library matching (Section 2.4) of the corresponding GC-FTIR spectra at each peak's maxima, as reported in Supplementary information Table S1. Consistent correlation of the library match with the given injected isomer was observed, with only one dissenting match, being for the third match for 1-nitropropane erroneously matched to nitroethane; alkyl chain homologue matching may be less specific for FTIR, although for this small dataset matching appears good. Comparisons were done on two setups as outlined in Supplementary information Figure S1, where (a) the terminal end of the analytical column was connected directly to the FID (GC-FID) and (b) the LP outlet was connected to the FID (GC-FTIR-FID). The total column length remained the same for both configurations. The overlaid chromatograms for the same test mixture separately injected on the two configurations at 50 °C and at varying split ratios and temperature ramps is given in Figure 1.

Retention times and full width half maximum (FWHM) values for the chromatograms of Figure 1 are presented in Table 1. These values were not calculated for the solvent peak (peak 1) due to its high concentration.

Table 1. Comparison of GC chromatographic FID peaks between direct FID and post-light-pipe FID results at various split ratio and temperature ramp combinations. Retention times and full width half maximum (FWHM) values are presented for peaks 2 to 5 depicted in Figure 1. Peaks 2, 3, 4 and 5 correspond to the compounds 2-butanol, 2-pentanone, 1-nitropropane and *m*-xylene respectively.

Conditions	Peak no.	GC-FID t_R (min)	GC-FTIR-FID t_R (min)	t_R Difference (min)	GC-FID FWHM (min)	GC-FTIR-FID FWHM (min)
A. split 100:1 ramp 10 °C min ⁻¹	2	2.81	2.78	0.03	0.023	0.064
	3	3.25	3.23	0.02	0.026	0.061
	4	3.72	3.70	0.02	0.045	0.073
	5	5.20	5.17	0.02	0.038	0.069
B. split 10:1 ramp 5 °C min ⁻¹	2	2.97	2.96	0.01	0.061	0.074
	3	3.59	3.58	0.00	0.078	0.079
	4	4.37	4.35	0.02	0.131	0.140
	5 [#]	6.64	6.68	−0.04	0.155	0.139
C. split 20:1 ramp 5 °C min ⁻¹	2	2.97	2.93	0.03	0.040	0.070
	3	3.58	3.56	0.02	0.049	0.072
	4	4.32	4.29	0.03	0.096	0.114
	5	6.64	6.62	0.01	0.095	0.108

[#] Overloaded peak.

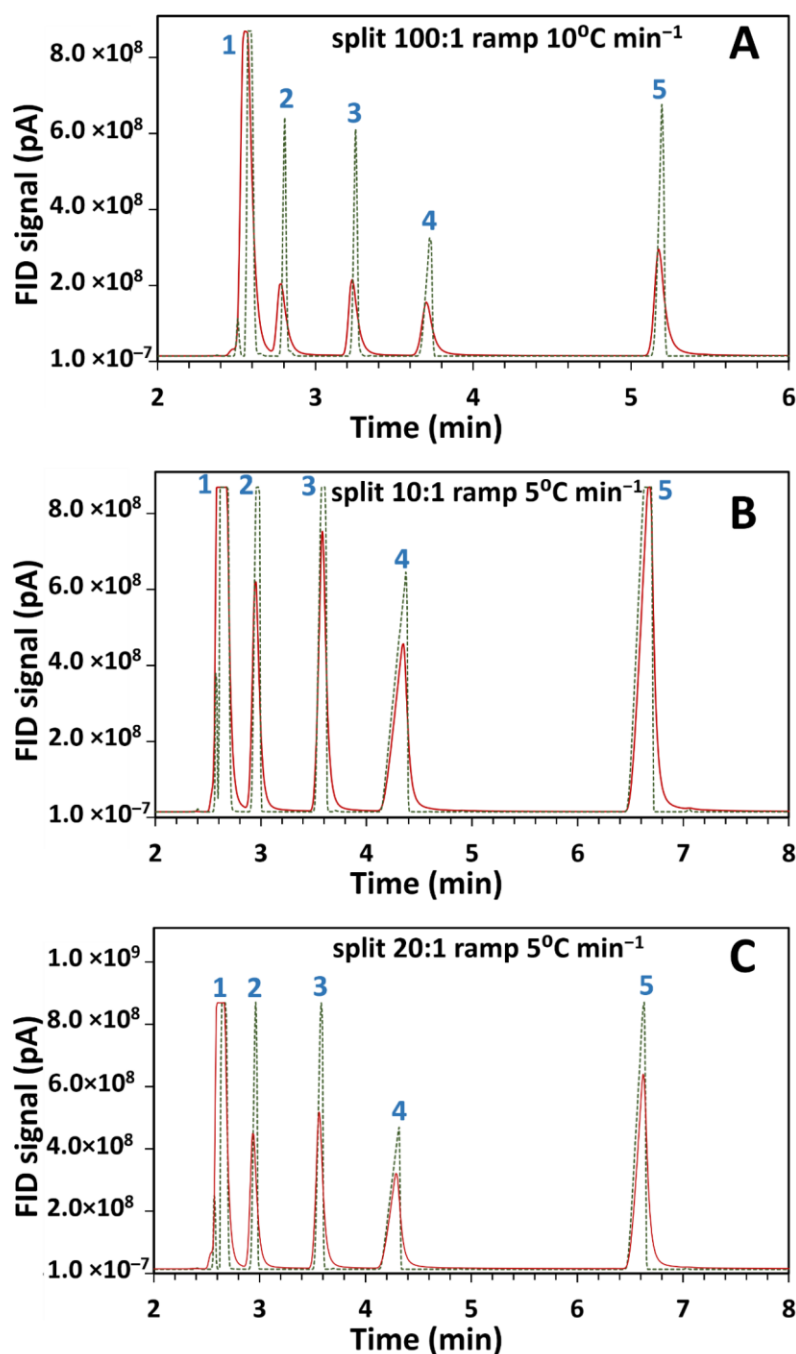


Figure 1. Comparison of flame ionisation detector (FID) results for overlaid chromatograms of gas chromatography-Fourier transform infrared-FID (GC–FTIR–FID) (continuous line) and GC–FID (dotted line) using a standard component mix injected at 50 °C and analyzed with different split ratios and temperature ramps as (A) 100:1, 10 °C min⁻¹, (B) 10:1, 5 °C min⁻¹, and (C) 20:1, 5 °C min⁻¹. Components corresponding to the peaks are (1) dichloromethane (DCM) (solvent peak), (2) 2-butanol, (3) 2-pentanone, (4) 1-nitropropane and (5) *m*-xylene.

Comparison of peak widths between the two setups revealed an observed reduction in peak height and concomitant peak broadening in the GC–FTIR–FID configuration. In light-pipe GC–FTIR this could be ascribed to the dispersion of the chromatographic peak within the volume of the LP. Excessive band broadening can reduce separation efficiency resulting in poorer resolution in chromatographic systems. However, FTIR spectra in the gas phase display reduced spectral band broadening compared

to those in condensed- or liquid-phases. Although gas-phase spectra are less common in literature than liquid-phase spectra, they are less confusing to interpret since the latter may contain multiple narrow bands within a broad band. From Figure 1A, the light-pipe contributes about a two-fold increase in peak width.

Effect of Varying Parameters on Signal-to-Noise (SNR) Ratio

The importance of having good signal-to-noise-ratio (SNR) in optical systems is not to be underestimated. The SNR determines the sensitivity of an instrument and relates to the measurement precision [22]. Attempts to improve SNR in LP GC–FTIR systems include optimising volume/length ratios to minimise chromatographic peak broadening [23], variations in the optical configurations [24], introduction of rapid scanning interferometers [25] and the use of suitable low-noise detectors [26]. The photoconductive liquid-nitrogen-cooled MCT detector used here, is well suited for LP measurements because of its sensitivity being almost two orders of magnitude greater than its pyroelectric predecessors [27]. The LP (and TL) needs to be maintained at a T sufficiently high to prevent condensation of GC solutes. High T has disadvantages by contributing to the LP acting as an IR source and increasing the intensity of the unmodulated radiation [28], which in turn could negatively affect the linear response of the MCT detector and the SNR [29].

This system's ability to maintain measurement with a good SNR was validated where LP (and TL) T were raised in 40 °C increments (120, 160, 200, 240 and 280 °C) to monitor its effect on SNR. The resulting root mean square (RMS) intensity of absorbance as a function of time is illustrated in Supplementary information Figure S2 for each LP T setting and is seen to increase with T . SNR was calculated by taking the ratio of the peak height of the 2936 cm^{-1} C–H stretch (signal) against the peak-to-peak noise of the 2200–2000 cm^{-1} region. This wavelength range was chosen as it displays the greatest single beam intensity [22]. A plot of this SNR against increasing LP T is illustrated in Supplementary information Figure S3A. The negative trend with T is consistent with prior studies on LP T effect on SNR, with the SNR in some GC–FTIR systems was seen to decrease by a factor of up to 10 with an increase of LP T up to 300 °C [28]. Thus, the LP should be maintained at as low a T as possible, consistent with ensuring no condensation in the LP.

Similarly, the effect of variations in FTIR resolution and carrier gas flow on SNR was validated. GC requires rapid data acquisition and adequate interferometer scan rates (i.e. number of sampling data points) to avoid chromatographic resolution degradation whilst providing sufficient GC peak characterisation ability. Supplementary information Figure S3B depicts the SNR trend for spectra collected under increasing optical resolution settings of 0.5, 1, 2, 4, 8, 32 and 64 cm^{-1} . The band broadening evident for lower resolution scans such as 64 cm^{-1} (and the high scan speed required by higher resolution) depicted in Supplementary information Figure S3D confirms the suitability of using spectral resolutions of 4 cm^{-1} or 8 cm^{-1} in routine use. The carrier gas flow conditions have an effect on migration of zones along the GC column [30] and variations in this affect the retention time of chromatographic peaks and peak widths. SNR was plotted as a function of carrier gas flows of 1.0, 1.5, 2.0 and 2.5 mL min^{-1} . As expected, increases in carrier gas flow contributed to progressively shorter analysis times and reduced retention times of the compound as evident in Supplementary information Figure S3E. This however was accompanied by a progressive reduction in SNR as seen in Supplementary information Figure S3C. Further, due to the sequential arrangement of FTIR and FID detection, the retention time of the same peak in GC–FTIR and GC–FID differed slightly as would be expected and is depicted in Supplementary information Figure S4.

LP-based spectrum bands are quite broad and most vapour-phase spectra of molecules have a bandwidth of at least 10 cm^{-1} . This minimises the necessity for measuring spectra at high resolutions, with GC–IR spectral measurements at 4 or 8 cm^{-1} resolution sufficing [31]. This can result when FTIR spectrometers measure 5–20 interferograms when operated in their highest scan speed.

3.2. Co-Eluting Isomer Analysis

The popularity of GC–MS for the analysis of complex mixtures has been unsurpassed due to its ease of use, applicability to multiple analytes, superior analyte detectability and identification capability based on mass spectrum libraries [32,33]. Its inability to differentiate isomers, which have almost identical mass spectra, has been amply discussed in literature [17,34]. MS data for such isomers can be ambiguous, resulting in similar fragmentation patterns from the molecular ion. In contrast, discrete vibrational and rotational absorption bands [35] in localised positions in FTIR spectra give rise to unique spectra, rendering a “fingerprinting” role, which can correlate to structural characteristics of the GC effluent molecules. Preliminary studies using *o*-, *m*- and *p*-cresol isomers validated the ability of this system to demonstrate the complementary nature of GC–MS and GC–FTIR as shown in Supplementary information Figure S5.

Essential oils consist of compounds that belong to diverse classes of compounds with various functional groups and structures [36], some of which may also have different isomeric forms. They include compounds including those with unsaturated bonds, branched and cyclic compounds, as well as oxygenated analogues. GC–FTIR spectra of selected essential oil standard compounds were obtained to validate the system’s applicability in identifying isomeric compounds that have similar mass spectra. Resulting GC–FTIR spectra of the essential oils geraniol, eugenol, limonene, α -pinene, β -pinene and γ -terpinene are depicted in Supplementary information Figure S6(A–F respectively) showing characteristic absorption bands in both functional and fingerprint regions. Ambiguities arising from the similarities in mass spectra of isomeric compounds, here α -pinene, β -pinene and γ -terpinene [Figure S6(G–I)], yield mismatches in library searches rendering a failure in MS identification. This can be resolved using the distinct FTIR spectra of these essential oils [Figure S6(D–F) respectively]. This complementary identification of FTIR and MS is a valuable tool in the characterisation of isomeric essential oil compounds in both one-dimensional and multidimensional GC.

Many components in essential oils overlap in GC analysis due to the similarity in their retention indices. It is common to require essential oils to be analysed on two complementary stationary phases in order to calculate retention indices on each phase to aid in identification. Thus, the analysis of essential oils depends on both successful separation as well as identification of their components. The strategy of using a combination of detection methods benefits the identification and evaluation of such similar compounds [37]. Although the separation of essential oils can be improved by the use of multidimensional GC [38], separation of most co-eluting essential oils on one-dimensional GC remains a challenge.

The ability to use this system to separately observe the spectra of the coeluting essential oils *p*-cymene and limonene on a single dimension was confirmed. *p*-cymene and limonene were mixed in the ratios of 1:9, 2:8, 3:7, 4:6, 5:5, 6:4, 7:3, 8:2 and 9:1 in hexane. Solutions of only *p*-cymene and limonene were also prepared in hexane and analysed. A single unresolved chromatographic peak was observed for both components as a result of deliberate coelution (Figure 2B). The spectrum on each side of the peak apex (Figure 2A) corresponding to a 0.04 absorbance (i.e., at 3.49 and 3.74 min, Figure 2C) was extracted and a library search conducted on each spectrum. In each instance of the different ratio mixtures, *p*-cymene was observed to be the early eluting isomer and limonene eluting as the later isomer. For example, in the sample of 5:5 limonene to *p*-cymene, the spectrum at 3.49 mins gave a search score of 0.87 for *p*-cymene and the spectrum at 3.74 mins gave a result of limonene with a search score of 0.95.

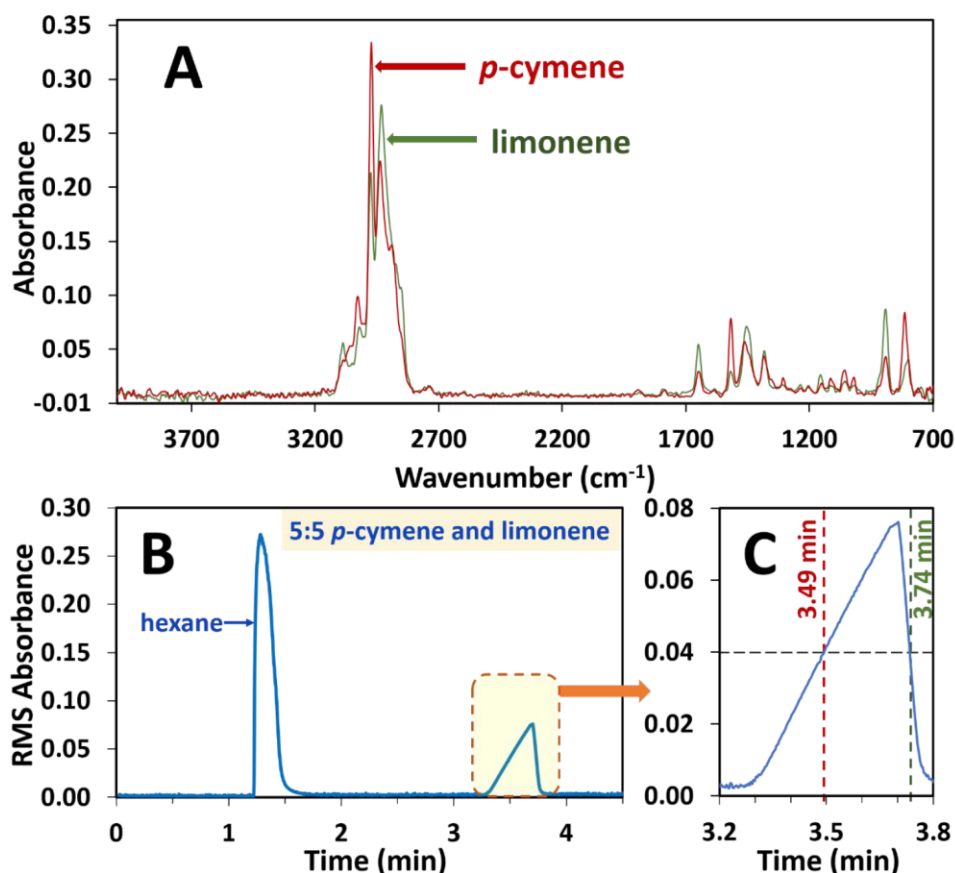


Figure 2. Depiction of extraction of spectra at 0.04 RMS absorbance intensity of the single unresolved chromatographic peak due to co-eluting components in a 5:5 ratio mixture of *p*-cymene and limonene essential oil standards. *p*-cymene and limonene often overlap on GC columns and are deliberately overloaded here to illustrate the power of FTIR to deconvolute overlapping peaks. (A) Spectrum of *p*-cymene at 3.49 min and spectrum of limonene at 3.74 min, both at 0.04 RMS absorbance. (B) RMS absorbance chromatogram with the overloaded peak, which is enlarged (C) to illustrate the extraction of each spectrum at 0.04 RMS absorbance.

3.3. GC×FTIR Analysis of Oximes

The reversible molecular interconversion, in which chemical species show transformation on the time scale of chromatographic separation, is referred to as dynamic GC (DGC). This invariably involves isomers, which might be rotamers or involve other transformations and the efforts to better differentiate these isomers over the years have included both one-dimensional and multidimensional GC methods [39]. Here, on-column isomerisation ($A \rightleftharpoons B$) results in incompletely resolved peaks which have a characteristic broadening or plateau region between the terminal peaks known as the ‘interconversion region’ (Figure 3B). This has been observed in oximes, imines with the general formula $RR'C=NOH$, where the configuration of substituents around the $C=N$ double bond produces *E* and *Z* isomers. Due to the isomers having similar (equivalent) mass spectra, conventional one-dimensional GC hyphenated to MS fails to separately identify or deconvolute the peak envelope or render information on the distribution of the individual isomers. In contrast the FTIR spectra of these isomers are distinct (Figure 3C). The suitability of light-pipe GC–FTIR for dynamic GC studies of oxime isomers was amply demonstrated in our recent studies [18], where the isomer profiles were traced using absorption bands stronger in each isomer, as well as by chemometric methods.

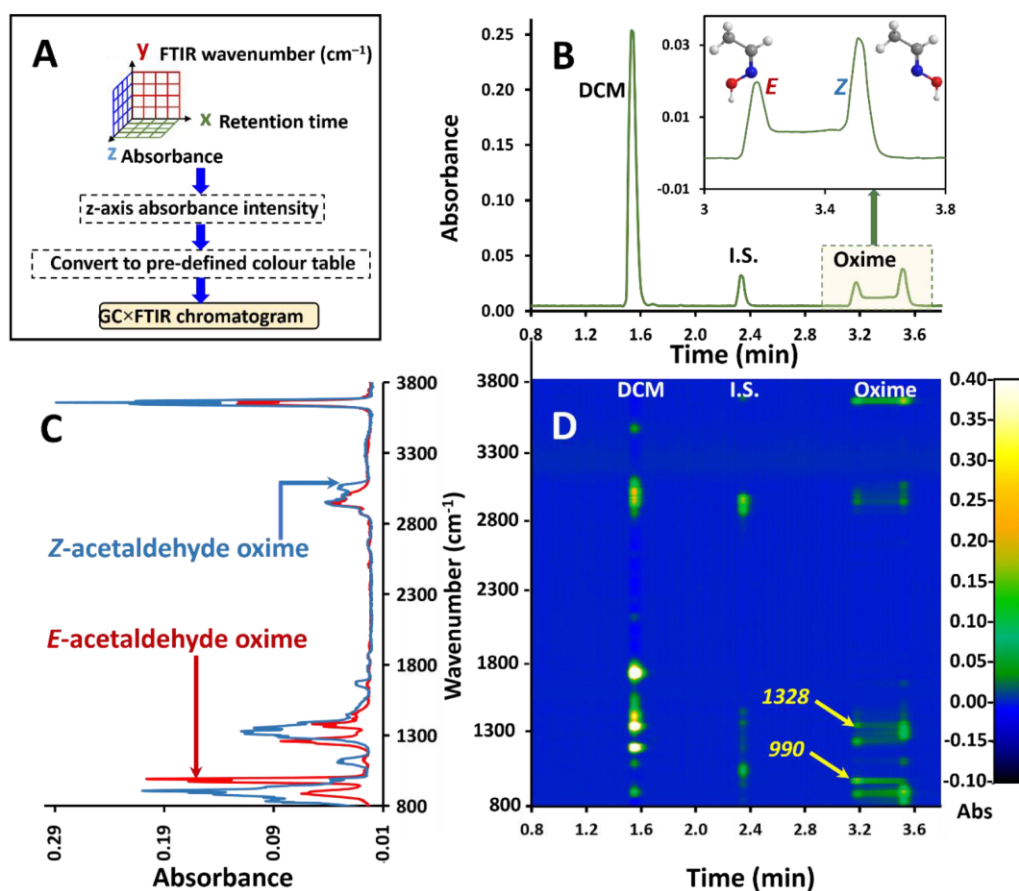


Figure 3. (A) Flow chart of the approach to GC×FTIR. (B) GC–FTIR RMS response profile of interconversion of *E* and *Z* acetaldehyde oximes on the GC PEG phase column. (C) Overlay of corresponding FTIR spectra for *E* and *Z* acetaldehyde oxime acquired from the GC–FTIR experiment. (D) GC×FTIR 2D colour contour profile illustrating absorbance responses for each compound in the time/wavenumber space. Arrows 990 and 1328 refer to the bands at 990 cm⁻¹ and 1328 cm⁻¹ which are stronger and more selective for the *E* and *Z* isomer respectively.

Here we use a GC×FTIR, ‘two-dimensional’ approach, proposed by Wang and Edwards [40] for ‘spectrometric resolution’ of close-eluting C₂-naphthalene isomeric mixtures, to independently trace the two oxime isomers. Whilst multidimensional separations focus on multiple column configurations, the multidimensional analysis system here can also be applied to instances where a detector is used as a separate second dimension to the first dimension GC separation, as proposed for MS where the molecular ion mass corresponds to a mass-domain separation dimension [41]. In a similar manner, Wang [42] recently presented a GC×VUV study of a diesel sample as a 2D analysis approach with VUV data collected over the range 125–430 nm, contrasting the result with GC×GC–FID. Whilst it was concluded that “All structural features are readily visualized in a manner complementary to two-dimensional gas chromatography, GC×GC,” it must be acknowledged that most features will correspond to incompletely resolved components and so represent overlapping VUV spectra.

Thus, GC×FTIR renders a two-dimensional presentation of GC retention time against the FTIR response for chemical species, with its inherent value in isomer mixture resolution. Here, in addition to its ability to detect and identify compounds, the FTIR enables spectrum display in the wavenumber dimension, together with separation in the time dimension by GC. The FTIR result is based on its ability to discriminate/separate functional groups or different component mixtures, based on differences of their absorption band attributes, rather than a physical separation. In conventional GC–FTIR presentation, the root mean square (RMS) of the total absorbance is plotted against retention time.

In GC×FTIR, the whole spectrum for each retention data point is plotted and aligned vertically along the retention time axis, with their respective intensities in the third dimension (perpendicular to the 2D plane). This results in a 3D chromatogram with retention time on the x-axis, FTIR wavenumber on the y-axis and absorbance on the z-axis (or as a 2D contour plot of spectrum intensity) as depicted in the flow chart in Figure 3A. Converting the z-axis to a predefined colour scale renders a 2D plane presentation. The GC×FTIR result is shown in Figure 3D, with the RMS absorbance chromatogram given in Figure 3B and overlaid FTIR spectra given in Figure 3C. The polyethylene glycol (PEG) stationary phase was chosen due to its polar nature which is known to promote interconversion. FTIR spectra were recorded at 4 cm^{-1} resolution. This technique can plot multiple spectra in 3D space as demonstrated using a simple GC application.

Such 2D/3D plots allow for a comprehensive overview of the spectroscopic/separation information achievable by FTIR detection in GC. For instance, it might be of use in determining the purity of compound elution. For example, the band at 990 cm^{-1} is stronger for the *E* isomer (Figure 3D, arrowed, 990) which is confirmed by the contour plot at an elution time of 3.2 min and wavenumber of 990 cm^{-1} . This is accompanied by a decay of the distribution of contour intensity at this wavelength which implies the gradual decrease of the *E* isomer with progressing elution time. Likewise, on Figure 3D, arrow 1328 (more selective for the *Z* isomer) shows an increase in contour intensity of the 1328 cm^{-1} band through to 3.255 min which is the elution time of original injected *Z* isomer. Previous attempts to trace the individual profiles of oximes undergoing dynamic interconversion have used contour plots in multidimensional and comprehensive 2D GC experiments [43,44].

The above discussion corresponds to the acetaldehyde oxime isomer elution. A chromatogram of a mixture of acetaldehyde oxime and propionaldehyde oximes is also depicted in the Supplementary information Figure S7A, displaying the expanded region of oximes to highlight the different bands corresponding to the interconversion regions of the *E* and *Z* isomers together with the corresponding GC×FTIR colour contour plot over the same retention time scale (Figure S7B) and an expanded region (Figure S7C) displaying IR bands corresponding to terminal (a, 4.4 min) and (c, 4.9 min) and an intermediate elution (b, 4.7 min) position of P.O. which shows absorption bands characteristic of both isomers. To the best of our knowledge this is however the first time multidimensional separations and contour plots in the form of a GC×FTIR experiment have been used with one-dimensional GC and FTIR spectroscopy to study isomer distribution of interconverting species. This is of value in recognising co-eluting isomers and suggests where deconvolution of spectra may be used in a simpler operator-friendly manner with a linear GC–FTIR presentation.

3.4. Multivariate Analysis of Co-Eluting Isomers

The capability of the GC–FTIR instrument in terms of rapid scan speeds is significant for both qualitative and quantitative analysis. Direct quantification of GC–FTIR data is possible as IR absorption obeys the Beer-Lambert law, where the absorbance (A) can be related to concentration of an absorber (c) and path length (l) as $A = \varepsilon cl$, where ε is molar absorptivity. Despite the best FTIR spectrometers having relatively poor sensitivity, the quantification ability of FTIR can be demonstrated [12] and is also of use in compound characterisation [45]. We validated the ability of this system to carry out univariate quantitative analyses—analysis of a single variable—with the IR detector's linear range response using several compounds with varying functional groups. Calibration curves for FTIR data can be constructed using peak area or peak absorption maxima as demonstrated in Supplementary information Figures S8 and S9. The R^2 values of *o*-cresol (Figure S8A), ethylbenzene (Figure S8B), α -pinene (Figure S9A) and γ -terpinene (Figure S9B) were 0.997, 0.996, 0.979 and 0.9662 respectively. Conditions of analysis are tabulated in Supplementary information Table S2.

As opposed to univariate data analysis, multivariate data analysis, which assesses multiple variables, is a growing trend in predicting the response or change in a chemical system using the development of models. As such, the development of multivariate models that relate to multi-wavelength spectrum responses to variations in analyte concentrations has been proved to

be valuable in the quantitative analysis of FTIR spectra [46,47] with the advantages of being fast, non-destructive and often cheap with the ability to be used in complex mixtures as well. The efficiency of these models to predict the concentration of new samples outweighs that of calibration curves based on a single wavelength of the FTIR spectrum. One such multivariate calibration approach, partial least squares regression (PLSR) was used to determine its applicability to GC–FTIR analysis of isomeric species, which is a useful test of co-eluting positional isomers. PLSR uses the whole FTIR spectrum region rather than a specific absorption band for analysing the component of interest and establishes a linear relationship between a known variable set (X) and predicted variables (Y). Here X constitutes the known concentration and Y the predicted values based on the spectra acquired. A set of latent variables (LVs) explain the source of variation in the Y block correlated to the X vector are computed to yield the latent variables which are used to calculate the regression vector b as set out in Equation (1), where e is the error vector (i.e., residuals).

$$Y = Xb^T + e. \quad (1)$$

In this study, the co-eluting isomers *m*- and *p*-cresol were chosen due to their FTIR spectra having marked differences, whilst having close similarity of mass spectra which precludes their individual quantification (Supplementary information Figure S2). The PLSR model was developed using a calibration data set X ($M \times N$) prepared using *m*- and *p*-cresol isomers in the ratios 0:10, 1:9, 2:8, 4:6, 6:4, 8:2, 9:1 and 10:1. The validation set had these isomers in ratios of 3:7, 5:5 and 7:3. Spectra were obtained in *.spc format with a resolution of 4 cm^{-1} with an initial GC oven T of 90°C increased to 135°C at the rate of 5°C min^{-1} .

Spectrum pre-processing was Savitzky–Golay second-derivative polynomial order 3 and 15 points of smoothing. Data were excluded from the regions 1699–2841, 3106–3159, 3715–3733 and $3735\text{--}4000 \text{ cm}^{-1}$ to reduce the effect of noise. Two data points were removed as outliers due to high Q residuals and Hotelling T^2 plots to enable better prediction. The coefficient of determination (R^2) for the calibration and validation sets were measured as well as the root mean square error of calibration (RMSEC) and root mean square error of prediction (RMSEP). The PLSR model was seen to follow a linear regression of near perfect linearity with a R^2 value of 0.99 and thus was confirmed to be suitable to use as a prediction model as demonstrated in Figure 4A. The RMSEC was 0.38 which reflects the internal prediction accuracy. Figure 4C shows the loading plots of the regression vector for *m*-cresol corresponding to the PLSR model together with the labelling of the most significant bands [767 cm^{-1} , 777 cm^{-1} (C–H bending), 1134 cm^{-1} , 1158 cm^{-1} , 1158 cm^{-1} (C–O stretching), 3649 cm^{-1} and 3662 cm^{-1} (O–H stretching)]. When tested using the validation set a R^2 prediction value of 0.88 and an RMSEP of 0.57 was obtained by the prediction set presented in Figure 4B, which represents the external predictive ability. The variability here is due to the decreasing sensitivity and IR response of the MCT detector below 700 cm^{-1} . In both Figure 4A,B the green dotted line represents the expected proportional 1:1 fit of the samples and the red continuous line represents the fit obtained using the model and test data.

The low value of RMSEP and high value of R^2 indicate the accuracy of this approach. This confirms the suitability of combining GC–FTIR data with the multivariate calibration method of PLS regression for quantifying coeluting isomer mixtures, especially for isomeric species with identical mass spectra.

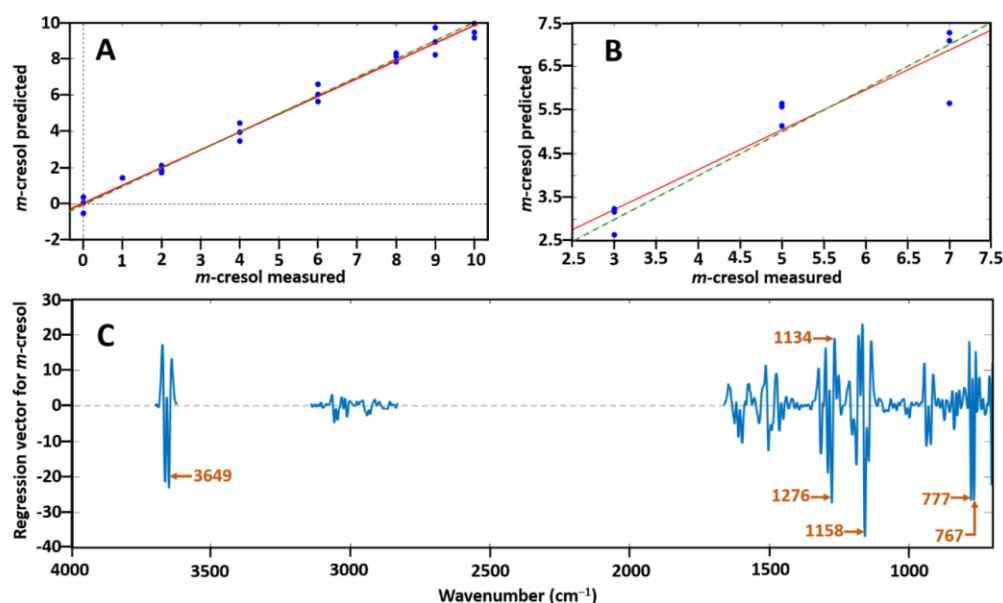


Figure 4. (A) Predicted *m*-cresol concentration ratio vs. measured *m*-cresol concentration ratio with the use of the partial least squares (PLS) regression model; (B) prediction set of *m*-cresol; and (C) loadings plot corresponding to the PLS model with labelling of the most significant bands which allow prediction of *m*-cresol from *p*-cresol. In both (A) and (B) the green dotted line represents the expected 1:1 proportional fit whilst the red continuous line shows the fit calculated by the model on the test data.

4. Conclusions

One of GC–FTIR’s greatest strengths is its ability to differentiate functional groups or chemical structures for resolved compounds. This is largely achieved by the distinct combination of peaks in the absorption spectrum, which creates a unique pattern for individual compounds. In contrast, MS library searches rely largely on defined fragmentation patterns (mass; intensity) of the molecule and these usually comprise less informative structural details. Identification is commonly achieved by the closest match of an acquired spectrum to the ‘hit-list’ of compound spectra submitted to reference libraries [32]. As aptly outlined by Ausloos et. al. [48], the structure identification ability of MS library searches depends mainly on the abundance and diversity of that structure in the library database of reference compounds—and it is possible to retrieve a ‘proposed MS library match’ even if the compound is not present in the library. Due to the complexity of ions which can be generated by dissociation, electron-ionisation mass spectra cannot be reliably predicted. This is mainly because these ions can undergo multiple pathways to achieve a given ion, the dependence of the mass spectrum on experimental conditions and the possibility of ions rearranging before dissociation [49]. Contrasting the progress in MS detection for GC in recent decades, there is a corresponding scarcity of GC–FTIR literature. However, a revival of interest in condensed phase GC–FTIR and the development of other spectroscopic detectors such as the VUV has reinvigorated the value of spectroscopic detectors and complementary identification approaches in chemical structure deduction. The relatively lower sensitivity characteristic of light-pipe GC–FTIR systems contrasts with its favourable identification power. The success of GC–FTIR optimisation rests upon a compromise of chromatography and spectroscopy and when used in combination with the spectrometric data of GC–MS can result in greater confidence in component identification rendering dual-qualitative information. Ongoing research is directed at setting up multidimensional configurations and combining alternative GC techniques. We believe applications to a range of samples to further demonstrate the value of using multiple detection methodologies will yield results with reliable and absolute identification of compounds, adding new dimensions to analytical capabilities of FTIR and similar spectroscopic detection techniques with GC.

Supplementary Materials: The following are available online at <http://www.mdpi.com/2297-8739/7/2/27/s1>. The detailed captions for these Figures and Tables are included in the supplementary file. Figure S1: Instrumental setup schematic for the light-pipe GC–FTIR–FID system., Figure S2: Effect of increasing light-pipe (and transfer line) temperatures on the root mean square intensity absorbance of GC–FTIR chromatograms of nonane., Figure S3: Effect of increasing LP and TL T , varying FTIR resolution and varying flow on signal-to-noise ratio calculations., Figure S4: GC–FTIR and GC–FTIR–FID chromatograms of 5% *o*-cresol in MeOH at varying injection volumes of (a) 1.5 μ L, (b) 2.0 μ L and (c) 3.0 μ L., Figure S5: Virtually identical GC–MS spectra for *o*-, *m*- and *p*-cresol isomers and their corresponding GC–FTIR spectra., Figure S6: GC–FTIR spectra of α -pinene, β -pinene, geraniol, γ -terpinene, limonene and eugenol essential oil standard compounds., Figure S7: GC \times FTIR colour contour plot of acetaldehyde oxime (A.O.) and propionaldehyde oxime (P.O.) elution with FTIR spectra corresponding to P.O. isomers at different positions over the dynamic P.O. peak., Figure S8: Calibration curves for peak area of *o*-cresol and peak height of ethylbenzene and GC–FTIR spectra for *o*-cresol and ethylbenzene together., Figure S9: Calibration curves for α -pinene and γ -terpinene at their absorption maxima and maximum absorption peak responses of α -pinene and γ -terpinene., Table S1: Library match results for elution of compounds used for GC–FID and GC–FTIR–FID peak comparison., Table S2: Chromatography conditions for univariate calibration of select compounds depicted in Figure S8 and Figure S9.

Author Contributions: Conceptualization, P.J.M. and J.S.Z.; methodology, J.S.Z., S.B., J.S.P.S., H.D.W. and Y.N.; software, J.S.Z.; formal analysis, J.S.Z. and H.D.W.; writing—original draft preparation, J.S.Z.; writing—review and editing, Y.N., P.J.M. and J.S.Z.; supervision, P.J.M. and B.R.W.; funding acquisition, P.J.M. All authors have read and agreed to the published version of the manuscript

Funding: This work was supported by the Australian Research Council, Linkage Grant scheme, with partner PerkinElmer (Grant LP150100465). Funding from PerkinElmer to the Monash University GRIP program is also acknowledged. Monash University support to J.S.Z. and H.D.W. for Deans' Research Scholarships is acknowledged.

Acknowledgments: Assistance given by Chadin Kulsing to J.S.S.P and J.S.Z. and assistance in PLSR to J.S.Z. by David Perez-Guaita, Zach Richardson and Miguela Martin is greatly appreciated.

Conflicts of Interest: The authors declare no conflict of interest.

References

- Poole, C.F. Ionization-based detectors for gas chromatography. *J. Chromatogr. A* **2015**, *1421*, 137–153. [[CrossRef](#)]
- Zavahir, J.S.; Nolvachai, Y.; Marriott, P.J. Molecular spectroscopy—Information rich detection for gas chromatography. *TrAC Trends Anal. Chem.* **2018**, *99*, 47–65. [[CrossRef](#)]
- Wilson, I.D.; Brinkman, U.A.T. Hyphenation and hypenation: The practice and prospects of multiple hyphenation. *J. Chromatogr. A* **2003**, *1000*, 325–356. [[CrossRef](#)]
- Santos, I.C.; Schug, K.A. Recent advances and applications of gas chromatography vacuum ultraviolet spectroscopy. *J. Sep. Sci.* **2017**, *40*, 138–151. [[CrossRef](#)] [[PubMed](#)]
- Nolvachai, Y.; Kulsing, C.; Marriott, P.J. Pesticides analysis: Advantages of increased dimensionality in as chromatography and mass spectrometry. *Crit. Rev. Environ. Sci. Technol.* **2015**, *45*, 2135–2173. [[CrossRef](#)]
- Andersson, J.T. Detectors. In *Practical Gas Chromatography: A Comprehensive Reference*; Dettmer-Wilde, K., Engewald, W., Eds.; Springer: Berlin/Heidelberg, Germany, 2014; pp. 205–248. [[CrossRef](#)]
- Gachot, G.; Grugeon, S.; Jimenez-Gordon, I.; Eshetu, G.G.; Boyanov, S.; Lecocq, A.; Marlair, G.; Pilard, S.; Laruelle, S. Gas chromatography/Fourier transform infrared/mass spectrometry coupling: A tool for Li-ion battery safety field investigation. *Anal. Methods* **2014**, *6*, 6120–6124. [[CrossRef](#)]
- Skoog, D.A. *Principles of Instrumental Analysis*, 6th ed.; Thomson, Brooks/Cole: Belmont, CA, USA, 2007.
- Visser, T. FT-IR detection in gas chromatography. *TrAC Trends Anal. Chem.* **2002**, *21*, 627–636. [[CrossRef](#)]
- Visser, T. Gas Chromatography/Fourier Transform Infrared Spectroscopy. In *Handbook of Vibrational Spectroscopy*; Griffiths, P.R., Chalmers, J.M., Eds.; John Wiley & Sons, Ltd.: Chichester, UK, 2006; pp. 1605–1626. [[CrossRef](#)]
- Sciarrone, D.; Schepis, A.; De Grazia, G.; Rotondo, A.; Alibrando, F.; Cipriano, R.R.; Bizzo, H.; Deschamps, C.; Sidisky, L.M.; Mondello, L. Collection and identification of an unknown component from: *Eugenia uniflora* essential oil exploiting a multidimensional preparative three-GC system employing apolar, mid-polar and ionic liquid stationary phases. *Faraday Discuss.* **2019**, *218*, 101–114. [[CrossRef](#)]
- Demirgian, J.C. Gas chromatography—Fourier transform infrared spectroscopy—Mass spectrometry. A powerful tool for component identification in complex organic mixtures. *TrAC Trends Anal. Chem.* **1987**, *6*, 58–64. [[CrossRef](#)]

13. Wilkins, C.L. Directly-linked gas chromatography–infrared–mass spectrometry (GC/IR/MS). In *Handbook of Vibrational Spectroscopy*; John Wiley & Sons, Ltd.: Chichester, UK, 2006; pp. 1627–1633. [[CrossRef](#)]
14. Krock, K.A.; Ragunathan, N.; Wilkins, C.L. Multidimensional gas chromatography coupled with infrared and mass spectrometry for analysis of Eucalyptus essential oils. *Anal. Chem.* **1994**, *66*, 425–430. [[CrossRef](#)]
15. Cooper, J.R.; Wilkins, C.L. Utilization of spectrometric information in linked gas chromatography–Fourier transform infrared spectroscopy–mass spectrometry. *Anal. Chem.* **1989**, *61*, 1571–1577. [[CrossRef](#)]
16. Cai, J.; Lin, P.; Zhu, X.L.; Su, Q. Comparative analysis of clary sage (*S. sclarea* L.) oil volatiles by GC–FTIR and GC–MS. *Food Chem.* **2006**, *99*, 401–407. [[CrossRef](#)]
17. Ragunathan, N.; Krock, K.A.; Klawun, C.; Sasaki, T.A.; Wilkins, C.L. Gas chromatography with spectroscopic detectors. *J. Chromatogr. A* **1999**, *856*, 349–397. [[CrossRef](#)]
18. Zavahir, J.S.; Nolvachai, Y.; Wood, B.R.; Marriott, P.J. Gas chromatography–Fourier transform infrared spectroscopy reveals dynamic molecular interconversion of oximes. *Analyst* **2019**, *144*, 4803–4812. [[CrossRef](#)]
19. Poole, C.F. Spectroscopic Detectors for Identification and Quantification. In *The Essence of Chromatography*; Elsevier Science: Amsterdam, The Netherlands, 2003; pp. 719–792. [[CrossRef](#)]
20. White, R.L. Chromatography–IR, methods and instrumentation. In *Encyclopedia of Spectroscopy and Spectrometry*, 3rd ed.; Tranter, G.E., Koppenaal, D.W., Eds.; Academic Press: Oxford, UK, 2017; pp. 251–255. [[CrossRef](#)]
21. Mark, H.; Workman, J., Jr. Experimental designs: Part 8— β , the power of a test. In *Chemometrics in Spectroscopy*; Academic Press: Amsterdam, The Netherlands, 2007; pp. 101–102. [[CrossRef](#)]
22. Blitz, J.P.; Klarup, D.G. Signal-to-noise ratio, signal processing, and spectral information in the instrumental analysis laboratory. *J. Chem. Educ.* **2002**, *79*, 1358–1360. [[CrossRef](#)]
23. Giss, G.N.; Wilkins, C.L. Effects of lightpipe dimensions on gas chromatography/Fourier transform infrared sensitivity. *Appl. Spectrosc.* **1984**, *38*, 17–20. [[CrossRef](#)]
24. Henry, D.E.; Giorgetti, A.; Haefner, A.M.; Griffiths, P.R.; Gurka, D.F. Optimizing the optical configuration for light-pipe gas chromatography/Fourier transform infrared spectrometry interfaces. *Anal. Chem.* **1987**, *59*, 2356–2361. [[CrossRef](#)]
25. Brissey, G.M.; Henry, D.E.; Giss, G.N.; Yang, P.W.; Griffiths, P.R.; Wilkins, C.L. Comparison of gas chromatography/Fourier transform infrared spectrometric Gram–Schmidt reconstructions from different interferometers. *Anal. Chem.* **1984**, *56*, 2002–2006. [[CrossRef](#)]
26. Theocharous, E.; Birch, J.R. Detectors for mid- and far-infrared spectrometry: Selection and use. In *Handbook of Vibrational Spectroscopy*; John Wiley & Sons, Ltd.: Chichester, UK, 2006; pp. 349–367. [[CrossRef](#)]
27. Griffiths, P.R.; Heaps, D.A.; Brejna, P.R. The gas chromatography/infrared interface: Past, present, and future. *Appl. Spectrosc.* **2008**, *62*, 259A–270A. [[CrossRef](#)] [[PubMed](#)]
28. Griffiths, P.R.; de Haseth, J.A. Coupled Techniques. In *Fourier Transform Infrared Spectrometry*; John Wiley & Sons, Inc.: Chichester, UK, 2006; pp. 481–507. [[CrossRef](#)]
29. Brown, R.S.; Cooper, J.R.; Wilkins, C.L. Lightpipe temperature and other factors affecting signal in gas chromatography/Fourier transform infrared spectrometry. *Anal. Chem.* **1985**, *57*, 2275–2279. [[CrossRef](#)]
30. Grob, R.L. Theory of gas chromatography. In *Modern Practice of Gas Chromatography*, 4th ed.; Grob, R.L., Barry, E.F., Eds.; John Wiley & Sons, Inc.: Chichester, UK, 2004; pp. 23–63. [[CrossRef](#)]
31. Griffiths, P.R. Gas chromatography | Infrared spectroscopy. In *Encyclopedia of Analytical Science*, 3rd ed.; Worsfold, P., Poole, C., Townshend, A., Miró, M., Eds.; Elsevier: Amsterdam, The Netherlands, 2013; Volume 4, pp. 186–192. [[CrossRef](#)]
32. Milman, B.L. General principles of identification by mass spectrometry. *TrAC Trends Anal. Chem.* **2015**, *69*, 24–33. [[CrossRef](#)]
33. Milman, B.L.; Zhurkovich, I.K. Mass spectral libraries: A statistical review of the visible use. *TrAC Trends Anal. Chem.* **2016**, *80*, 636–640. [[CrossRef](#)]
34. Sasaki, T.A.; Wilkins, C.L. Gas chromatography with Fourier transform infrared and mass spectral detection. *J. Chromatogr. A* **1999**, *842*, 341–349. [[CrossRef](#)]
35. Pavia, D.L.; Lampman, G.M.; Kriz, G.S.; Vyvyan, J.R. *Introduction to Spectroscopy*, 5th ed.; Cengage Learning: Stamford, CT, USA, 2015.
36. Do, T.K.T.; Hadji-Minaglou, F.; Antonioti, S.; Fernandez, X. Authenticity of essential oils. *TrAC Trends Anal. Chem.* **2015**, *66* (Suppl. C), 146–157. [[CrossRef](#)]

37. Li, Y.-Q.; Kong, D.-X.; Wu, H. Analysis and evaluation of essential oil components of cinnamon barks using GC–MS and FTIR spectroscopy. *Ind. Crops Prod.* **2013**, *41*, 269–278. [[CrossRef](#)]
38. Marriott, P.J.; Shellie, R.; Cornwell, C. Gas chromatographic technologies for the analysis of essential oils. *J. Chromatogr. A* **2001**, *936*, 1–22. [[CrossRef](#)]
39. Wong, Y.F.; Kulsing, C.; Marriott, P.J. Switchable enantioselective three- and four-dimensional dynamic gas chromatography–mass spectrometry: Example study of on-column molecular interconversion. *Anal. Chem.* **2017**, *89*, 5620–5628. [[CrossRef](#)]
40. Wang, F.C.-Y.; Edwards, K.E. Separation of C2-naphthalenes by gas chromatography × Fourier transform infrared spectroscopy (GC × FT-IR): Two-dimensional separation approach. *Anal. Chem.* **2007**, *79*, 106–112. [[CrossRef](#)]
41. Wang, F.C.-Y.; Qian, K.; Green, L.A. GC × MS of diesel: A two-dimensional separation approach. *Anal. Chem.* **2005**, *77*, 2777–2785. [[CrossRef](#)]
42. Wang, F.C.-Y. GC × VUV study of diesel: A two-dimensional separation approach. *Energy Fuels* **2020**, *34*, 1432–1437. [[CrossRef](#)]
43. Kulsing, C.; Nolvachai, Y.; Wong, Y.F.; Glouzman, M.I.; Marriott, P.J. Observation and explanation of two-dimensional interconversion of oximes with multiple heart-cutting using comprehensive multidimensional gas chromatography. *J. Chromatogr. A* **2018**, *1546*, 97–105. [[CrossRef](#)] [[PubMed](#)]
44. Nolvachai, Y.; Kulsing, C.; Trapp, O.; Marriott, P.J. Multidimensional gas chromatography investigation of concentration and temperature effects of oxime interconversion on ionic liquid and poly(ethylene glycol) stationary phases. *Anal. Chim. Acta* **2019**, *1081*, 200–208. [[CrossRef](#)] [[PubMed](#)]
45. Kempe, J.; Bellmann, C.; Meyer, D.; Windrich, F. GC-IR based two-dimensional structural group analysis of petroleum products. *Anal. Bioanal. Chem.* **2005**, *382*, 186–191. [[CrossRef](#)] [[PubMed](#)]
46. Richardson, Z.; Perez-Guaita, D.; Kochan, K.; Wood, B.R. Determining the age of spoiled milk from dried films using attenuated reflection Fourier transform infrared (ATR FT-IR) spectroscopy. *Appl. Spectrosc.* **2019**, *73*, 1041–1050. [[CrossRef](#)] [[PubMed](#)]
47. Toziou, P.-M.; Barmapalexis, P.; Boukouvala, P.; Verghese, S.; Nikolakakis, I. Quantification of live *Lactobacillus acidophilus* in mixed populations of live and killed by application of attenuated reflection Fourier transform infrared spectroscopy combined with chemometrics. *J. Pharm. Biomed. Anal.* **2018**, *154*, 16–22. [[CrossRef](#)] [[PubMed](#)]
48. Stein, S. Mass spectral reference libraries: An ever-expanding resource for chemical identification. *Anal. Chem.* **2012**, *84*, 7274–7282. [[CrossRef](#)]
49. Ausloos, P.; Clifton, C.L.; Lias, S.G.; Mikaya, A.I.; Stein, S.E.; Tchekhovskoi, D.V.; Sparkman, O.D.; Zaikin, V.; Zhu, D. The critical evaluation of a comprehensive mass spectral library. *J. Am. Soc. Mass Spectrom.* **1999**, *10*, 287–299. [[CrossRef](#)]



© 2020 by the authors. Licensee MDPI, Basel, Switzerland. This article is an open access article distributed under the terms and conditions of the Creative Commons Attribution (CC BY) license (<http://creativecommons.org/licenses/by/4.0/>).

3.4 Published supplementary material

Relationships in Gas Chromatography—Fourier Transform Infrared Spectroscopy—Comprehensive and Multilinear Analysis

Junaida Shezmin Zavahir, Jamieson S. P. Smith, Scott Blundell, Habtewold D. Waktola, Yada Nolvachai, Bayden R. Wood and Philip J. Marriott

Published in *Separations* Volume 7 – Issue 2, June 2020

Supplementary material

Article

Relationships in Gas Chromatography—Fourier Transform Infrared Spectroscopy—Comprehensive and Multilinear Analysis

Junaida Shezmin Zavahir ¹, Jamieson S. P. Smith ¹, Scott Blundell ², Habtewold D. Waktola ¹, Yada Nolvachai ¹, Bayden R. Wood ³ and Philip J. Marriott ^{1,*}

¹ Australian Centre for Research on Separation Science, School of Chemistry, Monash University, Wellington Road, Clayton, VIC 3800, Melbourne, Australia; junaida.ismail@monash.edu (J.S.Z.); jamiesonspsmith@gmail.com (J.S.P.S.); habtewold.waktola@monash.edu (H.D.W.); yada.nolvachai@monash.edu (Y.N.)

² Monash Analytical Platform, School of Chemistry, Monash University, Wellington Road, Clayton, VIC 3800, Melbourne, Australia; scott.blundell@monash.edu

³ Centre for Biospectroscopy, School of Chemistry, Monash University, Wellington Road, Clayton, VIC 3800, Melbourne, Australia; Bayden.Wood@monash.edu

* Correspondence: Philip.Marriott@monash.edu; Tel.: +61-3-9905-9630; Fax: +61-3-9905-8501

List of Figure Captions and Tables

Figure S1. Instrumental setup schematic for the light-pipe GC–FTIR–FID system.

Figure S2. Effect of increasing light-pipe (and transfer line) temperatures on the root mean square intensity absorbance of GC–FTIR chromatograms of nonane.

Figure S3. Effect of increasing LP and TL T, varying FTIR resolution and varying flow on signal-to-noise ratio calculations.

Figure S4. GC–FTIR and GC–FTIR–FID chromatograms of 5% o-cresol in MeOH at varying injection volumes of (a) 1.5 μ L, (b) 2.0 μ L and (c) 3.0 μ L.

Figure S5. Virtually identical GC–MS spectra for o-, m-, and p-cresol isomers and their corresponding GC–FTIR spectra.

Figure S6. GC–FTIR spectra of α -pinene, β -pinene, geraniol, γ -terpinene, limonene and eugenol standard compounds.

Figure S7. GC \times FTIR colour contour plot of acetaldehyde oxime (A.O.) and propionaldehyde oxime (P.O.) elution with FTIR spectra corresponding to P.O. isomers at different positions over the dynamic P.O. peak.

Figure S8. Calibration curves for peak area of o-cresol and peak height of ethylbenzene, and GC–FTIR spectra for o-cresol and ethylbenzene together.

Figure S9. Calibration curves for α -pinene and γ -terpinene at their absorption maxima, and maximum absorption peak responses of α -pinene and γ -terpinene.

Table S1. Library match results for elution of compounds used for GC–FID and GC–FTIR–FID peak comparison.

Table S2. Chromatography conditions for univariate calibration of select compounds depicted in Figure S8 and Figure S9.

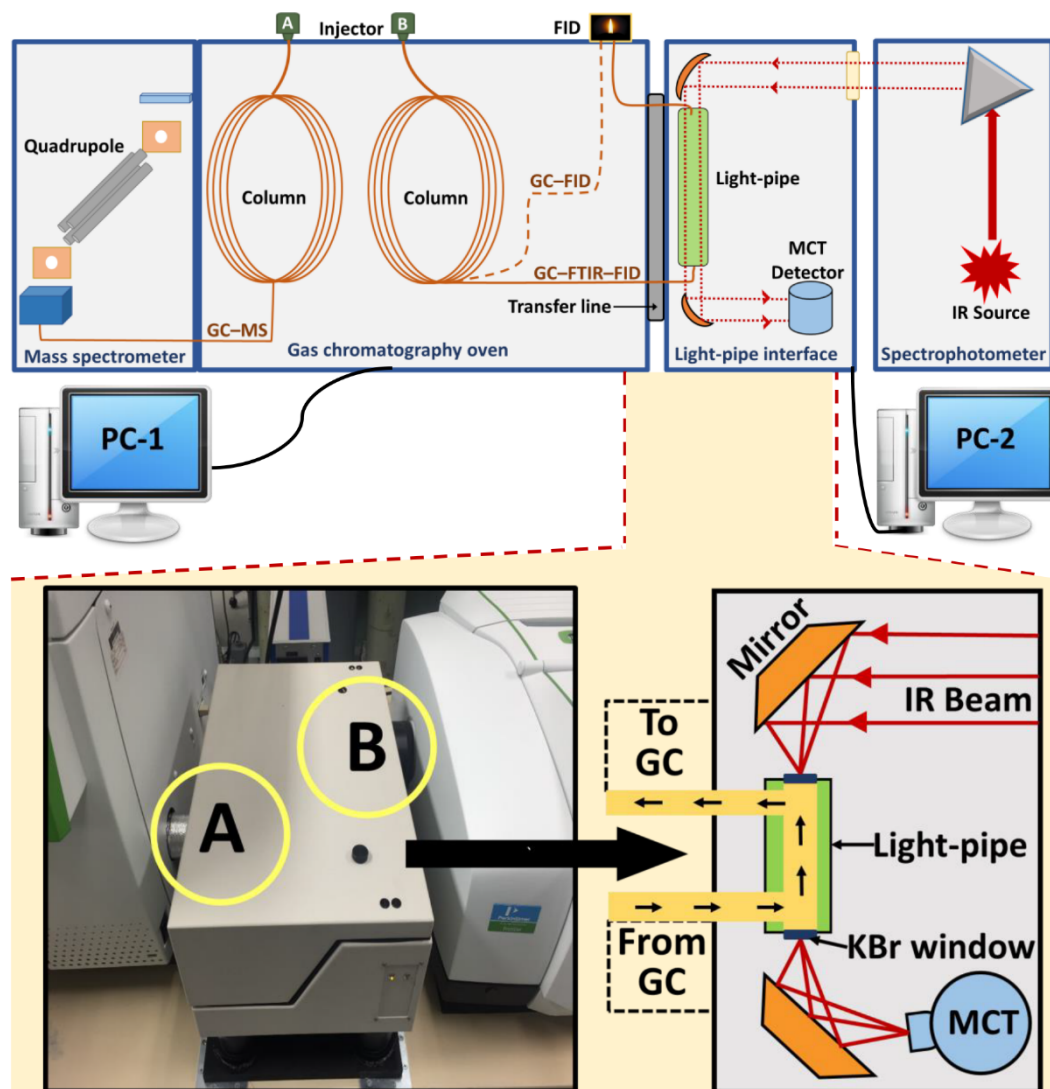


Figure S1. Instrumental setup schematic for the light-pipe GC-FTIR-FID system where the GC is hyphenated to a spectrophotometer via the light-pipe interface. The dashed line within the GC oven represents column configuration for GC-FID setting where the sample does not travel through the light pipe. The enlarged view below shows connection of the LP interface to the right hand side of the GC oven via an insulated transfer line (at A), the IR radiation input (at B) and the IR beam path from the spectrophotometer source to the MCT detector via the light-pipe through which the GC carrier gas flows.

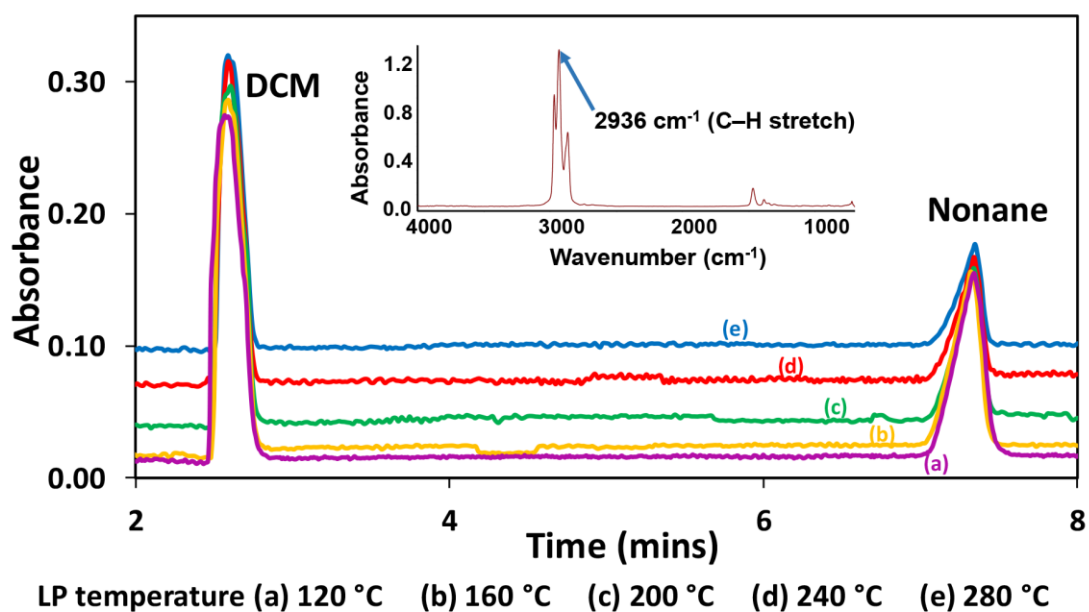


Figure S2. Effect of increasing light-pipe (and transfer line) temperatures of 120 °C, 160 °C, 200 °C, 240 °C and 280 °C respectively on the root mean square intensity absorbance of GC-FTIR chromatograms of nonane. The FTIR spectrum of nonane is inset.

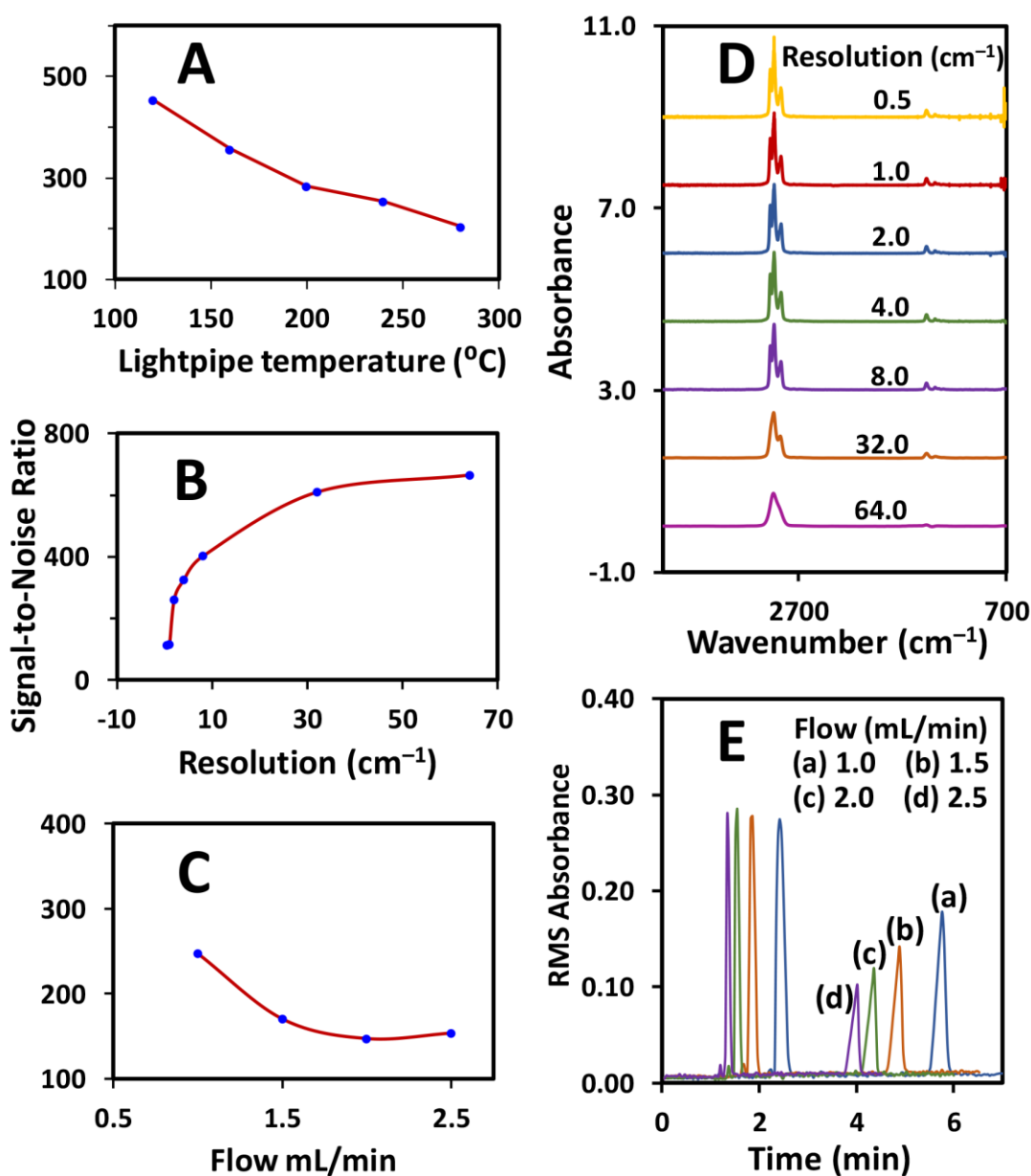


Figure S3. Effect of (A) increasing LP and TL T , (B) varying FTIR resolution and (C) varying flow on signal-to-noise ratio calculations made on the peak height of 2936 cm⁻¹ band of nonane. Effect of resolution change on spectral peak shape is depicted in (D) and change in retention time of root mean square absorbance chromatographic peak *vs.* carrier gas flow rate is depicted in (E). Analysis was at an initial T of 50 °C increased at 10 °C/min to 110 °C.

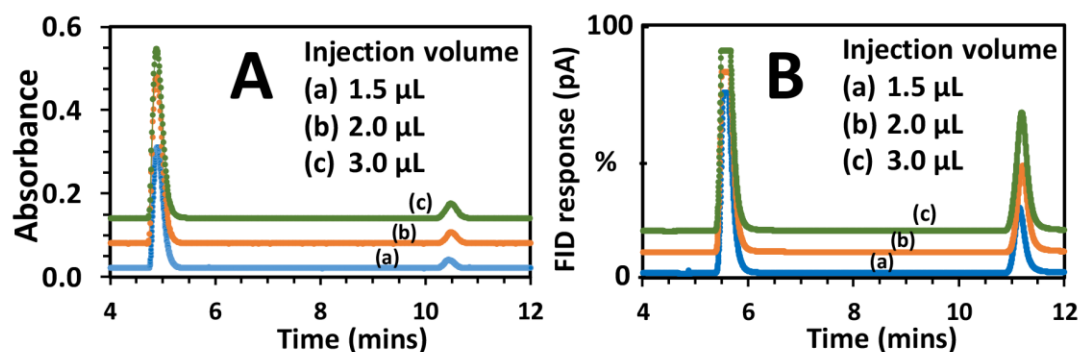


Figure S4. (A) GC-FTIR and (B) GC-FTIR-FID chromatograms of 5% (v/v) *o*-cresol in MeOH at varying injection volumes of (a) 1.5 µL, (b) 2.0 µL and (c) 3.0 µL, demonstrating the difference in peak retention times for the additional pathlength in (B). Samples were injected at an initial GC oven T of 65 °C, heated at 10 °C/min, to a final T of 150 °C. FTIR data collection used 8 cm⁻¹ resolution.

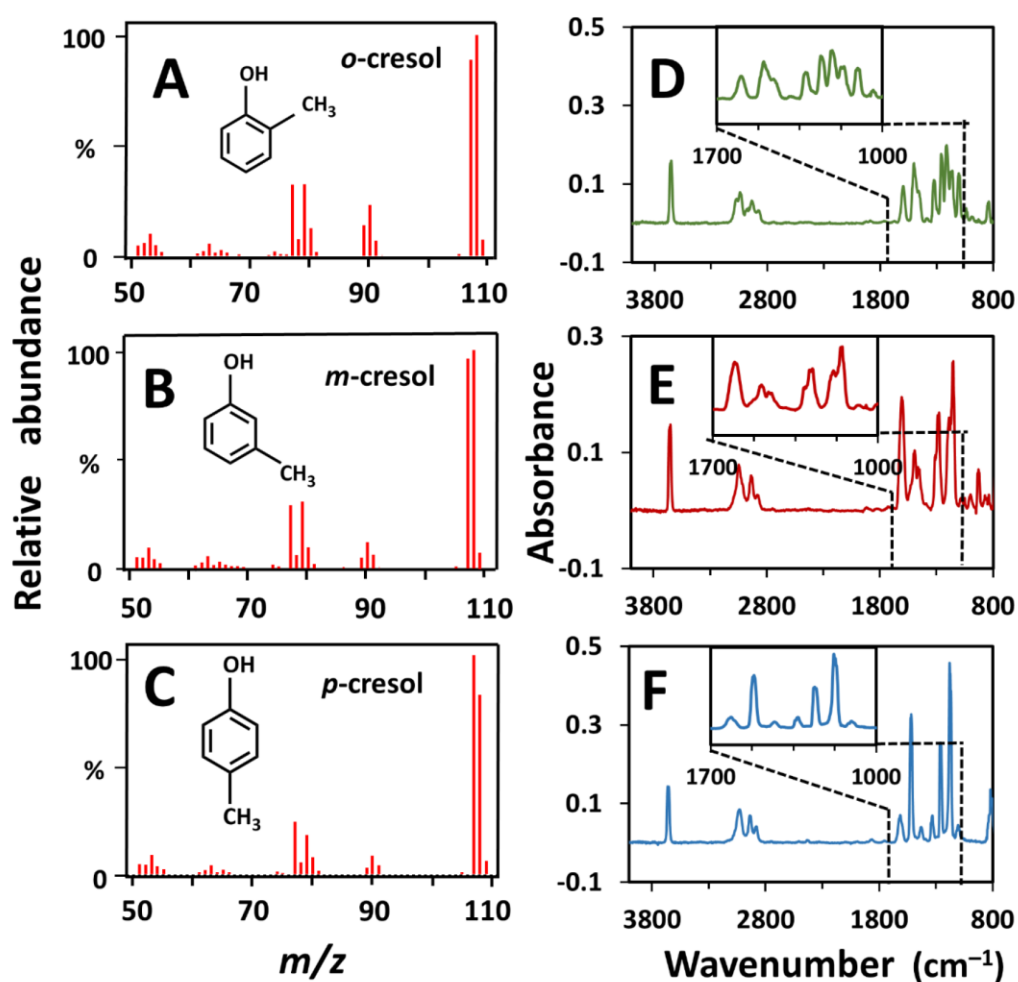


Figure S5. Very similar GC-MS spectra (Left) for (A) *o*-, (B) *m*-, and (C) *p*-cresol isomers and their corresponding GC-FTIR spectra (Right) (D, E and F); the latter display significant differences in the

vicinity of their fingerprint region at 1800–800 cm^{-1} . The FTIR region 1700–1000 cm^{-1} enlarged inset demonstrates their spectrum differences. Cresol isomer solutions in DCM were detected by FTIR at an oven T programme of 50 $^{\circ}\text{C}$, heated at 5 $^{\circ}\text{C}/\text{min}$, to 180 $^{\circ}\text{C}$.

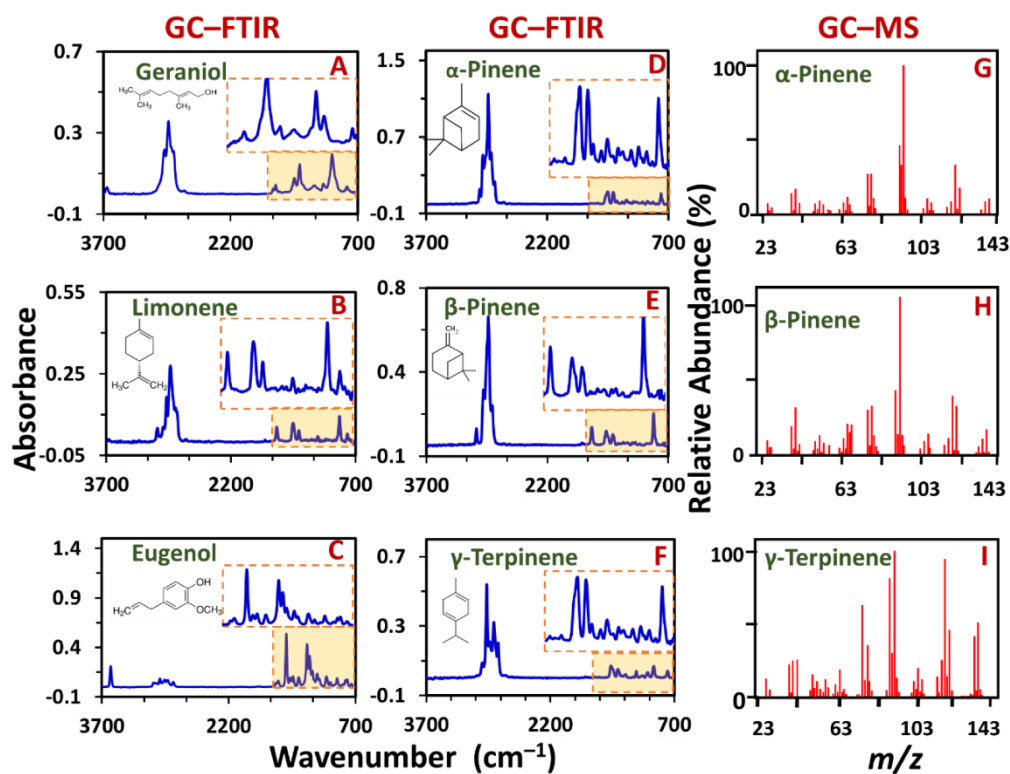


Figure S6. GC-FTIR spectra of α -pinene, β -pinene, geraniol, γ -terpinene, limonene and eugenol essential oil standard compounds (A–F) obtained at an initial T of 100 $^{\circ}\text{C}$ (1 min hold), heated at 5 $^{\circ}\text{C}/\text{min}$ to the elution T of the compounds, with the spectrum inset region 1700 cm^{-1} –700 cm^{-1} enlarged to demonstrate their differences. GC-MS spectra for (G) α -pinene, (H) β -pinene and (I) γ -terpinene show similarities in contrast to their respective GC-FTIR spectra (D, E and F).

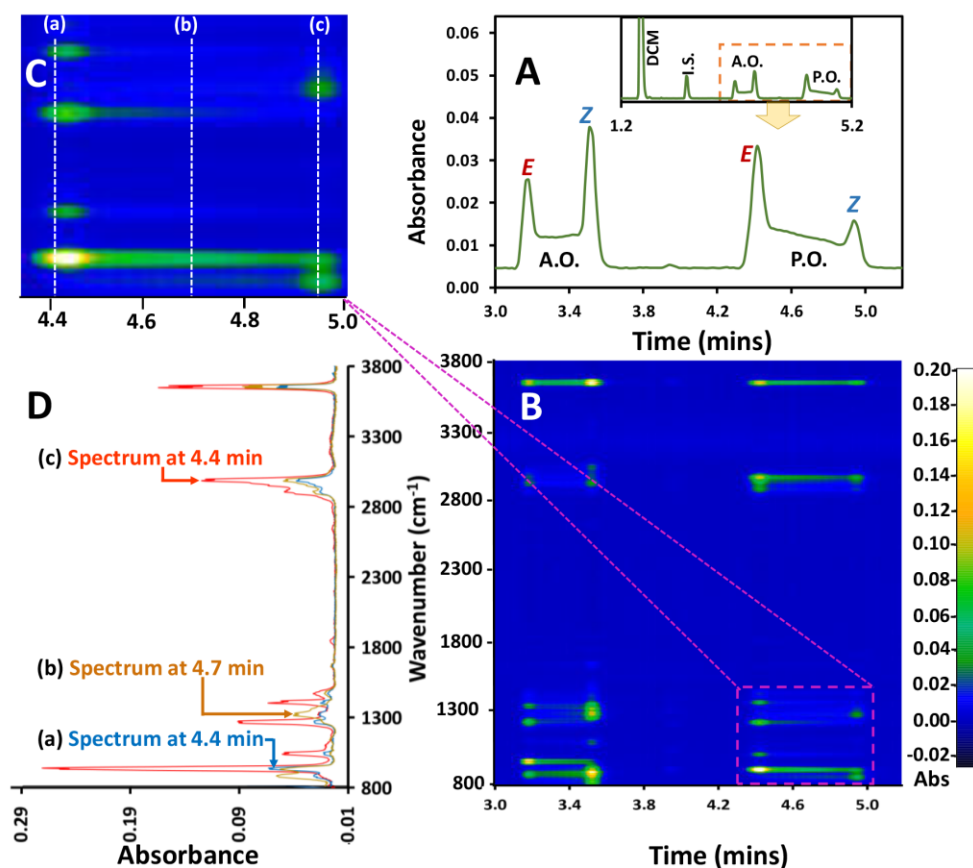


Figure S7. (A) Enlarged view of the GC-FTIR root mean square intensity profile of acetaldehyde oxime (A.O.) and propionaldehyde oxime (P.O.) interconversion region on GC PEG phase; the entire chromatogram is inset. (B) GCxFTIR 2D colour contour profile presented over the same retention time scale as (A), showing the IR spectrum bands of the interconversion region. (C) The boxed region in (B) is expanded to display IR bands corresponding to terminal (a, 4.4 min) and (c, 4.9 min) and an intermediate elution (b, 4.7 min) position of P.O. (D) Overlay of FTIR spectra acquired from the GC-FTIR experiment corresponding to terminal peaks of P.O., at 4.4 min (a) and at 4.9 min (c), and at an intermediate elution time of 4.7 min (b) which now shows absorption bands characteristic of both isomers.

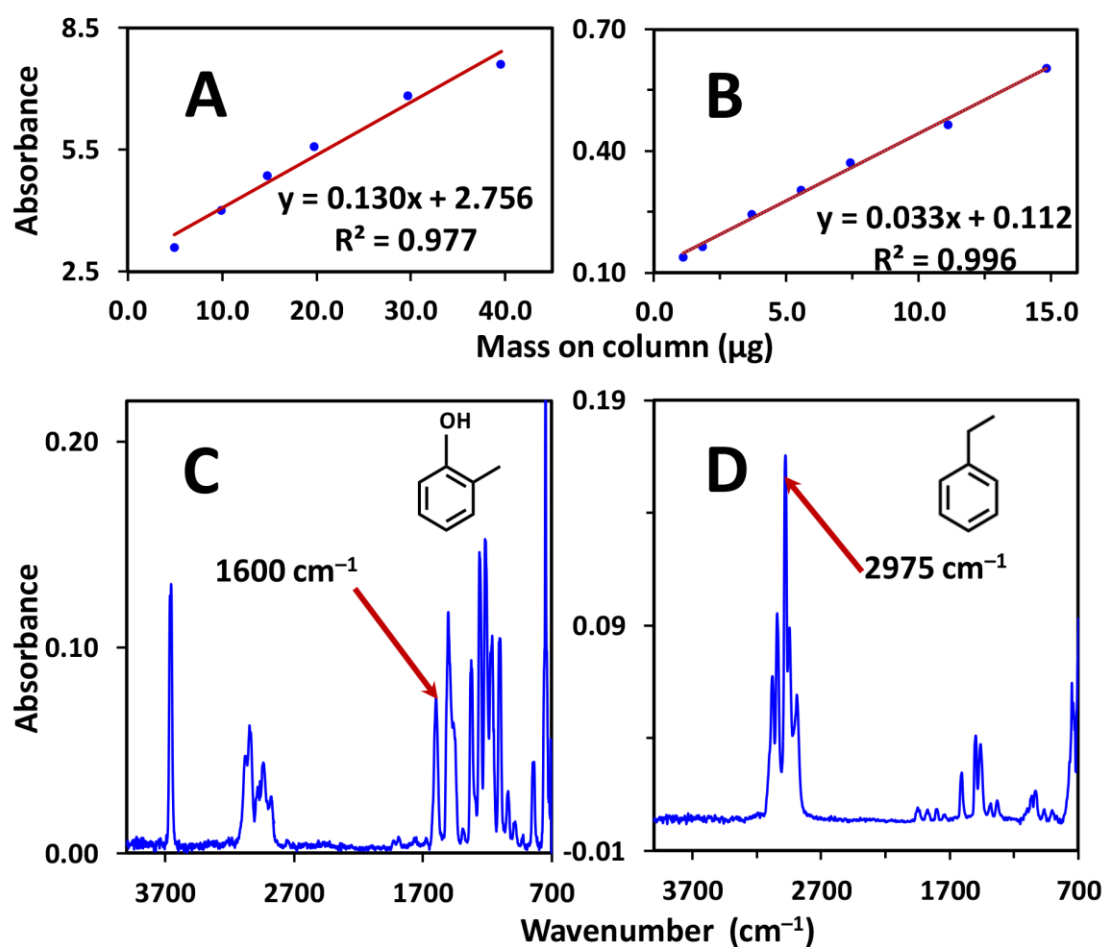


Figure S8. Calibration curves for (A) peak area of *o*-cresol and (B) peak height of ethylbenzene. The corresponding GC-FTIR spectra for (C) *o*-cresol and (D) ethylbenzene together with the specific peak responses used for quantification.

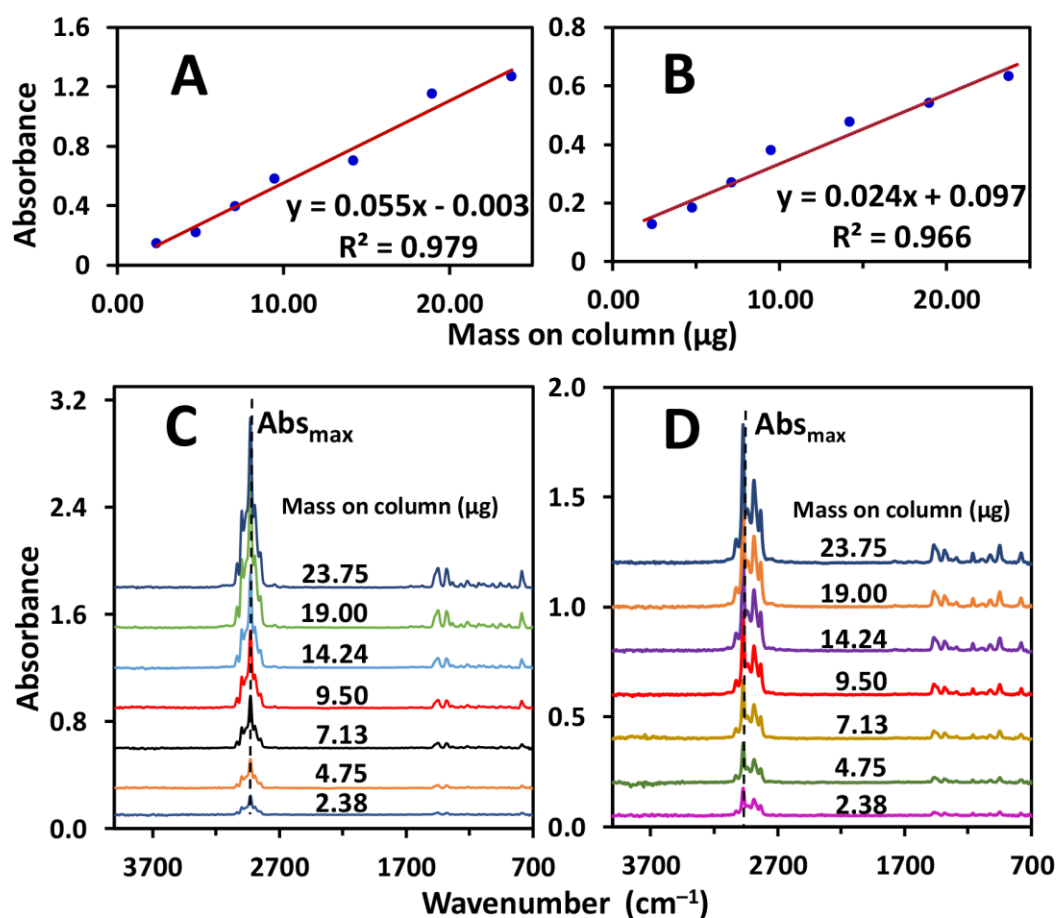


Figure S9. Calibration curves for (A) α -pinene and (B) γ -terpinene at their absorption maxima. Maximum absorption peak responses at different concentrations of (C) α -pinene and (D) γ -terpinene.

Table S1. Top three hits for the library match results for each compound eluted in the GC–FTIR–FID peak comparison experiment depicted in Figure 1 of the main manuscript. Library hits are for the FTIR spectra obtained from each FTIR peak, using the databases listed in Section 2.4 Software.

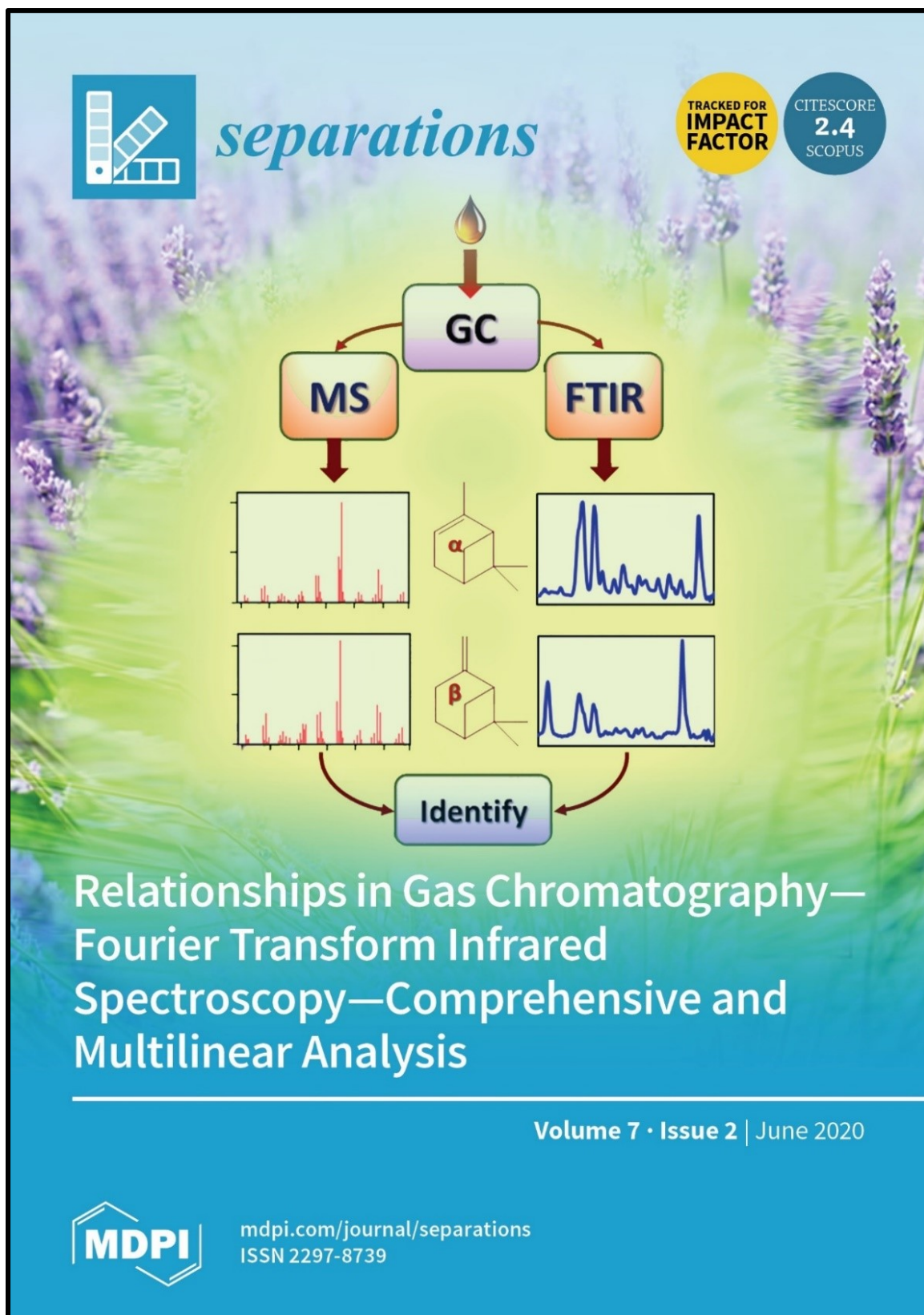
Elution order	Retention time t_R (min)	Search score	Search reference compound
1	2.6	0.9320	Dichloromethane; Methylene chloride
		0.8913	Dichloromethane, 99+%
		0.8742	Methane, dichloro-
2	2.9	0.9942	2-Butanol
		0.9930	2-Butanol
		0.9926	2-Butanol
3	3.5	0.9840	2-Pentanone
		0.9748	2-Pentanone
		0.9746	2-Pentanone
4	4.3	0.9973	1-Nitropropane, 98%
		0.9716	1-Nitropropane
		0.9601	Nitroethane, 96%
5	6.6	0.9898	Benzene, 1,3-dimethyl-
		0.9862	<i>m</i> -Xylene, 99%

0.9861	<i>m</i> -Xylene, 1,3-Dimethylbenzene
--------	---------------------------------------

Table S2. Chromatography conditions for univariate calibration of select compounds *o*-cresol, ethylbenzene, α -pinene and γ -terpinene depicted in Figure S8 and Figure S9.

	<i>o</i> -cresol	ethylbenzene	α -pinene	γ -terpinene
Injection volume (μ L)	2	1.5	1	1
Split ratio	20:1	10:1	2:1	2:1
Flow (mL/min)	1	1.5	2	2
Initial oven <i>T</i> ($^{\circ}$ C)	50	50	100	100
<i>T</i> ramp ($^{\circ}$ C/min)	10	10	5	5

3.5 Invited cover page of the journal issue the article was published in



Chapter 4

Gas Chromatography–Fourier Transform Infrared Spectroscopy Reveals Dynamic Molecular Interconversion of Oximes

J. Shezmin Zavahir^a, Yada Nolvachai^a, Bayden R. Wood and Philip J. Marriott^a

- ^a Australian Centre for Research on Separation Science, School of Chemistry, Monash University, Wellington Road, Clayton, Melbourne, VIC 3800, Australia
- ^b Centre for Biospectroscopy, School of Chemistry, Monash University, Wellington Road, Clayton, Melbourne, VIC 3800, Australia

Contents

4.1	Chapter synopsis.....	139
4.2	Graphical abstract published in journal issue	142
4.3	Article	143
4.4	Published supplementary Material.....	154

4.1 Chapter synopsis

Gas chromatography (GC) separation in general involves inert and non-reactive partitioning of analytes between the stationary and mobile phases to yield a resolved, single, Gaussian or near-Gaussian peak in the chromatogram for each respective compound. Some compounds, such as conformational and configurational isomers (diastereomers, enantiomers etc.) which exhibit thermally-fluxional behaviour, however can undergo on-column molecular transformations which distort the chromatographic peak shape. This can result in broadening, overlapping or incomplete resolution of peaks, which is usually characterised in the chromatogram by a plateau region between two terminal peaks. This arises from the ‘reaction’ $A \rightleftharpoons B$, where A and B are resolved on the column, and the energetics is sufficient to allow reaction. This on-column isomerisation, or dynamic interconversion, is a result of isomers which undergo molecular transformations during the chromatographic separation and is known as dynamic GC (DGC). Whilst GC as a physical method is a dynamic process, it is the molecular fluxionality as described here that dynamic GC refers to.

Dynamic GC – and its analogous HPLC method – is a rather unique but still fascinating phenomenon. The novel interconverting peak shape should ‘contain’ all the information related to each component, but most GC detectors are unable to record the precise amounts of each antipode since for example the FID only provides the overall profile, and the mass spectra of A and B will be identical for isomers.

Oximes are a group of chemical compounds belonging to the imines with the general formula $RR'C=NOH$, which can exist in the *E* and *Z* stereoisomer forms. Based on our previous studies they have proved to be well-suited model compounds for the study of interconversion processes in DGC. This has been an area in which analysts have focused on for many years to better understand the various chemical, thermodynamical and chromatographic processes involved in the phenomenon. Many have investigated the use of the high-resolution separation achieved by multi-dimensional GC (MDGC) in the study of this interconversion process, and perhaps most revealing has been the various configurations of comprehensive two-dimensional GC (GC×GC) with heart cutting techniques being explored to physically separate the isomers on two hyphenated columns. Here, column stationary phases such as polyethylene glycol (PEG) have been

seen to enhance the rate of interconversion for studying the individual isomers. Other studies have included molecular simulations, time-resolved techniques, enantioselective column usage, studying of reaction kinetics, stopped-flow chromatographic techniques, quantum mechanical studies, use of different stationary phase combinations, etc.

Nevertheless, one-dimensional GC–mass spectrometry (GC–MS) approaches have seen little success in this field due to the similarity of mass spectra of the *E* and *Z* isomers of such oximes. In contrast, the Fourier transform infrared (FTIR) spectra of these isomers are unique with marked differences in the position and intensity of their absorption bands. This study thus explores the use of one-dimensional GC with FTIR detection, as a novel approach in the study of dynamic interconversion behaviour. Here we use the light-pipe GC–FTIR system described and validated in Chapter 2 to investigate the molecular on-column isomerisation of oxime species. This is a valuable extension to the capabilities of the GC–FTIR hyphenation explored in Chapter 3, but here is specifically focussed on the processes and physical GC parameters that affect the kinetics, and re-iterates the complementary power of MS and FTIR detection in the identification of GC separated compounds.

The on-line acquisition of FTIR spectra aids in investigating the elution profile of individual isomers, especially within the characteristic plateau formation of the chromatogram. Using two oxime species, acetaldehyde and propionaldehyde oxime, for comparison, a range of analyses and data processing approaches were inspected. The uniqueness of individual FTIR spectra, especially in the fingerprint region of 1500–600 cm^{-1} , act as ‘molecular fingerprints’ for compounds. The use of this feature in providing unambiguity to compounds of various chemical classes was explored in Chapter 3 and an extension of the same capability to provide unambiguity to *E* and *Z* isomers of oximes is used in this Chapter. The molecular interconversion studies in this Chapter also benefit from the GC×FTIR comprehensive style analysis using two-dimensional colour contour plots as set out in Chapter 3. Here the isomers’ elution profile was assessed by observing the decay in the distribution of the colour intensity at a particular wavenumber band for each isomer using this spectroscopic/separation information.

Further, in this Chapter the characteristic stronger absorption bands for each isomer was chosen to retrace the single isomer profiles and decipher identity and elution order of the isomers. Multivariate curve resolution, a popular and powerful soft-modelling

chemometric method was adopted to analyse this multicomponent system, resolve the peaks and further confirm the identity of the compounds. This was supported also by molecular simulation of the isomer spectra and comparison to experimental spectra obtained by the in-house designed GC–FTIR system. The system was assessed for the most suitable FTIR data acquisition settings and chromatographic conditions. The effect of varying flow and isothermal temperature on the characteristic DGC peak profile was also observed. This was followed by the comparison of FTIR root mean square absorbance chromatogram to the FID chromatogram obtained with the same settings.

This Chapter thus continues on from the previous 3 Chapters to highlight the value of the molecular spectroscopic detection technique of FTIR when hyphenated to GC in unambiguous compound identification and reveals the role of GC–FTIR in revealing previously unexplored areas of the dynamic molecular interconversion of oximes.

4.3 Article

Gas chromatography–Fourier transform infrared spectroscopy reveals dynamic molecular interconversion of oximes

Junaida Shezmin Zavahir, Yada Nolvachai, Bayden R. Wood and Philip J. Marriott

Published in *Analyst*, Volume 144, pp. 4803–4812, July 2019



Analyst

PAPER

Cite this: *Analyst*, 2019, **144**, 4803

Gas chromatography–Fourier transform infrared spectroscopy reveals dynamic molecular interconversion of oximes†

J. Shezmin Zavahir,^a Yada Nolvachai,^a Bayden R. Wood ^b and Philip J. Marriott ^{*a}

This study reports gas chromatography (GC) combined with Fourier transform infrared (FTIR) spectroscopy to investigate the elution profiles of individual oxime isomers undergoing characteristic interconversion (dynamic chromatography) in GC. The use of a light-pipe FTIR interface enables on-line acquisition of FTIR spectra, which in turn render unambiguous identification of the individual molecules. Here, acetaldehyde oxime and propionaldehyde oxime were chosen for comparison of elution behaviour under varying temperature and carrier flow velocities. The choice of selective responses (wavenumber selectivity), which were relatively stronger for each isomer, enabled display and retracing of the individual isomer over the chromatographic time scale and thus provided characteristic single isomer profiles. Chemometric data analysis using the multivariate curve resolution technique further confirmed this isomer elution profile. Simulation of the spectrum for each isomer allowed comparison with instrument-generated FTIR spectra to confirm the elution order of *E* and *Z* isomers. The effect of changing chromatographic parameters (temperature, flow) on interconversion rates and/or extents were studied and the corresponding change in FTIR spectrum intensity was noted. The GC–FID data acquired concurrently with GC–FTIR analyses ratified isomerisation chromatographic profiles.

Received 30th May 2019,
Accepted 30th June 2019

DOI: 10.1039/c9an00990f

rsc.li/analyst

Introduction

The dynamic interconversion behaviour or reversible first order reactions that may occur during gas chromatographic (GC) elution have been observed for various chemical compounds and systems, and is commonly referred to as dynamic GC (DGC). These instances almost invariably involve isomers that undergo sterically hindered rotations, twisting mechanisms, inversions, rearrangements or such processes.¹ This interesting yet niche area has been studied over the years with an aim to extend the application base of compounds that undergo this process, improve the separation, or investigate parameters that alter the extent of interconversion.^{2–4} To better differentiate the (two or more) isomers involved, methods based on both single dimension and multidimensional GC systems have been studied.^{5–7} Instead of physical

resolution of the isomers, or independent (unique) analysis of the response of each isomer, an understanding of each isomer's profile can be gleaned by mathematical interpretation of the overall unresolved envelope.⁸

On-column isomerisation ($A \rightleftharpoons B$) results in incompletely resolved or overlapping GC peaks usually characterised by peak broadening or formation of a plateau region between terminal isomer peaks A and B^{9,10} as depicted in Fig. 1(a–d). The plateau region observed is a result of differences in retention factors between the original injected compound and its product as one isomer undergoes isomerisation to the other isomer, at some position along the column. The conditions used in GC analysis greatly influences the dynamic process as indicated by the extent of interconversion, which is observed through this plateau interconversion zone of the chromatogram. This is a result of a combination of molecular equilibria either within one or more of the phases ($A_m \rightleftharpoons B_m$ or $A_s \rightleftharpoons B_s$) or between the different phases ($A_m \rightleftharpoons A_s$ or $B_m \rightleftharpoons B_s$), although the latter largely controls the chromatographic elution process. The mobile and stationary phases are denoted by the subscripts *m* and *s* respectively, as depicted in Fig. 1(e). Many studies have been conducted on the kinetics^{11,12} and thermodynamics^{3,11,13,14} which largely determine the equilibria involved in this reversible process.

^aAustralian Centre for Research on Separation Science, School of Chemistry, Monash University, Wellington Road, Clayton, VIC 3800 Melbourne, Australia.

E-mail: Philip.Marriott@monash.edu; Fax: +61 3 99058501; Tel: +61 3 99059630

^bCentre for Biospectroscopy, School of Chemistry, Monash University, Wellington Road, Clayton, VIC 3800 Melbourne, Australia

† Electronic supplementary information (ESI) available. See DOI: 10.1039/c9an00990f

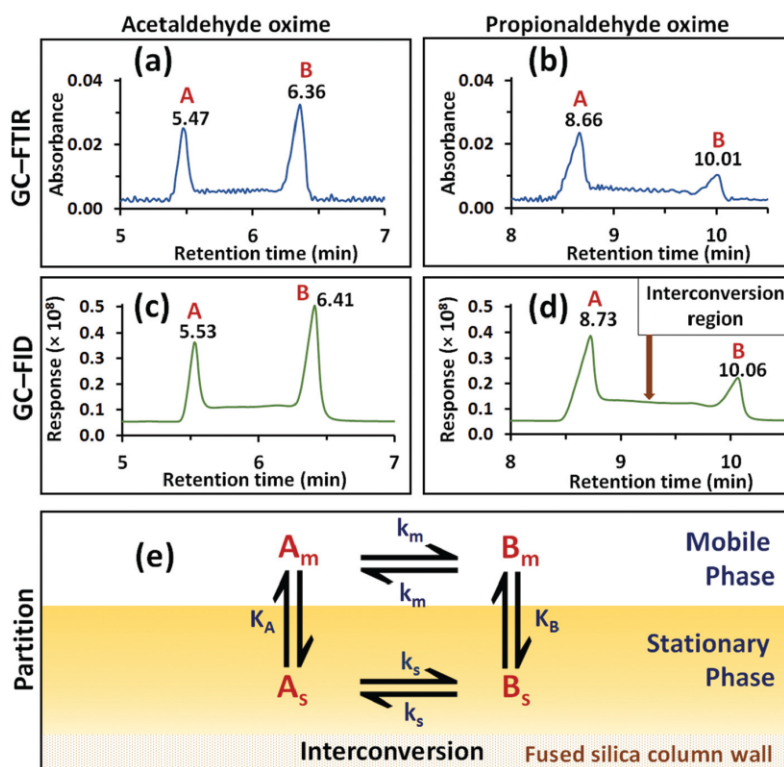


Fig. 1 Chromatograms with peak retention times of acetaldehyde oxime and propionaldehyde oxime in both GC–FTIR (a and b) and GC–FID (c and d). Both isomers have greater retention times in the GC–FID chromatograms since there is a delay of ca. 0.05–0.07 min between FTIR and FID recorded peaks. Very similar elution profiles are seen at each detector.

A particular application has been the observation of interconversion seen in oximes – imines with the general formula of $RR'C=NOH$ and for most studies of observation of this process, $R=H$ – which are important in both chemical and biological systems.^{15,16} Rotation around the C–N bond and inversion *via* sp -hybridization of the N atom^{3,17} have been proposed for the isomerisation of such oximes, which exist as *E* and *Z* isomers based on the configuration of substituents around the C=N double bond. These are used with confidence for studies on interconversion processes since the magnitude of their energy barrier is readily observed at the temperature at which they are chromatographed. The temperature is relatively low, usually <150 °C, and so they also have a labile configuration during GC analysis.⁶ They exhibit this effect most noticeably on wax (poly(ethylene)glycol) type phases, but do show this behaviour on some ionic liquid phases.

Among the various detectors used in GC, the mass spectrometer (MS) and flame ionisation detector (FID) are the most common choices. Over the years detection methods used for GC studies on the interconversion process include FID^{3,6,18} and various MS methods.^{5,7,19,20} Recent dynamic GC studies have employed comprehensive two-dimensional gas chromatography (GC \times GC) methods. However, conventional one dimen-

sional (1D) GC coupled to mass spectrometers fail to deconvolute, or separately identify the two isomers of the peak envelope due to the isomers usually having the same mass spectra. Thus there is limited direct information available on the individual abundances of each isomer over the total distribution. This calls for spectroscopic detectors such as the vacuum ultraviolet (VUV) or FTIR detector, which should better differentiate isomers. Despite the reduced sensitivity that FTIR offers compared to VUV, the wealth of information related to molecular functionalities and structures offered by FTIR detection should favour its general suitability for identification. In cases such as dynamic chromatographic studies, FTIR detection can play a role in identification of the isomers at each position throughout the envelope. This is because the molecular vibrational and fine-structure properties of the IR absorptions being different for each of the isomers, thus creating unique molecular isomer specific fingerprints.²¹ The technique employed in this study combines infrared spectroscopic detection with a 1DGC experiment.

The GC–Fourier transform infrared detection (GC–FTIR) system used here, depicted in ESI Fig. S1,[†] enables online detection by combining GC with an IR source *via* an interface housing a light-pipe,²² which constitutes a highly reflective

heated flow cell. This chemical tool combines the advantages of separation by GC with unambiguous identification of separated components using FTIR detection, which in turn denotes a unique signature for each component.²³ The chromatographic information generated by GC–FTIR – a plot of the total FTIR absorbance detected as a plot of time – can be further converted into informative chromatographic plots related to elution of each isomer using an isomer-specific response. This is also needed because the light-pipe renders some spectra void of useful information due to the absence of components present in the light-pipe at the time between GC peaks. Thus the reconstruction of spectroscopic data is generally needed and is carried out by Gram-Schmidt (GS) vector orthogonalisation or creation of functional group (FG) chromatograms.^{24,25}

Unlike MS spectra, the FTIR spectra of the two *E* and *Z* oxime isomers are distinct. Upon chromatographically separating the two isomers, the FTIR spectrum of each terminal GC peak is obtained. This method observes the time profile of the two individual isomers by choosing to follow an IR absorbing response prominent in the FTIR spectrum of each isomer. In addition, the use of the flame ionisation detector (FID) subsequent to the FTIR detector confirms chromatographic peak patterns seen after the light-pipe. In recent times multivariate analysis methods have been used widely to obtain both qualitative and quantitative data.^{26,27} The ability to use time based spectroscopic data generated in this study enables chemometric methods to be applied to further understand isomer elution profiles. Spectroscopic techniques have been a much sought after means of determining composition of reaction mixtures.^{28,29} To the best of our knowledge FTIR as a detection method has not been used with GC for the purpose of studying interconversion in oximes.

Experimental

Sample preparation

Acetaldehyde oxime (acetaldoxime; 99%, Sigma-Aldrich, St Louis, MO) and propionaldehyde oxime ($\geq 96\%$, Sigma-Aldrich, St Louis, MO) were prepared in acetone (Merck KGaA, Darmstadt, Germany). The internal standard used was butan-1-ol (99.5%, Merck, Kilsyth, Australia), also prepared in acetone. 20% (v/v) samples of the oxime mixtures were prepared in acetone with 250 μL of 20% (v/v) butan-1-ol added.

Instrumentation

A GC–FTIR system was used comprising of a PerkinElmer Clarus 680 GC equipped with an autosampler and flame ionisation detection (FID) (PerkinElmer Inc., Shelton, CT). A PIKE FTIR accessory (PIKE Technologies, Madison WI) was used as an interface to couple the GC to the IR source, which was a PerkinElmer Frontier SP8000 Fourier transform IR (PerkinElmer Inc., Bucks, UK) with a mid-infrared source. The PIKE accessory consisted of a gold-coated heated gas cell (light-pipe) with dimensions 120 mm length \times 1 mm I.D. path-length, fitted with 13 mm \times 2 mm thick KBr windows at either

end. IR radiation was recorded by a Mercury Cadmium Telluride (MCT) detector cooled to -196°C by liquid nitrogen for infrared detection.

Compounds were injected into the GC at an inlet temperature of 230°C with a 2 μL volume and 10 : 1 split unless specified. GC oven temperatures were operated isothermally, between 80°C and 140°C . Helium (99.99%) was used as carrier gas with flow rates varying from 1.5 mL min^{-1} to 4 mL min^{-1} . FID temperature was 250°C with acquisition rate of 12.5 Hz.

A HP-INNOWax (30 m \times 0.32 mm I.D. \times 0.5 μm d_f; Agilent Technologies) column consisting of a polyethylene glycol (PEG) stationary phase was chosen due to its polar nature, which apparently promotes the interconversion process. This connected the GC injection port to the light-pipe inlet *via* a deactivated fused silica (DFS) transfer line capillary (0.5 m \times 0.25 mm I.D., Agilent Technologies Mulgrave, Australia) using a universal press-tight connector (Restek, Bellefonte, PA). The light-pipe outlet was similarly connected to the FID using another DFS capillary (0.5 m \times 0.25 mm I.D.). Both inlet and outlet transfer line columns were housed within a heated insulated transfer line.

The GC conditions employed were varied depending on the analysis goals to either promote or limit the interconversion of the isomers. This was achieved by a range of settings including that of carrier gas flow rate, GC oven temperature, light-pipe temperature and FTIR data acquisition.

Real time spectrum results were obtained with weak apodisation at scan range of $4000\text{--}700\text{ cm}^{-1}$, at optical resolution of 4 cm^{-1} , with a scan speed of 1 cm s^{-1} , which corresponds to 0.92 spectra per s (0.92 Hz). Light-pipe and transfer line temperatures were maintained at a minimum of 10°C higher than the maximum temperature of the GC oven program.

Software

FID data were recorded using PerkinElmer TurboMass (v 6.1.2.2048) software. Software used for FTIR data was PerkinElmer Spectrum Timebase v3.1.3.0042 for data acquisition, and PerkinElmer Spectrum v10.4.2.27 for spectrum processing. MCR data analysis was processed under Matlab R2017b from MathWorks (Natick, MA) using the MCR-ALS 2.0 graphical user interface.

IR spectrum simulation

The geometry optimisations and frequency calculations of acetaldehyde oxime isomers were carried out using the M06-2X³⁰/aug-cc-pVDZ^{31,32} level of theory.^{33,34} All calculations were performed using Gaussian09.³⁵ Avogadro³⁶ was used for molecule and IR spectrum visualisation.

Results and discussion

FID/FTIR correlation

Dynamic chromatography studies in the past³⁷ confirmed that a polar wax-type stationary phase column is the most suitable

to promote molecular interconversion for oximes, hence the choice of a PEG column for this study. A range of analyses was performed, initially to select suitable chromatographic conditions. Short-chain alcohols have been previously used as the internal standard (I.S.) for dynamic chromatography experiments of oximes. Thus butan-1-ol was chosen, and it eluted after the solvent but before the oxime isomers. Preliminary experience with FID, as reported elsewhere, was initially conducted to observe interconversion,⁶ and confirm the extent of interconversion on the PEG stationary phase, prior to performing analyses using the GC–FTIR–FID configuration.

Parameter settings of the interferometer and FTIR data acquisition influence the root mean square (RMS) absorbance chromatogram as well as the FTIR spectrum in GC–FTIR analysis. The root mean square (RMS) absorbance chromatogram essentially presents the full FTIR response *versus* retention time. The apodisation process, removing of side lobes (feet or “podes”) of the IR spectrum, is conducted by multiplying the interferogram by a suitable weighting function prior to the Fourier transformation process.³⁸ This effectively compromises between reducing the amplitude of side lobes and the resulting deterioration of spectral resolution. Interferograms processed in the absence of apodisation have a lesser signal-to-noise ratio (SNR) than that in which apodisation has been applied. Of the three Norton Beer apodisation functions (strong, medium and weak) offered by the Spectrum Timebase software, weak apodisation was chosen for this study. The zero-path-difference (ZPD) point in interferograms corresponds to the position where interference production is maximum due to the moving mirrors of the spectrophotometer. Although an ideal interferometer would produce totally symmetrical interferograms, this is not so in practice. The process of phase correction (PC) is used to ensure the sample intervals of moving mirrors are in the same phase and hence tally with a path difference of zero³⁹ thus removing the asymmetry of the interferogram. The analyses were performed using 3 main PC settings offered by the Timebase software – background, self and magnitude – were compared. The ‘self’ PC setting phase corrects the sample spectrum from the interferogram and the background spectrum from its interferogram. ‘Background’ PC uses the background spectrum to phase correct the sample spectrum and is routinely used for samples that strongly absorb infrared. Often used at lower resolutions, the ‘magnitude’ PC is a result of calculating the magnitude spectrum – those that are subject to ordinate errors in low transmission regions. The commonly applied data point resolutions in on-line vapour phase GC–FTIR systems are 4 cm^{−1} or 8 cm^{−1}.²² Comparison of resolution, phase correction and scan speed settings were carried out to obtain appropriate settings to be used for FTIR data acquisition here, the results of which are shown in ESI Fig. S2.† Thus, data acquisition was carried out with a resolution of 4 cm^{−1}, magnitude phase correction settings, and 1 cm s^{−1} scan speed.

GC–FTIR–FID analysis was conducted with the injected constituents travelling through the light-pipe to the FID, as depicted in ESI Fig. S1.† The 1D GC chromatogram obtained

in an isothermal chromatographic analysis at 90 °C with flow of 3 mL min^{−1} using sequential FTIR and FID detection demonstrated the typical dynamic chromatographic interconversion profile of the two terminal *E* and *Z* peaks with a plateau region between them, shown in Fig. 1. Here, the acet-aldehyde oxime, which elutes first, has a higher initial amount of isomer B than isomer A, whereas for propionaldehyde oxime, a relatively higher amount of isomer A is seen. The retention time of FID chromatograms were greater by about 0.05 min than the respective FTIR chromatograms under the conditions here, due to compounds passing through the light-pipe before entering the FID. Fig. 1(e) sketches the equilibria (*k* values; rate constant) for the dynamic interconversion system $A_m \rightleftharpoons B_m$ and $A_s \rightleftharpoons B_s$ for isomers A and B that may arise in the stationary (s) and mobile (m) phases. Each isomer's retention time is determined by its distribution constant K_A and K_B values between the m and s phases.

Infrared spectrum processing

The effects of instrumental noise contributions by interferometers play a significant role in the signal output and hence SNR of GC–FTIR chromatograms.⁴⁰ The inherent noise in light-pipe based instruments contribute largely to the reduced SNR of the chromatogram. Thus, mathematical integration of interferogram signals to result in smoothing and reconstruction of GC–FTIR chromatograms is conducted – which effectively reduces noise – to obtain a significantly higher SNR.⁴¹ This aids in clarifying the existence of peaks which can be more apparent when data are smoothed, and obtaining qualitative information, as in this case of allowing the oxime terminal peaks to be observed with clarity.

Chromatograms generated in GC–FTIR represent a plot of the total IR detector response as a function of separation on a time scale, and are shown as a RMS absorbance plot. The most common procedures for converting this structure-specific information to reconstructed chromatograms include the Gram-Schmidt (GS) vector orthogonalisation, and the functional group (FG) chromatogram (known as chemigrams) method.⁴² Of these, the GS process uses a non-orthogonal set of linearly independent functions to construct an orthogonal basis. The intensity of a GS chromatogram relates to the difference of the interferogram vectors to the orthogonal axes used for the background subspace specification. Since this depends on the difference in the interferogram measured in the presence of an analyte in the light-pipe (at a level above the detection limit) and that measured when analyte is absent in the light-pipe, GS chromatograms do not necessarily depend on the IR absorbance.^{23,25} The FG chromatogram in contrast uses the chromatography–IR absorbance spectrum, where the integrated absorbance of selected regions are plotted against elution time. Since these predefined regions represent specific functional groups or vibrations, this method can be used to trace the elution profile of specific structural elements (*e.g.* the wavenumber of a selected absorbing band in FTIR) in GC separated compounds of various nature.⁴³ The Timebase software

used for FTIR data collection in this study is able to create both GS and FG chromatograms.

In this study, the construction of GS chromatograms (with 30 spectra) provides reconstructed chromatograms giving significantly improved clarity and SNR. Fig. 2a demonstrates the improved SNR chromatographic reconstruction achieved by the GS process for both acetaldehyde oxime and propionaldehyde oxime at an isothermal analysis at 90 °C with column flow of 3 mL min⁻¹ compared with the RMS absorbance result of GC-FTIR. Comparison of the original GC-FTIR (Fig. 2a) and GC-FID (Fig. 2b) chromatograms are also made with the latter retaining the peak profile expected. From this point onwards GS chromatograms will be used for comparison of chromatograms with varying chromatographic conditions.

E and *Z* isomer trace profiles using FTIR

Identification of individual *E* and *Z* isomers underlying the interconversion profile for a 1DGC separation is impossible when using detectors such as MS and FID. Standalone spectroscopic methods have been used widely for isomer differentiation of aldehyde oximes,^{44,45} with FTIR detection enabling identification by providing infrared spectra which differ in some of the isomer absorption bands. This characteristic is hence useful in GC detection of such isomers. Although the infrared spectrum of oximes have three general characteristic

absorption bands which correspond to the stretching vibrations of O-H (3600 cm⁻¹), C-N (1665 cm⁻¹) and N-O (945 cm⁻¹),⁴⁶ they differ in the fingerprint region below 1500 cm⁻¹. This is readily seen in the recorded IR spectra which correspond to the terminal A and B peaks (refer to Fig. 1) of the acetaldehyde oxime and propionaldehyde isomer mix which show clear differences in their FTIR absorption spectra, as depicted in ESI Fig. S3.†

Efforts to deduce the structure and stable forms of oxime isomers have included gas phase ¹H NMR studies,⁴⁷ conformational energy studies,¹⁵ microwave spectra,⁴⁸ DFT and *ab initio* MP2 methods, infrared spectroscopy,⁴⁹ etc. Previous experimental analyses using GC-FID with PEG and non-polar columns have generally shown the *E* isomer of acetaldehyde oxime to elute before that of its *Z* counterpart.³⁷ This was confirmed using spectrum simulations in which the simulated spectrum for the *E* isomer of acetaldehyde oxime corresponded to the experimental FTIR spectrum of the isomer which eluted first (A) in GC-FTIR analysis. The same conclusion is observed for the later eluting isomer (B) which correlates to the simulated *Z* acetaldehyde oxime isomer as seen in Fig. 3.

Based on the differences in intensities of spectroscopic absorption bands of the two isomers, absorption band(s) that were noticeably stronger in one isomer compared to the other isomer were chosen. Thus, the absorption band at 991 cm⁻¹

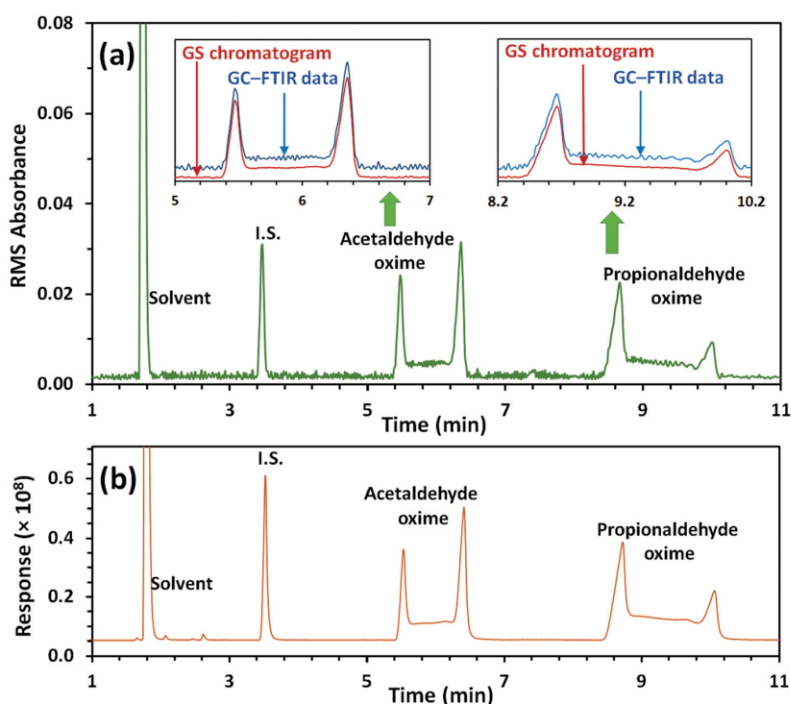


Fig. 2 (a) GC-FTIR showing comparison of non-processed GC-FTIR chromatograms together with the Gram-Schmidt (GS) chromatograms for acetaldehyde oxime and propionaldehyde oxime inset. (b) The analogous GC-FID chromatographic result using the same GC conditions. Internal standard (I.S.) = butan-1-ol.

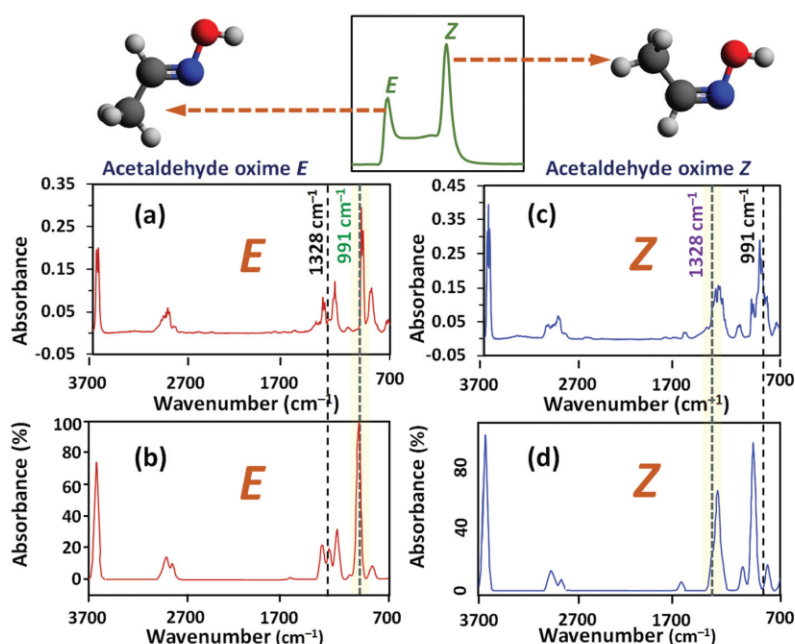


Fig. 3 FTIR spectra and molecular models of *E* and *Z* isomers of acetaldehyde oxime corresponding to the respective peaks of the chromatographic profile. (a) and (c) correspond to the FTIR spectrum of the 2 peaks in order of elution. (b) and (d) are the simulated spectra of the two isomers and are seen to correspond to their respective FTIR spectra.

for the C–H out of plane bending vibration, was chosen since it was stronger for the *E* isomer (Fig. 3a, b and 4a). Similarly, the C–H stretching vibration band at 1328 cm^{−1} was chosen as being comparatively stronger in the *Z* isomer (Fig. 3c, d and 4a). By choosing these selective absorption bands, a chemigram of each chosen wavenumber value can be plotted against the elution time of the GC-FTIR chromatogram. The result is an elution profile selective to each isomer, as presented in Fig. 4b.

Use of chemometric techniques in hyphenated chromatography using spectroscopic or spectrometric detectors has gained popularity, amongst which the Multivariate Curve Resolution (MCR) method is useful to decompose data matrices and recover pure response profiles in unresolved mixtures with minimal assumptions about the data set.⁵⁰ 1DGC as well as GC × GC with MS detection have used MCR methods for such deconvolution.⁵¹ Employing MS however, can be of limited use when isomers with similar mass spectra are to be analysed in instances where they coelute. MCR has been used successfully with liquid chromatography-IR analysis for resolving overlapping chromatographic peaks.⁵² Thus, the advantage offered by MCR to simultaneously identify and quantify analytes using online IR detection can be used here to study the pure chromatographic profiles of two individual IR-absorbing oxime isomers.

MCR is mathematically based on the bilinear model represented in eqn (1) below, where *D* is a data matrix containing spectra in which *C* consists of the matrix of concentrations

and *S*^T refers to the matrix of reference spectra. Here *E* refers to the matrix of residual noise not described by MCR.

$$D = CS^T + E \quad (1)$$

In using the MCR for a typical GC-FTIR analysis, the model outlined by eqn (1) can express *D*, *C* and *S*^T as the sum of the pure signals in the original GC-FTIR matrix, the matrix of the RMS absorbance chromatogram and the matrix of FTIR spectra respectively, as demonstrated in Fig. 4e. Spectra for MCR analysis were collected at specific data points of RMS absorbance chromatograms. In the example cited in Fig. 4c–f, 26 FTIR spectra were acquired from a chromatogram section (2.64–2.92 min) corresponding to the elution of acetaldehyde oxime in an isothermal GC analysis at 120 °C with column flow of 3 mL min^{−1}. MCR results were obtained using a predefined number of 2 components, which correspond to the two oxime isomers. Fig. 4f shows the MCR recovered concentration profiles of the two components which directly corresponds to the profile seen in Fig. 4b, thus confirming the elution profile of the two acetaldehyde oxime isomers within the interconversion zone. MCR recovered pure spectra (Fig. 4c and d) and spectra recovered from the peak apex of GC peaks (Fig. 4a) are similar, confirming the elution order of the oximes.

Effect of varying chromatographic parameters

The two main chromatographic parameters that affect the rate of interconversion are the oven temperature, *T*, and column

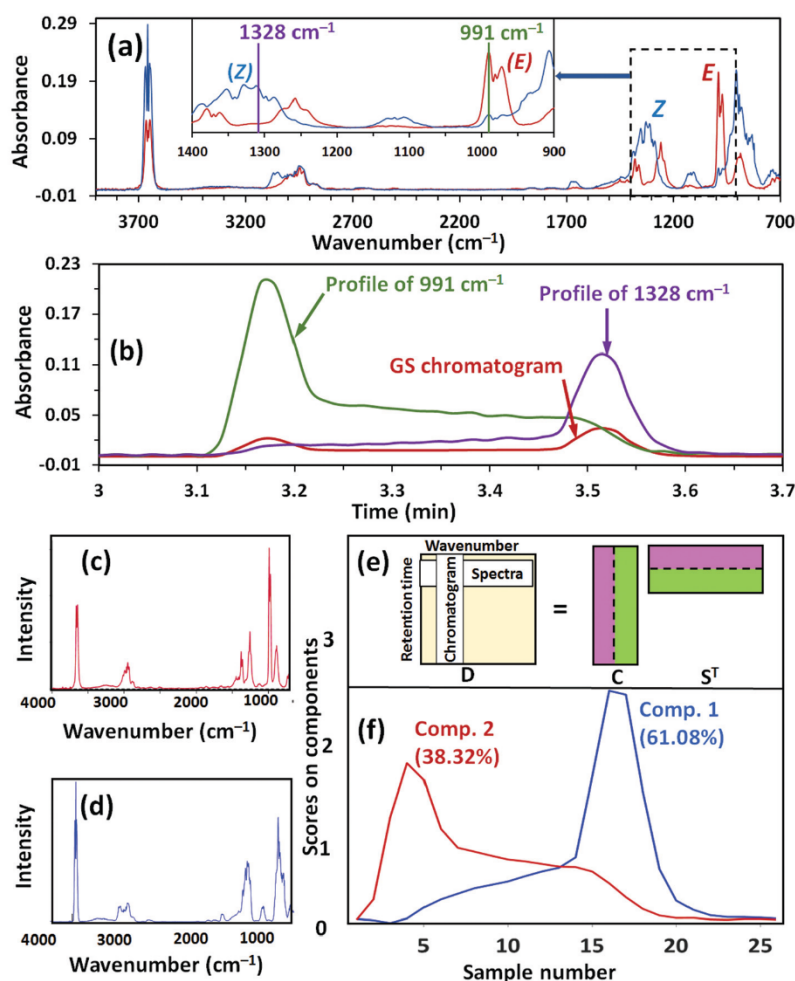


Fig. 4 (a) The IR spectra of *E* and *Z* acetaldehyde oxime isomers in the 1400–900 cm⁻¹ region enlarged (inset). (b) Plot of time based elution profiles of the IR spectra absorbances at 991 cm⁻¹ and 1328 cm⁻¹, shown in comparison to the original GS chromatogram. (c) and (d) MCR resolved spectra. (f) MCR resolved profiles of c and d. (e) Bilinear model used for MCR analysis of GC–FTIR data set which is the product of matrices of pure concentration profiles and spectra.

carrier gas flow rate which affects residence time. Increased T should increase the extent of plateau, as the rate constant increases (although retention time will decrease), and decreased carrier flow velocity will increase the plateau as time increases. This corresponds to a greater probability of each isomer undergoing an isomerisation event. Injection of the acetaldehyde and propionaldehyde oxime isomer mixture into the PEG column with varying isothermal oven temperatures show an interesting and expected change in the GC–FTIR dynamic chromatogram shape and elution pattern, shown in Fig. 5. Analyses were conducted at a constant flow of 3.0 mL min⁻¹ and light-pipe temperature of 150 °C. Previous studies have confirmed that changes in oven temperature (T) influence the extent of interconversion of oxime isomers.^{5,6}

Corresponding GC–FID chromatograms that compare with these GC–FTIR results are shown in ESI Fig. S4†. At relatively low temperatures some interconversion is evident with the observation of the characteristic plateau shape between the terminal peaks. The pattern at $T = 100$ °C changes with increasing T such that the distance between the terminal peaks corresponding to their resolution or respective retention time separation gradually decreases (Fig. S4†). This is accompanied by a gradual rise in the relative response of the plateau region with respect to the baseline and terminal unconverted isomers, A and B, or C and D for acetaldehyde and propionaldehyde oxime respectively. The increase in T contributes to an increase in the extent of interconversion. Substantial interconversion is seen at $T = 130$ °C, and at $T =$

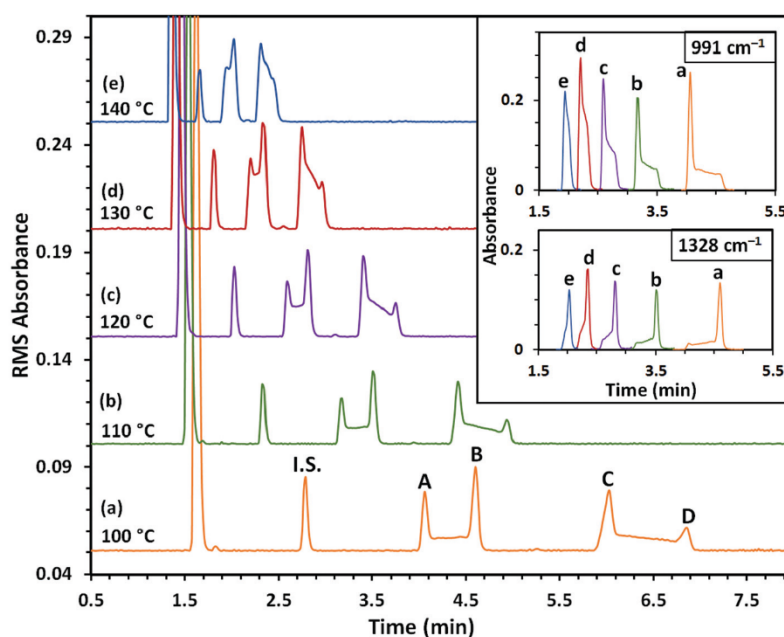


Fig. 5 Chromatograms of increasing isothermal temperatures of (a) 100 °C, (b) 110 °C, (c) 120 °C, (d) 130 °C and (e) 140 °C, at a light-pipe temperature of 150 °C and column flow of 3.0 mL min⁻¹. A and B correspond to the peaks of acetaldehyde oximes and C and D to those of propionaldehyde oxime. I.S.; internal standard. Profiles of wavelengths 991 cm⁻¹ and 1328 cm⁻¹ corresponding to the retention times of acetaldehyde oxime are inset.

140 °C the terminal antipodes are almost unresolved for acetaldehyde oxime but propionaldehyde oxime displays evidence of the plateau with terminal antipodes still discernible. At higher T reduced resolution will lead to antipode peaks and plateau being unresolved. Depicted in the inset in Fig. 5 are the corresponding trends in the selective profiles of the absorbances of the E isomer (991 cm⁻¹) and the Z isomer (1328 cm⁻¹). These are data that cannot be obtained with non-selective detectors that are unable to provide selective response

to the individual isomers. The only way to achieve comparative data is to mathematically deconvolute the profile with predicted or assumed rate constants and equilibria into its component A and B species. The alternative GC \times GC experiment⁷ was able to resolve the isomers on the second column to provide physical chromatographic deconvolution. Increase in oven T was also accompanied by an increase in the intensity of absorption bands in the IR spectra corresponding to the GC peaks as shown in ESI Fig. S5.[†]

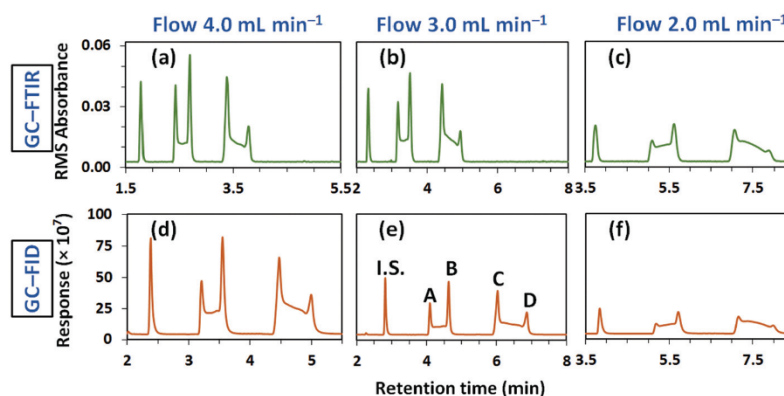


Fig. 6 GC–FTIR (a, b and c) and GC–FID (d, e and f) chromatograms of acetaldehyde oxime (A and B) and propionaldehyde oxime (C and D) isomer mixtures at decreasing flows of 4.0 mL min⁻¹ (a and d), 3.0 mL min⁻¹ (b and e) and 2.0 mL min⁻¹ (c and e), at $T = 110$ °C.

The effect of changing column flow on the extent of interconversion between the oxime analogues is evident in both GC–FTIR and GC–FID chromatograms. Chromatographic analyses were conducted with decreasing column flows from 4.0 mL min^{−1} to 2.0 mL min^{−1} while keeping the oven *T* constant at 110 °C and light-pipe *T* of 120 °C. Decreasing the column flow in successive analyses leads to an increase in the retention time, corresponding to residence or reaction time, and hence extent of interconversion between the isomers. Longer residence time of the oxime molecules in the column promotes interconversion between the isomers. This increases separation of the A and B antipodes, extends the plateau region between the isomers, and hence lowers its height difference from the baseline as evident in Fig. 6.

Conclusions

The interconversion process in 1DGC with respect to reversibly labile species, where the energy of interconversion and the prevailing GC conditions are suitable, may lead to a profile that separates the isomers and allows observation of a plateau between them. More common GC detectors often are unable to independently record a unique response to each isomer, for example the MS detector will usually not reliably distinguish each of the isomers. This study exploits the advantages of a FTIR detector to provide spectra that differentiate the two isomers, to then examine the chromatographic pattern of each isomer based on their unique absorbances at specific wavenumbers. The GC–FTIR experimental approach used here offers the possibility of interpreting the interconversion profiles of the two isomers underlying the interconversion region of the original chromatogram. The temperature dependency of the overall chromatographic peak shape is observed according to the FTIR's RMS absorbance response, then by the individual isomer shape change with varying temperature. Likewise the effect of carrier flow rate, where reduced flow rate increases the residence time and the extent of interconversion. The overall profile is comparable between FTIR and FID detectors.

Conflicts of interest

There are no conflicts to declare.

Acknowledgements

Support for this work was provided by the Australian Research Council Linkage Grant scheme with partner PerkinElmer (Grant LP150100465). The authors acknowledge the funding from PerkinElmer to the Monash University GRIP program. Support for a Deans Research scholarship to JSZ from the Monash University is also acknowledged. Dr David Perez-Guaita's advice on chemometrics is appreciated.

References

- 1 C. Dugave and L. Demange, *Chem. Rev.*, 2003, **103**, 2475–2532.
- 2 P. J. Marriott and Y. H. Lai, *J. Chromatogr. A*, 1988, **447**, 29–41.
- 3 O. Trapp, R. Shellie, P. Marriott and V. Schurig, *Anal. Chem.*, 2003, **75**, 4452–4461.
- 4 L. Pasti, A. Cavazzini, M. Nassi and F. Dondi, *J. Chromatogr. A*, 2010, **1217**, 1000–1009.
- 5 C. Chifuntwe, F. Zhu, H. Huegel and P. J. Marriott, *J. Chromatogr. A*, 2010, **1217**, 1114–1125.
- 6 S. Kröger, Y. F. Wong, S.-T. Chin, J. Grant, D. Lupton and P. J. Marriott, *J. Chromatogr. A*, 2015, **1404**, 104–114.
- 7 C. Kulsing, Y. Nolvachai, Y. F. Wong, M. I. Glouzman and P. J. Marriott, *J. Chromatogr. A*, 2018, **1546**, 97–105.
- 8 O. Trapp, G. Schoetz and V. Schurig, *Chirality*, 2001, **13**, 403–414.
- 9 J. Krupčík, J. Mydlová, P. Májek, P. Šimon and D. W. Armstrong, *J. Chromatogr. A*, 2008, **1186**, 144–160.
- 10 O. Trapp, *J. Chem. Inf. Comput. Sci.*, 2004, **44**, 1671–1679.
- 11 O. Trapp and V. Schurig, *Chem. – Eur. J.*, 2001, **7**, 1495–1502.
- 12 V. Schurig, M. Jung, M. Schleimer and F. G. Klärner, *Chem. Ber.*, 1992, **125**, 1301–1303.
- 13 S. Reich, O. Trapp and V. Schurig, *J. Chromatogr. A*, 2000, **892**, 487–498.
- 14 O. Trapp and V. Schurig, *J. Am. Chem. Soc.*, 2000, **122**, 1424–1430.
- 15 T. J. Venanzi and C. A. Venanzi, *J. Comput. Chem.*, 1988, **9**, 67–74.
- 16 S. Mukherjee, A. P. Bapat, M. R. Hill and B. S. Sumerlin, *Polym. Chem.*, 2014, **5**, 6923–6931.
- 17 F. Blanco, I. Alkorta and J. Elguero, *Croat. Chem. Acta*, 2009, **82**, 173–183.
- 18 P. Marriott, O. Trapp, R. Shellie and V. Schurig, *J. Chromatogr. A*, 2001, **919**, 115–126.
- 19 N. Isoherranen, M. Roeder, S. Soback, B. Yagen, V. Schurig and M. Bialer, *J. Chromatogr. B: Biomed. Sci. Appl.*, 2000, **745**, 325–332.
- 20 Y. F. Wong, C. Kulsing and P. J. Marriott, *Anal. Chem.*, 2017, **89**, 5620–5628.
- 21 J. S. Zahir, Y. Nolvachai and P. J. Marriott, *TrAC, Trends Anal. Chem.*, 2018, **99**, 47–65.
- 22 T. Visser, in *Handbook of Vibrational Spectroscopy*, ed. P. R. Griffiths and J. M. Chalmers, John Wiley & Sons, Ltd, Chichester, 2006, pp. 1605–1626.
- 23 P. R. Griffiths and J. A. de Haseth, in *Fourier Transform Infrared Spectrometry*, John Wiley & Sons, Inc., 2006, pp. 481–507.
- 24 P. R. Griffiths, Reference Module in Chemistry, in *Molecular Sciences and Chemical Engineering*, Elsevier, 2013.
- 25 R. L. White, in *Encyclopedia of Spectroscopy and Spectrometry*, ed. G. E. Tranter and D. W. Koppenaal, Academic Press, Oxford, 3rd edn, 2017, pp. 251–255.
- 26 H. Parastar, in *Data Handling in Science and Technology*, ed. A. M. de la Peña, H. C. Goicoechea, G. M. Escandar and A. C. Olivieri, Elsevier, 2015, vol. 29, pp. 293–345.

- | Paper | Analyst |
|---|--|
| 27 L. Violet, A. Mifleur, L. Vanoye, D. H. Nguyen, A. Favre-Réguillon, R. Philippe, R. M. Gauvin and P. Fongarland, <i>React. Chem. Eng.</i> , 2019, 4 , 909–918. | 38 P. R. Griffiths, in <i>Encyclopedia of Spectroscopy and Spectrometry</i> , ed. J. C. Lindon, G. E. Tranter and D. W. Koppenaal, Academic Press, Oxford, 3rd edn, 2017, pp. 428–436. |
| 28 S. Li, J. Lyons-Hart, J. Banyasz and K. Shafer, <i>Fuel</i> , 2001, 80 , 1809–1817. | 39 B. Stuart, in <i>Infrared Spectroscopy: Fundamentals and Applications</i> , John Wiley & Sons Ltd., West Sussex, 2004, ch. 3, pp. 15–44. |
| 29 R. Richard, Y. Li, B. Dubreuil, S. Thiebaud-Roux and L. Prat, <i>Bioresour. Technol.</i> , 2011, 102 , 6702–6709. | 40 G. M. Brissey, D. E. Henry, G. N. Giss, P. W. Yang, P. R. Griffiths and C. L. Wilkins, <i>Anal. Chem.</i> , 1984, 56 , 2002–2006. |
| 30 Y. Zhao and D. G. Truhlar, <i>Theor. Chem. Acc.</i> , 2008, 120 , 215–241. | 41 B. A. Hohne, G. Hangac, G. W. Small and T. L. Isenhour, <i>J. Chromatogr. Sci.</i> , 1981, 19 , 283–289. |
| 31 R. A. Kendall, T. H. Dunning Jr. and R. J. Harrison, <i>J. Chem. Phys.</i> , 1992, 96 , 6796–6806. | 42 J. A. de Haseth and T. L. Isenhour, <i>Anal. Chem.</i> , 1977, 49 , 1977–1981. |
| 32 D. E. Woon and T. H. Dunning Jr., <i>J. Chem. Phys.</i> , 1993, 98 , 1358–1371. | 43 S. Wachholz, U. Just, F. Keidel, H. Geißler and K. Käßler, <i>Fresenius' J. Anal. Chem.</i> , 1995, 352 , 515–520. |
| 33 V. Barone and M. Cossi, <i>J. Phys. Chem. A</i> , 1998, 102 , 1995–2001. | 44 S. Bank, W. D. Closson and L. T. Hodgins, <i>Tetrahedron</i> , 1968, 24 , 381–387. |
| 34 M. Cossi, N. Rega, G. Scalmani and V. Barone, <i>J. Comput. Chem.</i> , 2003, 24 , 669–681. | 45 K. Hosoi, H. Izawa, M. Kida, Y. Suzuki, K. Takahashi, M. Sakuma, M. Matsumoto, A. Mizoguchi, N. Kuze, T. Sakaizumi, P. G. Kolandaivel and O. Ohashi, <i>J. Mol. Struct.</i> , 2005, 735–736 , 325–334. |
| 35 M. J. Frisch, G. W. Trucks, H. B. Schlegel, G. E. Scuseria, M. A. Robb, J. R. Cheeseman, G. Scalmani, V. Barone, B. Mennucci, G. A. Petersson, H. Nakatsuji, M. Caricato, X. Li, H. P. Hratchian, A. F. Izmaylov, J. Bloino, G. Zheng, J. L. Sonnenberg, M. Hada, M. Ehara, K. Toyota, R. Fukuda, J. Hasegawa, M. Ishida, T. Nakajima, Y. Honda, O. Kitao, H. Nakai, T. Vreven, J. A. Montgomery Jr., J. E. Peralta, F. Ogliaro, M. J. Bearpark, J. Heyd, E. N. Brothers, K. N. Kudin, V. N. Staroverov, R. Kobayashi, J. Normand, K. Raghavachari, A. P. Rendell, J. C. Burant, S. S. Iyengar, J. Tomasi, M. Cossi, N. Rega, N. J. Millam, M. Klene, J. E. Knox, J. B. Cross, V. Bakken, C. Adamo, J. Jaramillo, R. Gomperts, R. E. Stratmann, O. Yazyev, A. J. Austin, R. Cammi, C. Pomelli, J. W. Ochterski, R. L. Martin, K. Morokuma, V. G. Zakrzewski, G. A. Voth, P. Salvador, J. J. Dannenberg, S. Dapprich, A. D. Daniels, Ö. Farkas, J. B. Foresman, J. V. Ortiz, J. Cioslowski and D. J. Fox, <i>Gaussian 09</i> , Gaussian, Inc., Wallingford, CT, 2009. | 46 A. M. Buswell, W. H. Rodebush and M. F. Roy, <i>J. Am. Chem. Soc.</i> , 1938, 60 , 2444–2449. |
| 36 M. Hanwell, D. Curtis, D. Lonie, T. Vandermeersch, E. Zurek and G. Hutchison, <i>J. Cheminf.</i> , 2012, 4 , 1–17. | 47 R. K. Harris and R. C. Rao, <i>Org. Magn. Reson.</i> , 1983, 21 , 580–586. |
| 37 P. Marriott, K. Aryasuk, R. Shellie, D. Ryan, K. Krisnangkura, V. Schurig and O. Trapp, <i>J. Chromatogr. A</i> , 2004, 1033 , 135–143. | 48 K. Hosoi, H. Izawa, M. Kida, Y. Suzuki, K. Takahashi, M. Sakuma, M. Matsumoto, A. Mizoguchi, N. Kuze, T. Sakaizumi, P. G. Kolandaivel and O. Ohashi, <i>J. Mol. Struct.</i> , 2005, 735–736 , 325–334. |
| | 49 A. Andrzejewska, L. Lapinski, I. Reva and R. Fausto, <i>Phys. Chem. Chem. Phys.</i> , 2002, 4 , 3289–3296. |
| | 50 A. de Juan, J. Jaumot and R. Tauler, <i>Anal. Methods</i> , 2014, 6 , 4964–4976. |
| | 51 L. W. Hantao, H. G. Aleme, M. P. Pedroso, G. P. Sabin, R. J. Poppi and F. Augusto, <i>Anal. Chim. Acta</i> , 2012, 731 , 11–23. |
| | 52 J. Kuligowski, G. Quintás, R. Tauler, B. Lendl and M. de la Guardia, <i>Anal. Chem.</i> , 2011, 83 , 4855–4862. |

4.4 Published supplementary material

Gas chromatography–Fourier transform infrared spectroscopy reveals dynamic molecular interconversion of oximes

Junaida Shezmin Zavahir, Yada Nolvachai, Bayden R. Wood and Philip J. Marriott

Published in *Analyst*, Volume 144, pp. 4803–4812, July 2019

Electronic Supplementary Material (ESI) for Analyst.
This journal is © The Royal Society of Chemistry 2019

Electronic Supplementary Information

**GAS CHROMATOGRAPHY–FOURIER TRANSFORM INFRARED
SPECTROSCOPY REVEALS DYNAMIC MOLECULAR
INTERCONVERSION OF OXIMES**

by

J. Shezmin Zavahir^a, Yada Nolvachai^a, Bayden R. Wood^b, Philip J.
Marriott^{*a}

^a Australian Centre for Research on Separation Science, School of Chemistry, Monash University,
Wellington Road, Clayton, VIC 3800, Melbourne, Australia.

^b Centre for Biospectroscopy, School of Chemistry, Monash University, Wellington Road, Clayton,
VIC 3800, Melbourne, Australia.

Submitted to:

Analyst

* Corresponding author: Tel. +61 3 99059630; fax. +61 3 99058501

Email: Philip.Marriott@monash.edu

Fig. S1. Instrumental schematic for the light-pipe GC–FTIR–FID system.

Fig. S2. Comparison of FTIR data acquisition settings (A) scan speed, (B) phase correction and (C) resolution.

Fig. S3. Infrared spectra corresponding to the two terminal peaks of acetaldehyde oxime (a and b) and propionaldehyde oxime (c and d).

Fig. S4. GC–FTIR and GC–FID chromatograms of acetaldehyde oxime (A and B) and propionaldehyde (C and D) oxime isomer mixes.

Fig. S5. Propionaldehyde oxime spectra acquired in GC–FTIR analyses.

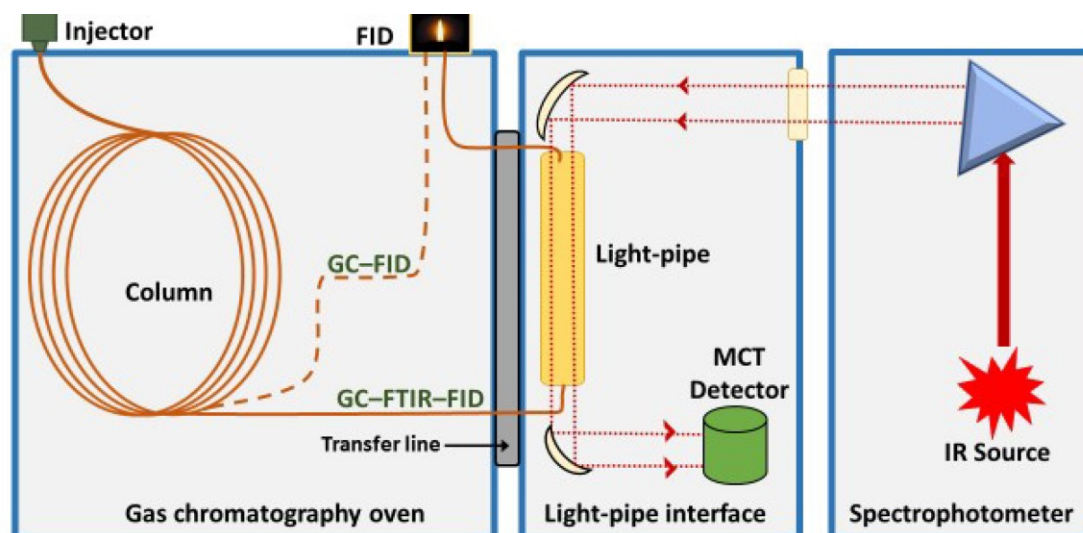


Fig. S1. Instrumental schematic for the light-pipe GC-FTIR-FID system where a GC is hyphenated to a spectrophotometer via a light-pipe interface. The dashed line represents column configuration for GC-FID setting where the sample does not travel through the light pipe.

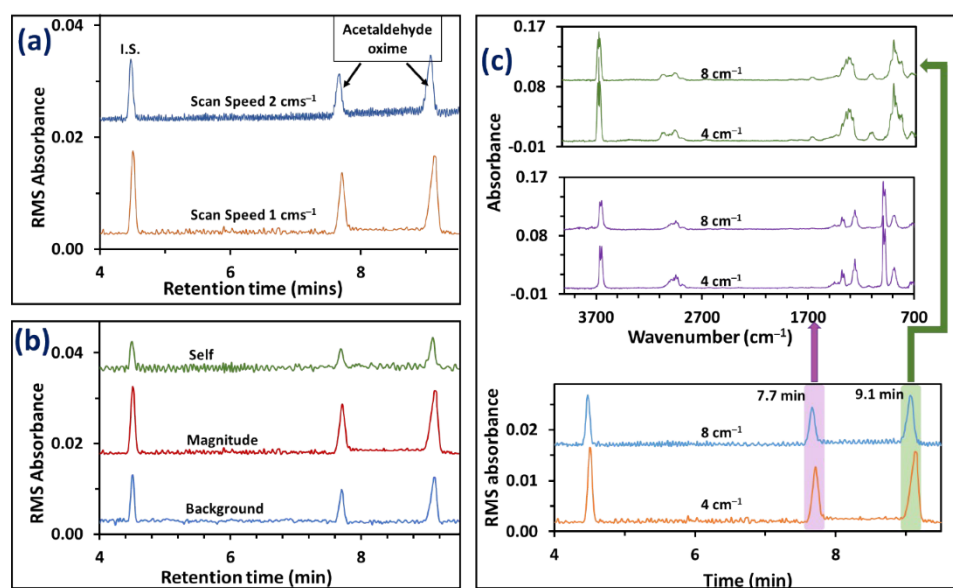


Fig. S2. Comparison of FTIR data acquisition settings (A) scan speed, (B) phase correction and (C) resolution, at isothermal oven T of 80 °C, flow of 3 mL min⁻¹. Peaks correspond to the I.S.; internal standard and dynamic chromatographic peaks of acetaldehyde oxime. In each, better SNR was observed using a scan speed of 1 cms⁻¹, magnitude phase correction and resolution of 4 cm⁻¹.

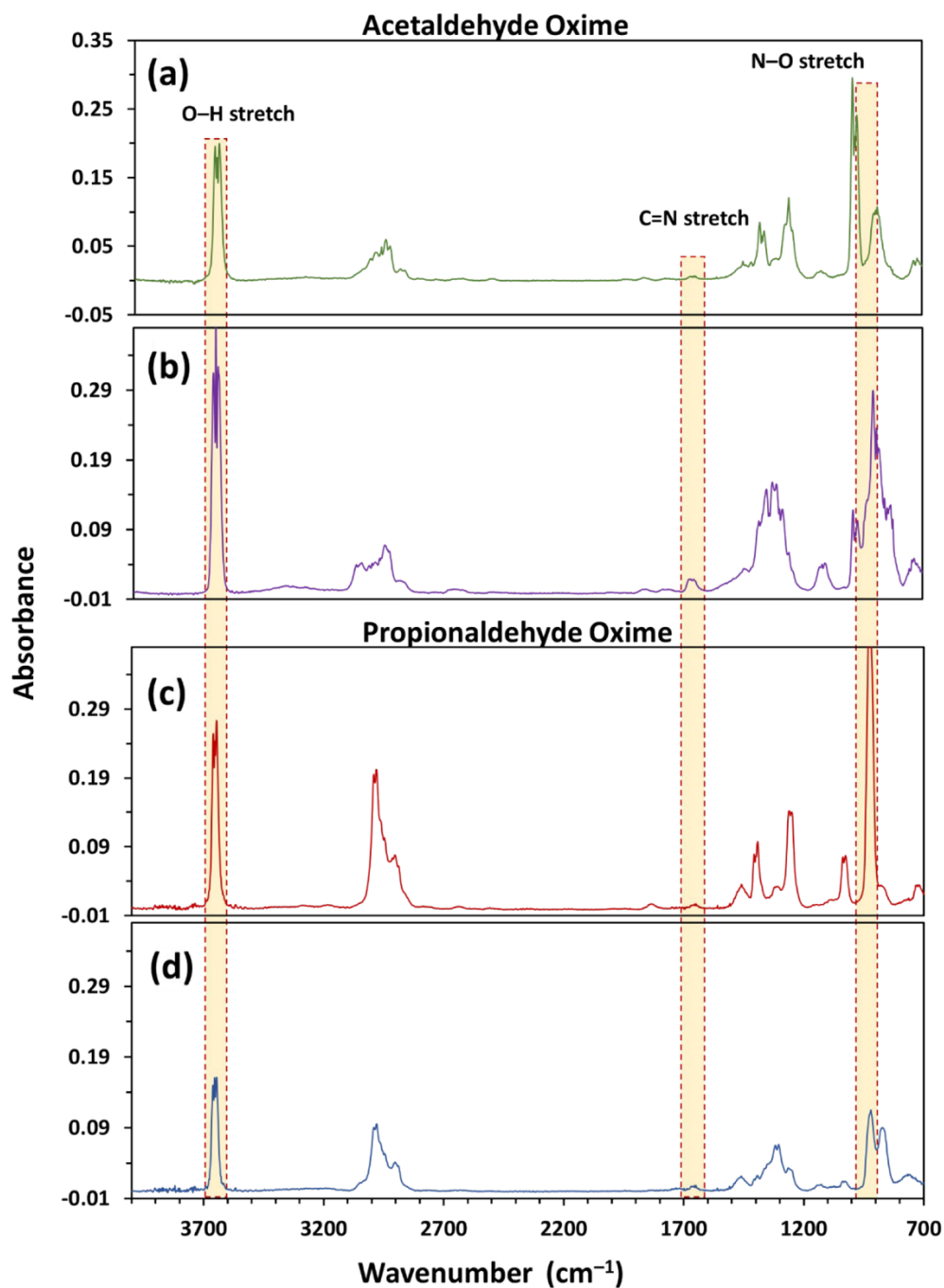


Fig. S3. Infrared spectra corresponding to the two terminal peaks of acetaldehyde oxime (a and b) and propionaldehyde oxime (c and d), demonstrating the differences in fingerprint region and absorption band intensities. Spectra were collected at $T = 130\text{ }^{\circ}\text{C}$ with a column flow of 3 mL min^{-1} . The image also shows the three bands characteristic to oximes, namely. O-H (3600 cm^{-1}), C-N (1665 cm^{-1}) and N-O (945 cm^{-1}). a and c correspond to the isomer which elutes first and b and d to the later eluting isomer for each compound.

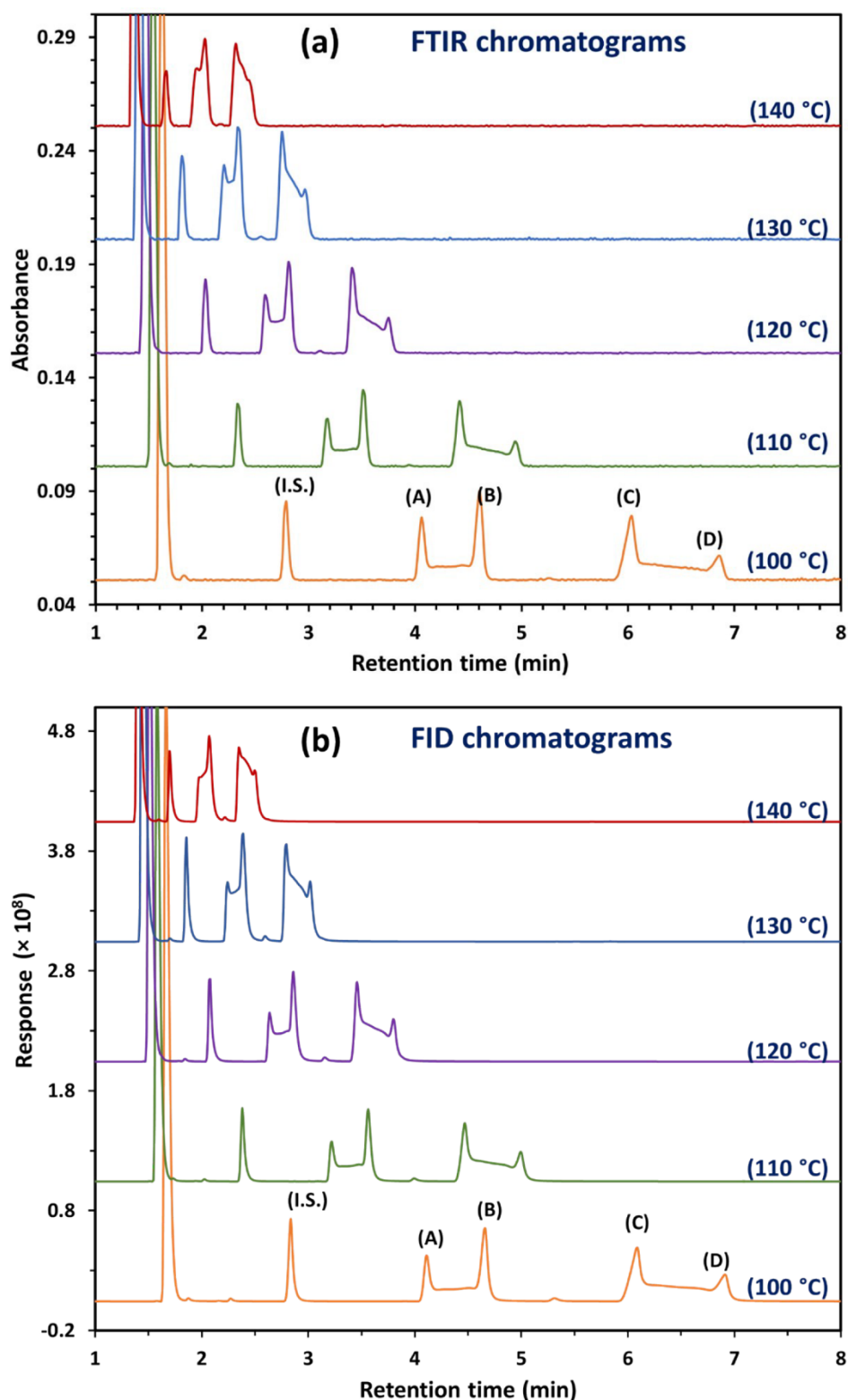


Fig. S4. GC–FTIR and GC–FID chromatograms of acetaldehyde oxime (A and B) and propionaldehyde (C and D) oxime isomer mixes at isothermal oven T of 100 °C, 110 °C, 120 °C, 130 °C and 140 °C. I.S.; Internal standard. Light-pipe temperature was maintained at 150 °C.

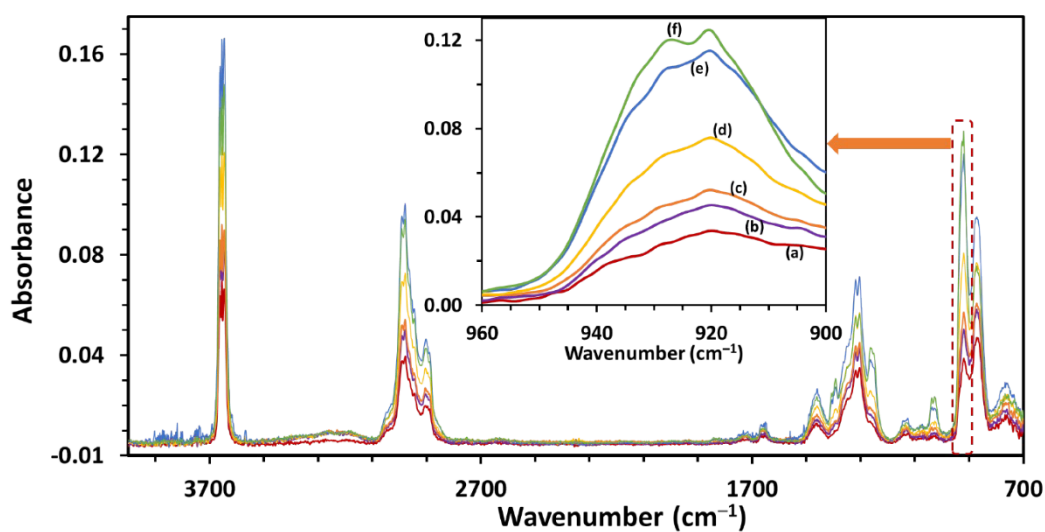


Fig. S5. Propionaldehyde oxime spectra acquired in GC–FTIR analyses with increasing isothermal temperatures of (a) 90 °C, (b) 100 °C, (c) 110 °C, (d) 120 °C, (e) 130 °C and (f) 140 °C, at a light-pipe temperature of 150 °C and column flow of 3.0 mL min⁻¹. Increased intensity of absorption bands is observed with increase in oven temperature.

Chapter 5

High resolution analysis of thermally oxidised aviation fuel — comprehensive two-dimensional gas chromatography vs high-resolution mass spectrometry

J. Shezmin Zavahir^a, Renée Webster^b, Federico Floris^c, Mark Barrows^c and Philip J. Marriott^a

^a Australian Centre for Research on Separation Science, School of Chemistry, Monash University, Wellington Road, Clayton, Melbourne, VIC 3800, Australia

^b Defence Science & Technology Group, Lorimer St, Fishermans Bend, VIC 3207, Australia

^c Department of Chemistry, University of Warwick, Coventry, CV4 7AL, UK

Contents

5.1	Chapter synopsis.....	2
5.2	Journal article manuscript prepared for submission	5
5.3	Supporting Information for article manuscript	36

5.1 Chapter synopsis

Being a complex matrix, aviation fuels can contain thousands of different compounds which makes the analysis of trace components a challenging task. These trace components can have a detrimental effect on the composition and quality of fuels. Thermal oxidation of fuels within the hot aircraft fuel system and during storage can form trace amounts of oxygenated components as well as other heteroatomic species which can alter the physicochemical properties of fuel and its performance. Of the other heteroatoms, the contribution of sulfur is crucial as formation of sulfur products can form deposits during fuel storage. Having a detailed knowledge of the trace constituents in aviation fuel is thus important to ensure its safety to be used in modern high-performance aircrafts. Often, the bulk hydrocarbon matrix of fuels makes it challenging to detect and/or identify the trace components using some analytical techniques.

This Chapter endeavours to study the molecular composition of four aviation fuels resulting from accelerated oxidative thermal stress. The fuels – two alternate fuels and two conventional fuels – are subjected to PetroOxy oxidation and studied with chosen analytical techniques. Focus is placed on identifying components which have undergone oxidation during the thermal stressing process.

At the commencement of this study, the fuels were analysed using the hyphenated light-pipe GC-FTIR system used in the experiments of previous Chapters. GC-FTIR proved to be unsuitable for the analytical purpose mainly due to the low sensitivity of light-pipe GC-FTIR which is insufficient to observe trace species. Thus, attenuated total reflectance-Fourier transform infrared spectroscopy (ATR-FTIR) was chosen to carry out FTIR analysis of the samples. ATR-FTIR is a low-cost, non-destructive and rapid analytical technique used in routine analysis of fuels, which evaluate various structural features of a sample based on its molecular vibrations. It is often coupled with chemometric methods to identify specific qualitative features in fuel samples. Here ATR-FTIR is used to analyse the aviation fuel samples with the multivariate analytical method of principal component analysis (PCA) which enables visualisation of the data on a single plot. Select regions of the infrared spectrum are chosen to conduct PCA analysis to detect any variation in the composition of oxygenates and hydrocarbons. This method however is insufficient to fully characterise the oxygenated components in fuels.

The field of petroleomics deals with the various approaches used to study petroleum related samples and render a detailed molecular characterisation of such samples. Here we use two high-resolution approaches which are commonly used in petroleomics investigations due to the wealth of information they provide, namely comprehensive two-dimensional chromatography hyphenated to time-of-flight mass spectrometry (GC×GC-TOFMS) and high-resolution mass spectrometry (HRMS) employing Fourier transform ion cyclotron resonance mass spectrometry (FTICR MS; also referred to as FT-ICR MS in literature).

Preliminary GC analyses of the fuel samples were conducted using one-dimensional GC (1DGC) to understand the fuel's overall profile. This was however unsuitable for analysing trace oxygenated species due to coelution with the bulk hydrocarbon matrix. With GC×GC analysis, the use of a polar – non-polar column configuration is implemented to aid components belonging to the bulk hydrocarbon matrix to be retained the most on the second dimension. 2D colour contour plots created from the total ion chromatograms (TICs) of the fuels enable grouping of compound classes and easy visualisation of the fuel's chemical profile. Using a standard component mix containing oxygenated compounds, a systematic data interpretation approach is adopted to develop an approach for the presence of oxygenated compounds in the thermally stressed fuels. Extracted ion chromatograms (EICs) are further constructed using accurate mass analysis made possible by the accurate mass TOFMS which can separate compounds containing ions of interest and identify specific compound groups.

FTICR MS is a foremost technique in the field of petroleomics due to its performance capabilities such as an ultrahigh resolving power and mass accuracy. The FTICR MS analysis used here employs atmospheric pressure photo-ionisation (APPI) which is well suited for a wide range of non-polar and low-polarity compounds. The broad band mass spectra of the FTICR MS which span a broad m/z range allows molecular formula assignments based on elemental composition and large molecule coverage. The extensive volume of data generated by FTICR MS is interpreted using various visualisation techniques which include Kendrick mass defect plots, double bond equivalence vs carbon number plots, heteroatomic class distribution plots, and van Krevelen diagrams of H/C versus O/C atomic ratios.

Using the merits of the two premier techniques of GC×GC–TOFMS and FTICR MS here we endeavour to achieve molecular speciation of the fuels with a focus on the oxygenated components. The two techniques are contrasted in their ability to produce the fine information needed to carry out complex mixture analysis. This study is conducted in collaboration with The University of Warwick, UK, where the FTICR MS analysis of fuels is conducted. The ongoing global COVID pandemic has affected the progress of this work. The current manuscript has been prepared for submission to the journal *Analytical Chemistry*. Both the manuscript and its related Supporting Information file has been presented in this Chapter.

**HIGH RESOLUTION ANALYSIS OF THERMALLY OXIDISED AVIATION FUEL —
COMPREHENSIVE TWO-DIMENSIONAL GAS CHROMATOGRAPHY VS HIGH-
RESOLUTION MASS SPECTROMETRY**

by

J. Shezmin Zavahir^a, Renée Webster^b, Federico Floris^c, Mark Barrows^c and Philip J.

Marriott^a

^a Australian Centre for Research on Separation Science, School of Chemistry, Monash University, Wellington Road, Clayton, VIC 3800, Melbourne, Australia.

^b Defence Science & Technology Group, Lorimer St, Fishermans Bend, VIC 3207, Australia

^c Department of Chemistry, University of Warwick, Coventry, CV4 7AL, UK

In preparation for submission to:

Analytical Chemistry

* Corresponding author:

Email : Philip.Marriott@monash.edu

Tel. +61 3 99059630; fax. +61 3 99058501

Keywords: aviation fuel; GC×GC; HRMS; FTICR MS; oxidation

ABSTRACT

The increasing appearance of alternate fuels in the market calls for reliable analytical techniques for their characterisation. This study reports the use of two high resolution (HR) techniques to study four select conventional and aviation fuels which have undergone accelerated thermal oxidative stress. Oxidation of aviation fuels can affect their heteroatomic composition, quality and performance. To analyse complex fuel matrices, use of comprehensive two-dimensional gas chromatography (GC×GC) with an accurate mass time-of-flight mass spectrometer (TOFMS), with its higher acquisition speed, accuracy and peak capacity, has a greater efficiency over one-dimensional gas chromatography. A “fingerprinting” type or group-type analysis of fuels is achieved using 2D contour plots and total ion chromatograms (TICs). Data are interpreted systematically using a standard component mix of oxygenates and extracted ion chromatograms (EICs) using the TICs resulting from GC×GC. HR mass spectrometry (MS) using Fourier transform ion cyclotron resonance MS (FTICR MS) can be successfully applied to fuel sample analysis. The combinations of a variety of data processing methods and visualisation tools facilitate interpreting the large volume of data generated when using FTICR MS for fuel analysis. The use of ATR–FTIR to visualise the differences in fuel compositions is also explored. A main aim of this study is also to evaluate the information derived from the advanced techniques of GC×GC and FTICR MS to yield an improved detailed molecular characterisation of the fuels. The complementary information rendered by these two methods benefit petroleomic investigations in comparison to a single approach.

INTRODUCTION

The current era recognises the ramifications of solely relying on traditional fossil fuels due to it being a finite and non-renewable resource. This overreliance on fossil fuels has an enormous impact on the environment and humanity with air and water quality deterioration, emission of transportation related gases, global warming and the negative impacts of petroleum-based products. There is increasing interest in promising substitutes such as alternately derived or synthetic fuels with favourable chemical properties, which are renewable, and have lower environmental impact compared to

fossil fuels. These can act as replacements for traditional fossil fuels and be sources of sustainable fuels in the aviation industry. They are produced via five main ASTM D7566-approved technologies ¹; (1) Hydroprocessed Ester and Fatty Acid Synthetic Paraffinic Kerosene (HEFA-SPK), (2) Fischer-Tropsch SPK (FT-SPK), (3) FT fuels with Synthetic Kerosene with Aromatics (FT-SKA), (4) Synthesized iso-paraffins (SIP), and (5) Alcohol to Jet (ATJ). Other pathways for alternate fuels are being continually explored and evaluated for their suitability by ASTM ².

With its role as both an engine coolant and propellant, jet fuel undergoes drastic short-term cyclic temperature changes leading to thermal stress with the potential for oxidation of hydrocarbons, which can affect the fuel's liquid-phase stability and performance ³. Such products can form insoluble deposits, alter the fuel properties, and have a direct influence on the operational safety of aircraft. With technology directed towards high performance aircraft with higher heat loads, there is an increased demand to improve oxidative thermal stability of jet fuels. Being complex matrices, interference result from the presence of bulk hydrocarbon compounds with the problem of identification of oxidised species and trace components contained therein ⁴⁻⁷. With the increased use of such fuels it is therefore imperative to understand the processes occurring in the fuel at a molecular level to preserve the final fuel's quality ⁸.

Thermal oxidation of a jet fuel is primarily governed by the fuel's composition which could contain thousands of individual species. Composition of the bulk hydrocarbons, account for ~99% of the fuel, whilst the remaining 1% is composed of trace chemical species such as sulfur, oxygen-containing heteroatomic entities, nitrogen and dissolved metal ^{3,9}. Jet fuel composition is mainly analysed using four analytical techniques namely; gas chromatography (GC), infrared (IR) spectroscopy, Raman spectroscopy and nuclear magnetic resonance spectroscopy.

Fourier transform infrared spectroscopy (FTIR) in the 4000–650 cm⁻¹ region has been used for both qualitative and quantitative analysis of various aviation fuels and biofuel blends, often employing chemometric modelling and multivariate techniques for data analysis ¹⁰. ATR-FTIR systems allow simple, low cost and rapid analysis of fuel samples of various origins ¹¹.

GC, a versatile tool with sensitivity and selectivity is valuable in analysing complex mixtures, such as fuel, and unravelling its constituents ¹². Identification of GC-separated analytes can be supported by various purpose-suited detector technologies ¹³. Despite being a mature technique, conventional one-dimensional GC (1DGC) – which uses a single-column – has shortcomings in that overlapping of peaks from different compound classes fail to achieve sufficient detectability and resolution, which affects qualitative and quantitative analysis of some compounds. This has driven the development of multidimensional GC (MDGC) which increases separation by using two or more columns of different selectivities. Its variant, the untargeted approach of comprehensive two-dimensional chromatography (GC×GC), uses the two-column approach on the total sample. Columns of different selectivities are used to render a better resolved chromatographic result, high peak capacity, improved sensitivity, ordered elution of compound classes and enhanced identification accuracy ¹⁴. It is thus apt for analysing complex hydrocarbon mixtures in the fuel industry such as aviation fuels, where compound class characterisation is of a greater focus than analysing all individual compounds, to provide a high-resolution gas chromatography (HRGC) separation of bulk and trace components ¹⁵. This enables a ‘fingerprinting’ or group-type analysis of the fuel to understand the various hydrocarbon and heteroatomic species within it, for differentiating various fuel types ¹⁶.

Hyphenation of GC×GC to time-of-flight mass spectrometry (TOFMS), GC×GC–TOFMS, provides additional identification using accurate mass analysis ¹⁷. The ability of a mass spectrometer to discriminate peak signals with similar mass-to-charge ratio (m/z) ions in a mass spectrum is referred to as its *resolution*. Based on this resolving power, mass spectrometers are classified as unit-mass resolution instruments (those which measure a compound’s nominal mass) and high-resolution mass spectrometry (HRMS) instruments (which can measure the mass to several decimal places; exact or accurate mass, with most modern HRMS instruments able to provide mass accuracies lower than 2 ppm) ¹⁸.

The field of ‘petroleomics’, focusses on the characterisation of petroleum at its molecular level to be able to correlate and ultimately predict its physicochemical properties as well as its behaviour ^{19, 20}. With its inherent complexity of components, which mainly belong to saturated hydrocarbons, aromatic hydrocarbons, resins and asphaltenes (SARA),

petrochemicals analysis commands the need for advanced analytical techniques²¹. Petroleomics investigations have benefitted greatly from GC-based methods such as GC×GC^{20, 22, 23}, and HRMS approaches^{24, 25}. GC×GC techniques enable the separation of hundreds of compounds in a sample in a single analysis²² with a higher peak capacity than 1D GC. HRMS approaches are facilitated by instruments such as Orbitrap MS and Fourier transform ion cyclotron resonance MS (FTICR MS) with various ionisation techniques, boasting resolutions beyond 1 000 000, a mass accuracy of sub ppm levels, and have the capability to produce quantitative elemental distribution patterns using various ionisation methods^{26, 27}. FTICR MS has proven itself to be a versatile tool with ultrahigh mass accuracy and resolution in the structural analysis of organic molecules over a wide range of molecular weights, well suited for petrochemical analysis^{26, 28}. The development of data interpretation and visualisation tools such as plots of Kendrick mass defect (KMD), double bond equivalence (DBE) vs carbon number, heteroatomic class distribution and van Krevelen diagrams play a pivotal role in the success of FTICR MS²⁶.

Of the many heteroatomic species present in petroleum, sulfur containing compounds (SCCs) hold a distinct position. Their speciation is important for downstream refining, upstream production and most importantly for the environmental and process optimization aspects arising from the emission products of their combustion^{29, 30}. However, due to the complexity of jet fuels the complete characterisation of its SCCs cannot be achieved using a single analytical method and requires multiple analytical techniques.

Recent advances in the technology and data interpretation methods for FTICR MS and GC×GC, and the development of mass spectrometric approaches for petroleomic samples²⁵ have made these techniques well suited for complex mixture analysis. The present study focuses on using high resolution GC with the GC×GC technique and the HRMS analysis approach using FTICR MS to analyse conventional and alternate aviation fuel samples which have undergone accelerated thermal oxidation. Figure 1 summarises the main approaches adopted to achieve the molecular characterisation of these fuels. The use of these approaches for analysis of oxygenates will also be highlighted and contrasts will be drawn between the two premier high-resolution approaches used to analyse the fuels.

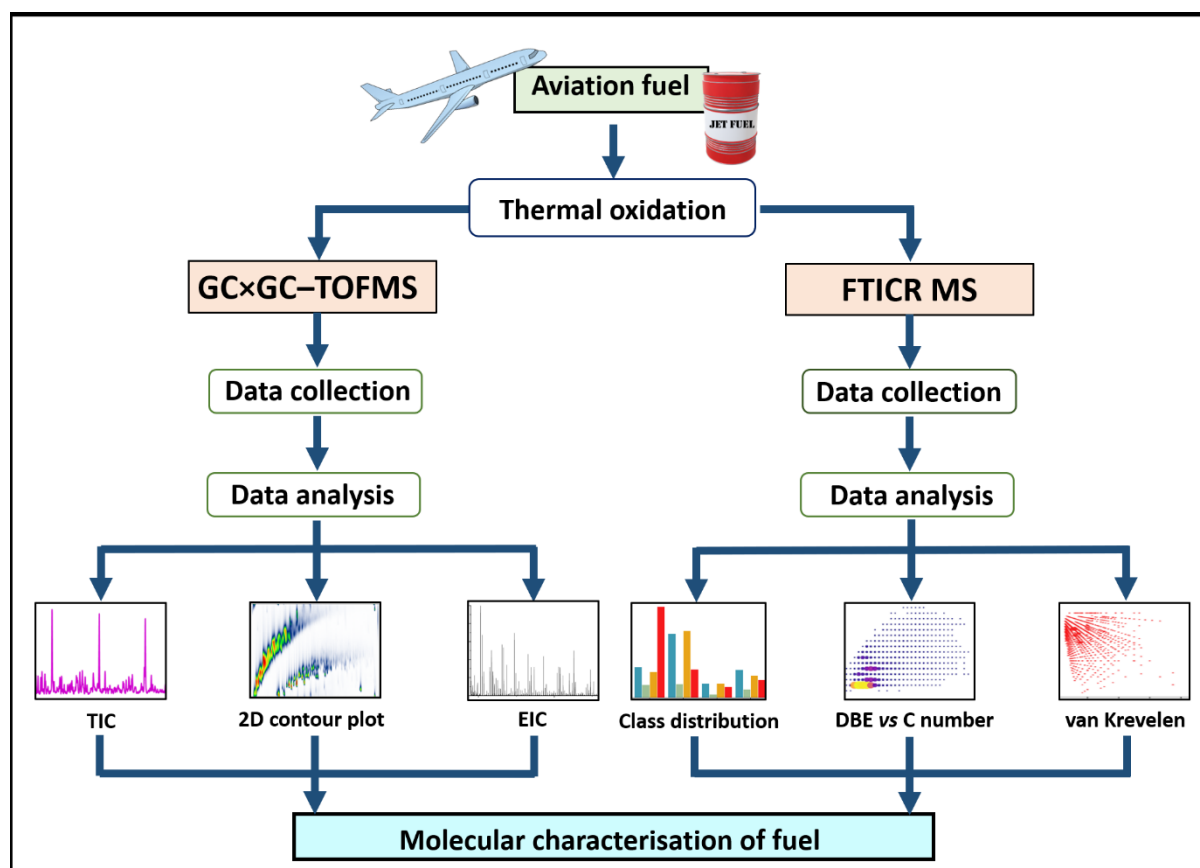


Figure 1. Flow chart contrasting GC×GC and HRMS approaches for the molecular characterisation of fuel. TIC, total ion chromatogram; EIC, extracted ion chromatogram; DBE vs C numbers, double bond equivalence versus carbon number.

EXPERIMENTAL SECTION

Fuel Samples

Four types of aviation fuel were selected to cover a range of feedstocks and processing technologies. Of these, two were alternate fuel samples; namely SPK (a synthetic paraffinic kerosene) and HTFT (a high temperature Fisher-Tropsch fuel) labelled A and B respectively. The two conventional fossil crude oil derived fuels were F-34 (a hydroprocessed fossil crude oil) and Merox (mercaptan oxidation process fossil crude oil) labelled C and D respectively. Each fuel type was thermally stressed using the PetroOxy oxidation system and included samples of initial (neat) and end (stress) stages of oxidation. The fuels were used “as is” containing any additives which may have been

added in the refinery process. The fuels comply with ASTM D1655³¹ and were stored at -18°C and used “as is” with no prior preparation or sample clean up. Table 1 summarises the details of the fuels.

Table 1. Details of fuels used in this study

Label	Source	Processing method
A	SPK	A synthetic paraffin kerosene
B	HTFT	High temperature Fischer–Tropsch synthesis
C	F-34	Hydroprocessed fossil crude oil
D	Merox	Mercaptan oxidation process fossil crude oil

Chemical Reagents and Sample Preparation

For GC analysis 50 μL of fuel sample was diluted in 950 μL analytical reagent-grade $\geq 99.8\%$ purity dichloromethane (DCM) (Merck, Kilsyth, Australia). A standard 10 000 mgL^{-1} stock solution of an oxygenate mixture containing selected polar and oxygenated compounds (purchased from Sigma-Aldrich; Castle Hill, Australia) as outlined in Table 2, which represent classes of compounds expected to be found in oxidised fuels, was prepared in DCM. This solution was diluted 100 times in DCM to obtain approximately 100 mgL^{-1} for each standard component concentration. For FTICR MS analysis fuel samples were diluted in a toluene/2-propanol 20/80% (v/v) solution (Honeywell Speciality Chemicals Seelze GmbH, Hannover, Germany) at 0.05 mg mL^{-1} .

ATR–FTIR Experiment

ATR–FTIR analysis was conducted using a Bruker Equinox 55 fitted with an MCT detector and single bounce diamond crystal as the internal reflection element (Bruker Optik, Ettlingen Germany). Spectra were collected with 16 background scans and 16 sample scans using a resolution of 4 cm^{-1} in the 4000–650 cm^{-1} range. Each sample was analysed in triplicate with background scans between each sample.

GC×GC–TOFMS Experiment

GC×GC separation was carried out using an Agilent 7890A GC (Agilent Technologies, Mulgrave, Australia) coupled to a 7200 accurate mass-time-of-flight mass spectrometer (accTOFMS; Agilent Technologies, Santa Clara, SA) equipped with a PAL3 Autosampler

(CTC Analytics AG, Zwingen, Switzerland). A polar/nonpolar capillary column configuration with a SolGel-WAX column (Trajan Scientific, Ringwood, Australia) in the first dimension (¹D; 30 m × 0.25 mm × 0.25 μm) and BPX5 column (SGE, Ringwood, Australia) as the second dimension (²D; 1 m × 0.1 mm × 0.1 μm); ¹D and ²D columns respectively were employed for GC×GC analysis. A deactivated Press-Tight connector (Restec Corporation, Bellefonte, PA) was used to connect the columns. An Everest model longitudinally modulated cryogenic system (LMCS; Chromatography Concepts, Doncaster, Australia) was used as a modulator. The modulator was held at a constant modulation temperature (T_M) of 0 °C and modulation period (P_M) of 9 s, with carbon dioxide as the cryogen coolant.

Experimentation was carried out using 0.5 μL injection volume of undiluted sample at a split ratio of 20:1 (except for the standard mixture at a split ratio of 50:1). The carrier gas (Helium; 99.999% purity) had a constant flow of 1.2 mLmin⁻¹. The GC oven program had an initial temperature of 50 °C, raised to 110 °C at 5 °Cmin⁻¹, then to 180 °C at 4 °Cmin⁻¹ and finally to 280 °C at 40 °Cmin⁻¹. MS transfer line T was maintained at 280 °C. The MS was operated at an ionisation voltage of 70 eV with data collected over the 43 to 400 m/z mass range. Routine calibration of the TOFMS rendered a mass accuracy of <5 ppm. Data acquisition rate was set at a nominal 50 Hz which equated to 47.38 Hz actual acquisition rate. To ensure oxygenates were not indigenous to the fuel, thermally oxidised fuels were analysed in duplicate and compared to neat (unoxidised) fuel as well as neat solvent.

Details for the one-dimensional GC–MS and GC–flame photometric detector (GC–FPD) experiments are included in the Supporting Information Tables S2 and S3 respectively.

High Resolution Mass Spectrometry Experiment

FTICR MS experiments were performed using a 12 Tesla solariX FTICR mass spectrometer (Bruker Daltonik GmbH, Bremen, Germany) coupled to an Apollo II APPI ion source operating in positive-ion mode. The diluted fuel samples were introduced by direct infusion to the ionisation source using a flow rate of 600 μL h⁻¹. The APPI source was operated with nitrogen at a pressure of 1.0 bar. Ions were accumulated in the collision cell for 0.05 s before detection and analysis. Broad band mass spectra data were recorded at 8MW with a detection range of m/z range of 98–3000. The MS data were

zero-filled and a Sine-Bell apodisation function was used before applying a fast Fourier transform. For the apodised data the measured mass resolving power at m/z 400 was 552,000 which allows to perform unique assignments of compositions with the molecular formula $C_cH_hN_nO_oS_s$, where subscripts c , h , n , o and s are the number of carbon, hydrogen, nitrogen, oxygen and sulfur respectively in each molecule. Each elemental composition is classified by its heteroatomic class (e.g. $N_nO_oS_s$ with a label “[H]” to indicate protonated adducts), carbon number, DBE, H/C and O/C ratio.

Software and data analysis

Data collection, processing and analysis for 1DGC–MS experiments were conducted using MassHunter v 10.0 (Agilent Technologies, Inc.) and using Agilent OpenLab CDS Chemstation version (Agilent Technologies) for 1DGC–FPD analysis.

ATR data were acquired using the Opus software version 6.0 (Bruker Optik GmbH) and chemometric data analysis was carried out using Quasar - Orange data mining toolbox v 3.0 (University of Ljubljana, Slovenia).

Instrument control, data acquisition and data analysis for GC×GC–TOFMS was carried out using MassHunter B.06.00. 2D contour plots for GC×GC were visualised by importing the data to Canvas W1.5.14.30115 (J&X Technologies Co., Ltd., Shanghai, China).

For HRMS, the data analysis and visualisation were performed with an in-house software developed at the University of Warwick, named KairosMS³². Obtained mass spectra were internally calibrated using the Bruker DataAnalysis software version 5.0 (Bruker Daltonik GmbH, Bremen, Germany) using a homologous series of a hydrocarbon class with double bond equivalent (DBE) of 8. The Composer software version 1.5.6 (Sierra Analytics, Modesto, CA, USA) was used to assign molecular compositions with a mass accuracy of up to 1 ppm using the chemical formula range constraints $C_{4-200}H_{4-1000}N_{0-20}O_{0-3}S_{0-3}$.

NIST 2011 version 2.0 aided in mass spectrum data matching and identification.

RESULTS AND DISCUSSION

ATR–FTIR analysis of thermally oxidised fuels

FTIR spectroscopy has been accepted as a reliable, accurate, fast and non-destructive method for analysing fuels of various origins including traditional fossil fuels, biofuels and other alternate fuels ^{33, 34}. The qualitative identification of specific vibrational bands can be used for compound structural determination which in turn reflect the fuel's composition and fuel properties. FTIR spectroscopy has been used in jet fuel stability tests ¹¹ and for evaluating the generation of products resulting from various processes, for example by monitoring the region of the carbonyl bond ($\sim 1740\text{ cm}^{-1}$) in biofuels to assess degree of oxidation ³⁵. Use of the ATR–FTIR technique to distinguish the thermally stressed fuel samples from their neat predecessors were done with undilute samples analysed in triplicate. The primary concern in these studies, and by extension to general fuel characterisation, is the relative sensitivity of the technique, and whether trace level analytes are able to be quantified.

Application of chemometrics through a range of multivariate techniques are increasingly used in comparative fuel sample analysis, mainly due to the increased reliability in comparison to univariate analysis and the ability to better extract information. Principal component analysis (PCA), a popular multivariate tool, simplifies complex multidimensional data to several relevant variables - the principal components (PC). PCA can evaluate relationships between samples of various fuels and biofuels ³⁶. Here, PCA was applied to the fuel samples in their neat and thermally stressed stages to identify variables which are affected by thermal processing, according to their importance and trends. Data obtained in triplicate using ATR–FTIR were exported to Orange Quasar software for PCA analysis. Supporting Information Figure S1 shows the average infrared spectrum for replicates of each fuel sample, with each inset showing the variations in part of the $2990\text{--}2850\text{ cm}^{-1}$ wavelength region. This corresponds to the C–H antisymmetric and symmetric stretch of aliphatic hydrocarbon compounds which was chosen due to the abundant hydrocarbons in these fuels. Thus, any changes in the hydrocarbon content due to conversion to oxygenated species should alter the C–H bond abundance in the samples. The red and blue regions depict the average of the neat and thermally stressed samples

respectively with a lower intensity of the C–H absorption band observed in most stressed samples, which could be attributed to oxidation processes.

The PCA scores and loading plots resulting from analysis of the fuels are shown in Figure 2. The first two principal components (PC1 and PC2) account for 77.2% of the cumulative normalised variance of the data set. PC1 accounts for 54.2% and PC2 for 23% with an additional 11.6% being explained by PC3. Strong PC1 loadings observed at 2955, 2943, 1465 and 1474 cm^{-1} are characteristic of stretching and bending vibrations of C–H bonds. The strong loadings on PC2 at 2957, 2922, 1470 and 1370 cm^{-1} are also characteristic of C–H bond containing groups. It is noted that neither of these relate to oxidation product bands. According to the chemical differences associated with oxidation which occurs as a result of thermal oxidative stress, the fuels are expected to be grouped on the PCA scores plot (Figure 2B). Although the alternate fuels SPK and HTFT showed clear grouping on the scores plot, this was not observed in the conventional fuels Merox and F-34, which could be attributed to the comparatively higher complexity of the conventional fuels. However, no clear grouping was apparent to enable distinguishing the two stages of thermal oxidation in each fuel and can be concluded that the PC1 and PC2 did not succeed in explaining the variance between the neat and stressed samples. The abundance of hydrocarbon containing groups, which masks the contribution by trace compounds, contribute to the presence of C–H bonds observed in PC1 and PC2 and therefore doesn't allow for a successful analysis of PCA.

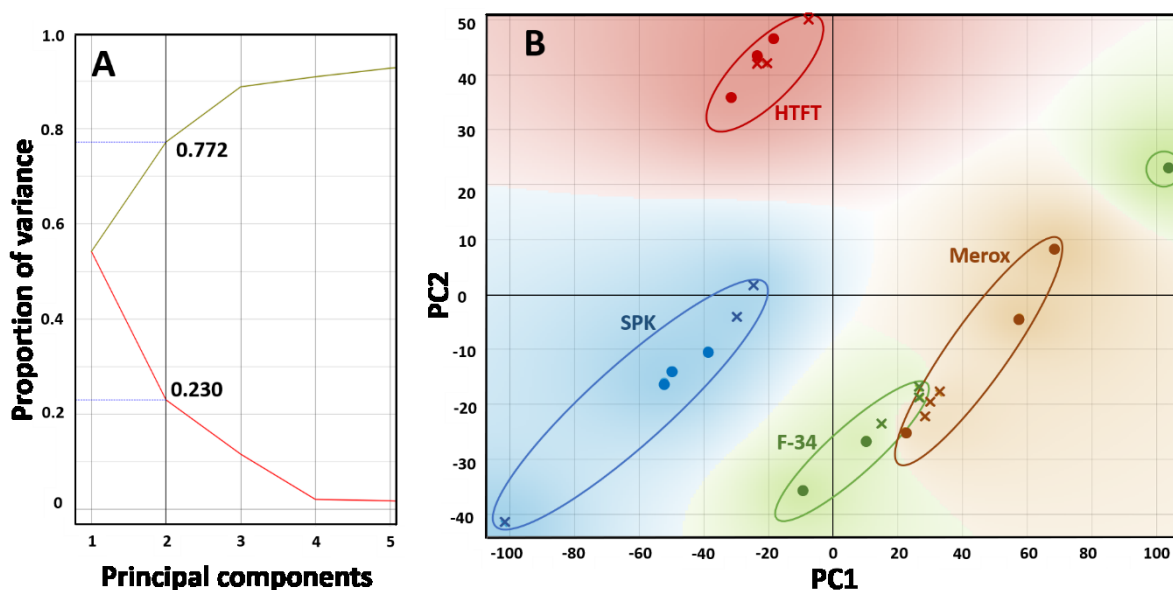


Figure 2. The PCA loadings plot (A) and the PCA scatter plot (B) of the 4 fuel samples each in the neat and stressed stages. Each fuel was analysed in triplicate and its zone is represented by a different colour as blue - SPK, red – HTFT, brown - Merox and green F-34. The crosses and circles represent the neat and thermally stressed samples respectively.

The infrared region of the carbonyl bond $C=O$ can be used to confirm the presence of carbonyl containing oxygenated products such as aldehydes, ketones and carboxylic acids, and compare oxidation levels before and after thermal oxidative stress³⁷. The $1740\text{--}1690\text{ cm}^{-1}$ region corresponding to the $C=O$ band can be used as an indication of oxidation using PCA analysis. The PCA scatter plot for PCA conducted on this FTIR region is presented in Supporting Information Figure S2 where there is separation seen in the clusters of neat and stressed fuels thus confirming the discrimination of the two stages by the presence of oxygenates in the latter. PC1 and PC2 explain 84.8% and 11.7% respectively of the total variability.

Being the most abundant heteroatom in petrochemicals, the evaluation of sulfur compounds in aviation fuels is important to assess their deposition, oxidation and effect on fuel quality upon undergoing thermal stress. Hence, PCA analysis was further conducted on select regions of the FTIR spectrum to assess the effect on sulfur compounds in fuels upon thermal oxidative stress. Here specific FTIR spectrum regions which show a strong peak intensity corresponding to various sulfur containing functional

groups as given in Supporting Information Table S1 were chosen for PCA analysis using these regions. The resulting PCA scores plots for select functional groups are presented in Supporting Information Figure S3. Here too the PC1 and PC2 failed to sufficiently explain the variance between the thermally stressed and neat samples.

GC×GC results of thermally oxidised fuel samples

One-dimensional (1D) GC with quadrupole mass spectrometry (GC–MS) analysis of the fuel samples were initially conducted using the settings given in Supporting Information Table S2, the resulting chromatograms of which are presented in Supporting Information Figure S4. Due to the complexity and large number of coeluting/overlapping compounds found in such fuels, 1DGC–MS used here with nominal mass fails to differentiate the various compound classes. Further, there is difficulty in separating the oxidation products present in low abundances – such as alcohols, aldehydes, ketones, furans, acids etc. – from the extensive matrix hydrocarbons³⁸. Such oxidised products also give poor library matches of mass spectra due to overlapping compounds, and unless a unique ion is available that doesn't respond to matrix compounds extracted ion chromatograms (EIC) for these chemical classes are poorly selective.

In contrast, GC×GC increases the peak capacity and provides an orthogonal means of separation through the use of two complementary stationary phases for ¹D and ²D of appropriate selectivity towards target classes. This results in an increased resolution of sample components, thereby proving to be particularly effective in studying these complex matrices by resolving underlying matrix material. This is of special value when target components are the focus of a study. The time-of-flight mass spectrometer (TOFMS) – which uses electron ionisation (EI) to produce fragment ions of molecules – is compatible as a detector for GC×GC experiments due to fast acquisition speed and modulated GC peak widths of 100–400 ms²⁵. Use of a high-resolution accurate mass TOFMS (accTOFMS) as a detector in this study is well suited for fuel samples, as accurate mass detection can achieve a maximum sampling rate of 50 Hz in full mass spectrum acquisition, overcome the interferences encountered in analysis of complex samples such as fuels and aid in non-target structural identification³⁹.

Figure 3 presents contour plots obtained for the total ion chromatogram (TIC) data from GC×GC–TOFMS analysis of the alternate and conventional fuels. The various compound classes are grouped for easy identification, an advantage of the 2D plot derived from GC×GC data that is not available to 1DGC data. A marked advantage of GC×GC compared to 1DGC is the ability to greatly increase the performance-oriented metric of peak capacity (n_c) – broadly described as the number of peaks which fits into a given separation – while keeping the analysis time constant. High $n_{c,2D}$ separation may be achieved through careful selection of the 1D and 2D column dimensions and their phase ratio (β)⁴⁰. β is the ratio of the volume of the mobile phase, V_M , to the volume of the stationary phase, V_S , and allows for method manipulations whilst maintaining the selectivity of the stationary phase. The polar – non-polar column configuration chosen here is well suited for aviation fuel analysis so that the abundant non-polar hydrocarbon components (such as alkanes) elute as the last-eluting and hence most retained class of compounds on the 2D column. This is useful, because these major components will not interfere with the earlier eluting, polar components; interference may occur if the abundant alkanes elute before the polar compounds¹². As depicted in Figure 3, this also provides good resolution of the aromatic hydrocarbons (e.g. single- and double-ring) which elute at a lower 2t_R value, from the straight-chain and branched hydrocarbons. Here the compound classes were grouped using the deconvolution of MassHunter software and NIST 2011 library.

As seen in Figure 3 the conventional crude oil derived fuels F-34 and Merox (Figures 3C and 3D) show significantly higher complexity over the synthetic fuels SPK and HTFT (Figures 3A and 3B). Comparison of the chemical components of the fuel types revealed the SPK and HTFT samples had a majority of straight chain and branched alkanes (first dimension retention time 1t_R ranging from 5.5–18 min and 5.5–13 min respectively) whilst the conventional fuels had additional significant proportions of aromatic compounds from the ~10 min 1t_R point. The relative amounts of mono- and diaromatic components were higher in the Merox sample than the F-34 sample which can be attributed to the latter's hydroprocessing technique.

Determination of the exact identities of the wide range of alkanes present here would be tentative since it is based on molecular ion fragmentation which would produce ambiguous mass spectra due to structural isomerism and similarities of homologous

compound mass spectra. Hence, library searching would also not yield confirmed matches due to the similar MS spectrum results for many compounds, and limited availability of standards to match the exhaustive list of compounds ⁷.

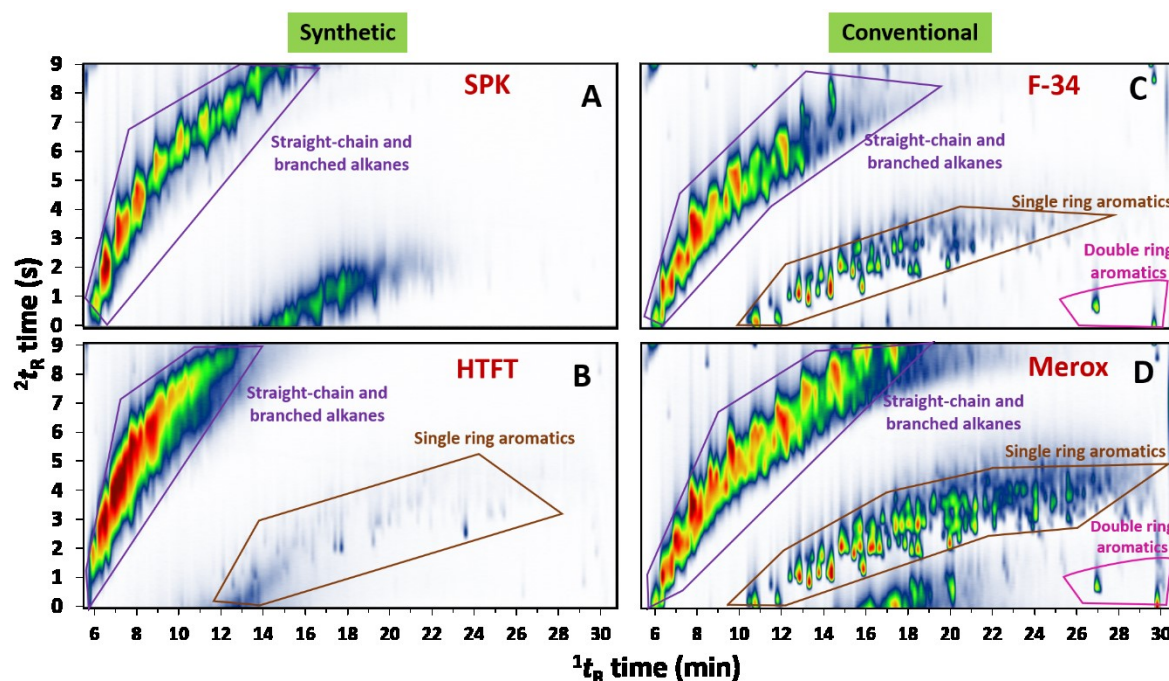


Figure 3. Contour plots of total ion chromatogram (TIC) data for synthetic and conventional fuel blends obtained by GC×GC analysis for (A) SPK, (B) HTFT, (C) F-34 and (D) Merox. The distinct classes of compounds have been grouped for easy identification on the 2D plot.

The 9-component standard mixture (consisting of 7 oxygenates, and toluene and naphthalene for reference) was used primarily to assist in identification of classes of oxidised species in the thermally stressed fuel samples. The colour contour plot for this standards mix is shown in Figure 4B and its peak identification is given in Table 2 which includes details of the compounds. Figure 4A is the modulated 1D format chromatogram which is then used to generate the 2D plot in Figure 4B, according to the modulation process (see below).

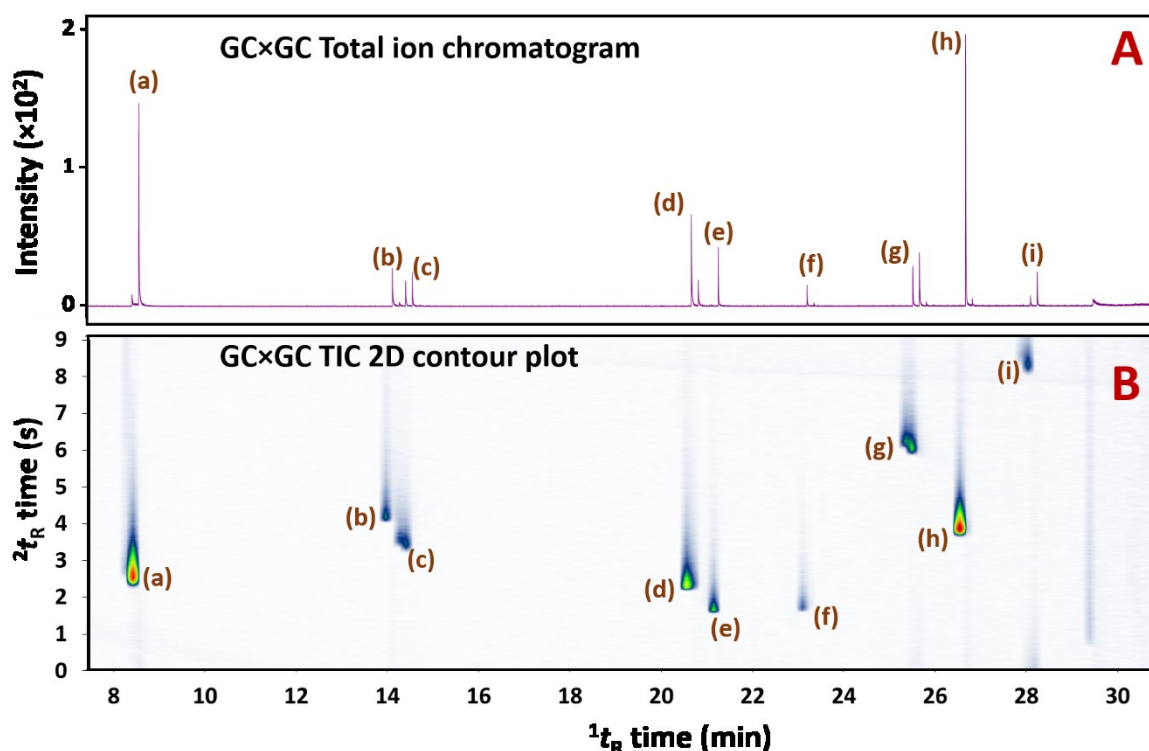


Figure 4. (A) GC×GC total ion chromatogram (TIC) of the 7-component standard oxygenate mixture with toluene and naphthalene co-added for reference, together with (B) the TIC 2D colour contour plot for the same mixture. Peak labelling (a–i) corresponds to the identification and details given in Table 2.

Table 2 Peak identification details of compounds in the standard oxygenate mixture and accurate mass of major fragment ions obtained from individual mass spectra of standards.

Peak	Compound name	Formula	Conc. (mg/L)	1 ^t _R (min)	2 ^t _R (s)	Exact mass [*]	Major fragment ions
a	toluene	C ₇ H ₈	103.3	8.00	2.49	92.1384	65.0373 [C ₅ H ₅] ⁺ 91.0543 [C ₇ H ₇] ⁺
b	octanal	C ₈ H ₁₆ O	100.9	13.55	4.09	128.2120 [*]	56.0624 [C ₄ H ₈] ⁺ 69.0679 [C ₅ H ₉] ⁺ 81.0696 [C ₆ H ₉] ⁺ 95.0859 [C ₇ H ₁₁] ⁺
c	cyclohexanone	C ₆ H ₁₀ O	99.9	14.00	3.38	98.0732 [*]	55.0177 [C ₄ H ₇] ⁺ 69.0329 [C ₅ H ₉] ⁺ 80.0627 [C ₆ H ₈] ⁺ [*] 98.0731 [C ₆ H ₁₀ O] ⁺

d	benzaldehyde	C ₇ H ₆ O	105.4	20.15	2.28	106.0419 *	77.0389 [C ₆ H ₅] ⁺ * 105.0336 [C ₇ H ₅ O] ⁺
e	octanol	C ₈ H ₁₈ O	94.9	20.75	1.68	130.2279 *	55.0545 [C ₄ H ₇] ⁺ 69.0703 [C ₅ H ₉] ⁺ 83.0843 [C ₆ H ₁₁] ⁺
f	methylfuranone	C ₅ H ₆ O ₂	110.2	22.67	1.69	98.0999*	* 57.0335 [C ₃ H ₅ O] ⁺ 85.0281 [C ₄ H ₅ O ₂] ⁺
g	dodecanal	C ₁₂ H ₂₄ O	103.1	25.10	5.99	184.3184 *	55.0544 [C ₄ H ₇] ⁺ 67.0548 [C ₅ H ₇] ⁺ 81.0693 [C ₆ H ₉] ⁺ 95.0835 [C ₇ H ₁₁] ⁺ 109.1035 [C ₈ H ₁₃] ⁺
h	naphthalene	C ₁₀ H ₈	93.8	26.15	3.78	128.1705	102.0460 [C ₈ H ₆] ⁺ 128.0626 [C ₁₀ H ₈] ⁺
i	hexanoic acid	C ₆ H ₁₂ O ₂	98.0	27.65	8.17	116.1583	55.0545 [C ₄ H ₇] ⁺ 71.0856 [C ₅ H ₁₁] ⁺ 83.0864 [C ₆ H ₁₁] ⁺ * 116.0922 [C ₆ H ₁₃ O ₂] ⁺

* These ions have an O atom, and so should be potential target fragment ions to locate the respective oxidative components in the 2D plot by using appropriate accurate mass values.

* The molecular ions of these oxidation products are generally of low abundance so will not be useful for accurate mass EIC presentations of 2D plots.

Since the conditions under which Figure 3 and Figure 4 were acquired are the same, then if any of these reference compounds happen to be in any of the samples, then their 2D retention positions should be the same. For example, an EIC of the HTFT stress sample with the m/z 128.0626 ion of naphthalene gives a modulated peak at 26.23 min as seen in Supporting Information Figure S5.

GC×GC can provide information on a range of specific trace components which may be difficult to separate from a complex hydrocarbon matrix using a 1DGC experiment due to the lack of dissimilarity with the bulk hydrocarbon mix, which can overburden the detector and challenge its sensitivity to trace compounds ⁷. In GC×GC analysis for oxygenates, the generation of EICs can be used together with the principle of mass defect

to differentiate mass fragment ions, and also molecular ions if they have adequate abundance, containing oxygen from those containing only hydrogen and carbon. If a class of oxidation products has a common fragment ion containing an 'O' atom, this would allow a common ion mass to represent that class, but from Table 2, this seems unlikely, perhaps except for the furanones. EICs are valuable in the analysis of complex fuel matrices, such as aviation fuel, where there is an abundance of hydrocarbons and a resulting presence of a background of hydrocarbons throughout the TIC. EICs using nominal masses are insufficient to analyse trace components, especially oxygenates, which may share ion fragments with the same nominal mass with other non-oxygenated components. The use of accurate masses to generate EICs for such samples is hence befitting, which is facilitated by the accurate mass TOFMS used in this study. The fast scan rate of 47.38 Hz used here is further desirable for GC×GC–TOFMS analysis to maintain sufficient resolution to detect narrow modulated peaks.

A systematic data interpretation approach was adopted to enable detection of the oxygenated compounds in the sample matrices using the standard compound mix. Here the modulation period (P_M) of 9 s generated multiple modulated peaks on the 1t_R axis of the TIC for some compounds, although it should be recognised that $P_M = 9$ s is a rather slow modulation setting, and is likely to produce only 1 or 2 modulated peaks owing to the small modulation ratio (M_R)⁴¹. The peak width at half height on the 1D column is expected to be about 5 s, so M_R is ~ 1.4 . This is due to the role played by the modulation phase, which refers to the timing of the modulation process and the profile of the peak entering the modulator. Since the time a peak enters the modulator is not controllable it may largely fit in to a single 9 s modulation and have a single maximum (in-phase) or have two maxima (180° out-of-phase). The repeatability of the modulated peaks in terms of representing the modulated period is relatively good, since in Figure 4A the respective modulated peaks of the same compound are almost exactly 9 s apart. For example, the two modulated peaks for benzaldehyde are at 20.188 min and 20.338, the difference of which equates to 9.0 s. Similarly, the peaks for cyclohexanone appear 9 s apart (8.94 s) at 13.907 min and 14.056 min.

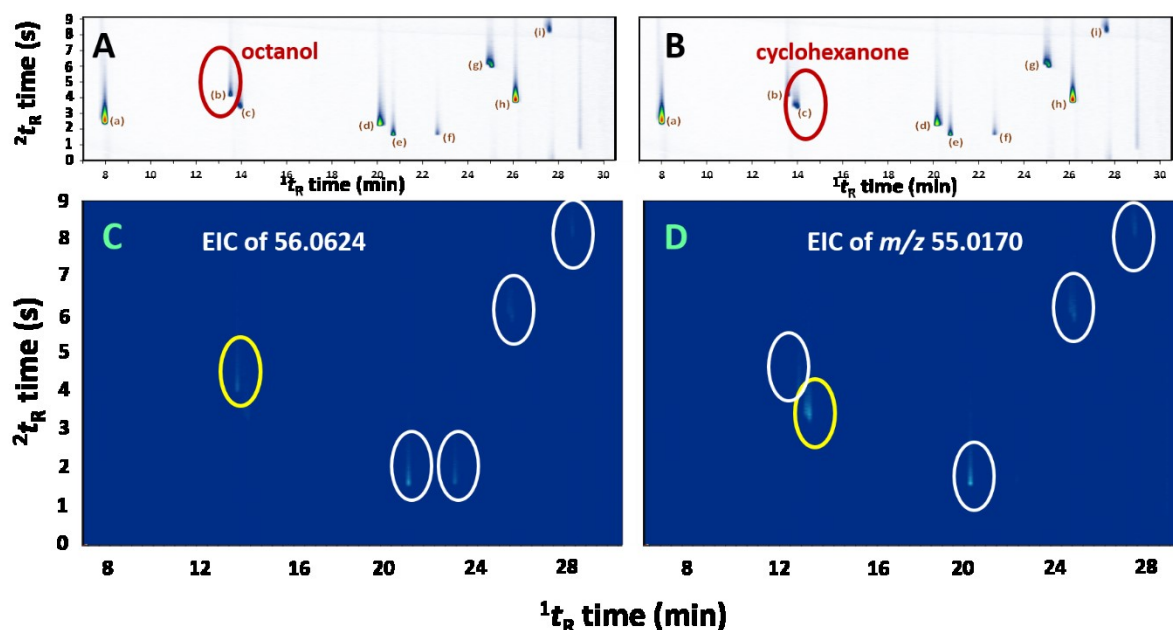


Figure 5. 2D colour contour plots for the EICs of (C) m/z 56.0624 obtained from octanol and of (D) m/z 55.0170 obtained from cyclohexanone. The TIC 2D contour plots of the standards mixture with has been included to highlight the position of (A) the octanol peak and (B) the cyclohexanone peak respectively.

The m/z 105.0336 ion resulting from the $[C_7H_5O]^+$ fragment ion of benzaldehyde cleavage resulted in an EIC 2D contour plot showing a modulated peak at the 1t_R and 2t_R of 20.15 min and 2.28 s respectively (Table 2). This aromatic benzoyl ion ($ArC\equiv O^+$) results from the cleavage of the terminal hydrogen. The molecular ion peak in ketones is prominent. The fragmentation of alkyl aromatic ketones occurs due to alkyl cleavage, which like the aromatic aldehydes result in the $ArC\equiv O^+$ fragment. This principle of fragmentation showing a specificity to oxygenates can be used for fuel sample analysis and thus the accurate mass fragment of m/z 105.0336 mass was used to extract chromatograms from the various aviation fuel samples to detect the presence of oxygenates originating from aromatic aldehydes and ketones. Figure 6 shows an example of this approach using the thermally stressed HTFT fuel sample.

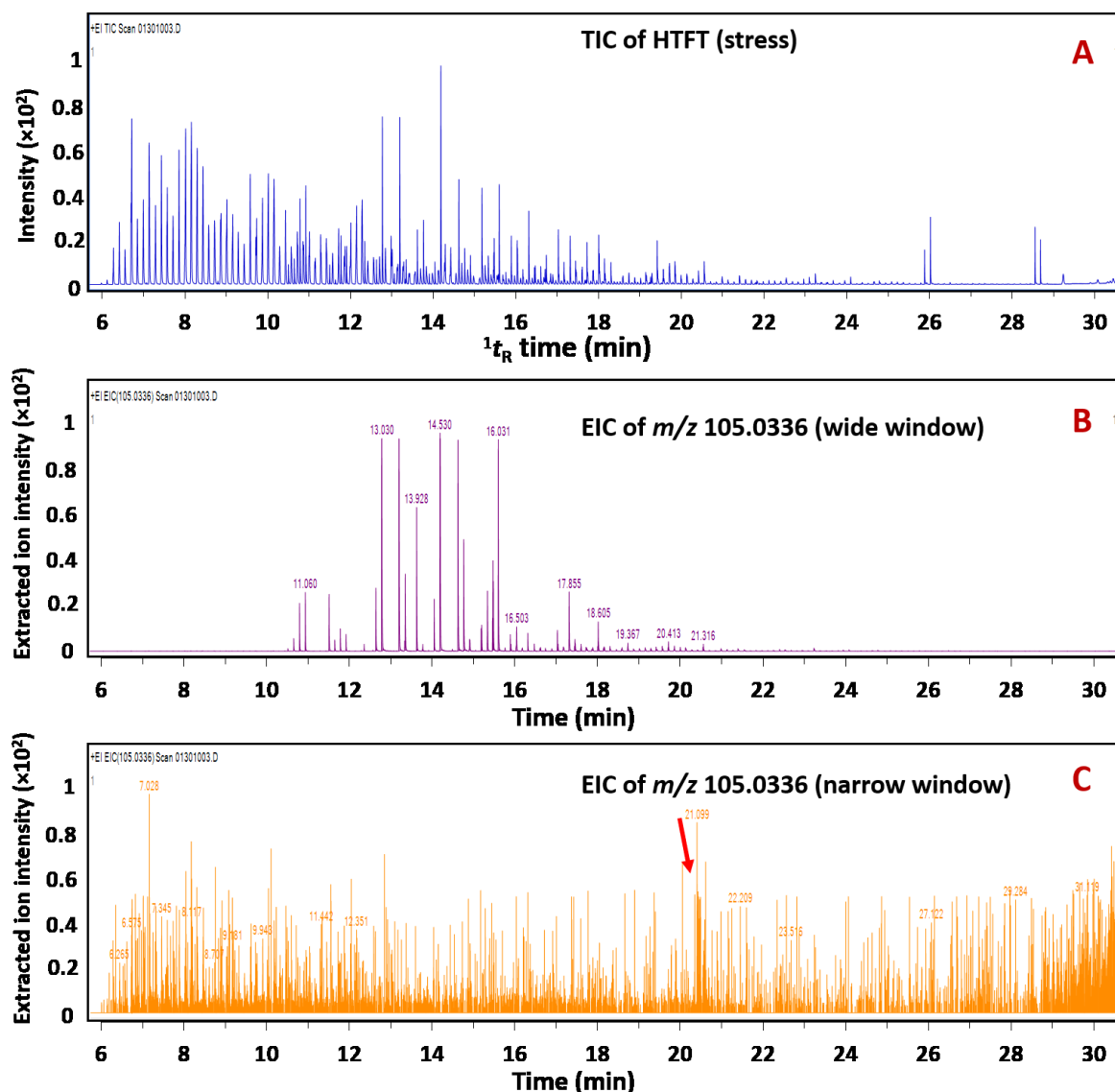


Figure 6. TIC of the thermally stressed HTFT fuel (A) together with the EICs at m/z of 105.0336 corresponding to the $\text{ArC}\equiv\text{O}^+$ fragment ion resulting from the cleavage of the oxygenated compounds aromatic aldehydes and ketones. (B) EIC obtained with a wide 300 ppm window and (C) obtained with a narrow 30 ppm window. The arrow shows where benzaldehyde is expected.

Figure 6 demonstrates the effect of choosing a suitable – or unsuitable – ppm window for EICs in GC \times GC data. Figure 6B and 6C show EICs for m/z 105.0336 obtained using a wide 300 ppm window and narrow 30 ppm window respectively. Benzaldehyde has a t_R of 20.15 min on the TIC for oxygenate standards (Table 2). If the peaks in Figure 6B show components which fragment to give the $\text{ArC}\equiv\text{O}^+$ ion, being the lowest mass of the $\text{ArC}\equiv\text{O}^+$ analogues, we expect to see a significant peak at this t_R of 20.15 min for the EICs and other alkylated benzaldehydes which would elute at a higher t_R . Further, a significant peak for

the $\text{ArC}\equiv\text{O}^+$ is not seen in Figure 6C; the benzaldehyde position is shown by the arrow. Hence we conclude that the peaks in Fig. 6B are not benzaldehyde analogues. A m/z 105 ion also occurs as a fragmentation ion for monoaromatics, at an accurate mass of $[\text{C}_8\text{H}_9]^+ = 105.0699$. Hence the narrow window excludes this ion, but the wide window captures this ion for the monoaromatics, and presents the suite of aromatics with this ion. The presence of monoaromatic compounds in the sample can be further demonstrated as below.

Demonstration of monoaromatic substitution selectivity

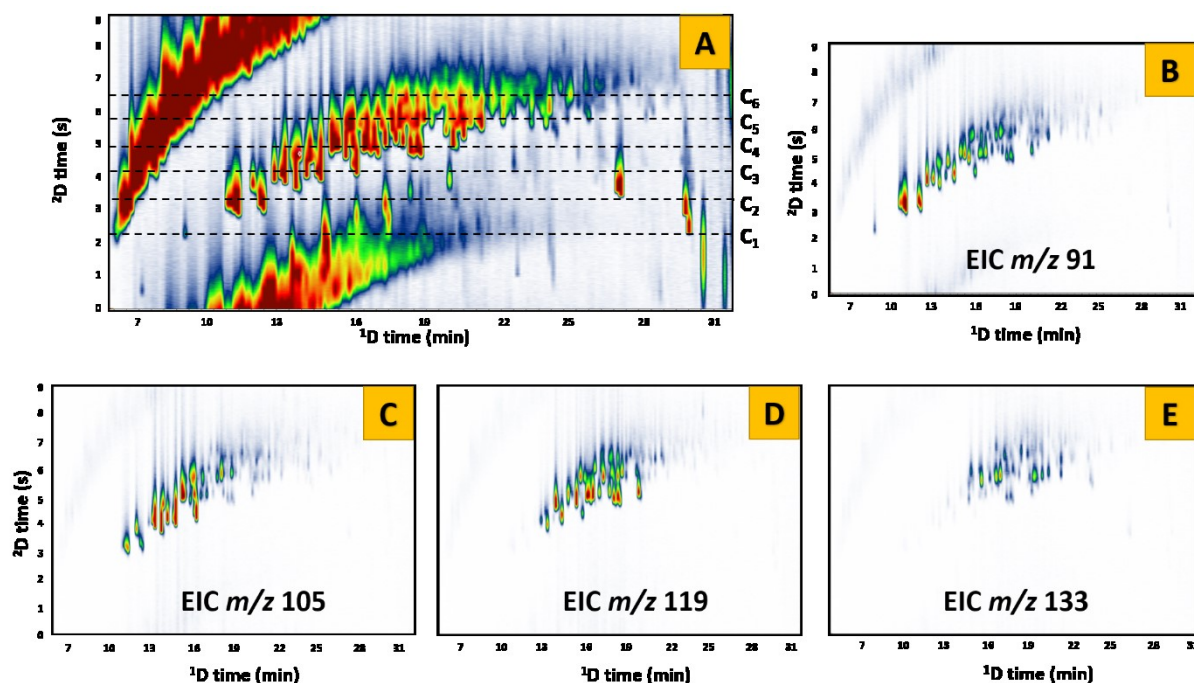


Figure 7. (A) TIC of the HTFT (stress) sample with the separation of various monoaromatic groups ($\text{C}_1 - \text{C}_6$). B–E show the EICs obtained from this TIC for the m/z values 91, 105, 119 and 133. For instance, the m/z 105 ion indicates C_2 and greater groups.

As seen in Figure 7, the selected ion masses for the specific monoaromatic groups can assist to identify the carbon number substitution on the benzene ring and propose these groups on the TIC as C_1 , C_2 , C_3 etc. Some example mass spectra and typical library hit compounds for such spectra are presented in Supporting Information Table S4. It should be reiterated that the mass spectra (based on fragmentation patterns) give only probable

hits for the library searches, and cannot be accurately identified unless complemented by detectors such as FTIR (based on the molecule's structure) which give a unique spectrum, and/or authentic standards. The EIC of m/z 105 gave a similar profile to the peaks obtained by the m/z 105.0336 wide window EIC in Figure 6B. Thus, to see the specific $\text{ArC}\equiv\text{O}^+$ ion a strong fragment would be necessary. The absence of sufficient information achieved using the accurate mass EIC for oxygenated compounds comes as a surprise to us here, since the samples were expected to comprise some oxygenates. It can be concluded that a number of operational conditions were not optimised to allow detection of the trace oxygenates. Clearly the ready fragmentation loss of oxygen groups e.g. in alcohols will lead to fragment ions comprising only C and H, so selection of a class-specific ion containing an O atom that represents a given class is not apparent. For benzaldehydes, greater response and sensitivity oxygenated compounds towards the m/z 105.0336 ion would require greater injection amounts, and splitless injection rather than the split conditions used here. The adoption of a soft ionisation technique that retains oxygen in the molecular / pseudo molecular ion will assist in selection of suitable EIC ions to correspond to all possible homologues of the oxygenates chemical class; chemical ionisation (CI) would be suggested in this regard.

The role of sulfur compounds as a trace component affecting the thermal stability of jet fuels has been studied ⁶. GC combined with sulfur selective detection, such as sulfur chemiluminescent detection (SCD) and flame photometric detection (FPD) in its sulfur mode, can be used for detecting sulfur species ⁴². Preliminary analysis for detection of the presence of sulfur compounds was conducted with 1DGC-FPD for the four fuel types using the settings given in Supporting Information Table S3. The resulting 1DGC chromatograms are shown in Supporting Information Figure S7 where, of the four fuel samples, only Merox demonstrated a significant presence of sulfur compounds. This is as expected because Merox fuels are produced using the mercaptan oxidation technology which converts mercaptans into disulfides. Although the 1DGC systems generally allow a simpler experimental setup and data analysis compared to multidimensional systems to investigate the presence of sulfur compounds in samples, they generally provide a reduced separation efficiency compared to GC×GC-FPD systems which also combine 1t_R and 2t_R . GC×GC-TOFMS has been shown to be successful in separating sulfur compounds from polyaromatic hydrocarbons and phenols, as well as the separation of sulfur isomers from one another – a feat not possible with 1DGC ⁴³. However, the detection of sulfur

compounds using GC×GC–TOFMS and EICs is not as straightforward as the detection of oxygenates due to the vast diversity of fragment ions for the various sulfur compound classes and is thus beyond the direct scope of this study.

Despite the abundant fragmentation observed, one shortcoming of using electron ionisation (EI) techniques, such as that in the TOFMS system available in this study, is often the very low presence of the molecular ion. In contrast mass spectrometers employing field ionisation (FI), atmospheric pressure photoionisation (APPI) chemical ionisation (CI) modes generate an abundance of molecular and protonated ions ³⁸, which may be better suited to avoid the lack of oxygen contained in the abundant fragment ions seen with EI. This would also be a similar concept to the ionisation process used in HRMS, reported below.

HRMS results of thermally oxidised fuel samples

FTICR MS, which produces results by combining both mass measurement and resolution in the same step, does not necessarily rely on the need for a pre-separation process prior to analysis as needed by the lower resolution time-of-flight or quadrupole MS. They may however benefit from coupling to chromatographic interfaces for sample purification, mixture separation or preconcentration. The HRMS technique used in this experiment uses atmospheric pressure photoionisation (APPI) as it is well suited for non-polar and low-polarity compounds which constitute a large proportion of complex petrochemical mixtures ⁴⁴ as evident in Figure 3. APPI is generally implemented by exposing analytes to an energy of ~10 eV emitted by a UV lamp. This also has the ability to generate MS signals for species over a wide range of compounds including non-polar entities which may not be accessed by other ionisation techniques such as electrospray ionisation (ESI) and atmospheric pressure chemical ionisation (APCI) ²⁵. APPI relies on the absorption of photons and hence is sensitive towards aromatic groups because aromatic groups are good chromophores for absorbing UV. In (+)-mode APPI, the chemical reaction which follows the absorption of photons generate both molecular (M^+) and protonated ($[M + H]^+$) ions. The use of toluene as a dopant in the APPI used in this study enhances the ion yield of ionisation because UV radiation readily ionises the dopant molecules and produces a large number of molecular ions and free radicals. Subsequently the dopant

ionises other molecules through electron or proton transfer and/or charge exchange reactions. Molecules such as saturates which are readily ionised by APPI also benefit from the use of dopants due to the resulting increase of ionised analyte molecules. Figure 8 shows the broadband positive-ion APPI FTICR mass spectra for the 4 fuels (neat and stress) where it is seen that the molecular weight distribution shifts to a higher m/z value in the stressed fuels.

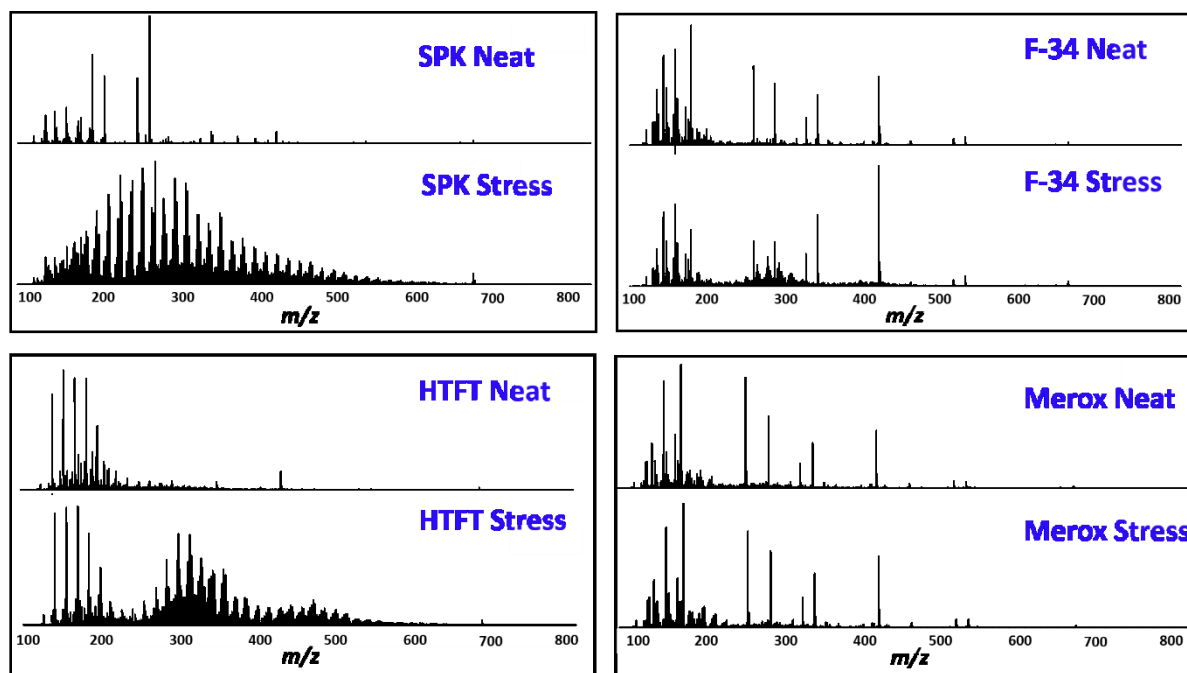


Figure 8. Broadband positive-ion APPI FTICR mass spectra for the 4 neat and stressed fuels.

Use of FTICR MS is accompanied by the possibility of resolving thousands of chemically distinct components or different elemental compositions using a single mass spectrum which spans a broad m/z range. This feature affords a unique characteristic signature referred to as a 'fingerprint' or 'profile' at the molecular level. The resulting increase in the number of m/z values increases the number of formulae which match an exact m/z value, as well as the probability of obtaining a correct result within a 1 ppm error window⁴⁵. This places value on the use of Kendrick mass defect (KMD) calculations which aid in analysing homologous series of compounds. The KMD is calculated as set out in Equations 1 and 2 using the nominal mass (14.000 00) and exact mass (14.01565 Da) of the CH_2 alkyl unit to sort members of the same heteroatom class.

$$\text{Exact Kendrick mass} = \text{IUPAC mass} \times (14.000\ 00 / 14.015\ 65) \quad (\text{Eq. 1})$$

$$\text{KMD} = (\text{nominal Kendrick mass} - \text{exact Kendrick mass}) \quad (\text{Eq. 2})$$

This renders the same KMD to ions differing by only one CH₂ group and hence such homologous series will align on the same horizontal line when the KMD is plotted against the nominal Kendrick mass. Such a separation based on alkylation using KMD aids in sorting complicated spectrum peaks to identify homologically related compounds, which is an advantage in identifying groups of related classes in petroleum samples ⁴⁶. The KMD plays a pivotal role in assigning molecular formulae, detecting the degree of unsaturation using the double bond equivalent (DBE), identifying the class of heteroatoms and in detecting minute changes in sample composition. The DBE (also referred to as number of rings plus double bonds) is given by Equation 3 where *c*, *h* and *n* denote the number of carbon atoms, hydrogen and halogen atoms, and nitrogen atoms respectively.

$$\text{DBE} = c - \left(\frac{h}{2}\right) + \left(\frac{n}{2}\right) + 1 \quad (\text{Eq. 3})$$

The DBE describes compound aromaticity and unsaturation whilst the carbon number represents the degree of alkylation, volatility and molecular weight. The DBE versus carbon number (DBE/C) plots are typically used in FTICR MS data analysis and enable visualisation of broad trends in the degree of alkylation (carbon number) and aromaticity (DBE), where each point on the graph corresponds to an assigned molecular formula, and thus facilitate comparative analysis of the compositional variation between complex samples. DBE calculations are mainly useful for compounds containing C and H and does not indicate double bonds between other elements such as N and O. This approach cannot be extended to DBE calculations for compounds when S or P are present since depending on their oxidation state S and P can show different valencies. This rule however has an exception in strictly reducing environments when it can be assumed that S is bivalent (e.g. sulfides and thiols) and P is trivalent (e.g. phosphines) ⁴⁷.

Compounds with similar heteroatom distribution are expected to show similar chemical properties and hence will influence the physical properties of the fuel in a similar manner. Thus, if a DBE plot displays such heteroatom relationships, then this will also represent the fuel's properties. This feature is exploited to compare the molecular composition of the four different neat fuel samples. The histogram in Figure 9 displays a comparison of the percentage of contribution to the total signal by the various heteroatom compound

classes of the four fuels in their neat stage. The DBE versus carbon number plots are inset for the HC[H] and O1 classes for the four fuels. Of these samples, the HTFT and Merox samples display the highest DBE values for both HC[H] and O1 classes. This denotes a high degree of unsaturation and presence of double bonds as explained in Equation 3. DBE values as high as 15 seen in the HTFT, F-34 and Merox samples convey the presence of aromatic compounds with as many as 4 or 5 condensed rings.

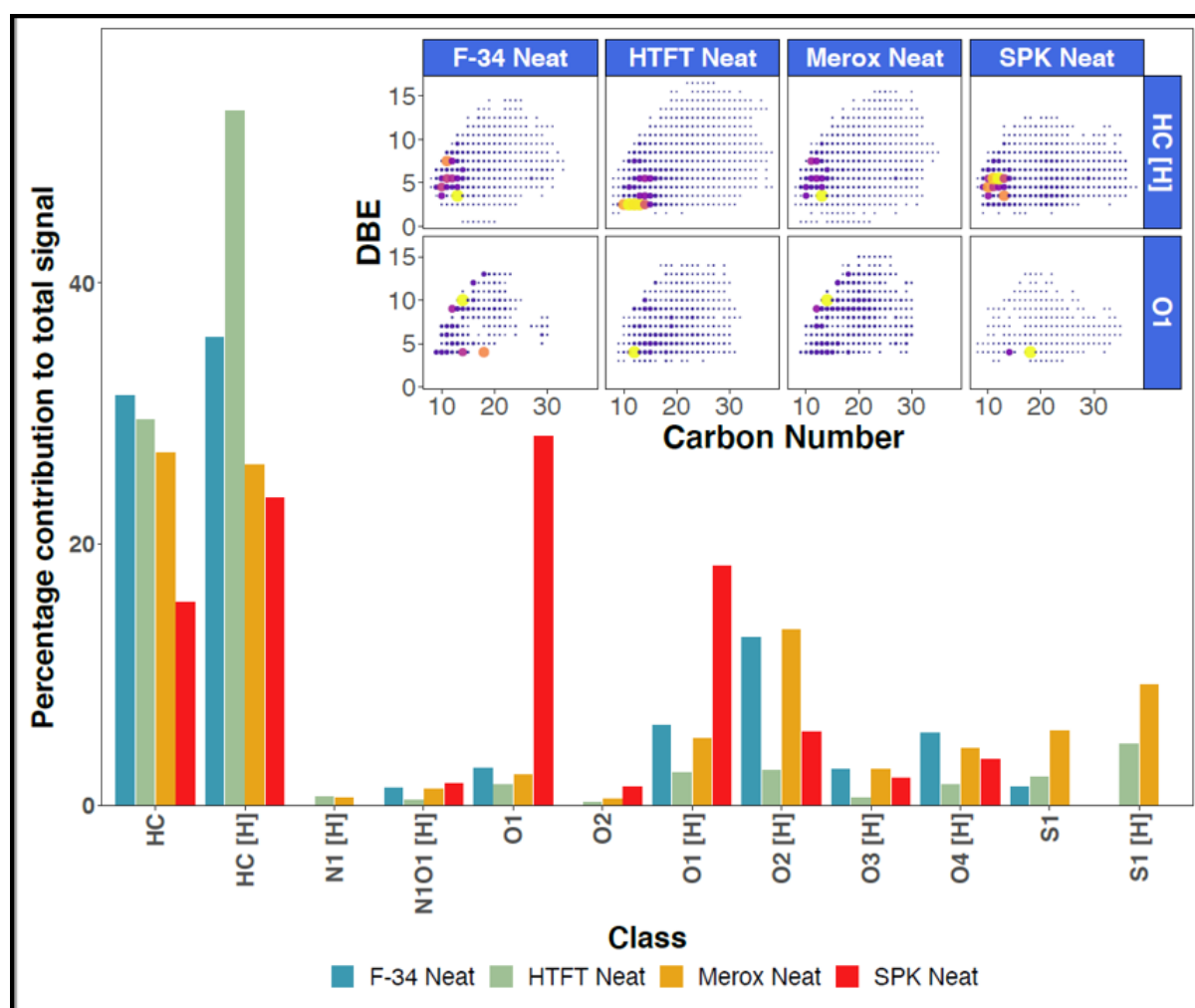


Figure 9. Comparison of the heteroatom class distribution and the percentage contribution to the total signal by the various classes for the four fuels in their neat stage.

Of significance here is the increased contribution by the HC (C_nH_n series) class in the HTFT fuel whereas the O1 class was highest in the SPK fuel. The S1 class ($C_nH_nS_1$ series) was most abundant in the Merox sample which agrees with GC-FPD results obtained (presented in Figure S7 of Supporting Information). With the allowable sulfur levels in

petrochemical products being continually decreased by regulatory demands, percentage contribution by S1 and S1[H] classes and sulfur speciation is of particular importance to the petroleum refining industry.

The histograms in Figure 10 present the relative abundance for the various compound classes detected in the four fuel types. The blue and red bars compare the abundance of neat and stressed stages respectively for each class. These results show that all four fuels had a comparatively lower abundance of HC classes and a higher abundance of O containing classes in the stressed fuels. Therefore, it could be inferred that in all cases the thermal stressing contributed to the oxidation of hydrocarbon species in neat samples to an increased prevalence of oxygenates in the stressed samples. This is further supported by van Krevelen plots.

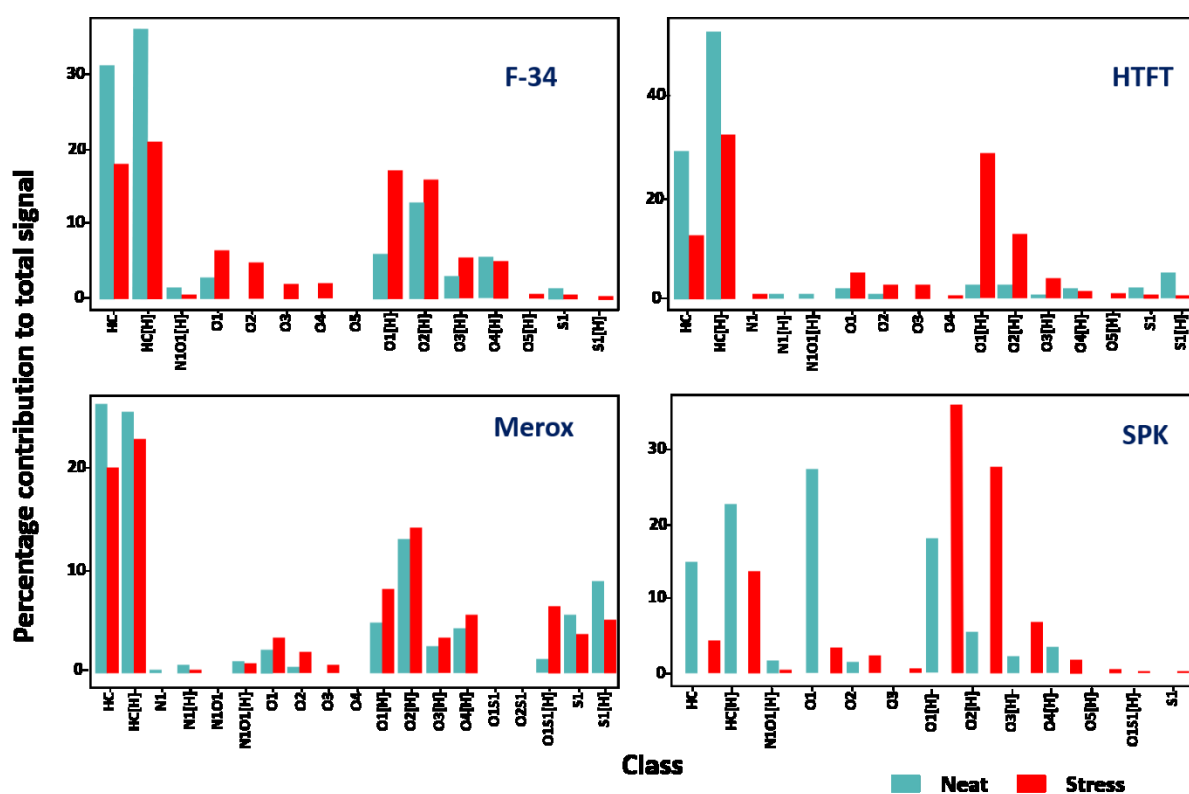


Figure 10. Histograms presenting the relative class distribution of the neat and stress stages of the four fuel types. Blue bars represent the neat stage and the red bars represent the thermally stressed stage.

Van Krevelen diagrams are an important graphical tool in complex mixture analysis using FTICR MS where a large number of molecules are displayed in a space defined by plotting

their H/C ratio against their and O/C ratios ⁴⁸. These diagrams enable comparing differentiating features of whole samples, and also visualising the chemical composition of compounds during a given process such as transforming to higher value-added products. They aid in extracting molecular information of the samples analysed which are readily generated from FTICR MS data and the assigned elemental composition of each mass spectrum peak. Here, van Krevelen diagrams were successfully used to analyse the four fuel types, each in their neat and thermally stressed stages as presented in Figure 11.

The distinct points on the van Krevelen diagram represent compounds with different compositions obtained by the atomic ratio of the compounds. These plots are advantageous in that compounds with similar structural characteristics are grouped in the same region of the plot. This enables the clear definition of compounds with distinct structural features – such as condensed aromatics, fatty acids etc. – and the ability to be distinguished from each other based on the variation in H/C and O/C. For example, the alignment of dots along lines as shown in Figure 11 consist of compounds belonging to the same alkylation series where the lines intersect at an H/C value of 2 on the y-axis. This corresponds to an elemental composition of $C_cH_cO_o$ which converts to $C_{c-n}H_{c-n}O_{o-n}$ when it loses $(CH_2)_n$ and the new y-axis and x-axis values for H/C and O/C respectively can be represented by Equation 4.

$$y = (h - 2n)/c - 2n; x = o/(c - n) \quad (\text{Eq. 4})$$

The elimination of n yields Equation 5.

$$y = 2 + (h - 2c)ox \quad (\text{Eq. 5})$$

Thus, the y-intercept for each alkylation series remains as 2 as evident in the van Krevelen plots in Figure 11(A–H) for the four fuel types.

Since major chemical classes of compounds have a specific H/C or O/C ratio, each class of compounds retains a specific location on the plot. Hence, when a sample undergoes a chemical reaction such as oxidation or condensation, this affects the unique location of points on the van Krevelen diagram due to the loss of C, H, O or N atoms ⁴⁹. This property is made use of in observing the changes in H/C and O/C ratios of fuels before and after thermal stressing as depicted in Figure 11.

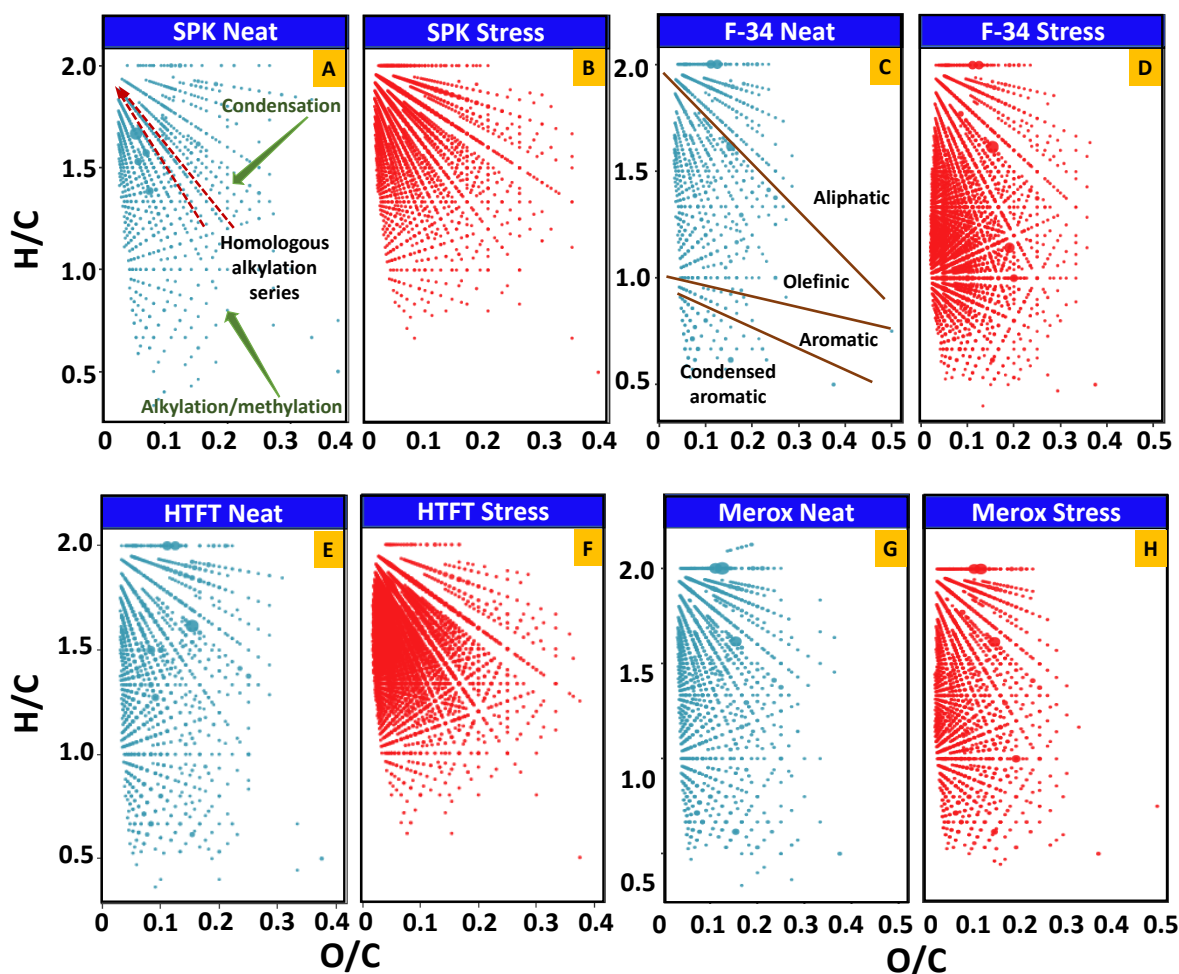


Figure 11. The van Krevelen diagrams for elemental data of the four types of fuel (neat and stressed stages). Compounds in homologous alkylation series appear along the lines that intersect at the H/C axis at an atomic ratio of 2, towards which alkylation increases. Condensation increases towards lower H/C values. Based on alkylation and aromaticity, the labelled regions can be identified as aliphatics, olefinics, aromatics and condensed

As illustrated in Figure 11A, alkylation increases towards higher atomic ratios on the H/C axis and condensation increases towards lower H/C ratios. Compounds in homologous series appear along definite lines leading to specific H/C ratio numbers. For example, homologous alkylation series converge at H/C value of 2 as explained in Equations 4 and 5. Van Krevelen plots can also be divided into specific regions⁵⁰ as seen in Figure 11C, where the common hydrocarbon classes seen in fuels – aliphatics, olefinics, aromatics and condensed aromatics – are depicted. In all neat fuel types, the species are concentrated in the region that spans between H/C values of 0.5–2.0. The lower limit of the H/C region increases in the thermally stressed samples and is most visible in the SPK sample where the region spans 1.0–2.0. This aligns with the GC×GC results presented in

Figure 2, where the SPK samples have the highest proportion of straight chain and branched alkanes.

Further, for each fuel type, the abundance of structures (dots on the plot) seen in the higher O/C values is greater for thermally stressed samples than their respective neat samples. This can be attributed to the higher oxygen content in the thermally stressed samples ⁵¹, indicating a higher degree of carboxylation and the presence of oxygenated species. The van Krevelen diagrams can thus be used in aviation fuel samples to successfully sort compounds which may possess common structural relationships.

Complementary analysis using GC×GC–TOFMS and HRMS for aviation fuel

The use of high-resolution techniques for fuel analysis can provide a greater breadth of information and a deeper understanding of the constituents in aviation fuels. The two techniques GC×GC and FTICR MS both have their strengths and weaknesses over the other technique in achieving this.

GC×GC provides superiority in chromatographic separation with structured chromatograms and allows the physical resolution of analytes in complex matrices. Its hyphenation to accurate mass TOFMS, as used in this study, renders the capability to produce better deconvoluted mass spectra with an increased mass resolution. TIC data generated by GC×GC–TOFMS can be readily visualised by 2D contour plots on which compound classes and their homologous composition can be grouped. This gives the ability to view a range of compound classes on a single plot; a task impossible with lower resolution 1DGC. Thus, both a quantitative and qualitative overview of the total sample can be gleaned. The well-defined chromatographic regions facilitate structural elucidation of eluted analytes. The union of the ordered elution of components on the 2D column and the subsequent analysis of the resulting mass spectrum of each peak enables identification of the analyte using a combination of approaches. This includes approaches such as EICs for specific accurate masses, peak deconvolution, generation of formula using the exact mass of fragment ions, library similarity searches etc. When used for identifying oxygenate species the EICs provide a distribution of the species and can be used to compare the fuels with its neat stages. A significant limitation related to this purpose arises when an O-containing compound has a poor molecular ion, and the

oxygenated moiety is lost via facile fragmentation, thereby not confirming the presence of O in the molecule. GC×GC–TOFMS enables a group-type speciation of compound classes, which can be manipulated to suit the sample type using various chromatographic stationary phases. In the study of oxygenates in fuel, GC×GC has the capability for unbiased separation of mixtures containing both polar and non-polar functional groups which is well-suited for complex mixtures which have components of varying polarities. The qualitative identification provided by GC×GC–TOFMS can be an excellent source of complementary information to FTICR MS. This is mainly because GC×GC–TOFMS can characterise non-polar compounds – subject to the ionisation process – that may not be measured effectively by FTICR MS ²⁶. Further, saturates and olefins have the tendency to fragment and undergo gas-phase reactions during ionisation and can often render difficulties in mass spectrum measurements. Here, the class distribution capabilities of GC separation support characterisation of matrix components.

In contrast to the chromatographic separation-based approach in GC×GC–TOFMS, FTICR MS investigates the elemental composition of samples and can simultaneously accumulate an extensive amount of information from a mere single mass spectrum. The enormous amount of data it yields is visualised using a range of plots such as DBE vs C number, KMD and van Krevelen plots. Although FTICR MS enables identification of homologous series, unlike GC×GC–TOFMS it lacks the ability to distinguish structural isomers which have the same heteroatomic composition ⁵², and where these isomers may affect fuel performance and quality. The suitability of the method is also challenged in the specific detection of compounds such as phenolics and organic acids with smaller molecular masses, irrespective of the ionisation method used ⁵³. Further, the Kendrick mass sorting capability of FTICR MS enables elemental composition assignments of masses 3× higher than that achievable by mass measurement accuracy methods alone ⁵⁴. FTICR MS application has enabled knowledge of up to 800 Da having polar functional groups e.g. ESI ionisation coupled to FTICR MS can be used to study oxygenated compounds and nitrogen containing entities ²⁹.

CONCLUSIONS

New methodologies for petroleomics applications are consistently being explored due to the wide variety of fuels needing analysis and identification of their components. Changes in the distribution of compound classes, changes in hydrocarbon content and variation in the composition of heteroatoms such as oxygenates is often observed to provide a molecular signature to the samples being analysed. The complexity of fuel samples promotes the approach of carrying out chromatographic separation of the fuel components by online or offline means prior to being analysed by HRMS systems ²⁴. GC×GC has proven itself to be a reliable source of information for complex sample analysis with greater efficiency than conventional 1DGC, yet is dependent on the capability of the detector it is hyphenated to. The accurate mass TOFMS is well suited for target and non-target analysis required in characterising complex matrices such as aviation fuels. Another powerful tool, FTICR MS takes advantage of its ability to render elemental composition, together with a multitude of data plotting methods to provide information on the heteroatom content of these fuels. This however has the disadvantages of not being quantitative with bias arising from the ionisation step and presenting an enormous device cost. This work investigated fundamental experimental requirements for correlating the oxidation of components in fuel samples based on high resolution analytical approaches. Thus, the marriage of information derived from the powerful duo in chemical analyses, HRMS approaches and HRGC experiments, gives a deeper insight to the detailed composition and molecular speciation of aviation fuels and continues to change the paradigm in petroleomics investigations.

ACKNOWLEDGEMENTS

Support for this work was provided by the Australian Research Council Linkage Grant scheme with partner PerkinElmer (Grant LP150100465). The authors acknowledge the funding from PerkinElmer to the Monash University GRIP program. Support for a Deans Research scholarship to JSZ from the Monash University is also acknowledged. Defence Science Technology Organisation are gratefully acknowledged for providing fuel samples.

REFERENCES

- (1) ASTM. In *Standard Specification for Aviation Turbine Fuel Containing Synthesized Hydrocarbons*; ASTM D7566-20c: ASTM International, West Conshohocken, PA, 2020.
- (2) Morgan, T. J.; Youkhana, A.; Turn, S. Q.; Ogoshi, R.; Garcia-Pérez, M. *Energy Fuels* **2019**, *33*, 2699–2762.
- (3) Jia, T.; Zhang, X.; Liu, Y.; Gong, S.; Deng, C.; Pan, L.; Zou, J.-J. *Chem. Eng. Sci.* **2021**, *229*, 116157.
- (4) Dounghthip, T.; Ervin, J.; Zabarnick, S.; Williams, T. *Energy Fuels* **2004**, *18*, 425–437.
- (5) Kulsing, C.; Rawson, P.; Webster, R. L.; Evans, D. J.; Marriott, P. J. *Energy Fuels* **2017**, *31*, 8978–8984.
- (6) Rawson, P. M.; Webster, R. L.; Evans, D.; Abanteriba, S. *Fuel* **2018**, *231*, 1–7.
- (7) Webster, R. L.; Rawson, P. M.; Kulsing, C.; Evans, D. J.; Marriott, P. J. *Energy Fuels* **2017**, *31*, 4886–4894.
- (8) Beccaria, M.; Siqueira, A. L. M.; Maniquet, A.; Giusti, P.; Piparo, M.; Stefanuto, P.-H.; Focant, J.-F. *J. Sep. Sci.* **2021**, *44*, 115–134.
- (9) Striebich, R. C.; Contreras, J.; Balster, L. M.; West, Z.; Shafer, L. M.; Zabarnick, S. *Energy Fuels* **2009**, *23*, 5474–5482.
- (10) Vozka, P.; Kilaz, G. *Fuel* **2020**, *268*, 117391.
- (11) Heneghan, S. P.; Locklear, S. L.; Geiger, D. L.; Anderson, S. D.; Schulz, W. D. *J. Propul. Power* **1993**, *9*, 5–9.
- (12) Tran, T. C.; Logan, G. A.; Grosjean, E.; Ryan, D.; Marriott, P. J. *Geochimica et Cosmochimica Acta* **2010**, *74*, 6468–6484.
- (13) Zavahir, J. S.; Nolvachai, Y.; Marriott, P. J. *TrAC Trends Anal. Chem.* **2018**, *99*, 47–65.
- (14) Marriott, P. J.; Nolvachai, Y. In *Sep. Sci. Technol.*, Snow, N. H., Ed.; Academic Press, 2020, pp 41–68.
- (15) Blomberg, J.; Schoenmakers, P. J.; Beens, J.; Tijssen, R. J. *High Resol. Chromatogr.* **1997**, *20*, 539–544.
- (16) Striebich, R. C.; Shafer, L. M.; Adams, R. K.; West, Z. J.; DeWitt, M. J.; Zabarnick, S. *Energy Fuels* **2014**, *28*, 5696–5706.
- (17) Van Deursen, M.; Beens, J.; Reijenga, J.; Lipman, P.; Cramers, C.; Blomberg, J. *J. Sep. Sci.* **2000**, *23*, 507–510.
- (18) Agüera, A.; Martínez-Piernas, A. B.; Campos-Mañas, M. C. In *Applications in High Resolution Mass Spectrometry*, Romero-González, R.; Frenich, A. G., Eds.; Elsevier Inc.: Amsterdam, Oxford, Cambridge, 2017, pp 59–82.
- (19) Marshall, A. G.; Rodgers, R. P. *Proc. Natl. Acad. Sci.* **2008**, *105*, 18090–18095.
- (20) Pollo, B. J.; Teixeira, C. A.; Belinato, J. R.; Furlan, M. F.; Cunha, I. C. d. M.; Vaz, C. R.; Volpato, G. V.; Augusto, F. *TrAC Trends Anal. Chem.* **2021**, *134*, 116111.
- (21) Pereira, I.; de Aguiar, D. V. A.; Vasconcelos, G.; Vaz, B. G. In *Fundamentals and Applications of Fourier Transform Mass Spectrometry*, Kanawati, B.; Schmitt-Kopplin, P., Eds.; Elsevier, 2019, pp 509–528.
- (22) Pollo, B. J.; Alexandrino, G. L.; Augusto, F.; Hantao, L. W. *TrAC Trends Anal. Chem.* **2018**, *105*, 202–217.
- (23) Nizio, K. D.; Mginitie, T. M.; Harynuk, J. J. *J. Chromatogr. A* **2012**, *1255*, 12–23.
- (24) Lozano, D. C. P.; Thomas, M. J.; Jones, H. E.; Barrow, M. P. *Annu. Rev. Anal. Chem.* **2020**, *13*, 405–430.
- (25) Borisov, R. S.; Kulikova, L. N.; Zaikin, V. G. *Pet. Chem.* **2019**, *59*, 1055–1076.
- (26) Cho, Y.; Ahmed, A.; Islam, A.; Kim, S. *Mass Spectrom. Rev.* **2015**, *34*, 248–263.

- (27) Gutiérrez Sama, S.; Barrère-Mangote, C.; Bouyssière, B.; Giusti, P.; Lobinski, R. *TrAC Trends Anal. Chem.* **2018**, *104*, 69–76.
- (28) Rodgers, R. P.; Marshall, A. G. In *Asphaltenes, Heavy Oils, and Petroleomics*, Mullins, O. C.; Sheu, E. Y.; Hammami, A.; Marshall, A. G., Eds.; Springer New York: New York, NY, 2007, pp 6–93.
- (29) Marshall, A. G.; Rodgers, R. P. *Acc. Chem. Res.* **2004**, *37*, 53–59.
- (30) Han, Y.; Zhang, Y.; Xu, C.; Hsu, C. S. *Fuel* **2018**, *221*, 144–158.
- (31) ASTM. In *Standard Specification for Aviation Turbine Fuels*; ASTM D1655-20d: ASTM International, West Conshohocken, PA, 2020.
- (32) Gavard, R.; Jones, H. E.; Palacio Lozano, D. C.; Thomas, M. J.; Rossell, D.; Spencer, S. E.; Barrow, M. P. *Anal. Chem.* **2020**, *92*, 3775–3786.
- (33) Mahamuni, N. N.; Adewuyi, Y. G. *Energy Fuels* **2009**, *23*, 3773–3782.
- (34) Fodor, G. E.; Kohl, K. B.; Mason, R. L. *Anal. Chem.* **1996**, *68*, 23–30.
- (35) Araújo, S. V.; Rocha, B. S.; Luna, F. M. T.; Rola, E. M.; Azevedo, D. C. S.; Cavalcante, C. L. *Fuel Process. Technol.* **2011**, *92*, 1152–1155.
- (36) Brandão, L. F. P.; Braga, J. W. B.; Suarez, P. A. Z. *Energy & Environment* **2018**, *31*, 733–754.
- (37) Bacha, K.; Ben-Amara, A.; Vannier, A.; Alves-Fortunato, M.; Nardin, M. *Energy Fuels* **2015**, *29*, 4345–4355.
- (38) Beccaria, M.; Siqueira, A. L. M.; Maniquet, A.; Giusti, P.; Piparo, M.; Stefanuto, P. H.; Focant, J. F. *J. Sep. Sci.* **2021**, *44*, 115–134.
- (39) Mitrevski, B.; Marriott, P. J. *J. Chromatogr. A* **2014**, *1362*, 262–269.
- (40) Parsons, B. A.; Pinkerton, D. K.; Synovec, R. E. *J. Chromatogr. A* **2018**, *1536*, 16–26.
- (41) Khummueng, W.; Harynuk, J.; Marriott, P. J. *Anal. Chem.* **2006**, *78*, 4578–4587.
- (42) Chin, S. T.; Wu, Z. Y.; Morrison, P. D.; Marriott, P. J. *Anal. Methods* **2010**, *2*, 243–253.
- (43) Machado, M. E.; Caramão, E. B.; Zini, C. A. *J. Chromatogr. A* **2011**, *1218*, 3200–3207.
- (44) Purcell, J. M.; Hendrickson, C. L.; Rodgers, R. P.; Marshall, A. G. *Anal. Chem.* **2006**, *78*, 5906–5912.
- (45) Sleighter, R. L.; Hatcher, P. G. *J. Mass Spectrom.* **2007**, *42*, 559–574.
- (46) Hughey, C. A.; Hendrickson, C. L.; Rodgers, R. P.; Marshall, A. G.; Qian, K. *Anal. Chem.* **2001**, *73*, 4676–4681.
- (47) Reemtsma, T. *J. Chromatogr. A* **2009**, *1216*, 3687–3701.
- (48) Van Krevelen, D. *Fuel* **1950**, *29*, 269–284.
- (49) Kim, S.; Kramer, R. W.; Hatcher, P. G. *Anal. Chem.* **2003**, *75*, 5336–5344.
- (50) Willoughby, A.; Wozniak, A.; Hatcher, P. G. *Atmospheric Chemistry and Physics* **2014**, *14*, 10299–10314.
- (51) Kramer, R. W.; Kujawinski, E. B.; Hatcher, P. G. *Environ. Sci. Technol.* **2004**, *38*, 3387–3395.
- (52) Orlov, A. A.; Zhrebker, A.; Eletskaya, A. A.; Chernikov, V. S.; Kozlovskaya, L. I.; Zhernov, Y. V.; Kostyukevich, Y.; Palyulin, V. A.; Nikolaev, E. N.; Osolodkin, D. I.; Perminova, I. V. *Scientific Reports* **2019**, *9*, 12066.
- (53) Michailof, C. M.; Kalogiannis, K. G.; Sfetsas, T.; Patiaka, D. T.; Lappas, A. A. *Pet. Chem.* **2016**, *5*, 614–639.
- (54) Ryan P. Rodgers, T. M. S., and Alan G. Marshall. *Anal. Chem.* **2005**, *77*, 20 A–27 A.

Supporting Information

High resolution analysis of thermally oxidised aviation fuel — comprehensive two-dimensional gas chromatography vs high-resolution mass spectrometry

J. Shezmin Zavahir^a, Renée Webster^b, Federico Floris^c, Mark Barrows^c and Philip J. Marriott^a

^a Australian Centre for Research on Separation Science, School of Chemistry, Monash University, Wellington Road, Clayton, VIC 3800, Melbourne, Australia.

^b Defence Science & Technology Group, Lorimer St, Fishermans Bend, VIC 3207, Australia

^c Department of Chemistry, University of Warwick, Coventry, CV4 7AL, UK

Preparation for submission to:

Analytical Chemistry

* Corresponding author:

Email: Philip.Marriott@monash.edu (P. J. Marriott)

Tel: +61 3 99059630

Fax : +61 3 99058501

List of Figure Captions and Tables

Figure S1. ATR–FTIR spectrum for the fuels SPK, F-34, HTFT and Merox with the inset for each fuel showing the average spectrum for the C–H stretching region. The red and blue regions show the average of the neat and thermally stressed samples respectively.

Figure S2. PCA scatter plots for the infrared region of 1740–1690 cm^{-1} corresponding to carbonyl groups of the oxygenates carboxylic acid, aldehydes and ketones for fuel samples. Neat stage denoted by crosses and thermally stressed stage by circles. Colours corresponding to the fuels are blue – SPK; red – HTFT; green – F-34; and brown – Merox.

Figure S3. PCA score plots for some select infrared regions as described in Table S1 for specific sulfur containing functional groups. The corresponding mid IR wavenumber regions are (A) 2580–2500 cm^{-1} , (B) 1060–1020 cm^{-1} , (C) 1220–1190 cm^{-1} and, (B) 1050–770 cm^{-1} .

Figure S4. 1D GC–MS chromatograms of the four fuel types (A) with the comparative chromatograms of neat and thermally stressed stages for each fuel type Merox (B), F-34 (C), SPK (D) and FT (E).

Figure S5. Naphthalene peak indicated on the TIC of the standard mixture (A). The TIC of the HTFT (stress) samples is seen in (B) with the EIC of the m/z 128.0626 corresponding to the $[\text{C}_{10}\text{H}_8]^+$ ion of naphthalene (C). It is seen that the retention time of naphthalene in both (A) and (C) are the same at 26.233 min.

Figure S6. Total ion chromatogram (TIC) of the standard component mixture (A) and the mass spectra corresponding to the oxygenated species (B–H). Lower case peak labels on A correspond to the respective mass spectra.

Figure S7. 1DGC–FPD chromatograms of (a) Merox, (b) SPK (c) HTFT and (d) F-34 fuels showing the presence of sulfur compounds in the Merox sample.

Table S1. Functional group and frequency range descriptions for groups of sulfur containing compounds analysed by PCA.

Table S2. Operational parameters for one-dimensional gas chromatography mass spectrometry (1DGC–MS) experiments

Table S3. Operational parameters for one-dimensional gas chromatography with flame photometric detection (1DGC–FPD) experiments.

Table S4. Examples of mass spectra and typical compounds belonging to various carbon number substitution compounds found in the monoaromatic region of the HTFT (stress) fuel.

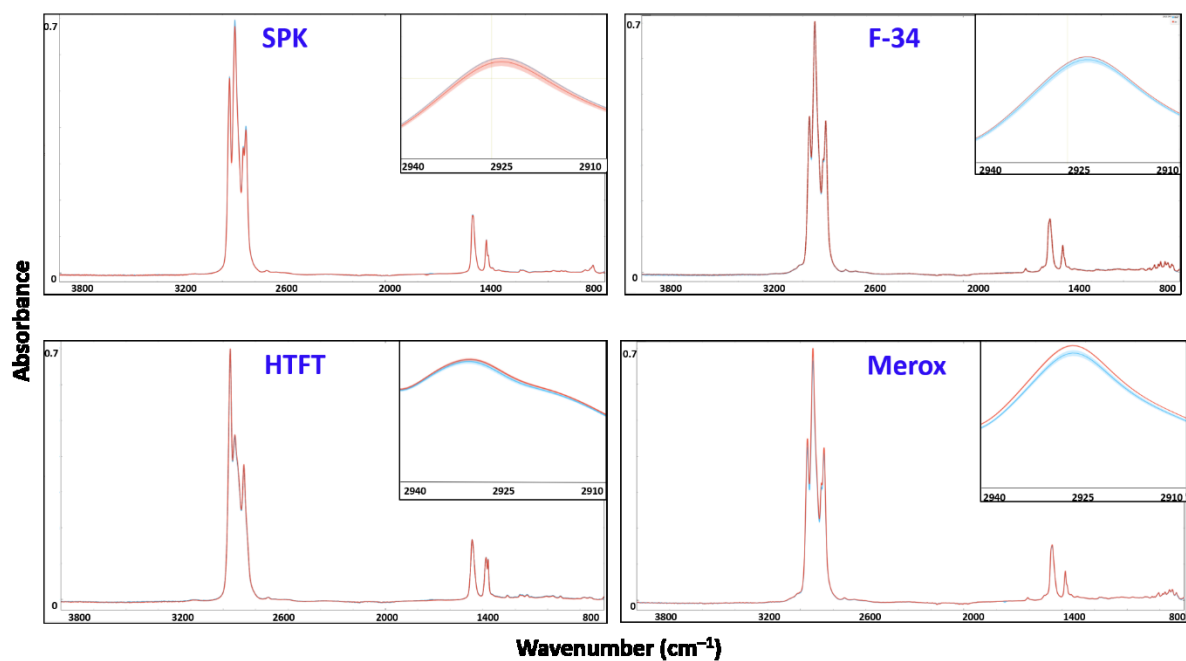


Figure S1. ATR-FTIR spectrum for the fuels SPK, F-34, HTFT and Merox with the inset for each fuel showing the average spectrum for the C-H stretching region. The red and blue regions show the average of the neat and thermally stressed samples respectively.

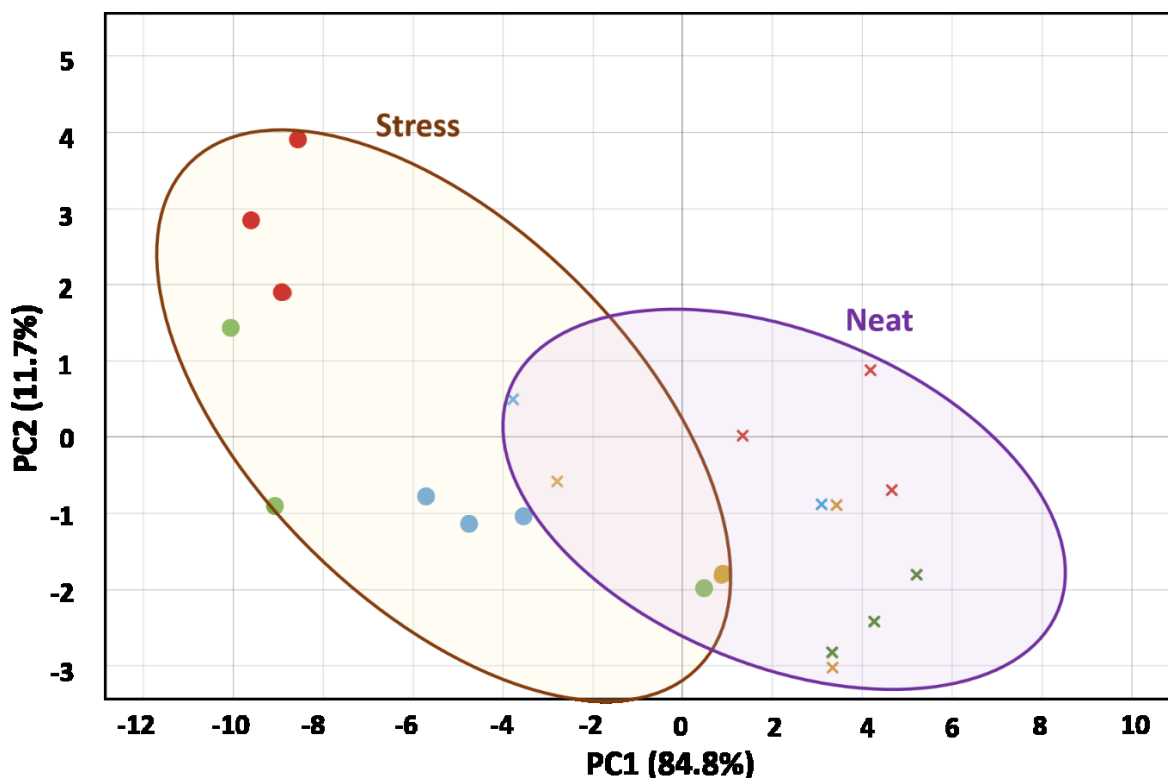


Figure S2. PCA scatter plots for the infrared region of 1740–1690 cm^{-1} corresponding to carbonyl groups of the oxygenates carboxylic acid, aldehydes and ketones for fuel samples. Neat stage denoted by crosses and thermally stressed stage by circles. Colours corresponding to the fuels are blue – SPK; red – HTFT; green – F-34; and brown – Merox.

Table S1. Functional group and frequency range descriptions for groups of sulfur containing compounds analysed by PCA.

Group	Class of compounds	Frequency range (cm^{-1})	Mode of vibration
S-H	Thiols	2580–2500	S-H stretch
S=O	Sulfoxides	1060–1020	S=O stretch
S=O	Dialkyl sulfites	1220–1190	S=O stretch
SO ₂	Sulfones, sulphonamides, sulfonic acids, sulfonates, sulfonyl chlorides	1390–1290	SO ₂ antisymmetric stretch
SO ₂	chlorides	1190–1120	SO ₂ symmetric stretch
SO ₂	Dialkyl sulfates and sulfonyl fluorides	1420–1390	SO ₂ antisymmetric stretch
SO ₂		1220–1190	SO ₂ symmetric stretch
S-O-C	Dialkyl sulphites and sulfates	1050–770	S-O-C stretch

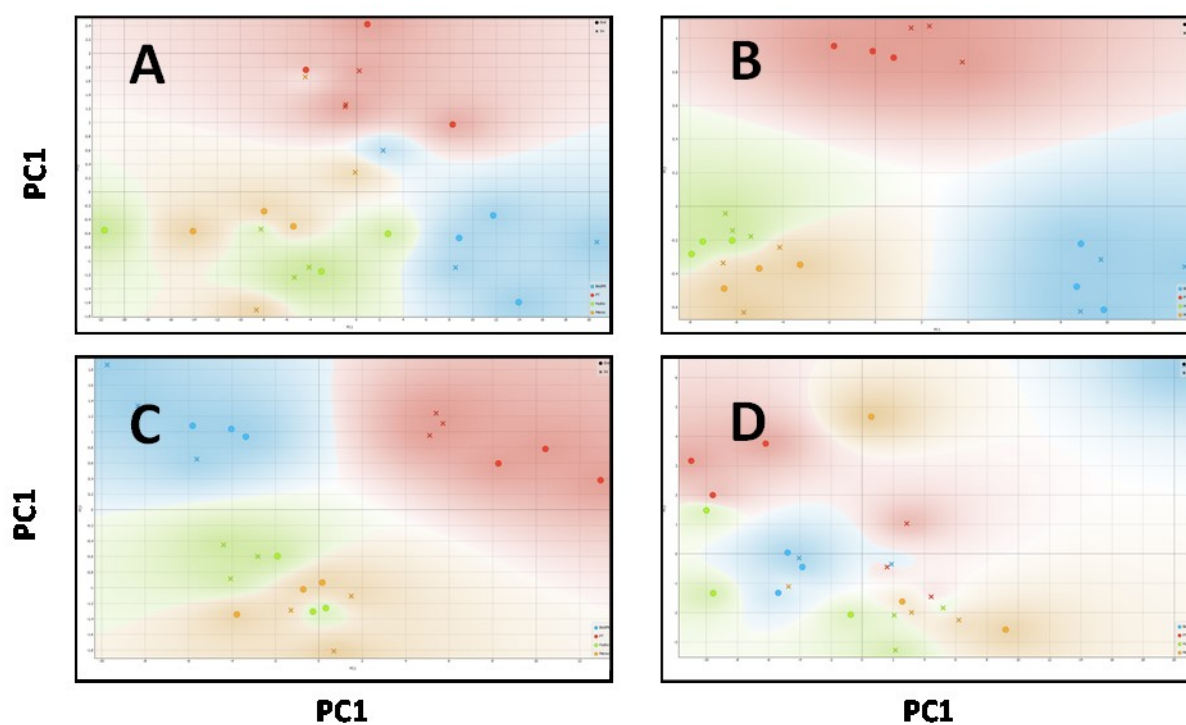


Figure S3. PCA score plots for some select infrared regions as described in Table S1 for specific sulfur containing functional groups. The corresponding mid IR wavenumber regions are (A) 2580–2500 cm⁻¹, (B) 1060–1020 cm⁻¹, (C) 1220–1190 cm⁻¹ and, (B) 1050–770 cm⁻¹.

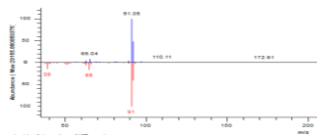
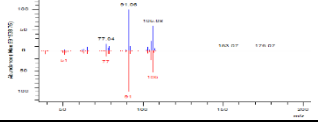
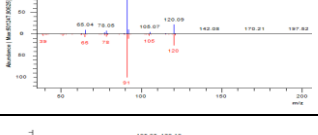
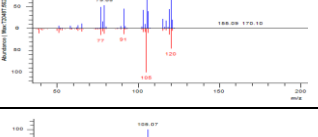
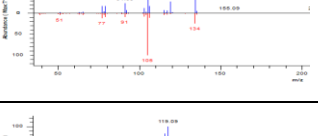
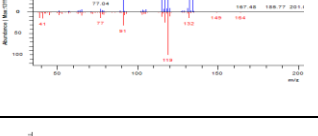
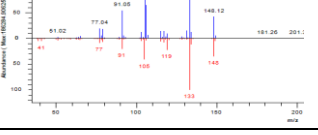
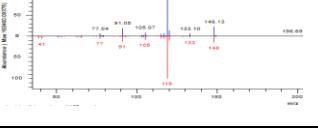
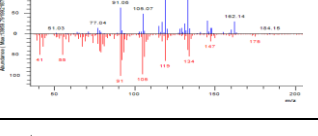
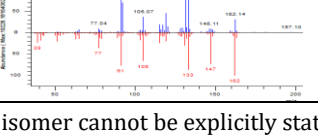
Table S2. Operational parameters for one-dimensional gas chromatography mass spectrometry (1DGC-MS) experiments

Gas chromatograph model	Agilent 7890A (Agilent Technologies, Santa Clara, CA)
Mass spectrometer model	Agilent 7000 Triple quadrupole mass spectrometer (Agilent Technologies, Santa Clara, CA)
Non-polar capillary column	
Sample preparation	50
Injection volume	1
	°C
Split ratio	200:1
Carrier gas	He, 99.999%
Carrier gas flow	1.2 mL/min, constant flow
GC oven program	Initial temperature of 50 °C to 250 °C at 4 °C /min
MS transfer line temperature	280 °C
MS ionisation voltage	70eV
Mass range	43 to 700 <i>m/z</i>

Table S3. Operational parameters for one-dimensional gas chromatography with flame photometric detection (1DGC–FPD) experiments.

Gas chromatograph model	Agilent 7890A (Agilent technologies, Santa Clara, CA) fitted with a flame photometric detector
Polar capillary column	SUPELCOWAX-10 (Sigma-Aldrich Co., St Louis, MO)
Sample preparation	1:5 dilution in DCM
Injection volume	1
	°C
Split ratio	20:1
Carrier gas	H ₂ , 99.999% purity
Carrier gas flow	1.5 mL/min, constant flow
GC oven program	Initial temperature of 100 °C to 250 °C at 4 °C /min, held for 30 min
FPD detector temperature	280 °C
FPD detector mode	S mode at 100 Hz
Gas flow rate	H ₂ :Air:N ₂ at 50:60:20 mL/min
Data collection and processing software	Agilent OpenLab CDS Chemstation version(Agilent Technologies)

Table S4. Examples of mass spectra and typical compounds corresponding to various carbon number substitution compounds found in the monoaromatic region of the HTFT (stress) fuel.

Class	Example $^{\dagger}t_R$ (min)	$^{\ddagger}2t_R$ (s)	Example mass spectrum	Examples of typical compounds
C ₁	8.758	2.293		toluene
C ₂	11.081	3.136		*dimethyl benzene (xylenes) *ethylbenzene
C ₃	12.508	4.075		*propyl benzene *1-ethyl-2-methyl- benzene *1,2,4-trimethylbenzene * methyl propyl benzene
	14.4581	4.327		
C ₄	14.908	5.120		*1,2-diethylbenzene *1-methyl-3-propyl benzene *cymene (<i>ortho, meta, para</i>) *2-ethyl-1,4-dimethyl benzene
	17.581	5.207		
C ₅	17.758	5.769		*1-ethyl-3-(1-methylethyl) benzene *1,1-dimethylpropyl benzene *1-ethylpropyl benzene
	18.808	5.883		
C ₆	20.1582	6.606		*1-ethylbutyl benzene *1,2,4-triethyl benzene *3-ethyl-1,2,4,5-tetramethyl- benzene
	20.758	6.479		

* Substitution pattern or the specific isomer cannot be explicitly stated for the indicated mass spectrum.

 ‡ Retention times are indicative for the specific examples shown

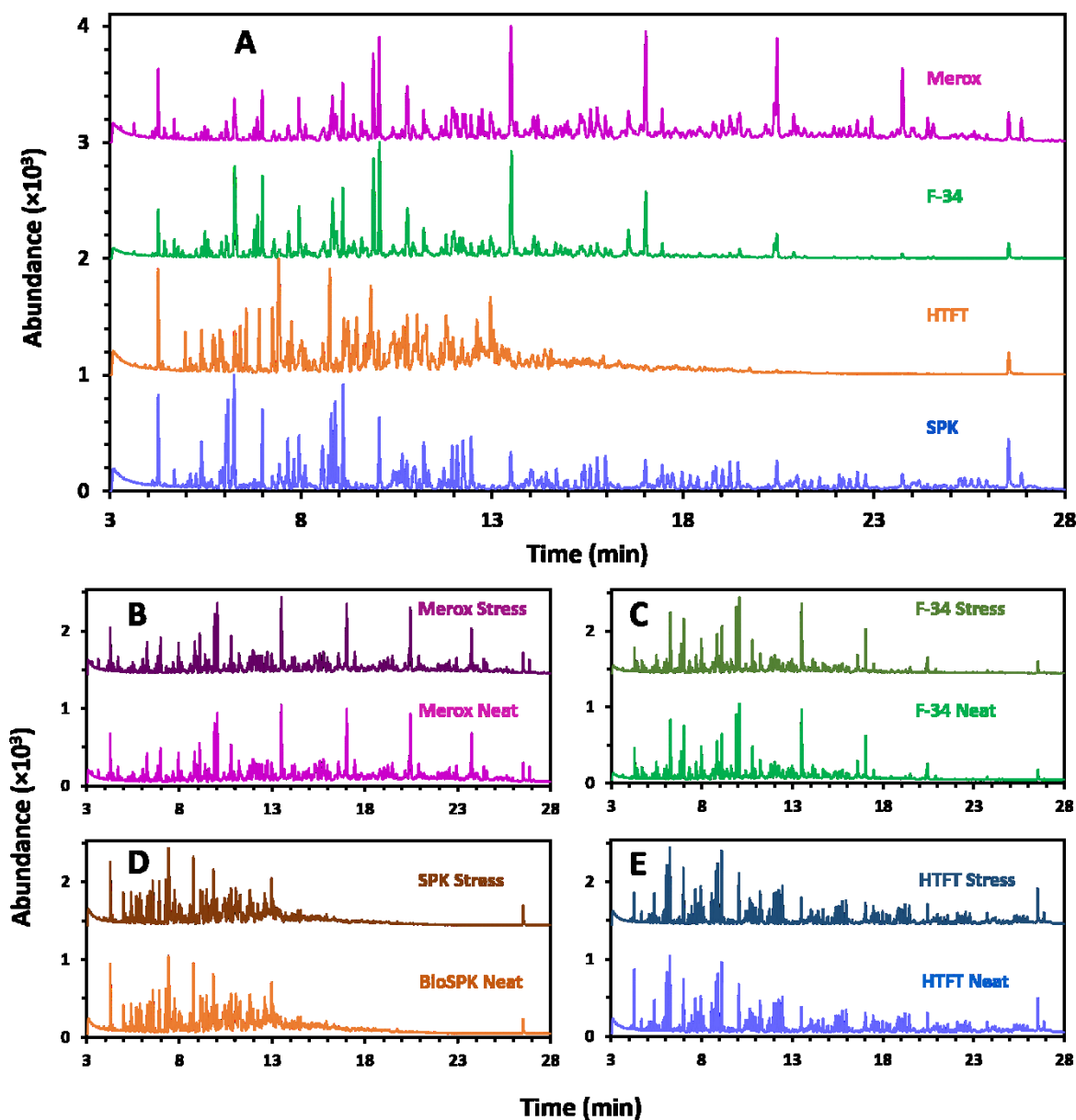


Figure S4. 1D GC-MS chromatograms of the four fuel types (A) with the comparative chromatograms of neat and thermally stressed stages for each fuel type Merox (B), F-34 (C), SPK (D) and FT (E).

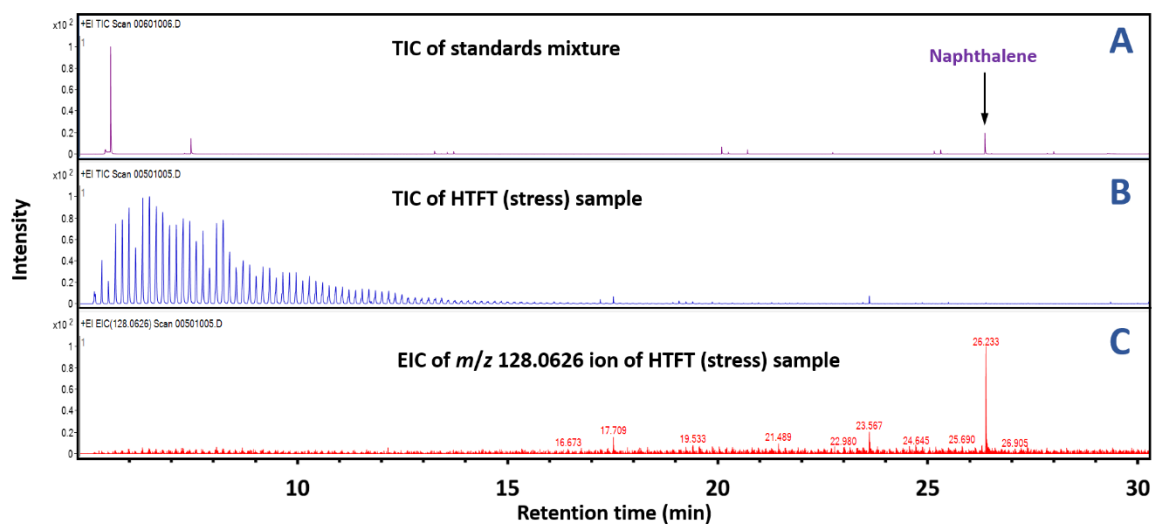
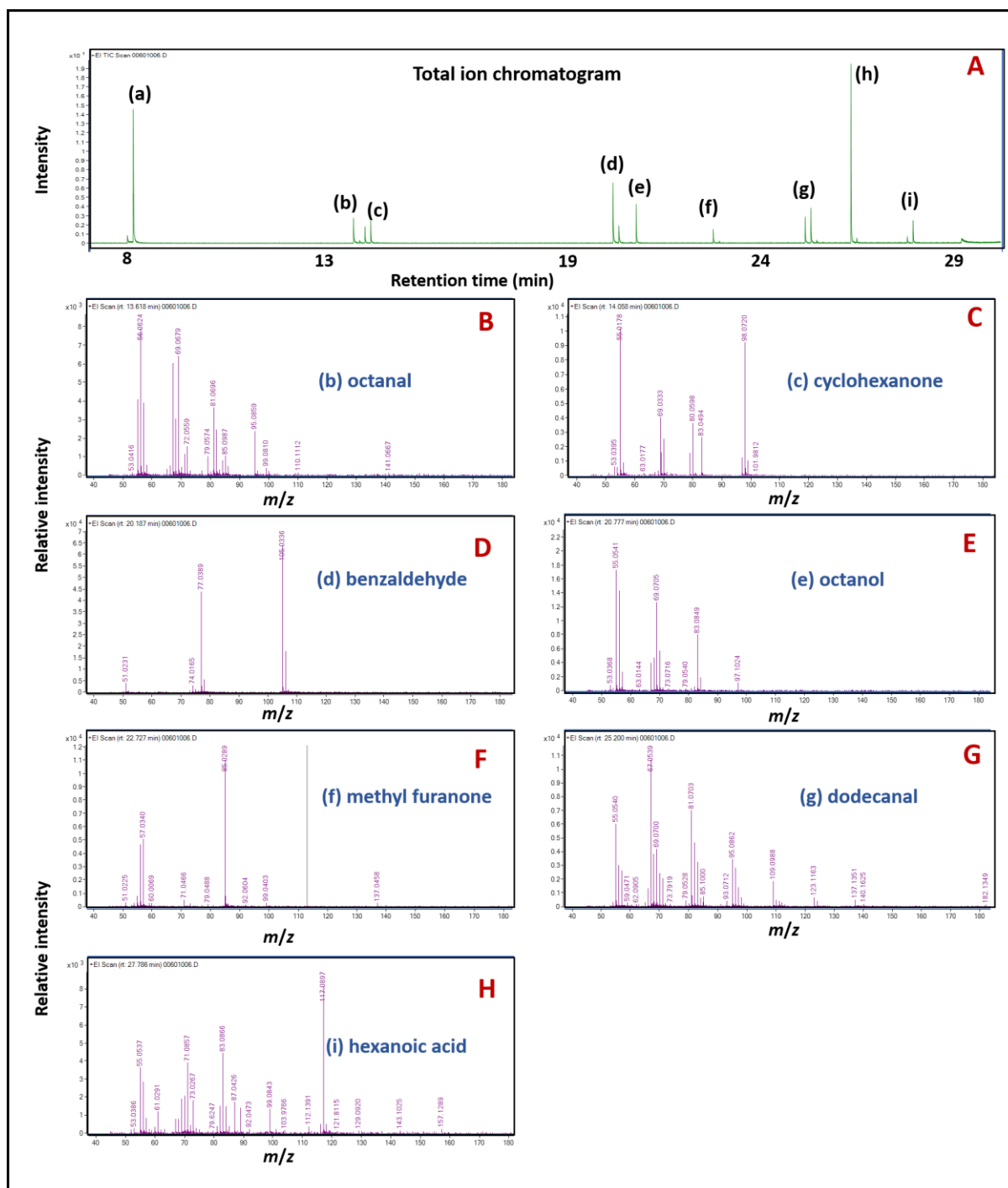


Figure S5. Naphthalene peak indicated on the TIC of the standard mixture (A). The TIC of the HTFT (stress) samples is seen in (B) with the EIC of the m/z 128.0626 corresponding to the $[C_{10}H_8]^+$ ion of naphthalene (C). It is seen that the retention time of naphthalene in both (A) and (C) are the same at 26.233 min.



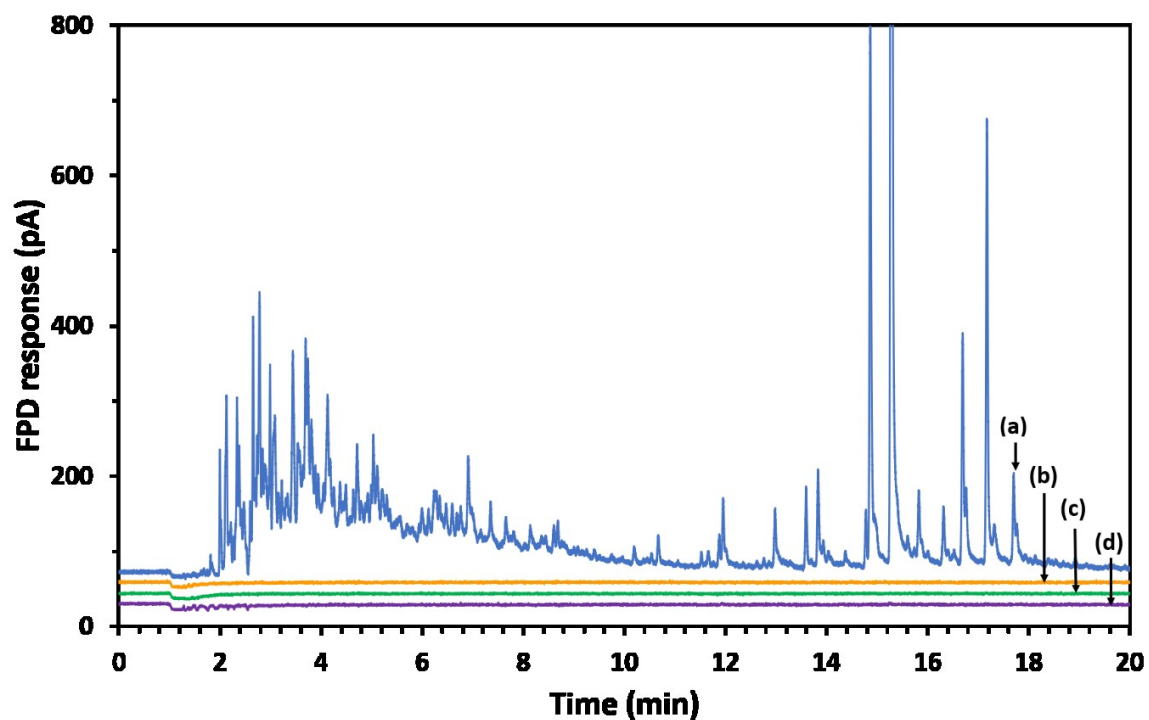


Figure S7. 1DGC–SPD chromatograms of (a) Merox, (b) SPK (c) HTFT and (d) F-34 fuels showing the presence of sulfur compounds in the Merox sample.

Chapter 6

Conclusions and future prospects

6.1 Conclusions

The need for unambiguous chemical analysis of components remains a priority for analysts irrespective of the complexity or origin of the sample to be analysed. The various Chapters in this Thesis endeavour to systematically bring together the advances in some important analytical techniques, mainly using the versatile and mature technique of gas chromatography together with the identification capabilities of spectrometric detection and spectroscopic detection – Fourier transform infrared spectroscopy in particular. The mass spectrometer has been and remains a powerful analytical tool referred to as the ‘gold standard’ for good reason – its reliability, reproducibility and utility cannot be overlooked; in full scan mode it can give an immediate suggestion as to molecular identity and so, many analysts rely heavily on this capability. Despite its superiority and sensitivity, the mass spectrum can be limited in its identification capabilities when relying on a library match against a compound in a database, which may not give an accurate identification. The simple example where an organic compound not present in the MS library may probably still generate a high library match is testimony to the problem of unquestioned reliance on MS library matching. Here additional confirmation needs to be sought using retention indices and comparison to spectra of authentic standards – the latter not always being a feasible option due to the high cost of or lack of availability of such standards. The various studies in this thesis thus align to shed light on the capabilities of other approaches, which overcome the shortcomings of solely relying on mass spectrometry (MS), whilst exemplifying their benefits by application to a wide range of compound classes.

A majority of the studies employ a hyphenated GC–FTIR system with a light-pipe interface which allows for real time analysis of GC eluted analytes. The first Chapter introduces the basic knowledge and concepts together with the underlying principles of the techniques and analytical approaches used in the Chapters which follow. This also includes a comprehensive

literature review of the current state of the existing technologies and capabilities. Chapter 2 is placed as a methodology Chapter which details the various instrumentation, methods and experimental approaches used in the thesis Chapters which followed. Here a combination of relevant theoretical and instrumental approaches allowed preliminary validation studies conducted using the GC–FTIR system. Chapter 3 builds upon the capabilities of the GC–FTIR technique to analyse various compound classes and highlights the uniqueness of FTIR spectra. A feature here was the comprehensive style presentation of GC×FTIR which enabled a simultaneous spectroscopic/separation visualisation of data. This Chapter reiterates the capabilities of GC–FTIR and its value to component identification. Chapter 4 employs the accurate identification capabilities of FTIR spectra in the specific task of identifying oxime isomers which undergo dynamic on-column isomerisation on GC columns. Chapter 5 applies the techniques of two premier technologies – specifically high-resolution MS and comprehensive two-dimensional GC (GC×GC) – to study and attempt to give molecular speciation to aviation fuels which have undergone accelerated thermal stress.

During various stages of this Thesis one of the main limitations has been the low sensitivity of the light-pipe GC–FTIR system, as highlighted in Chapter 1, to enable analysis of samples as complex as the aviation fuels. The inability to successfully conduct EICs on the fuel samples in Chapter 5 came as a surprising result and it would have been ideal to vary chromatographic parameters and reanalyse the samples. Unfortunately, the samples could not be immediately reanalysed due to the breakdown of the TOF MS instrument during the devastating School of Chemistry flood and the Covid-19 pandemic, and the inability to have it repaired during this time as a result of the pandemic's effect.

As demonstrated in the various Chapters, FTIR possesses a ‘molecular fingerprinting’ ability owing to its unique spectrum. This and other molecular spectroscopic detection techniques constitute an important part of supporting varying levels of molecular identification to GC separated constituents. Apart from those that directly depend on molecular emission from specific elemental constituents of a sample (FPD, SCD, NCD), the role of spectroscopy imparts important qualitative as well as quantitative analysis. Both spectroscopic and MS detection rely on the information derived from their respective ‘spectrum’ which may impart

information to either the molecular electronic absorption pattern of the species, or the structural features of the molecule (carbon-proton bond moieties, functional groups, bond connectivity, bond fragmentation, bond vibrations). However, apart from extensive MS libraries, other techniques have limited GC database records. Of the various MS approaches tandem mass spectrometry (MS/MS or MS²), where two or more mass analysers are combined, enable robust large-scale analysis capabilities and offer specificity with hopefully a very good identification with precursor/product matching; this makes it a common go-to tool for drug testing and metabolomics.

These spectroscopic and spectrometric approaches converge at the analyst's hands to provide to a greater or lesser extent, an insight into the molecule's structure, and so contributes to its identification.

6.2 Future prospects

Both, the advantages of the techniques used in this thesis as well as the limitations they pose, point towards topics to be addressed in the future as well as recommendations associated with the respective techniques.

Advances and future prospects in mass spectrometry

The shortcomings in identification capabilities of single quadrupole MS hyphenated to the GC can be overcome by modern high-resolution MS methods or combinations of various MS techniques such as MS/MS to accomplish a higher level of identification. Developments in vital software tools, data processing, data interpretation methods and visualisation means are proposed to address the growing size and complexity of data generated by ultrahigh resolution instruments. This continues to open newer avenues to analyse complex matrices such as petroleum-related samples. Here, ultra-high resolution achieved by Orbitrap and Fourier transform ion cyclotron resonance MS continue to allow for record levels of

compositional details to a wide variety of “omics” fields such as petroleomics, metabolomics, transcriptomics, proteomics, lipidomics etc. Such high-resolution MS techniques can benefit from the hyphenation to separation approaches such as liquid chromatography or GC.

Advances and future prospects in gas chromatography

Similar to MS, GC can achieve additional high-resolution analysis success as a stand-alone technique mainly due to the various advances in GC separation methodologies. Here, multidimensional GC techniques have evolved over the decades to achieve enhanced capabilities that significantly eclipse 1DGC. Of these GC×GC has emerged as an accessible tool, and when hyphenated to multichannel detectors can separate, detect and ‘tentatively identify’ thousands of analytes. With the correct choice of the best stationary phase and column set to achieve the selectivity required to suit the sample, as well as powerful data interpretation tools such as chemometrics, the applications base of GC×GC will continue to expand. Something that has not been sufficiently explored is the role of correlation of structure with retention in GC×GC which would be a recommendation for future study. With the popularity of GC×GC increasing in R&D ventures, such structure-retention predictions may enable more absolute identification.

Modern GC based methods continue to see new developments in software, column stationary phases, and various components of its instrumentation. MS will continue to be a dominant technology for GC, and with increased access to accurate mass MS, opportunities for precise empirical formula deduction is of great qualitative and quantitative assistance. Although olfactometry detection cannot be defined in the classical spectroscopic instrumental sense, its hyphenation to GC provides characterisation of a molecule’s odour activity, which is a function of molecular structure. With its complex, selective and variable performance, linking this to an MS creates an apt tool to detect low levels of odour active compounds. In the same vein, electroantennography detection (EAD), which uses the response of e.g. insect receptors towards specific compounds, find considerable application in molecular characterisation using GC–EAD. Modifications in GC instrument configurations to

accommodate two or more column stationary phases which can offer resolution of a variety of component polarities could be undertaken.

Advances and future prospects in Fourier transform infrared spectroscopy

As analysts who strive to render an accurate molecular identification to compounds, the complementary power of MS and information rich spectroscopic detectors cannot be overlooked. However, if FTIR is to be a more accepted technique in the future reliable and simplified interfacing which provide sufficient sensitivity must be addressed. Here, interfaces which enable direct deposition of GC effluent on a cryogenically-cooled ZnSe disk, such as that seen in the GC-FTIR instrument by Dani Instruments™, allows for acquisition of solid-phase FTIR spectra which feature sharper bands than gas phase spectra acquired in light-pipe GC-FTIR systems. The higher sensitivity advantages of such direct-deposition interfaces find applications in fields such as Forensics and R&D in which exact identification of substances, afforded by techniques such as FTIR, is crucial.

It is unlikely that NMR will be more than a curiosity, unless again the interface and analyte detectability are addressed. Off-line prep-scale NMR with GC is a much more accepted approach, and should be further promoted. Of the spectroscopic techniques, the emerging GC-VUV technique seems to offer a truly 'disruptive' technology as a universal platform offering a sensitive, quantitative, qualitative method, which further research continues to most surely extend and confirm, with the reported ease of set-up an important feature. Further, with the development of computational approaches and simulations a deeper molecular level understanding can be achieved. Such molecular modelling will enable improved correlation of simulation with experiment whilst predicting theoretical and practical insights into the identification and behaviour of molecules. With the uniqueness of spectra offered by spectroscopic techniques, more complete database availability will no doubt be of great value.

Advanced techniques will always be more challenging to implement and optimise compared to their conventional counterparts. But newer technologies will surely continue to enter the

arena of GC and endeavour to extend its capabilities, whilst MS and spectroscopic detectors will be a driving force in the greater aspiration of reliable detection. The outcomes of this thesis thus contributes to render a practical insight in to the various reliable and advanced technologies used to achieve the ultimate goal of unambiguous chemical component identification.

Appendix A – Published article from which Chapter 1 excerpts are obtained

Trends in Analytical Chemistry 99 (2018) 47–65



Contents lists available at ScienceDirect

Trends in Analytical Chemistry

journal homepage: www.elsevier.com/locate/trac

Molecular spectroscopy – Information rich detection for gas chromatography



J. Shezmin Zavahir, Yada Nolvachai, Philip J. Marriott*

Australian Centre for Research on Separation Science, School of Chemistry, Monash University, Wellington Road, Clayton, VIC 3800, Melbourne, Australia

ARTICLE INFO

Article history:
Available online 1 December 2017

Keywords:
VUV detection
FTIR detection
Mass spectrometry detection
FPD detection
NMR detection
Chemiluminescence detection
UV detection
Gas chromatography
MDGC
Hyphenation

ABSTRACT

Molecular spectroscopic detection plays a crucial role in gas chromatography (GC). Some detectors constitute element-selective spectroscopy, where an element-containing species generates the detected signal, e.g. flame photometric detection (S, P, Cu); chemiluminescence detection (S, N). These respond with selective response, usually with excellent analyte detectability and reduced matrix interferences. Classical molecular spectroscopic detectors – Fourier transform infrared, nuclear magnetic resonance, ultraviolet – respond by giving a spectrum characteristic of the (intact) molecule. Molecular structure response plays multi-faceted roles: it produces a unique spectrum of a molecule, provided it is resolved by the column and presented to the detector as a single compound; or the chromatogram can be generated by responding to the total signal, or selectively to a given component of the signal. This review summarises the response, sensitivities, applicability, and recent literature reports of molecular spectroscopic detection. Hyphenation with dual detection and brief comments on multidimensional GC is included.

© 2017 Elsevier B.V. All rights reserved.

1. Introduction

Gas chromatography (GC) has proven to be an invaluable technique in the analytical separation of inorganic or organic volatile compounds, in which gaseous analytes of a sample are transported through a column (today, normally a capillary column) by a carrier gas (the mobile phase). It has become an important tool in diverse applications in an extraordinarily wide range of fields. Its advantages over most other techniques for monitoring volatile chemicals are its high analyte detectability, linear range, exceptional resolving power, relatively good precision, fast analysis, and comparatively low cost. Excellent separation accompanies simultaneous qualitative and/or quantitative information of separated compounds, thus making reliable, efficient and sensitive detection, potentially with identification, possible.

1.1. Comments on detection criteria

A GC detector can be any physical technique which has the ability to be hyphenated with GC experiments, and which offers on-line or quasi-on-line dynamic response to compounds being analysed. This enables exploitation of the advantages of both the GC

separation and the physical process constituting the detection method. The ability of the detector's response to reproduce a compound's elution profile is paramount. Several features may characterise an ideal detector. The foremost of these is a detectability sufficient to yield a signal at the desired concentration level for the component(s) in a sample. Analyte detectabilities may be in the range of 10^{-8} – 10^{-15} g of solute per s. Based upon their response characteristics, chromatographic detectors may be classified as mass sensitive or concentration sensitive. Whilst mass sensitive detectors often are destructive towards the compounds of the sample and respond to changes in mass per unit time (g/s), the latter tend to be non-destructive and respond to changes in mass per unit volume (g/mL). When choosing a detector its analyte detectability – sometimes referred to in literature as 'sensitivity' – (response per unit mass or concentration of sample [1]) vs selectivity (normally, the ability to distinguish a certain functional group or element within the molecule or matrix without interferences from other components [2]) is to be considered. Although it may be desirable that the response factor (a measure of the response of a detector per mass of compound) of the detector should be similar for all analytes, it is not a pre-requisite for effective detection. Furthermore, stability, ease of use, predictability and reliability are also favoured properties when selecting appropriate detectors [3]. GC detectors can also be categorised based on the mechanism by which they respond to analytes; universal detectors theoretically

* Corresponding author. Fax: +61 3 99058501.
E-mail address: Philip.Marriott@monash.edu (P.J. Marriott).

should detect all solutes, whilst selective detectors respond to only a particular class of compounds – usually according to some heteroelement (i.e. neither carbon, nor hydrogen) in the compound. In addition to the most important feature of producing a good signal, the three factors – noise, time constant and cell volume – also play a role in a detector's efficacy.

Since the invention of the first GC detector in the 1950s [4], a broad range of detectors with varied selectivity and function have been introduced [5]. Apart from a few examples, there has been little revolutionary innovation in detection in GC in the past five years. However, continual incremental improvements in detector designs occur, such as miniaturisation, modifications to detection cell volume, and microelectronics in data control, acquisition and storage, as well as data display and analysis [6]. Higher flow rate (e.g. with make-up gas) may have the effect of dilution or reduced detectability. Despite improvements made in analytical GC instrumentation, complex sample analysis still remains a hurdle, and steps to simplify the sample by pre-treatment to deliver discrete fractions of the sample to the instrument may be advised, where whole sample introduction proves too difficult a separation task [7]. Selective detection may be considered one way to simplify a total sample response; sample preparation may be targeted to suit the detector used.

1.2. Comments on multidimensional gas chromatography

Inadequate chromatographic separation, which may result when a single column (one dimensional; 1D GC) is used, may be overcome by multidimensional GC (MDGC), which also effectively delivers fewer overlapping compounds to the detector. MDGC conventionally employs (at least) two columns of different selectivity (different stationary phases) [8], connected sequentially via a sampling device positioned between the two columns. The two approaches of MDGC are (i) the conventional heart-cut (H/C) method of subjecting a target portion of the first column to the second, or (ii) comprehensive two-dimensional GC ($GC \times GC$) where the entire sample is subjected to two column separation, according to the criteria Giddings espoused [9]. A well-detailed series of reviews by Adahchour *et al.* delves into the significance as well as the various instrumental, developmental and application aspects of $GC \times GC$ [10–13]. A figure included in Section 8 (see later, Fig. 6) illustrates various options from 1D GC to MDGC arrangements. MDGC has greater resolving power and may improve detection limits, removing underlying chemical interferences, with larger analyte peak capacity than 1D GC [14,15]. The development of new hardware such as micro-fluidic switches [16] and cryogenic modulators render MDGC distinct advantages over 1D GC towards both quantitative and qualitative analysis [17]. MDGC has been used in conjunction with a variety of detectors in many applications, generally with excellent quantitative and qualitative results [18,19].

1.3. Comments on data handling

The analysis of chromatographic detection results is continually improving with the development of various software to suit the detection method and criteria. Conversion of the analog signal originating from the detector to a computer-compatible digital signal, enables convenient data handling by the analyst [20]. Digitised time and signal magnitude are generated by sampling the detector output at the required frequency (data points per s). The rate of data acquisition of chromatographic data affects precision of factors such as peak retention times, area repeatability, peak resolution of closely eluting compounds, etc. [21]. In the move to faster GC analysis, detector acquisition rate is a critical need. Very 'fast' GC

peaks may have a width at half peak height of <0.5 s, so an acquisition rate of about 50 Hz is appropriate for adequate quantitative analysis. However, influencing factors such as detector electronics and extended path length flow cells or larger internal volume of some detectors may not be suited to such speed. Treating large quantities of data thus generated by complex matrices, benefit greatly from the use of chemometric techniques [22]. Use of multivariate data analysis in both 1D GC and MDGC can provide information otherwise inaccessible [23]. The problem of deconvolution of co-eluting peaks can be solved by dedicated software which deconvolute spectra results to render better identification of compounds [24].

Data presentation of both 1D and MDGC methods rely on the fundamental property of retention time, which may be transformed to retention index data (*I*) [25], and peak detection – the ability to distinguish an analyte signal from the background noise and other analyte signals [18]. Where confirmation of molecular structure based on spectroscopic detection is required, it is preferable that the molecule be detected as a unique species in the detector. This requires either adequate separation from other matrix material (best achieved with MDGC), or an effective deconvolution procedure which is able to spectroscopically isolate just the response of the target molecule.

1.4. Comments on mass measurement molecular ionisation detection

Over the years, ionisation detectors – those which detect gas phase ionised molecules – have been used widely in GC and their detailed structure, modes and principles have been previously reviewed [19,26,27]. The mass spectrometer (MS) is the most widely adopted ionisation detector in GC capable of giving molecular information. It is not the purpose of this review to revisit this area at length, since MS is a spectrometric technique rather than spectroscopic. However since it provides molecular structure information, and is proposed as the 'gold standard' detector to support identification as well as provides a benchmark in universal detection, comment on MS must be made here. Over 85% of GC analyses [28] are or can be carried out using an MS, giving reliable qualitative and quantitative analysis. It is one of the most powerful tools for identification of chemical components, based on m/z ratios of analytes and their fragment ions. Of all 'molecular structural' detectors, MS – despite the complexity and the management and maintenance requirements of its instrumentation [29] – is readily hyphenated with the GC experiment by simply attaching the column to the MS interface. It gives a very high 'production rate' of valuable information enhanced by the availability of sophisticated and comprehensive databases with well-developed strategies for comparison of spectra. The detection limit of this technique is about 0.25 pg [14]. Since the inception of GC hyphenated with MS (GC–MS) in the 1950s [30], this technique has become one of the most information-rich tools for volatile chemical analysis; it is normally applied by using electron ionisation (EI) [chemical ionisation (CI) is used less frequently] at vacuum, with MS conditions usually based on a standard 70 eV ionisation energy. Standard database libraries have >240,000 spectra, plus a collection of specialist libraries related to specific applications; library spectrum entries are relatively independent of instrumental design [14,31,32]. However for compound identification, a GC–MS spectrum alone may be insufficient for adequate characterisation, especially for untargeted analysis in complex matrix samples, primarily due to the similarity of spectra for closely related compounds. Assignment of molecular identity to peaks in GC–MS may lead to erroneous results, especially if authentic standards are not available to compare exact retentions and confirm mass spectra.

Various aspects of chemical identification using MS and chromatography have been amply expounded by Milman [33–35]. Multi-dimensional MS (MS/MS) can be performed in order to improve selectivity and also signal-to-noise (S/N) ratio. This approach involves further fragmentation of the primary ion(s) and selective monitoring of product ions by using different MS scanning routines, such as triple quadrupole (QqQ) or quadrupole time-of-flight (qTOF) with MS/MS capability, or with MSⁿ capability by using an ion trap MS (ITMS). Xian *et al.* reviewed recent advances in high resolution mass spectrometric (HRMS) approaches [36]. Although limited by the (currently) reduced size of their databases [24], mass spectrum deconvolution software plays a further role in identification of co-eluting peaks. Recent advances in MS includes application of GC × GC–TOFMS for non-target compound analysis in saffron [37], food safety and quality analysis using MS [38], GC × GC with soft and hard ionisation TOFMS in environmental analysis [39], use of QqTOF and QqQ-MS/MS for nutraceuticals analysis [40], multiple reaction monitoring (MRM) analysis with GC × GC–QqQMS for essential oil analysis [41] and the combination of MS/MS and exact mass analysis in shale oil analysis [42]. Such methods allow high confidence in compound analysis based on ¹I, ²I retention index values, accurate mass MS, and MS fingerprint data.

Although hyphenation with MS provides useful information such as specific *m/z* of precursor/product ions of analytes, it has limitations in differentiating isomers or compounds with very similar fragmentation patterns, and analysing labile and low mass compounds. MS may fail to provide absolute identification of compounds, which may further demand functional group identification, proton structural environment, electronic transitions or 3D structures. This emphasises the need for detectors which may provide alternate or complementary information to MS. The hyphenation of spectroscopic detectors may thus offer atomic and molecular information which can very often complement information derived from other sources, for improved compound identification.

1.5. Comments on spectroscopy

Spectroscopy may be broadly defined as the study of the interactions between electromagnetic radiation and matter. Whilst

atomic spectroscopy relates mainly to transitions which take place when changes to atomic electronic configurations occur, molecular spectroscopy considers the energy states corresponding to nuclei vibrations and rotations within a molecule, or molecular electronic transitions. The energy of a molecule, according to the Born-Oppenheimer approximation, is given as the sum of electronic energy (*E*_{el}), vibrational energy (*E*_{vib}) and rotational energy (*E*_{rot}).

$$E = E_{el} + E_{vib} + E_{rot}$$

It is this energy change which takes place by the absorption, emission, resonance or scattering by functional groups, bonds, vibrations, or atoms within the molecules that leads to specific patterns in the molecular spectroscopy spectrum. The absorbance-based methods within the electromagnetic spectrum rely on the ratio of radiation power measurements; one before a beam has passed through an analyte medium (*P*₀) and the other after (*P*), leading to transmittance (*T*) and absorbance (*A*) measurements, which are related by the relationship $A = -\log T$ and $T = \log P_0/P$. For monochromatic radiation, absorbance follows the Beer-Lambert law; $A \propto c$, where *c* = the absorbing species concentration. Also $A = \epsilon cL$, where *L* = path length through the sample, whose molar absorptivity (referred to as *extinction coefficient* in older literature [43]) = ϵ .

Thus, molecular spectroscopy, with its potential complexity, provides useful information on molecular properties. For instance, the relatively simple UV–vis band spectrum of molecules with low resolution spectrometers, contrasts with the infrared spectrum with its high degree of detail of the very same molecule. Needless to say, the MS offers a further contrast to these spectroscopies, and dual detection where MS occupies one detection dimension is of obvious interest. Molecular spectroscopy offers information quite distinct to MS, and is of importance in chromatographic analysis in order to improve compound identification, and to further understand the chemical construction of compounds eluted from the column, leading to the development of hyphenation with spectroscopic detectors in GC.

Based on the above interaction between matter, energy and hyphenation with different operations in GC, molecular spectroscopic detectors can be classified as shown in Fig. 1.

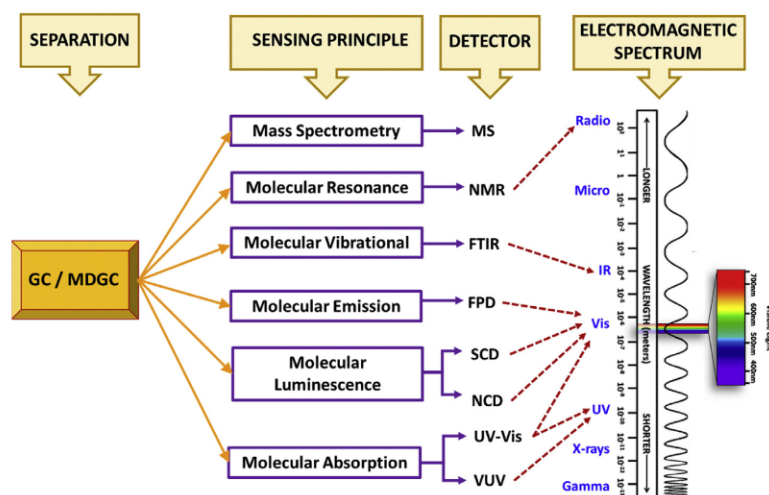


Fig. 1. Diagram illustrating different hyphenations with spectroscopic detectors in GC and MDGC (MDGC is intended to also imply GC × GC where applicable).

Depending on need, GC detectors can be chosen for detection of either atomic or molecular species. Although spectroscopic detectors in GC have been reviewed previously [44,45], there has been a dearth of recent reviews. GC detectors based on atomic spectroscopy provide atomic or elemental selective detection. Of these, the atomic emission detector (AED), a highly selective detector based on atomic emission, is the most prominent and widely hyphenated atomic detector to GC (GC–AED); it has been the focus of many reviews and chapters [46–49]. Atomic spectrometric detectors for GC, including the GC–AED, were reviewed by Li *et al.*, in 2016 covering theory, operational characteristics, analytical performance and practical applications [3]. In contrast the scope of this review is to present a broad view of the various molecular spectroscopic detectors used in GC, and highlight a few emerging detectors in this area. Although the AED is not a ‘molecular spectroscopic’ detector, it will not be discussed in detail in this review, however, reference and comparison to the AED will be made where applicable when element-selective detection is discussed. Due to superior detection limits, many available standard protocols, and widely established databases, MS technologies have overwhelmed less popular molecular spectroscopic methods, for hyphenation with GC. But the latter have their specific niche applications, and need to be considered.

2. GC–Fourier transform infrared spectroscopy (GC–FTIR)

Perhaps 30+ years ago, FTIR had surprisingly quite a few devotees. Personal enquiry suggests that method difficulties, poor reliability, and lack of support for system maintenance and upgrades saw many abandon the technique. With its ability to provide a wealth of molecular vibrational (and fine-structure) information, related to molecular functionalities and structures, FTIR spectroscopy is recognised as a detector which can be a universal and yet molecular qualitative detection method, providing complementary information to mass-based ionisation detectors in GC. The absorption of infrared radiation leads to molecular vibrations within molecules. Due to the varied bond lengths and strengths between atoms in a molecule, the frequency of radiation absorption varies with molecular bonds and vibration modes. Since IR absorbances are very specific to stretches/wagging/rocking etc. vibrations of molecules, the IR signal fingerprint can be directly predicted based on quantum chemistry. The prediction is especially useful when approximate confirmation of functional groups, isomer structures or closely related structures of a compound is required [50]. This further extends to the use of FTIR to differentiate geometric (*cis/trans* or *E/Z*) isomers [51]. The unique spectrum obtained for each molecule also encapsulates information from the intact molecule, as opposed to molecular fragments seen in MS. Common FTIR spectrometers consist of an infrared source, an interferometer, sample compartment, detector, amplifier and a computer for Fourier transformation. The hyphenated GC–FTIR instrument ‘simply’ requires replacement of the sample compartment, and design of the light source/detector arrangement. The mercury cadmium telluride (MCT) detector, the most used detector in GC–FTIR instrumentation, allows rapid data acquisition. Various reviews have explored GC–FTIR as a source of spectroscopic detection [52,53]. Why did FTIR lose most of its allure? The emergence of MS, with its many options, keen marketing, reliability, plethora of available methods, and immediate access to a ‘molecular answer’ has a powerful reinforcement effect in GC–MS. The FTIR, by contrast, which generally is more difficult to maintain, has a lower detectability for analytes [54]. With FTIR’s main attribute being its molecular selectivity and identification – which is more-or-less also provided by MS – consigning FTIR to a historical curiosity might be understood. It is necessary to directly confront this perception.

2.1. Development of GC–FTIR hyphenation

GC–IR was introduced in the 1960s [55], initially using packed columns. The 1980s saw approaches to hyphenate capillary column GC with spectroscopic methods for molecular detection, to improve analytical identification [56,57].

FTIR spectrophotometers are more sensitive compared to dispersion type instruments. Improved interfaces between GC and FTIR allow for simpler hyphenation, whilst the interface should retain GC resolution as well as improve interaction of the IR beam with eluted analytes. Such interfacing enables GC effluent detection by either an on-line approach using flow-through cells, or quasi-on-line methods where the effluent is concentrated and immobilised on a trapping medium [58]. Four main interface types are available for GC–FTIR [59].

The light-pipe interface is most commonly used [58]; GC effluent passes into the light-pipe through which IR radiation transmits, for collection of gas phase spectra. Introduced in 1964 [60], and re-designed by Azaragga [61], a heated gas phase IR flow cell with high reflectivity gold-coated internal surface and IR-transparent windows at either end facilitate reflection of the IR beam through the cell. The flow-through design offers real-time analysis, which other interface types may not. Although common, the light-pipe is least sensitive (ng range).

In matrix isolation-FTIR (MI-FTIR), GC effluent in a matrix of cold inert gas (argon) is directed under vacuum for cryogenic trapping onto the surface of a gold-plated collection disc. Trapped analytes undergo interrogation via an IR beam. Costly and complex, MI-FTIR provides high sensitivities, and low detection limits to 100s of pg [62], a sensitivity comparable to some MS methods. Low temperature trapping in GC–MI-FTIR renders sharp and narrow IR peaks due to minimal thermal band broadening.

Direct-deposition (DD) FTIR positions an IR microscope very close to the deposition site of GC analytes. Effluent is directed *in vacuo* onto a cooled (liquid N₂) moving infrared substrate (ZnSe). With high sensitivity and a lower detection limit than the light-pipe design, DD can detect at sub-ng levels of analyte with no pre-concentration. In a study of FAMES, DD-FTIR had better capacity than the light-pipe to characterise complex mixtures of variable concentration [63].

Both matrix isolation and cryotrapping (Xe matrix gas; liquid N₂ coolant) [64] in a cryotrapping-matrix isolation GC–FTIR interface study reported sub-ng detection limits. Detectability is improved by using a longer light-pipe; this can reduce GC resolution. Design compromises analyte detectability and resolution, with purging He or N₂ gas to tune IR sensitivity and GC resolution. The I.D. and length of the cell are typically 0.3–1.0 mm and 50–100 mm, respectively, and so is compatible with the average peak volume from GC capillaries [65]. Fig. 2 represents a GC–FTIR setup with various interface types indicated.

GC–FTIR scanning is generally carried out over 4000–600 cm^{−1}; a background scan may precede the sample scan. Derivatisation of compounds benefits FTIR detection by either improving the detectability by an increased IR response [66], or by enabling identification of compounds inaccurately identified by MS [67]. GC–FTIR enables the unambiguous structural elucidation of structures as well as confirmation of an unknown based on spectroscopic identification and chromatographic retention time (*t_R*). Retention index (*I*) data in GC or MDGC allows a preliminary screen of possible compound identity. FTIR allows functional group analysis to detect hydroxyl, aromatic, aliphatic, amine, nitrile etc. groups [68], since each functional group has a characteristic vibrational absorption, which can be used for qualitative, or quantitative purposes. GC–FTIR spectra can be searched against available reference spectra in digital spectral database libraries for

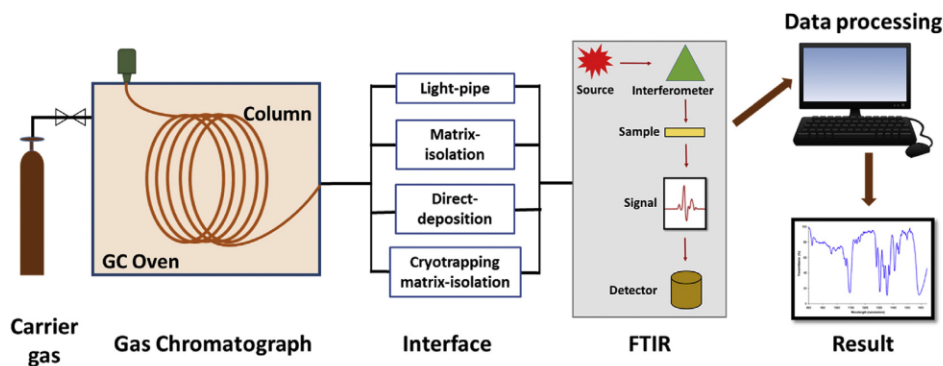


Fig. 2. Schematic diagram illustrating the GC–FTIR set up with various interfaces and data processing.

individualised identity of a compound, and potentially class identity [69]. Since homologues show similar, but not identical, IR spectra, library searches of unknown compounds will often match the homologue, which may assist structural elucidation. The development of a two-dimensional separation approach, defined as GC \times FTIR, was presented with GC capillary column separation as the first dimension and spectroscopic separation as the second dimension in the analysis of a C₂-naphthalene isomeric mixture [70]. Unambiguous elucidation of structures in unknown substances thus calls for spectroscopic tools, such as FTIR, to complement MS.

2.2. Applications of GC–FTIR

With one of GC–FTIR's successes residing in its ability to differentiate between geometric isomers, it finds application as a complementary method to GC–MS [58,71] with applications covering several disciplines as outlined below.

As novel substances increasingly appear in psychoactive substances and illegal drugs, there is a need to identify substances whose isomers very often have different biological activities. GC–FTIR complements GC–MS detection for structural elucidation of designer drug studies [72]. The sensitivity of FTIR spectra towards even minor changes in a molecule's structure to provide “fingerprinting” of molecules, is an asset in forensic and clinical studies [73]. An expert system built using artificial neural networks dedicated to identification of amphetamines, confirms the efficiency and relevancy of GC–FTIR-based systems over GC–MS for modelling classes of compounds [52].

Increasing awareness in food and dietary supplement adulteration calls for methods to be developed for proper identification and quantification of isomers showing biological activity; the power of FTIR to differentiate structural isomers is especially of use in food adulteration studies [53]. Target components include geometric isomers in complex mixtures such as fatty acid methyl esters, essential oils, edible fats and oils. The *cis/trans* geometry of double bonds in the natural oil conjugated linoleic acid, often used in dietary supplements, was confirmed in GC–FTIR by differentiation in the 3000 cm^{−1} region of the spectrum [74] as seen in Fig. 3.

In comparing GC–MS and GC–FTIR for clary sage oil volatiles, an MS search proposed a component at *t_R* = 49.19 min as nerol (96% probability) or geranyl acetate (91% probability). The presence of two strong bands at 1700 and 1200 cm^{−1} in the FTIR spectrum identified the compound as geranyl acetate with a 98% probability library match [75]. Interfacing FTIR to MDGC systems incorporating cryogenic trapping was introduced in the early 1990s [76]. This can be used for qualitative analysis of complex mixtures [77]. The large

amount of data produced in a single GC–FTIR run calls for appropriate hard and software. High scan speeds of 1–10 scans per second suffice this need [78].

Quantitative analysis of GC–FTIR can be obtained by one of four methods; chromatographic peak height, chromatographic peak area, absorbance value of the spectral peak or integrated area of spectral peak [78]. Analyte detectability can be increased with techniques such as large volume injections and solid phase extraction [79]. LODs of 0.1–1 µg/L were achieved using pre-selected wave number regions (2820–2980 cm^{−1}, 1640–1670 cm^{−1}, 1520–1580 cm^{−1} and 1000–1050 cm^{−1}) in a study to determine micro-contaminants in water [80]. Further identification and/or quantification applications of GC–FTIR include the structural elucidation of natural saccharides [81], marine origin complexes [82], toxicological compounds [83], insect pheromones [84], pinene degradation studies [85], pharmaceutical analysis [86], isomeric studies on drugs of abuse [87], chemical weapons convention analyses [66], characterisation of petroleum hydrocarbon [88], compound identification in fentanyl metabolites [89] and essential oil adulteration studies [90].

3. GC–nuclear magnetic resonance (GC–NMR)

Amongst all spectroscopic tools, nuclear magnetic resonance (NMR) is considered to have the highest capability of distinguishing diastereomers and enantiomers (constitutional and configurational isomers; enantiomers when shift reagents are used). Upon absorbing radio frequency energy, electrons around nuclei create strong and homogenous magnetic fields. The resulting characteristic chemical shifts provide information on the dynamics, reaction states, chemical environments and structure of molecules [1]. NMR is therefore an information rich tool for assigning structures based on molecular connectivity, for the arrangement of carbons and protons in a molecule. Off-line NMR is relatively widely reported for GC separations, usually for preparative scale collection where individual resolved compounds are separately collected for transfer to NMR [91,92]. Depending on the amount of material collected, a variety of NMR techniques can be employed for characterisation purposes, including ¹H, ¹³C, and multidimensional NMR methods; this is the primary reason for developing a strategy with supporting NMR information, in order to confirm the structure of a compound. Of all spectroscopic methods, it provides a most robust interpretation of the entire spectrum [93] also by which the three-dimensional molecular structure of a molecule may be determined. Absorption of electromagnetic radiation is measured in the 4–900 MHz radio-frequency region. The most useful isotopes used in NMR are those with a spin value of *I* = 1/2. This is most

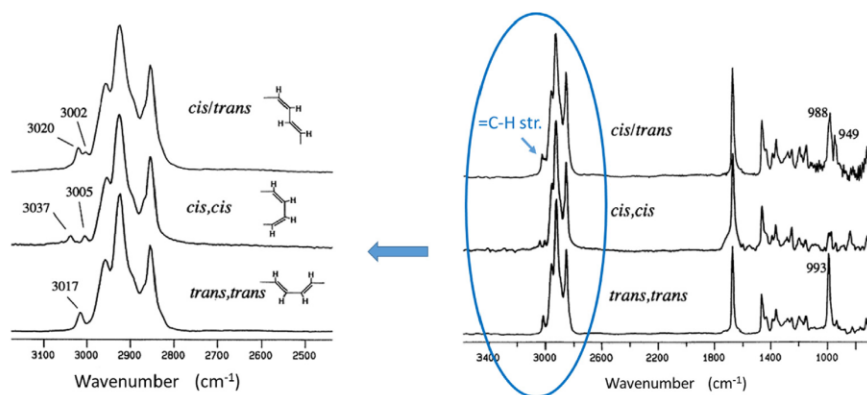


Fig. 3. GC-DE-FTIR spectra observed at 8 cm^{-1} resolution discriminates between CLA geometric isomers as shown for DMOX derivatives. Adapted from Ref. [74] with permission.

commonly seen for the relevant element isotopes ^1H , ^{13}C , ^{19}F , and ^{31}P , thus enabling the analysis of many compounds in organic chemistry, and of relevance to gas chromatography.

Hyphenating GC to capillary NMR gives the best spectroscopic elucidation of structures of unknown compounds [94]. This is outlined in a recent review of capillary NMR detection in separation science, seen largely as most relevant to liquid chromatography (LC-NMR), but with comment on CE-NMR and GC-NMR [69,95].

3.1. Development of GC-NMR hyphenation

The LC-NMR hyphenation finds significant application in many fields [96,97]. Although initially reported in the 1960s [98], on-line coupling of GC to NMR has been much more problematic as continuous recording of NMR spectra was not possible. Sample handling difficulties and low signal-to-noise (S/N) ratio of spectra at atmospheric pressure delayed development of this technique [95].

Development of high-field NMR magnets partly overcomes the hurdle of poor S/N in NMR [99], along with hyperpolarisation methods [100] and spectrum processing [101] techniques. Analyte detectability of NMR is significantly poorer compared to MS and IR methods, and implementation is considerably more technically demanding since the NMR flow cell must be located in a strong magnetic field. Detectability, chromatographic resolution and spectrum resolution depend on the optimum flow rate, aided by recent developments in flow cell design [102]. Most knowledge in this area comes from developments in LC-NMR, rather than GC-NMR. Continuous-flow NMR micro-coil probe developments support improved LODs [95]. Technical design improvement in magnet and cryogenic probe technology improve analyte detectability [103,104]. Both probe design and optimum flow rate must be balanced to achieve best resolution and intensity. Advances in and uses of micro-coil capillary flow probe NMR spectroscopy in relation to GC have been recently reviewed [105,106].

3.2. Applications of GC-NMR

Molecular stereo-chemical interpretation from GC-NMR provides complementary information to MS [107–110]. Capillary-NMR was first used for structure analysis in 2007/8 for volatile model compounds dichloromethane, tetrahydrofuran, acetone, and diethyl ether, using continuous-flow solenoid micro-coil ^1H NMR measurements at 400 Hz [102], and for separation of stereoisomers and enantiomers of *cis*- and *trans*-1,2-dimethylcyclohexane [101] as well as investigations using enantioselective GC separation of

racemic 2,4-dimethylhexane whose enantiomers showed identical NMR spectra but different retention times [111].

Application of off-line NMR analysis of microscale capillary-preparative MDGC, with multiple sample injections and repeat collection of a single compound provides both high resolution, and increased amounts for the identification of volatile compounds [91]. Geraniol was resolved from co-eluting compounds in this study, followed by a study of 1- and 2-methylnaphthalenes in crude oil (at natural abundance of ca. 0.2%) [92]. In the latter case, the use of an internal standard, dimethoxybenzene, gives a simple NMR spectrum, and provides comparative quantitative knowledge about the compounds to be collected in the prep-capillary experiment. Spectrum resolution and proton connectivities in NMR can be enhanced by 2D NMR methods [68], and in all cases increased acquisition time improved S/N levels [112]. In one report [113], polyaromatic catalyst products which had equivalent mass spectra, were analysed by capillary GC collection and off-line ^1H NMR, and spectrum similarities were found amongst the different products for the reactions conducted. In some cases crystals were grown after the prep-scale capillary GC collection, completing X-ray structural analysis.

NMR spectroscopy shows a relatively poorer analyte detectability and higher limits of detection in comparison to other spectroscopic detection techniques [95]. NMR spectroscopists traditionally refer to the sensitivity (or analyte detectability) as the S/N for a given analyte concentration, or concentration sensitivity (S_c). This largely depends on the active detection volume of the probe [114]. Detection limits in the low-nanogram range have been provided by modern solenoidal microprobes [102]. A 2009 review outlines an increase of analyte detectability in successful GC-NMR experiments using a system containing a microprobe with a detection volume of approximately 200 μL . Here LODs were reduced to 200 μg from 3 mg as seen in previous attempts [95]. Thus, good data in modern NMR instruments could be obtained from relatively small sample quantities, although the amounts are still considerably in excess of those needed for MS and other spectroscopic detectors, both in off-line and on-line methods, and at a significant cost in experimental effort. The greatest advantages of NMR as a GC detector lies in its structural elucidation possibilities; its non-destructive nature is also useful, although its routine on-line hyphenation is unlikely in the near future.

4. Visible and ultra-violet absorption based detectors

Absorption spectroscopy in the visible and UV region is a valuable quantitative tool for molecular analysis, although lacking

detailed structural elucidation. The UV–vis detector, which obeys the Beer–Lambert law for absorbance, is much more commonly employed in liquid chromatography (LC) methods, but also offers useful possibilities in GC, both qualitative and quantitative.

Passing polychromatic UV or vis radiation through a medium causes bonding electrons to be excited, enabling correlation of absorption bands to bonds of the molecules it passes through, leading to molecular absorption. Functional groups have different absorptivities, so produce different sensitivities, and also different absorption maxima. Therefore the wavelength is tuned to the absorption bands needed to suit the compound of interest's molecular structure. Being broad band absorptions, there is limited scope for structural identification by use of UV–vis spectra.

In recent times the UV–vis region and the vacuum UV (VUV) regions of the electromagnetic spectrum have been used to develop absorption based instrumentation for GC detection, to measure substances based on absorption spectra of light in the gas/vapour phase. They are non-destructive towards analytes, making sequential detection possible *e.g.* VUV/MS.

4.1. Gas chromatography–ultraviolet-visible spectroscopy

The UV and visible regions span 10–400 nm and 400–700 nm regions respectively. This section on UV will exclude the VUV region. UV–vis spectroscopy is a routine analytical tool for many organic, inorganic and biological species, and a commonly used technique for quantitative analysis in environmental, chemical and forensic laboratories [68]. Since absorption maxima and molar absorptivities vary among different components, concentration cannot be determined by peak response alone. Rather than fixed wavelength detection, a variable wavelength, diode-array type detector is most useful, to allow a time program to be used to measure each component at their maximum absorption wavelengths. As with GC–FTIR and GC–MS, gas chromatography–ultraviolet detection (GC–UV) falls into the same category of full scan analysis.

4.1.1. Development of GC–UV hyphenation

UV detectors generally employ a deuterium (D_2) discharge lamp light source for wavelengths 190–380 nm, and a tungsten (W) lamp for greater wavelengths. Versatility and better analyte detectability can be achieved by variable-wavelength detectors, incorporating broadband D_2 , xenon or W lamps and a monochromator, which allow components to be measured at their maximum absorption wavelength. The UV detector also comprises of an optical system housing, wavelength selection, mirrors or windows, and flow cells.

Photodiode array (PDA) detectors, commonly used in column liquid chromatography (LC) [115] allow simultaneous acquisition of a wide range of UV–vis wavelengths, so both chromatographic and spectrum information are obtained. A given wavelength can be selected to print out an equivalent single-wavelength response chromatogram, or used to prepare calibration data. Thus, the PDA is suitable for quantitative and qualitative analysis [116].

Use of UV detection in GC has been modest. The wide availability of alternative detection – *e.g.* FID – is probably the main factor. Compared with FID, gas phase absorption sensitivity of molecules in the UV range is limited, and it is more difficult to interface between the GC experiment, flow cell, and passage of light, combining to complicate gas phase chromatographic separation with UV–vis. Since the first application of GC–UV, presented by Kaye in the early 1960s [117], UV-spectroscopy in GC has developed in fits and starts. Increased environmental awareness in the 1970s promoted assessment of polynuclear aromatic (PNA) compounds. Early studies [118–121] sought to improve instrument design to increase

limits of detection and analyte detectability. Condensation of hot GC effluent within the UV detector is avoided by heating both the GC transfer-line to the UV-detector, and the UV-flow cell [122]. Total flow can be made up with carrier gas N_2 flow [123].

4.1.2. Applications of GC–UV

Lagesson *et al.*'s extensive study lead to commercial production of a GC–UV instrument, demonstrating structural isomer differentiation by GC–UV, and identification of organic and inorganic compounds over 168–380 nm [120]. Thermal desorption prior to analysis revealed that the GC–UV method had clear advantage over GC–MS for aromatic or conjugated compounds [124]. This was extended to analysis of alcohols and phenols [121], wine [125], indoor dust [123] and biomass ash [126]. An improved method for analysis of aromatic volatiles in coal tar pitch was also reported [127]. Development of GC–pyrolysis–UV detection (GC–PUD), to selectively detect functional groups in nitro organic explosives, gave characteristic UV spectra of nitrobenzene, 2,4-dinitrotoluene and tetraol with linear responses [128]. Recently, GC–UV was shown to display a real time three dimensional result of retention time vs wavelength, enabling processes to be followed visually as a tool for continuous monitoring and simultaneous analyte and decomposition product detection [129].

GC–UV, enabling both qualitative and quantitative analysis, offers acceptable analyte detectability with limits of detection in the nanogram range. Individual compounds as well as chemical classes of compounds in a sample are supported by well-defined UV-spectra, unaffected by solvent effects or the detector's temperature [126]. The resulting vapour phase spectra are suited to compound classification as well as computer based searches for unknowns against a reference library. These include organic and inorganic compounds, and selective analysis for chemical classes such as pyridines, naphthalenes, aliphatic aldehydes etc.

Reliable quantitative determination, based on the Beer–Lambert law, allows acceptable analyte detectability with limits of detection in the ng range. Such quantitation can be obtained by GC–UV using standards of known concentrations against the absorption of the compound. This was exemplified in the analysis of polycyclic aromatic hydrocarbons (PAHs) in biomass combustion ash, permitting detection limits of 15 μg of PAHs per kg of biomass combusted [126]. A quantitative study of volatile organic compounds (VOC) in indoor dust confirmed that analyte detectability of UV methods was on par with that of MS, contrasting to the poorer detectability of FTIR [97]. GC separation was combined with UV absorption for the rapid measurement of PNA compounds in air to quantitatively analyse coke oven effluents [130], extended to a 'tentative' method for PAH determination in automobile exhaust, achieving a 0.1 μg lower limit of detection [131]. Derivatisation of alcohols and phenols to their respective benzoates assisted in decreasing the detection limits of GC–UV analysis [121]. Recent reports of using GC–UV show the ability to measure elemental mercury in natural gas or light hydrocarbons with a 1.7 $\mu\text{g}/\text{m}^3$ detection limit [132]. Despite these characteristics, GC–UV–vis has been a niche area of limited acceptance within the GC–detection sphere. The recent development of vacuum UV detection (next section) may reverse this trend.

4.2. GC–vacuum ultraviolet detection (GC–VUV)

Vacuum ultraviolet (VUV) radiation corresponds to absorption of light by high energy electronic transition of bonded and non-bonded electrons. A 2016 review refers to the 120–200 nm region as far UV (FUV) with 'vacuum UV' referring to operation that normally requires use of spectrometers held under vacuum to reduce background absorption [133]. However, the term VUV will

be used here since this has become synonymous with the detection technique.

Most compounds have limited absorption in UV–vis, but strong absorption in the VUV region; where the absorption cross-section is much stronger. Renewed interest in VUV as a universal detector for GC analytes (GC–VUV) arises from its good general analyte detectability, whilst exhibiting some selectivity. This mass-sensitive detector is broadly applicable to qualitative and quantitative analysis. VUV detectors have the added ability to differentiate *cis*–/*trans*–isomers, similar to other molecular spectroscopic techniques, due to their different absorption maxima. GC–VUV data can be used to deconvolute co-eluting molecules, and perform pseudo-absolute quantification. It may provide information in areas where MS may fail, resulting in a non-destructive, universal detector able to give full scan absorption spectra. A recent comprehensive review outlines the features, instrumentation, applications and performance of GC–VUV [28].

4.2.1. Development of GC–VUV

Most molecules absorb in the VUV region, and these molecular absorption spectra provide valuable qualitative information [134]. Early UV or VUV detectors had a limited ability to transmit light <168 nm [135,136]. The combination of GC with a UV detector in the 122 nm wavelength region provided detection of a variety of analytes but apparently lacked qualitative analysis ability as compared to a FID [137]. Some early studies in the VUV region were restricted to synchrotron facilities [138]. It is desirable for detectors to generate linear signal responses in this region, and suitable light sources that produce continuous, high intensity radiation, whilst overcoming significant background absorption, has delayed the development of bench-top analytical instruments [139]. Schug and co-workers progressed a range of techniques related to the GC–VUV system. A commercial benchtop VUV detector for GC capable of collecting wavelength absorptions in the 120–240 nm range, represents the latest advancement in GC–VUV detectors [139], and successfully addresses many shortcomings posed by earlier spectroscopic detector technologies. Similar to earlier instruments, this has a D₂ light source, heated GC transfer line, makeup gas, flow cell and grating. Coated reflective optics and back-thinned charge-coupled device (CCD) enable simultaneous collection of high quality VUV absorption data over 115–240 nm for presentation of absorption spectra of GC peaks.

VUV gas phase absorptivity of chemical classes across the wavelength range does not vary greatly, resulting in predictability of class-response (*i.e.* similar response factors). Fast GC–VUV applications are supported by data acquisition rates as high as 100 Hz. Good repeatability of VUV spectra allow software deconvolution of multiple closely related, overlapping spectra, to provide analyte

differentiation, as seen in the analysis of co-eluting dimethylnaphthalene isomers [140] and mixtures of permanent gases [141]. Selective identification of classes of molecules can be achieved using digitally created ‘spectral filters’, which project GC signals for specified absorption wavelength ranges. This can improve detection limits, or assist in distinguishing between different compound classes by reducing the impact of the background matrix components.

Time interval deconvolution (TID) permitting integration of GC–VUV data sets was recently devised, assisting in faster and better speciation of constituents in a sample than conventional methods [142]. A pseudo-absolute quantification method for GC–VUV eliminates errors by performing reliable quantitative analysis, without the need for calibration [143], to model and accurately predict detector response [144]. GC–VUV has been proven to be a complementary technique able to offer good selectivity in complex mixture analysis [140].

4.2.2. Applications of GC–VUV

In practice, GC–VUV can be applied to a plethora of areas including petrochemicals, environmental science, agrochemicals, forensics, food technology and flavour analysis – probably as broad as GC–MS, with successful analysis of a myriad of compounds including fixed gases, PAHs, pesticides, alkanes, steroid hormones, drug compounds, fatty-acids, terpenes etc. [28].

GC–VUV provides the ability to distinguish isomers and other compounds, so complements and in this respect extends beyond GC–MS, especially in measuring small or labile compounds, and differentiating isomeric species. The best analyte detectability obtained by VUV is seen for organic compounds containing molecules with aromatic groups and heteroatoms; it is suited to analysing complex sample matrices. This was used in a qualitative and quantitative study of a terpene mixture using a 125–160 nm spectrum filter, with deconvolution of co-eluting peaks [145]. Fig. 4 represents the isomer differentiating ability of the VUV detector, obtained from the hyphenated GC–VUV instrument, illustrated for α - and γ -terpinene, and *cis*- and *trans*-nerolidol.

GC–VUV is useful for chemical monitoring, exemplified in the analysis of 38 pesticides; the strong absorption of aromatic species in the 160–200 nm region helped differentiate aromatic pesticides from their non-aromatic counterparts and integration of absorbance responses increased analyte detectability [146]. Software ability to deconvolute co-eluting peaks has been used for authentication studies of vanilla extract [147]. Although most fatty acid (FA) screening and profiling is done with GC–MS, ambiguous results can be produced in *cis*–/*trans*–isomer differentiation. This can be overcome by GC–VUV, which has been used recently in the analysis of FA methyl esters, for fatty acid profiling of commercial foods [148].

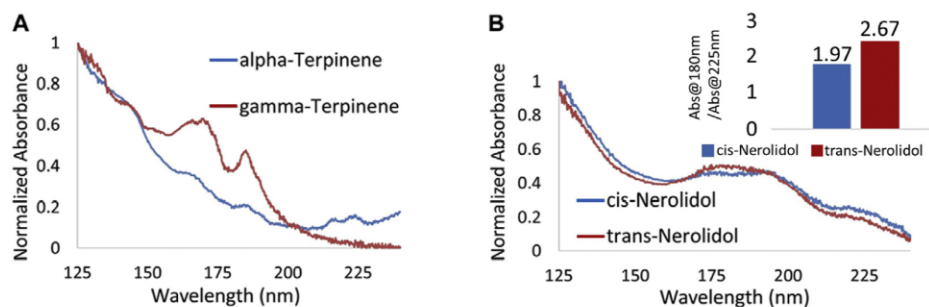


Fig. 4. Spectra of isomeric (A) terpenes and (B) nerolidols obtained by GC–VUV. The ratio of normalised absorption for 180 nm and 225 nm is illustrated as an inset in (B). Adapted from Ref. [145] with permission.

Complex petroleum products are analysed for varied purposes. GC–VUV has been used to determine hydrocarbon group-type in diesels [149]. Detection limit enhancement or distinguishing different classes of compounds can be achieved using spectrum filters. They can be chosen for light absorption by saturated compounds using 125–160 nm filters or unsaturated compounds using 170–240 nm filters. Strong absorbance of monoaromatics in the 180–200 nm range and naphthalene compounds in the 210–220 nm range, was employed to selectively identify these compounds in jet and diesel fuel without the need for deconvolution [140]. GC–MS analysis of the 209 PCB congeners, with complex $^{35}\text{Cl}/^{37}\text{Cl}$ isotope molecular and fragment-ion patterns, causes analytical difficulties. GC–VUV however can distinguish these congeners based on their distinctive absorption spectra, including VUV software-based deconvolution of congeners not resolved chromatographically [150]. Recently GC–VUV was used to distinguish isomers in designer drugs resulting in distinctive spectra, making this a useful tool in forensic analysis of seized drugs [151].

This detector is suitable for fast GC and GC \times GC due to its fast acquisition rates and signal averaging ability [28]. The increased separation capacity of multidimensional GC can be coupled with detection of isomeric compounds which are hard to distinguish with the conventional method using MS based detectors, such as studies on naphthalene [139] and *cis*–/*trans*–fatty acid distribution [148]. Compounds that give poor molecular ions and/or poor MS fragment information may be favourably analysed using GC–VUV. Insufficient acquisition speed and high detection limits have impeded hyphenation of GC \times GC with some optical spectroscopic detectors. The VUV detector was successfully used in a proof-of-concept study for hydrocarbon fuels using cryomodulation GC \times GC [152]. The analysis of highly polar VOCs present at trace quantities in breath gas via GC \times GC–VUV gave LODs in the lower nanogram range [29]. Comparison of the GC \times GC–TOFMS results for the same sample established the potential of GC \times GC–VUV as a complementary method to MS detection techniques. Some maintenance advantages of VUV compared with MS, such as not needing high vacuum and pumps, are relevant to clinical environments. VUV detection coupled with polar ionic liquid GC phases has been reported for the separation of *cis*–/*trans*–fatty acids and their methyl esters [153].

VUV spectroscopy follows the quantitative Beer–Lambert law and produces more featured absorption spectra than that of UV. The mass on-column detection limits for representatives of different chemical class analytes were reported to range from 15 pg (benzene) to 246 pg (water) [139]. A 2017 study profiling various vanilla extract samples showed target analyte LODs between 0.42 and 2.0 $\mu\text{g}/\text{mL}$. A comprehensive database of VUV absorption spectra is yet to emerge. Meanwhile information obtained from recorded synchrotron spectra can be used to obtain absolute information of absorptivities across a range of wavelengths. These data together with suitable software enhance quantitative analysis [147]. GC–VUV eliminates ionisation inefficiencies that are encountered in MS analysis. With its ability to continuously and rapidly acquire full spectroscopic absorption data and present it as a single chromatographic response, GC–VUV can be promisingly applied to many fields as a universal detector; the future of this emerging detection tool across many application areas will be exciting.

5. Molecular emission based detectors

An upper energy state atom or molecule transition to a lower energy state emits electromagnetic radiation, where the energy state of the emitted photon is equal to the energy difference between the two states. Different electron transitions have specific energy difference, which gives rise to different radiated energy,

resulting in an emission spectrum. Molecular emission GC detectors normally correspond to element species in a molecule, which produce small-molecule excited state species as a result of a flame or chemical reaction, with corresponding characteristic radiation. Although the AED mainly provides information based on atomic emission spectroscopy, it is of value in analysis requiring multi-element approaches. The resulting AED spectra can be used with corresponding mass spectra to characterise compounds [48,80,154]. Similarly, the uniqueness of molecular emission corresponding to an element's spectrum plays an important role in identifying compounds containing that element using molecular emission based GC detectors.

5.1. GC–flame photometric detection (GC–FPD)

Based upon photometric detection by flame emission in a hydrogen–air flame, the flame photometric detector (FPD) has been used as a GC detector since its inception in the late 1960s [155]. Used mainly for the sensitive and selective detection of organic compounds containing sulfur (S) and phosphorus (P) compounds, it responds well to other elements including iron group metals, lead, tin, boron, antimony, arsenic, selenium, germanium, etc. [156–158]. Although reviewed previously [159,160], the FPD is included here as a molecular spectroscopic technology; recent studies are included.

In the FPD, GC effluent burns in a H_2 -rich flame where combustion products lead to some specific excited state small molecules which subsequently decay and emit light. This chemiluminescent reaction generates a band emission, usually with multiple emission maxima. The emitted light passes through a filter which selects light unique to the desired species. A photomultiplier tube (PMT) records and amplifies the signal response. A thermal filter may be located between the chemiluminescence region and the PMT to isolate visible and UV radiation, and reduce background noise from the PMT.

Selectivity towards S and P compounds – the two most commonly measured by FPD – arise from selected optical filters which isolate the respective emission bands for passage to the PMT; S compounds produce excited S_2^* with a S selective filter transmitting ~ 394 nm or at other maxima. P compounds produce excited HPO^* , with a P selective filter usually transmitting at ~ 526 nm.

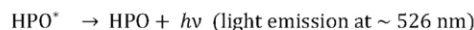
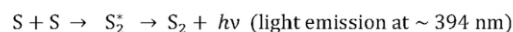
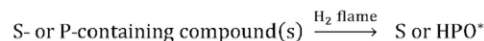
Scheme 1 is a representative description of this process.

Changing from one element to another is only a matter of swapping the FPD filters, although a different flame composition is often required.

Generally the FPD has high analyte detectability, simplicity, comparatively low price, stability, ease of use and good selectivity, and detects very low quantities of sulfur and/or phosphorus compounds. Modifications of the FPD have been proposed to overcome some limitations.

5.1.1. Development of GC–FPD

The initial single channel (single element) FPD was followed soon after by a dual-detection system (S + P) so that compounds



Scheme 1 Production of light emission with S and P selective filters for the FPD.

containing S, or P, or both could be recorded. Replacing a reflector in the initial design with a second filter/photomultiplier combination gave rise to this dual-channel FPD [161] and allowed the atomic ratio between S and P in a molecule to be measured. Large solvent volumes could extinguish the flame, overcome by switching H₂ and air inlets, to form a dual flame photometric detector (dFPD) [162] and gave a more uniform, reproducible response [1] yet with a reduced analyte detectability.

The FPD has a non-linear, often quadratic, sulfur response dependency with amount, due to atomic S recombination to produce S₂^{*} [159], and a variable, non-uniform response factor over a broad range of analytes due to the variation in S₂ emission intensity [163,164] (partly overcome by the dual-flame FPD), and analyte response quenching by even moderate amounts of co-eluting hydrocarbons [165].

The non-linear nature of S response was chemically tackled by doping the flame with a sulfur compound (e.g. CS₂) to create a background of sulfur [166]. Other modifications included different flame burners [167] and geometric modifications [166]. It is advisable to ensure spectral response ratios remain constant when dual-channel models are used [168].

Trace determination of sulfur compounds exacerbate sulfur quenching affects in analysis of complex samples. Many solutions have been suggested to combat quenching, such as operating in a linear mode rather than the conventional quadratic mode, with a twenty-fold greater tolerance to quenching [169]. Sulfur-emission quenching was reduced with unconventional combustion mechanisms, including the pulsed-FPD (PFPD) [170] and reactive flow detector (RFD). The PFPD pulses the flame to separate the S₂^{*} chemiluminescence from the hydrocarbon background, which isolates the flame zones in which these arise [171]. Although it had improved selectivity, analyte detectability, heteroatom selectivity, quenching reduction, and hydrogen consumption rate, it had negative effects with column flow and combustor surface [172]. Simultaneous S and C compound analysis was proposed by introducing flame ionisation to the FPD, via a pulsed flame photometric ionisation detector (PFPID) [173]. Such PFPDs are continually being optimised for new applications for GC [174].

Introduction of a counter-current FPD (μ FPD) method with small opposing flows of hydrogen and oxygen [175–177] gave rise to a more sensitive and robust version than the dFPD. Adaptation of this design to a multiple microflame (mFPD) format resulted in analytes travelling through several small flames burning in a series towards signal monitoring at the final analytical flame. Comparison of the single, dual and multiple flame modes of the FPD showed the mFPD had excellent analyte detectability and response characteristics as well as improved resistance to analyte emission quenching [178]. A new linear mFPD response mode, monitoring sulfur via HSO^{*} emission at 750 nm, showed improved hydrocarbon quenching response in comparison to the conventional single flame S₂^{*} mode. Linearity was over about 4 orders of magnitude, with detection limits nearing 5.8×10^{-11} g/s and selectivity of S:C of approximately 3.5×10^3 [179]. This model was further improved to create a stainless steel mFPD to additionally allow for analyte emission monitoring in the multiple flames [180].

Singh and co-workers substituted the optical filters with a rotating variable interference filter to monitor 100 data points over a range from 400 to 700 nm for signal averaging, adjusting background and other processing functions [181]. This resulted in a loss of analyte detectability despite additional understanding of the response. Dual wavelength FPD instruments have been developed containing a single burner and two PMT housings; one with an S-filter and another with a P-filter, enabling it to acquire either or both S mode (FPD/S) and P mode (FPD/P) [182]. Performance of this detector is therefore a compromise as optimum gas flows for HPO^{*}

and S₂^{*} are quite different. Minimising operation time and increasing separation speed in GC makes faster GC method options more attractive. With the commercially available FPDs reaching data-acquisition rates of >100 Hz they can be used for fast GC methods [183].

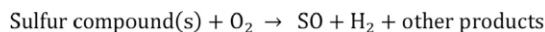
5.1.2. Applications of GC–FPD

Although GC–FPD is used largely for studies on pesticides [184–186], it is also used routinely for e.g. studies in environmental emissions [187–189], petroleum products [190,191], food production [192,193], human health risk [194,195], and Chinese medicinal wine [196]. Techniques such as purge and trap (PT) can be linked to GC–FPD systems for more efficient analysis when on-site sampling is required [197]. This much used spectroscopic detector can be used in conjunction with the MS for compound identification in matrices [198]. The quantification ability of the GC–FPD can yield LODs in the 0.0005–0.004 mg/kg range as reported by Rahman et al. [192].

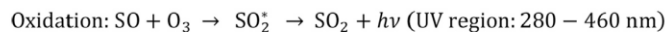
Use of the FPD has been extended to hyphenation to GC \times GC [19], first reported in 2010 for the detection of S- and P-compounds by using a dual channel FPD system in both the S₂ and HPO modes. The fast peak generation of GC \times GC was compatible with FPD acquisition, and was used in analysing pesticides [199,200], and S compounds in petroleum [182,201]. In a study benchmarking candidate detectors for multi-residue pesticide analysis by GC \times GC, FPD(P) performed better than FPD(S) as the latter had a poorer peak shape (tailing factor of 3.36–5.12) and a 10–20 fold poorer analyte detectability compared to its P mode [202]. The GC \times GC–FPD(P) suitability, its improved resolution, and P selectivity in comparison to 1D GC–FPD was confirmed in the study of organophosphorus pesticides and esters in standards, soil and food matrices [199,200]. The FPD performed well in comprehensive two-dimensional GC (GC \times GC–FPD(S)) for evaluation of S speciation and quantification in shale oil [203]. Separation of S-containing compounds from hydrocarbon matrix in the second dimension (²D) column greatly reduced quenching effects and improved the limit of detection by about 10-fold, and the S/N by about 100-fold. Limits of detection attained in such a comprehensive 2DGC–FPD system were reported to be 45 pg/s in the P-mode and 617 pg/s in the S-mode [182]. Linking this to a heart-cutting strategy, the potential to quantify S based on complete class separation have also been explored.

6. Molecular luminescence spectrometry detectors

The emission of light from an excited state of a molecule, referred to as molecular luminescence, may be brought about by fluorescence, phosphorescence or chemiluminescence. Chemiluminescence results when the species' excitation is caused by a chemical reaction. The resulting optical emission can be used for qualitative and quantitative properties. Having inherently higher analyte detectability, luminescence methods have detection limits one to three orders of magnitude lower (*i.e.* better) than their absorption counterparts [68]. The presence of S and N compounds in a myriad of analytical samples makes their accurate determination imperative. The inadequacy of universal detectors to detect trace-levels of N and S components in a matrix demands element-selective detectors for industrial and research use. Fundamental studies [204] and application work [205] lead to development of S- and N-chemiluminescent detectors (SCD and NCD). Reactions of S- and N-containing compounds produces light energy as a product. The SCD and NCD have been reviewed many times, with different scopes [206–209]. Operating principles for SCD and NCD are similar, and they complement other detector techniques. Of the element-selective detectors used in GC for successful S and N



Reduced pressure oxidation with O_3 in the ozone reactor [222]:



Scheme 2 Reduction and oxidative combustion in the SCD.

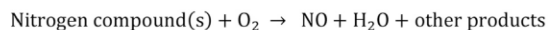
determination, the AED is a multi-element method as opposed to the SCD and NCD which are specific for a single element [210]. Unlike the FPD, the AED and SCD show linear responses for S [210,211].

6.1. Development of GC–chemiluminescence detectors

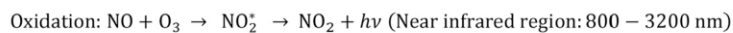
Chemiluminescent detectors were developed mainly with ozone as reactant [206]. The sensing region is preceded by a conversion step, usually via high-temperature pyrolysis, of analytes to sulfur monoxide (SO) or nitric oxide (NO), enabling downstream S- and N- detection. The ozone reaction zone is a light-tight gas chamber where the SO or NO species and ozone mix to give a metastable species. Emission is detected using a PMT. Selectivity for the desired chemiluminescence signal is by an optical filter between the chamber and PMT. The detector normally comprises an ozone generator, and a vacuum pump to keep the reaction chamber pressure low for chemiluminescent reaction efficiency.

Chemiluminescent detectors show many advantageous features over other element-selective methods [207]. The high response factor to the analyte of interest (S or N) over other substances leads to excellent selectivity with values of 10^7 for NCD and flame-based SCD and 10^8 for non-flame SCDs over carbon [206,212]. Since chemiluminescence occurs against a dark background, it has negligible background interference, so the SCD and NCD have very high analyte detectability to their respective elements, with better detectability than FPD towards S. Both SCD and NCD exhibit a linear response, proportional to the heteroatom concentration. An equimolar response of these detectors simplifies calibration for quantitative detection of unknown N/S analytes; recoveries of 86–107% for SCD and 90–110% [213] for NCD were reported. The SCD and NCD are somewhat less robust than the FPD.

Precise isolation of S-containing compounds from a matrix and their detection at trace levels can be problematic in GC analysis [19]. In 2016 Luong *et al.* reviewed the SCD outlining its history and recent advances [214]. Early commercial SCDs employed fluorine-induced detection [215–217]. Selectivity towards S species was improved by ozone-induced chemiluminescence, which combusts all S compounds in a H_2 flame to produce SO. Initially named the universal sulfur detector (USD), it had equimolar response to most S compounds, and good selectivity over hydrocarbons [218]. Improved versions of flameless designs [219], dual detection systems [220] and dual plasma systems [221] followed. The latter enhances SO production by using a lower O_2 -rich flame, and an upper H_2 -rich flame. The SCD was redesigned in 2016 for improved detector performance; increased selectivity, linear and equimolar response, stability and ease of use were design goals.



followed by the chemiluminescent reaction generating near-infrared emission



Scheme 3 Reduction and oxidative combustion in the NCD.

Reduction then oxidative combustion in the SCD is as follows [218] (Scheme 2).

The NCD and SCD are analogous technologies in respect of their design and implementation, and are conceptually similar in their underlying chemical processes and performance.

Coupling the redox chemistry of NO_2 with chemiluminescence produced the NCD as the redox chemiluminescence detector (RCD; 1985), following that of the SCD [223].

Universal reduction then oxidative combustion in the NCD is as follows (Scheme 3):

Most NCD applications generate NO by oxidative combustion, but N-nitroso compounds (nitrosamines) convert to NO by thermal cleavage [224], leading to a selective nitrosamine mode. The NCD has exceptional N selectivity over C. Like the SCD, it has very little or no quenching. Its response is linear and equimolar towards various N-compounds.

6.1.1. Applications of GC–SCD

The SCD preceded use of the FPD to determine S compounds by GC \times GC. Of main interest is the detector acquisition rate, expected to be > 50 Hz for GC \times GC applications. The separation, identification and quantification of S compounds in petroleum and pyrolysis products was reported [225].

The SCD is a good candidate for trace S analysis, with optimisation ensuring good compound-independent S response, unparalleled by other S-specific detectors [226]. Simple sample preparation steps suffice to yield analyte detectability in the sub-microgram region, due to the detector's selectivity [227]. Various GC detection methods for determining reduced S compounds (RSCs) in air was reviewed recently comparing the SCD to other S selective detectors including the FPD, PFPD and AED [228]. The SCD was reportedly superior in terms of its linear response, detectability and uniform S response, despite the robustness, low cost and wide applicability of the FPD(S) for such applications. Reduced SCD S-quenching by hydrocarbons, good equimolar response and excellent selectivity for S ($>10^7$) [219,222] also improved this detector over the FPD(S). It also showed better detection limits of ca. 20 ppb [229] in a dual plasma SCD system. Good correlation coefficients for S compound calibration (>0.9993), and detection limits in the pg of S s^{-1} level were achieved in 2016 with a modern version of the SCD [214]. A further system using cryotrapping sample preparation steps gave detection limits of 0.1–0.3 pg S s^{-1} for RSCs [230].

In addition to petrochemical and energy studies [231], SCD is also used for analysing photo-degradation [232], alcoholic beverages [233–235], flavours [236] and sewer waters [237]. Although S compounds may be reactive, and at low concentration systematic losses may arise, measurement of volatile organic S compounds

(VOSCs) have been studied using GC–SCD with pre-concentration steps such as static headspace injection [238] and thermal desorption [237]. Combining SCDs with MDGC is mostly used for qualitative and quantitative studies of S compounds in various petroleum products [225,239] as well as process water studies [240]. A 2017 review of the various detectors used for S characterisation highlights the use of both the SCD and FPDs [241]. In a pyrolysis oil study using different column sets and multiple detectors, the SCD and NCD were successful in conducting both quantitative and qualitative analysis [242].

6.1.2. Applications of GC–NCD

The SCD and NCD apparently have little mutual interference of their spectra, so provide good selectivity towards their respective element. Applications of the NCD have, like the SCD, been widest in petrochemicals [243]. Selective derivatisation of conjugated dienes with 4-methyl-1,2,4-triazoline-3,5-dione quantitatively introduces a N-containing moiety to allow GC–NCD detection and characterisation of the diolefins in petroleum [244]. The NCD's efficacy in trace N analysis is seen in studies including spices [245], the environment [246] and explosives [247].

Applications of GC \times GC–NCD make this detector useful to provide knowledge of molecular nitrogen species in sample matrices such as feedstock [248]. Other applications include analysis of volatile nitrosamines in meat products [249], acrylamides in starchy food [250] and quantitative analysis of urban air samples [251], and benefit from this separation-detection combination. In comparison of NCD to other detectors, it was reported to have improved equimolar response than NPD, FID and MS [252], and lower LOD and better repeatability than MS [253]. A study of nitrosamines in various meat samples rendered LODs in the 1.66–3.86 $\mu\text{g/L}$ range using GC \times GC with an NCD [249]. In recent comparisons of SCD and NCD to other detectors such as FID and TOFMS in GC \times GC of plastic waste pyrolysis oil [242] and shale oil [254], molecular speciation in the 2D plot supported ready identification of different S and N classes of compounds in the complex mixture. Although response tailing may be observed, this was not commented on, and it is not clear if this is a detector-based effect. Fig. 5 exemplifies group type analysis achieved through the NCD and SCD.

7. Detector figures of merit

Table 1 presents a summary of various analytical figures of merit for a variety of spectroscopic detectors.

8. Multiple detector hyphenation and selected applications of molecular detection

Multiple detectors hyphenated with GC provide additional information over and above that of a single detector [255,256]. They often allow monitoring and confirmation of compound identities with greater confidence Fig. 6.

There are many reasons why this is useful. For example, the electron-capture detector (ECD), an ionisation based detector [26] which responds in an element-selective manner to halogen-containing organic compounds, can be used with the FPD. This is especially useful for ultra-trace detection of a variety of classes of compounds such as pesticides, dioxins, PCBs, OP esters etc. With their inherent ability to provide structural information on a molecule's intact structure compared to the molecular fragments obtained in MS, as well as complementary information provided by isomer identification, molecular spectroscopic detectors are often hyphenated with MS. A non-destructive detector (e.g. FTIR, UV, VUV) may be serially hyphenated before another detector [28].

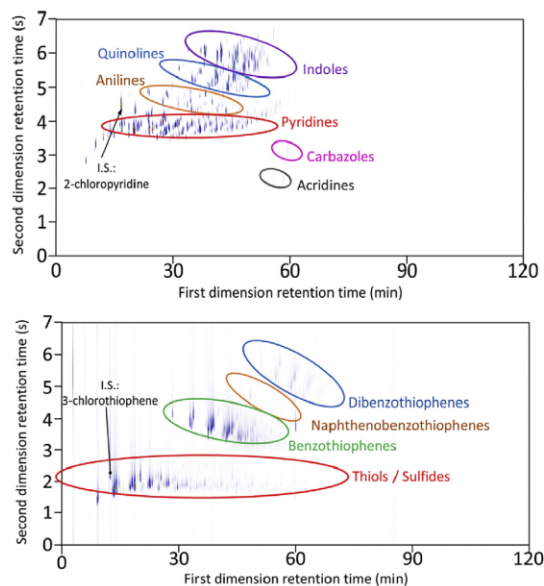


Fig. 5. (A) GC \times GC–NCD chromatogram with different nitrogen containing hydrocarbon groups and (B) GC \times GC–SCD chromatogram with different sulfur containing hydrocarbon groups of shale oil samples. Adapted from Ref. [254] with permission.

Hyphenation should produce better – qualitative and/or quantitative – results, such as spectroscopic detection using both MS and FTIR where the latter has capabilities for detailed isomer information [45]. The practice of multiple hyphenation and the ability of molecular spectroscopic methods such as UV–vis, FTIR, and NMR to provide complementary information to MS have been reviewed [256].

Of the molecular spectroscopic techniques, GC–FTIR/MS has been of especial interest. The first capillary GC–FTIR/MS arrangement was reported in 1982 [57], achieved by a variety of approaches such as tunable ratio post-column splitting with time-synchronised detection [58]. This can also be achieved by using two identical columns, switching between two detectors with an open cross splitter, or running the effluent stream through serially linked detectors [257]. Employing cryogenic IR methods is useful to minimise analyte detectability differences between the two detectors, but is not amenable to on-line methods. The diverse applications of GC–FTIR/MS include amino acid pyrolysis products [51], polymer pyrolysis studies [258], and flavour analysis [259]. In the latter study a multidimensional approach was used to isolate a specific region from a first column, then expand its retention on one of its second dimension columns. Each could then be recorded by using MS, FTIR or FID detection. Fig. 7 exemplifies a study using a parallel GC–FTIR/MS system to identify lithium battery degradation products in which FTIR show spectra different to each other, whilst MS displays similar spectra for ethylene oxide and acetaldehyde [260].

Simultaneous use of MS and PFPD(S) in an on-line system to analyse *Shochu* (Japanese beverage) identified short-chain esters contributing to fruity aroma and strong flavour from S compounds, which decreased with aging [261]. Simultaneous detection with element specific detectors can be carried out in MDGC using heart-cuts to demonstrate changes during processes such as aging of whisky. This was accomplished for characterisation of S compounds with a selectable one-dimensional/two-dimensional retention time locked GC–SCD/NCD/MS system [233]. The complementarity of

Table 1
Classification of detectors and relative analytical figures of merit for spectroscopic detectors.

Detector	Response classification	Mass/concentration sensitive	Linear range	Limit of detection (LOD)	Ref
FTIR	Spectrum of intact molecule	Concentration	10^3	10^{-9} g/mL	[80]
NMR	Spectrum of intact molecule	Concentration	10^1	10^{-4} g/mL	[95]
UV	Spectrum of intact molecule	Concentration	10^2	10^{-6} g/mL	[121]
VUV	Spectrum of intact molecule	Concentration	10^3	10^{-6} g/mL	[139]
FPD (S)	S ₂ emission	Mass	10^4	10^{-11} g/s	[3]
FPD (P)	HPO emission	Mass	10^4	10^{-12} g/s	[3]
SCD	SO ₂ emission	Mass	$>10^4$	10^{-12} g/s	[5]
NCD	NO ₂ emission	Mass	$>10^4$	10^{-12} g/s	[5]

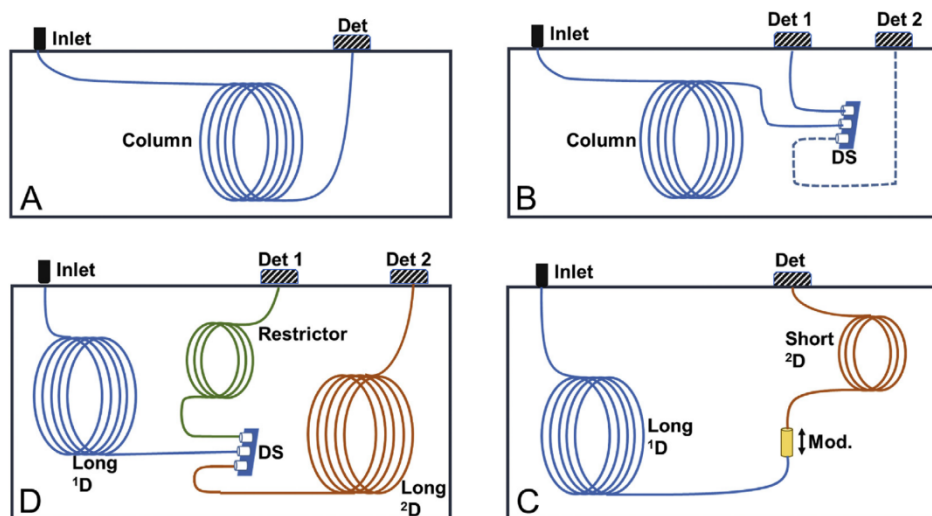


Fig. 6. Diagrams illustrating example experimental setups in (A) GC with single detector, (B) GC with DS enabling switching between two detectors, (C) GC \times GC and (D) H/C MDGC. ¹D, first column; ²D, second column; Det, detector; Mod., modulator; DS, Deans Switch.

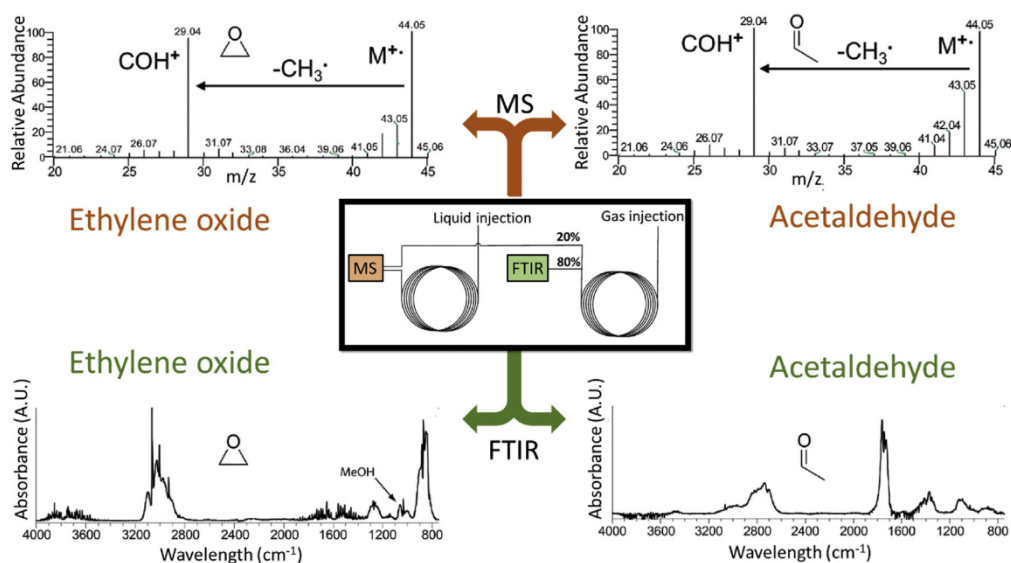


Fig. 7. Parallel GC–FTIR/MS system showing MS and FTIR spectra for ethylene and acetaldehyde. Adapted from Ref. [260] with permission.

information gained through parallel spectroscopic and spectrometric detection is also highlighted in the usage of GC–AED/MS. Here the molar mass information of mass spectrometry in conjunction with elemental composition provided by AED provides valuable information for identifying unknown compounds. This approach is of much value in identifying target and non-target compounds in various matrices [262,263]. The identification of compounds combining the detections by AED and MS can also be applied to comprehensive 2DGC [264].

Table 2 is a selective summary of typical applications of GC–molecular spectroscopic detector applications published since 2007.

9. Conclusion and future trends

Molecular spectroscopy techniques constitute important detection methods in GC. Apart from those that directly depend on molecular emission from specific elemental constituents of a sample (FPD, SCD, NCD), the role of spectroscopy includes both quantitative analysis, but more importantly qualitative analysis, to support varying levels of molecular identification. The information derivable from the respective 'spectrum' may be related to either structural features of the molecule (functional groups, bond connectivity, carbon-proton bond moieties, bond fragmentation, bond vibrations), or the molecular electronic absorption pattern of the species. These provide, to a greater or lesser extent, an insight into the molecule's structure, and so contributes to its identification. Although olfactometry detection cannot be defined in the classical spectroscopic instrumental sense, its hyphenation to GC provides characterisation of a molecule's odour activity, which is a function of molecular structure. With its complex, selective and variable

performance, linking this to an MS creates an apt tool to detect low levels of odour active compounds. In the same vein, electro-antennography detection, which uses the response of *e.g.* insect receptors towards specific compounds, find considerable application in molecular characterisation. The mass spectrometer has been and remains a powerful tool in the analyst's hands, and in full scan mode can give an immediate suggestion as to molecular identity. But the simplicity of this process can also be its biggest limitation – the first library match or 'hit' provided for a compound in the GC–MS experiment might not be the correct molecule. Modern high resolution MS methods or combinations of various MS techniques can accomplish a level of identification not achieved with a single quadrupole MS hyphenated to the GC. As with other spectroscopic detectors in GC, an extensive MS spectrum library will assist in giving a first approximation to the potential identity of a compound, and with an information rich detector such as FTIR, this might be reasonably accurate. But apart from extensive MS libraries, other techniques have limited GC database records. MS will continue to be a dominant technology for GC, and with increased access to accurate mass MS, opportunities for precise empirical formula deduction is of great qualitative and quantitative assistance. Reliable and simplified FTIR interfacing must be addressed if this is to be a more accepted technique in the future. It is unlikely that NMR will be more than a curiosity, unless again the interface and analyte detectability are addressed. Off-line prep-scale NMR with GC is a much more accepted approach, and should be further promoted. The emerging GC–VUV technique seems to offer a truly 'disruptive' technology as a sensitive, quantitative, qualitative method, which further research in the coming years will most surely extend and examine. Although the MS still remains the workhorse of GC detection techniques, and MS technologies continue to be refined in order to improve molecular

Table 2

Example applications of GC with various spectroscopic detectors published since 1997, including instances of multiple detector techniques.

Detection technique	Sample source	Comments/application	Ref
GC–FTIR	Alcoholic beverages	Methanol and ethanol identification and quantitation using library spectra	[69]
GC–FTIR	Chemical weapons	Trace analysis of convention related chemicals	[66]
GC–FTIR	Insect pheromones	Isomer identification	[84]
GC–FTIR	Designer drugs	Complementary structural elucidation to GC–MS analysis	[72]
MDGC–FTIR–MS	Fragrances	Irritant identification using spectral library identification	[257]
GC– ¹ H NMR, Off-line	Mix of diethyl ether, dichloromethane, tetrahydrofuran	Use of solenoid type micro coil for volatiles detection	[102]
GC– ¹ H NMR On-line	1,2-dimethylcyclohexane	Identification of volatile <i>cis/trans</i> -stereoisomers	[101]
GC– ¹ H NMR On-line	Unfunctionalised racemic chiral alkane	Separation and identification of enantiomers	[111]
MDGC– ¹ H NMR Off-line	Crude oil	Methylnaphthalene isomer identification in off-line NMR mode	[92]
MDGC–2D NMR Off-line	Essential oils	Volatile component identity confirmation	[91]
GC–UV	Biomass ash	PAHs and other organic compounds	[124]
GC–UV	Explosives	Enables simultaneous detection of target analyte and decomposition product	[129]
GC–VUV	Turpentine mixtures	Co-eluting peaks deconvoluted, quantitative analysis of terpenes	[145]
GC–VUV	FAME mix and food oils	Co-eluting peaks deconvoluted, <i>cis/trans</i> -isomeric differentiation of FAMES, fatty acid profiling of food oil	[148]
GC–VUV	Jet and diesel fuel	Computational deconvolution, speciation of dimethylnaphthalene in fuel	[140]
GC–VUV	Petroleum products	Timed interval deconvolution applied, hydrocarbon speciation	[142]
GC–VUV	Water	Natural and toxic gas analysis in Li battery run off	[141]
GC–VUV	Pesticide	Multiclass pesticide identification, isomer differentiation	[146]
GC × GC–VUV	Breath gas	Analysis of VOCs	[29]
PT–GC–pFPD	Seawater	Trace-level dimethylsulfide analysis	[197]
GC–FPD/P	Pepper	Analysis of toxic metabolites	[192]
GC–FPD	Sea water	Butyltin hydride extraction using quartz surface-induced tin emission FPD	[265]
GC × GC–FPD	Pesticides and Kerosene	S and P containing compounds identified. Higher detection limits than 1D GC–FPD seen.	[182]
GC × GC–FPD(S)	Shale oil	Sulfur speciation and quantification	[203]
GC × GC–FPD(P)	Spiked Diesel matrix	OP pesticides & esters	[199]
GC–SCD	Crude oil	Sulfur compound speciation	[231]
GC–NCD	Petrochemicals	Nitrogen compounds speciation and quantitation	[243]
GC × GC–NCD	Plastic waste pyrolysis oil	S- and N- containing groups identified	[242]
GC × GC–SCD			
GC–MS–FTIR	Li battery degradation	Identification of electrolyte degradation products	[260]
GC–SCD/NCD/MS	Whisky	Simultaneous detection of S and N compounds	[233]

identification through accurate mass and novel MS/MS methods, the systematic and informed application of a range of spectroscopic detection tools will no doubt benefit the unambiguous identification of GC separated compounds.

Acknowledgements

This work was supported by the Australian Research Council, Linkage Grant scheme, with partner PerkinElmer (Grant LP150100465). Funding from PerkinElmer to the Monash University GRIP program is also acknowledged. Monash University support for JSZ for a Deans Research Scholarship is acknowledged.

References

- [1] C.F. Poole, *The Essence of Chromatography*, Elsevier, Amsterdam, 2003.
- [2] B. Domon, R. Aebersold, Options and considerations when selecting a quantitative proteomics strategy, *Nat. Biotechnol.* 28 (2010) 710.
- [3] C. Li, Z. Long, X. Jiang, P. Wu, X. Hou, Atomic spectrometric detectors for gas chromatography, *Trends Anal. Chem.* 77 (2016) 139–155.
- [4] A. James, A. Martin, Gas-liquid partition chromatography: the separation and micro-estimation of volatile fatty acids from formic acid to dodecanoic acid, *Biochem. J.* 50 (1952) 679–690.
- [5] *Practical Gas Chromatography*, A Comprehensive Reference, Springer, Berlin, Heidelberg, 2014.
- [6] J.M. Miller, *Chromatography: Concepts and Contrasts*, second ed., Wiley, Hoboken, NJ, 2005.
- [7] B.H. Fumes, M.R. Silva, F.N. Andrade, C.E.D. Nazario, F.M. Lanças, Recent advances and future trends in new materials for sample preparation, *Trends Anal. Chem.* 71 (2015) 9–25.
- [8] J. de Zeeuw, J. Luong, Developments in stationary phase technology for gas chromatography, *Trends Anal. Chem.* 21 (2002) 594–607.
- [9] J.C. Giddings, Dynamics of zone spreading, in: *Dynamics of Chromatography: Principles and Theory*, Marcel Dekker Inc., New York, 1965, pp. 13–94.
- [10] M. Adachour, J. Beens, R.J.J. Vreuls, U.A.T. Brinkman, Recent developments in comprehensive two-dimensional gas chromatography (GC × GC): I. Introduction and instrumental set-up, *Trends Anal. Chem.* 25 (2006) 438–454.
- [11] M. Adachour, J. Beens, R.J.J. Vreuls, U.A.T. Brinkman, Recent developments in comprehensive two-dimensional gas chromatography (GC × GC). IV. Further applications, conclusions and perspectives, *Trends Anal. Chem.* 25 (2006) 821–840.
- [12] M. Adachour, J. Beens, R.J.J. Vreuls, U.A.T. Brinkman, Recent developments in comprehensive two-dimensional gas chromatography (GC × GC). III. Applications for petrochemicals and organohalogenes, *Trends Anal. Chem.* 25 (2006) 726–741.
- [13] M. Adachour, J. Beens, R.J.J. Vreuls, U.A.T. Brinkman, Recent developments in comprehensive two-dimensional gas chromatography (GC × GC). II. Modulation and detection, *Trends Anal. Chem.* 25 (2006) 540–553.
- [14] Y. Nolvachai, C. Kulsing, P.J. Marriott, Pesticides analysis: advantages of increased dimensionality in gas chromatography and mass spectrometry, *Crit. Rev. Environ. Sci. Technol.* 45 (2015) 2135–2173.
- [15] S.T. Chin, P.J. Marriott, Multidimensional gas chromatography beyond simple volatiles separation, *Chem. Commun.* 50 (2014) 8819–8833.
- [16] K.M. Sharif, S.-T. Chin, C. Kulsing, P.J. Marriott, The microfluidic Deans switch: 50 years of progress, innovation and application, *Trends Anal. Chem.* 82 (2016) 35–54.
- [17] J.A. Murray, Qualitative and quantitative approaches in comprehensive two-dimensional gas chromatography, *J. Chromatogr. A* 1261 (2012) 58–68.
- [18] L.L.P. van Stee, U.T. Brinkman, Peak detection methods for GC × GC: an overview, *Trends Anal. Chem.* 83 (2016) 1–13.
- [19] P.J. Marriott, Detector technologies and applications in comprehensive two-dimensional gas chromatography, in: L. Mondello (Editor), *Comprehensive Chromatography in Combination with Mass Spectrometry*, John Wiley & Sons, Inc, Hoboken, NJ., 2011, pp. 243–280.
- [20] J.T. Andersson, Detectors, in: K. Dettmer-Wilde, W. Engewald (Editors), *Detectors*, Springer, Berlin, Heidelberg, 2014, pp. 205–248.
- [21] R.C. Blase, K. Llera, A. Luspay-Kuti, M. Libardoni, The importance of detector acquisition rate in comprehensive two-dimensional gas chromatography (GC×GC), *Sep. Sci. Technol.* 49 (2014) 847–853.
- [22] K.M. Pierce, J.L. Hope, J.C. Hoggard, R.E. Synovec, A principal component analysis based method to discover chemical differences in comprehensive two-dimensional gas chromatography with time-of-flight mass spectrometry (GC×GC-TOFMS) separations of metabolites in plant samples, *Talanta* 70 (2006) 797–804.
- [23] K. Héberger, M. Görgényi, Principal component analysis of Kováts indices for carbonyl compounds in capillary gas chromatography, *J. Chromatogr. A* 845 (1999) 21–31.
- [24] S. Dagan, Comparison of gas chromatography–pulsed flame photometric detection–mass spectrometry, automated mass spectral deconvolution and identification system and gas chromatography–tandem mass spectrometry as tools for trace level detection and identification, *J. Chromatogr. A* 868 (2000) 229–247.
- [25] V.I. Babushok, Chromatographic retention indices in identification of chemical compounds, *Trends Anal. Chem.* 69 (2015) 98–104.
- [26] C.F. Poole, Ionization-based detectors for gas chromatography, *J. Chromatogr. A* 1421 (2015) 137–153.
- [27] R.P. Scott, *Chromatographic Detectors: Design, Function, and Operation*, CRC Press, 1996.
- [28] I.C. Santos, K.A. Schug, Recent advances and applications of gas chromatography vacuum ultraviolet spectroscopy, *J. Sep. Sci.* 40 (2017) 138–151.
- [29] B. Gruber, T. Groeger, D. Harrison, R. Zimmermann, Vacuum ultraviolet absorption spectroscopy in combination with comprehensive two-dimensional gas chromatography for the monitoring of volatile organic compounds in breath gas: a feasibility study, *J. Chromatogr. A* 1464 (2016) 141–146.
- [30] J. Holmes, F. Morrell, Oscillographic mass spectrometric monitoring of gas chromatography, *Appl. Spectrosc.* 11 (1957) 86–87.
- [31] S. Stein, Mass spectral reference libraries: an ever-expanding resource for chemical identification, *Anal. Chem.* 84 (2012) 7274–7282.
- [32] B.L. Milman, I.K. Zhurkovich, Mass spectral libraries: a statistical review of the visible use, *Trends Anal. Chem.* 80 (2016) 636–640.
- [33] B.L. Milman, Identification of chemical compounds, *Trends Anal. Chem.* 24 (2005) 493–508.
- [34] B.L. Milman, *Chemical Identification and its Quality Assurance*, Springer, Berlin, London, 2011.
- [35] B.L. Milman, General principles of identification by mass spectrometry, *Trends Anal. Chem.* 69 (2015) 24–33.
- [36] F. Xian, C.L. Hendrickson, A.G. Marshall, High resolution mass spectrometry, *Anal. Chem.* 84 (2012) 708–719.
- [37] M. Jiang, C. Kulsing, Y. Nolvachai, P.J. Marriott, Two-dimensional retention indices improve component identification in comprehensive two-dimensional gas chromatography of saffron, *Anal. Chem.* 87 (2015) 5753–5761.
- [38] X. Wang, S. Wang, Z. Cai, The latest developments and applications of mass spectrometry in food-safety and quality analysis, *Trends Anal. Chem.* 52 (2013) 170–185.
- [39] M.S. Alam, R.M. Harrison, Recent advances in the application of 2-dimensional gas chromatography with soft and hard ionisation time-of-flight mass spectrometry in environmental analysis, *Chem. Sci.* 7 (2016) 3968–3977.
- [40] G. Martínez-Domínguez, P. Plaza-Bolaños, R. Romero-González, A. Garrido-Frenich, Analytical approaches for the determination of pesticide residues in nutraceutical products and related matrices by chromatographic techniques coupled to mass spectrometry, *Talanta* 118 (2014) 277–291.
- [41] P.Q. Tranchida, F.A. Franchina, M. Zoccali, S. Pantò, D. Sciarrone, P. Dugo, L. Mondello, Untargeted and targeted comprehensive two-dimensional GC analysis using a novel unified high-speed triple quadrupole mass spectrometer, *J. Chromatogr. A* 1278 (2013) 153–159.
- [42] B. Mitrevski, P.J. Marriott, Evaluation of quadrupole-time-of-flight mass spectrometry in comprehensive two-dimensional gas chromatography, *J. Chromatogr. A* 1362 (2014) 262–269.
- [43] D.C. Harris, *Quantitative Chemical Analysis*, ninth ed., W.H. Freeman & Co, New York, 2016.
- [44] C.L. Wilkins, Hyphenated spectroscopic detectors for gas chromatography, in: C.F. Poole (Editor), *Gas Chromatography*, Elsevier, Amsterdam, 2012, pp. 349–354.
- [45] N. Ragnathan, K.A. Krock, C. Klawun, T.A. Sasaki, C.L. Wilkins, Gas chromatography with spectroscopic detectors, *J. Chromatogr. A* 856 (1999) 349–397.
- [46] L.L.P. van Stee, U.A.T. Brinkman, H. Bagheri, Gas chromatography with atomic emission detection: a powerful technique, *Trends Anal. Chem.* 21 (2002) 618–626.
- [47] J.T. Andersson, Some unique properties of gas chromatography coupled with atomic-emission detection, *Anal. Bioanal. Chem.* 373 (2002) 344–355.
- [48] L.L.P. van Stee, U.A.T. Brinkman, Developments in the application of gas chromatography with atomic emission (plus mass spectrometric) detection, *J. Chromatogr. A* 1186 (2008) 109–122.
- [49] H. Bagheri, M. Saraji, U.A.T. Brinkman, Environmental applications of gas chromatography-atomic emission detection, *Tech. Instrum. Anal. Chem.* 21 (2000) 211–238.
- [50] V.A. Basiuk, R. Navarro-González, Identification of hexahydroimidazo[1, 2-a]pyrazine-3,6-diones and hexahydroimidazo[1,2-a]imidazo[1,2-d]pyrazine-3,8-diones, unusual products of silica-catalyzed amino acid thermal condensation and products of their thermal decomposition using coupled high-performance liquid chromatography–particle beam mass spectrometry and gas chromatography–Fourier transform infrared spectroscopy–mass spectrometry, *J. Chromatogr. A* 776 (1997) 255–273.
- [51] V.A. Basiuk, R. Navarro-González, E.V. Basiuk, Pyrolysis of alanine and α -aminoisobutyric acid: identification of less-volatile products using gas chromatography/Fourier transform infrared spectroscopy/mass spectrometry, *J. Anal. Appl. Pyrolysis* 45 (1998) 89–102.
- [52] S. Gosav, R. Dinica, M. Praisler, Choosing between GC-FTIR and GC-MS spectra for an efficient intelligent identification of illicit amphetamines, *J. Mol. Struct.* 887 (2008) 269–278.

- [53] C. Cordella, I. Moussa, A.C. Martel, N. Sbirrazzouli, L. Lizzani-Cuvelier, Recent developments in food characterization and adulteration detection: technique-oriented perspectives, *J. Agric. Food Chem.* 50 (2002) 1751–1764.
- [54] P.R. Griffiths, D.A. Heaps, P.R. Bregina, The gas chromatography/infrared interface: past, present, and future, *Appl. Spectrosc.* 62 (2008) 259A–270A.
- [55] M.J.D. Low, Rapid infrared analysis of gas-chromatography peaks, *Chem. Commun.* (1966) 371–372.
- [56] T. Hirschfeld, The hy-phen-ated methods, *Anal. Chem.* 52 (1980) 226–232.
- [57] R.W. Crawford, T. Hirschfeld, R.H. Sanborn, C.M. Wong, Organic analysis with a combined capillary gas chromatograph/mass spectrometer/Fourier transform infrared spectrometer, *Anal. Chem.* 54 (1982) 817–820.
- [58] T. Visser, FT-IR detection in gas chromatography, *Trends Anal. Chem.* 21 (2002) 627–636.
- [59] C.J. Wurrey, Applications of gas chromatography-Fourier transform IR spectrometry in environmental analyses, *Trends Anal. Chem.* 8 (1989) 52–58.
- [60] P.A. Wilks, R.A. Brown, Construction and performance of an infrared chromatographic fraction analyzer, *Anal. Chem.* 36 (1964) 1896–1899.
- [61] L.V. Azarraga, Construction and performance of an infrared chromatographic fraction analyzer, *Appl. Spectrosc.* 34 (1980) 224–225.
- [62] M.M. Mossoba, R.A. Niemann, J.Y.T. Chen, Picogram level quantitation of 2,3,7,8-tetrachlorodibenzo-p-dioxin in fish extracts by capillary gas chromatography/matrix isolation/Fourier transform infrared spectrometry, *Anal. Chem.* 61 (1989) 1678–1685.
- [63] E. Sémon, S. Ferary, J. Auger, J.L. Le Quéré, Gas chromatography-Fourier transform infrared spectrometry of fatty acids: new applications with a direct deposition interface, *J. Am. Oil Chem. Soc.* 75 (1998) 101–105.
- [64] R.S. Brown, C.L. Wilkins, Cryogenically cooled interface for gas chromatography Fourier-transform infrared spectrometry, *Anal. Chem.* 60 (1988) 1483–1488.
- [65] N. Ragunathan, K.A. Krock, C. Klawun, T.A. Sasaki, C.L. Wilkins, Multispectral detection for gas chromatography, *J. Chromatogr. A* 703 (1995) 335–382.
- [66] P. Garg, A. Purohit, V.K. Tak, D. Dubey, Enhanced detectability of fluorinated derivatives of N, N-dialkylamino alcohols and precursors of nitrogen mustards by gas chromatography coupled to Fourier transform infrared spectroscopy analysis for verification of chemical weapons convention, *J. Chromatogr. A* 1216 (2009) 7906–7914.
- [67] S.D. Richardson, A.D. Thruston, T.V. Caughran, P.H. Chen, T.W. Collette, T.L. Floyd, K.M. Schenck, B.W. Lykins, G.-R. Sun, G. Majetich, Identification of new ozone disinfection byproducts in drinking water, *Environ. Sci. Technol.* 33 (1999) 3368–3377.
- [68] D.A. Skoog, Principles of Instrumental Analysis, sixth ed., Thomson, Brooks/Cole, Belmont, CA, 2007.
- [69] K. Sharma, S.P. Sharma, S. Lahiri, Novel method for identification and quantification of methanol and ethanol in alcoholic beverages by gas chromatography-Fourier transform infrared spectroscopy and horizontal attenuated total reflectance-Fourier transform infrared spectroscopy, *J. AOAC Int.* 92 (2009) 518–526.
- [70] F.C.-Y. Wang, K.E. Edwards, Separation of C2-naphthalenes by gas chromatography \times Fourier transform infrared spectroscopy (GC \times FT-IR): two-dimensional separation approach, *Anal. Chem.* 79 (2007) 106–112.
- [71] T.A. Sasaki, C.L. Wilkins, Gas chromatography with Fourier transform infrared and mass spectral detection, *J. Chromatogr. A* 842 (1999) 341–349.
- [72] A. Carlsson, S. Lindberg, X. Wu, S. Dunne, M. Josefsson, C. Åstot, J. Dahlén, Prediction of designer drugs: synthesis and spectroscopic analysis of synthetic cannabinoid analogues of 1H-indol-3-yl(2,2,3,3-tetramethylcyclopropyl) methanone and 1H-indol-3-yl(adamantan-1-yl)methanone, *Drug Test. Anal.* 8 (2016) 1015–1029.
- [73] B. Mile, Chemistry in court, *Chromatographia* 62 (2005) 3–9.
- [74] J.A. Roach, M.M. Mossoba, M.P. Yurawecz, J.K. Kramer, Chromatographic separation and identification of conjugated linoleic acid isomers, *Anal. Chim. Acta* 465 (2002) 207–226.
- [75] J. Cai, P. Lin, X.L. Zhu, Q. Su, Comparative analysis of clary sage (*S. sclarea* L.) oil volatiles by GC-FTIR and GC-MS, *Food Chem.* 99 (2006) 401–407.
- [76] P.A. Rodriguez, C.L. Eddy, C. Marcott, M.L. Fey, J.M. Anast, Combined two-dimensional GC/MS/matrix isolation FT-IR with a versatile sample introduction system, *J. Microcolumn Sep.* 3 (1991) 289–301.
- [77] C.L. Wilkins, Multidimensional GC for qualitative IR and MS of mixtures, *Anal. Chem.* 66 (1994) 295A–301A.
- [78] T. Visser, Gas chromatography/fourier transform infrared spectroscopy, in: P.R. Griffiths, J.M. Chalmers (Editors), *Handbook of Vibrational Spectroscopy*, vol. 2, John Wiley & Sons, Ltd, Chichester, 2002, pp. 1605–1626.
- [79] T. Visser, M.J. Vredenburg, A.P.J.M. de Jong, G.W. Somsen, T. Hankemeier, N.H. Velthorst, C. Gooijer, U.A.T. Brinkman, Improvements in environmental trace analysis by GC-IR and LC-IR, *J. Mol. Struct.* 408 (1997) 97–103.
- [80] T. Hankemeier, E. Hooijsschuur, R.J.J. Vreuls, U.A.T. Brinkman, T. Visser, On-line solid phase extraction-gas chromatography-cryotrapping-infrared spectrometry for the trace-level determination of microcontaminants in aqueous samples, *J. High Resolut. Chromatogr.* 21 (1998) 341–346.
- [81] R. Veness, C. Evans, Identification of monosaccharides and related compounds by gas chromatography-Fourier transform infrared spectroscopy of their trimethylsilyl ethers, *J. Chromatogr. A* 721 (1996) 165–172.
- [82] P. Doumenq, M. Guiliano, G. Mille, GC/FTIR potential for structural analysis of marine origin complex mixtures, *Int. J. Environ. Anal. Chem.* 37 (1989) 235–244.
- [83] J.C. Young, D.E. Games, Analysis of Fusarium mycotoxins by gas chromatography-Fourier transform infrared spectroscopy, *J. Chromatogr. A* 663 (1994) 211–218.
- [84] D.M. Vidal, C.F. Fávoro, M.M. Guimarães, P.H.G. Zarbin, Identification and synthesis of the male-produced sex pheromone of the soldier beetle *Chauliognathus fallax* (Coleoptera: Cantharidae), *J. Braz. Chem. Soc.* 27 (2016) 1506–1511.
- [85] W. Schrader, J. Geiger, D. Klockow, E.-H. Korte, Degradation of α -pinene on Tenax during sample storage: effects of daylight radiation and temperature, *Environ. Sci. Technol.* 35 (2001) 2717–2720.
- [86] K. Łaniewski, T. Wännman, G. Hagman, Gas chromatography with mass spectrometric, atomic emission and Fourier transform infrared spectroscopic detection as complementary analytical techniques for the identification of unknown impurities in pharmaceutical analysis, *J. Chromatogr. A* 985 (2003) 275–282.
- [87] T. Belal, T. Awad, J. DeRuiter, C.R. Clark, GC–IRD methods for the identification of isomeric ethoxyphenethylamines and methoxymethcathinones, *Forensic Sci. Int.* 184 (2009) 54–63.
- [88] K. Sharma, S. Sharma, S. Lahiri, Characterization and identification of petroleum hydrocarbons and biomarkers by GC-FTIR and GC-MS, *Pet. Sci. Technol.* 27 (2009) 1209–1226.
- [89] J. Guitton, M. Desage, S. Alamercury, L. Dutruch, S. Dautraix, J. Perdrix, J. Brazier, Gas chromatographic–mass spectrometry and gas chromatographic–Fourier transform infrared spectroscopy assay for the simultaneous identification of fentanyl metabolites, *J. Chromatogr. B* 693 (1997) 59–70.
- [90] K.A. Krock, N. Ragunathan, C.L. Wilkins, Multidimensional gas chromatography coupled with infrared and mass spectrometry for analysis of eucalyptus essential oils, *Anal. Chem.* 66 (1994) 425–430.
- [91] G.T. Eyres, S. Urban, P.D. Morrison, J.-P. Dufour, P.J. Marriott, Method for small-molecule discovery based on microscale-preparative multidimensional gas chromatography isolation with nuclear magnetic resonance spectroscopy, *Anal. Chem.* 80 (2008) 6293–6299.
- [92] G.T. Eyres, S. Urban, P.D. Morrison, P.J. Marriott, Application of microscale-preparative multidimensional gas chromatography with nuclear magnetic resonance spectroscopy for identification of pure methyl naphthalenes from crude oils, *J. Chromatogr. A* 1215 (2008) 168–176.
- [93] E. Becker, A brief history of nuclear magnetic resonance, *Anal. Chem.* 65 (1993) 295A–302A.
- [94] K. Patel, J. Patel, M. Patel, G. Rajput, H. Patel, Introduction to hyphenated techniques and their applications in pharmacy, *Pharm. Methods* 1 (2010) 2–13.
- [95] M. Kühnle, K. Holtin, K. Albert, Capillary NMR detection in separation science, *J. Sep. Sci.* 32 (2009) 719–726.
- [96] J.R. Kesting, K.T. Johansen, J.W. Jaroszewski, Hyphenated NMR techniques, *Adv. Biomed. Spectrosc.* 3 (2011) 413–434.
- [97] J. Buddrus, H. Herzog, J.W. Cooper, Coupling of hplc and NMR. 2. Analysis of flowing liquid chromatographic fractions by proton magnetic resonance in the presence of hydrogen-containing eluting solvents, *J. Magn. Reson.* 42 (1981) 453–459.
- [98] E. Brame Jr., Combining gas chromatography with nuclear magnetic resonance spectrometry, *Anal. Chem.* 37 (1965) 1183–1184.
- [99] T. Kiyoshi, M. Yoshikawa, A. Sato, K. Itoh, S. Matsumoto, H. Wada, S. Ito, T. Miki, T. Miyazaki, T. Kamikado, Operation of a 920-MHz high-resolution NMR magnet at TML, *IEEE Trans. Appl. Supercond.* 13 (2003) 1391–1395.
- [100] R. Adams, J. Aguilar, K. Atkinson, M. Cowley, P. Elliott, S. Duckett, G. Green, I. Khazal, J. Lopez-Serrano, D. Williamson, Reversible interactions with para-hydrogen enhance NMR sensitivity by polarization transfer, *Science* 323 (2009) 1708–1711.
- [101] M. Kühnle, D. Kreidler, K. Holtin, H. Czesla, P. Schuler, W. Schaal, V. Schurig, K. Albert, Online coupling of gas chromatography to nuclear magnetic resonance spectroscopy: method for the analysis of volatile stereoisomers, *Anal. Chem.* 80 (2008) 5481–5486.
- [102] M.D. Grynbaum, D. Kreidler, J. Rehbein, A. Pura, P. Schuler, W. Schaal, H. Czesla, A. Webb, V. Schurig, K. Albert, Hyphenation of gas chromatography to microcoil 1H nuclear magnetic resonance spectroscopy, *Anal. Chem.* 79 (2007) 2708–2713.
- [103] P.F. Flynn, D.L. Mattiello, H.D. Hill, A.J. Wand, Optimal use of cryogenic probe technology in NMR studies of proteins, *J. Am. Chem. Soc.* 122 (2000) 4823–4824.
- [104] H. Nagai, A. Sato, T. Kiyoshi, F. Matsumoto, H. Wada, S. Ito, T. Miki, M. Yoshikawa, Y. Kawate, S. Fukui, Development and testing of superfluid-cooled 900 MHz NMR magnet, *Cryogenics* 41 (2001) 623–630.
- [105] S.A. Korhammer, A. Bernreuther, Hyphenation of high-performance liquid chromatography (HPLC) and other chromatographic techniques (SFC, GPC, GC, CE) with nuclear magnetic resonance (NMR): a review, *Fresenius, J. Anal. Chem.* 354 (1996) 131–135.
- [106] O. Gökyay, K. Albert, From single to multiple microcoil flow probe NMR and related capillary techniques: a review, *Anal. Bioanal. Chem.* 402 (2012) 647–669.
- [107] C. Paiva, A. Amaral, M. Rodriguez, N. Canyellas, X. Correig, J. Ballecà, J. Ramalho-Santos, R. Oliva, Identification of endogenous metabolites in human sperm cells using proton nuclear magnetic resonance (1H-NMR) spectroscopy and gas chromatography-mass spectrometry (GC-MS), *Andrology* 3 (2015) 496–505.

- [108] A. Booker, A. Suter, A. Krnjic, B. Strassel, M. Zloh, M. Said, M. Heinrich, A phytochemical comparison of saw palmetto products using gas chromatography and ¹H nuclear magnetic resonance spectroscopy metabolomic profiling, *J. Pharm. Pharmacol.* 66 (2014) 811–822.
- [109] K. Skogerson, R. Runnebaum, G. Wohlgemuth, J. de Ropp, H. Heymann, O. Fiehn, Comparison of gas chromatography-coupled time-of-flight mass spectrometry and H-1 nuclear magnetic resonance spectroscopy metabolite identification in white wines from a sensory study investigating wine body, *J. Agric. Food Chem.* 57 (2009) 6899–6907.
- [110] J.A. Nazeam, H.A. Gad, H.M. El-Hefnawy, A.-N.B. Singab, Chromatographic separation and detection methods of *Aloe arborescens* Miller constituents: a systematic review, *J. Chromatogr. B* 1058 (2017) 57–67.
- [111] M. Kühnle, D. Kreidler, K. Holtin, H. Czesla, P. Schuler, V. Schurig, K. Albert, Online coupling of enantioselective capillary gas chromatography with proton nuclear magnetic resonance spectroscopy, *Chirality* 22 (2010) 808–812.
- [112] B. Gouilleux, B. Charrier, S. Akoka, F.-X. Felpin, M. Rodríguez-Zubiri, P. Giraudeau, Ultrafast 2D NMR on a benchtop spectrometer: applications and perspectives, *Trends Anal. Chem.* 83 (2016) 65–75.
- [113] C.P. Rühle, J. Niere, P.D. Morrison, R.C. Jones, T. Caradoc-Davies, A.J. Canty, M.G. Gardiner, V.-A. Tolhurst, P.J. Marriott, Characterization of tetra-aryl benzene isomers by using preparative gas chromatography with mass spectrometry, nuclear magnetic resonance spectroscopy, and X-ray crystallographic methods, *Anal. Chem.* 82 (2010) 4501–4509.
- [114] D.L. Olson, M.E. Lacey, J.V. Sweedler, Microcoils significantly boost NMR mass sensitivity and provide new detection opportunities: the Nanoliter Niche, *Anal. Chem.* 70 (1998) 257A–264A.
- [115] T. Schmid, B. Baumann, M. Himmelsbach, C.W. Klampfl, W. Buchberger, Analysis of saccharides in beverages by HPLC with direct UV detection, *Anal. Bioanal. Chem.* 408 (2016) 1871–1878.
- [116] D.G. Hatzinikolaou, V. Lagesson, A.J. Stavridou, A.E. Pouli, L. Lagesson-Andrasko, J.C. Stavrides, Analysis of the gas phase of cigarette smoke by gas chromatography coupled with UV-diode array detection, *Anal. Chem.* 78 (2006) 4509–4516.
- [117] W. Kaye, Far-ultraviolet spectroscopic detection of gas chromatograph effluent, *Anal. Chem.* 34 (1962) 287–293.
- [118] M. Novotny, F.J. Schwende, M.J. Hartigan, J.E. Purcell, Capillary gas chromatography with ultraviolet spectrometric detection, *Anal. Chem.* 52 (1980) 736–740.
- [119] V. Lagesson, J. Newman, Microcolumn gas-chromatography with ultraviolet detection and identification using a photodiode array spectrophotometer, *Anal. Chem.* 61 (1989) 1249–1252.
- [120] L. Lagesson-Andrasko, V. Legesson, J. Andrasko, The use of gas-phase UV spectra in the 168–330-nm wavelength region for analytical purposes. 1. Qualitative measurements, *Anal. Chem.* 70 (1998) 819–826.
- [121] I. Sanz-Vicente, S. Cabredo, J. Galban, Gas chromatography with UV-vis molecular absorption spectrometry detection: increasing sensitivity of the determination of alcohols and phenols by derivatization, *Chromatographia* 48 (1998) 542–547.
- [122] A. Nilsson, V. Lagesson, C.-G. Bornehag, J. Sundell, C. Tagesson, Quantitative determination of volatile organic compounds in indoor dust using gas chromatography-UV spectrometry, *Environ. Int.* 31 (2005) 1141–1148.
- [123] A. Nilsson, E. Kihlström, V. Lagesson, B. Wessén, B. Szponar, L. Larsson, C. Tagesson, Microorganisms and volatile organic compounds in airborne dust from damp residences, *Indoor Air* 14 (2004) 74–82.
- [124] H. Lagesson, A. Nilsson, C. Tagesson, Qualitative determination of compounds adsorbed on indoor dust particles using GC-UV and GC-MS after thermal desorption, *Chromatographia* 52 (2000) 621–630.
- [125] T. Cedrón-Fernández, C. Sáenz-Barrio, S. Cabredo-Pinillos, I. Sanz-Vicente, Separation and determination of volatile compounds in synthetic wine samples by gas chromatography using UV-visible molecular absorption spectrometry as detector, *Talanta* 57 (2002) 555–563.
- [126] P. Straka, M. Havelcova, Polycyclic aromatic hydrocarbons and other organic compounds in ashes from biomass combustion, *Acta Geodyn. Geomater.* 9 (2012) 481–490.
- [127] R.A. Greinke, I.C. Lewis, Development of a gas chromatographic-ultraviolet absorption spectrometric method for monitoring petroleum pitch volatiles in the environment, *Anal. Chem.* 47 (1975) 2151–2155.
- [128] R. Hodyss, J.L. Beauchamp, Multidimensional detection of nitroorganic explosives by gas chromatography-pyrolysis-ultraviolet detection, *Anal. Chem.* 77 (2005) 3607–3610.
- [129] J. Andrasko, L. Lagesson-Andrasko, J. Dahlén, B.H. Jonsson, Analysis of explosives by GC-UV, *J. Forensic Sci.* 62 (2017) 1022–1027.
- [130] T.D. Searl, F.J. Cassidy, W.H. King, R.A. Brown, An analytical method for polynuclear aromatic compounds in coke oven effluents by combined use of gas chromatography and ultraviolet absorption spectrometry, *Anal. Chem.* 42 (1970) 954–958.
- [131] E. Sawicki, Tentative method of analysis for polynuclear aromatic hydrocarbons in automobile exhaust, *Health Lab. Sci.* 11 (1974) 228–239.
- [132] R. Gras, J. Luong, R.A. Shellie, Direct measurement of trace elemental mercury in hydrocarbon matrices by gas chromatography with ultraviolet photometric detection. (Report), *Anal. Chem.* 87 (2015) 11429–11432.
- [133] Y. Ozaki, I. Tanabe, Far-ultraviolet spectroscopy of solid and liquid states: characteristics, instrumentation, and applications, *Analyst* 141 (2016) 3962–3981.
- [134] H.C. Lu, H.K. Chen, B.M. Cheng, J.F. Ogilvie, Absorption spectra in the vacuum ultraviolet region of small molecules in condensed phases, *Spectrochim. Acta Part A* 71 (2008) 1485–1491.
- [135] J. Driscoll, M. Duffy, S. Pappas, Capillary gas chromatographic analysis with the far-UV absorbance detector, *J. Chromatogr. A* 441 (1988) 63–71.
- [136] V. Lagesson, L. Lagesson-Andrasko, J. Andrasko, F. Baco, Identification of compounds and specific functional groups in the wavelength region 168–330 nm using gas chromatography with UV detection, *J. Chromatogr. A* 867 (2000) 187–206.
- [137] B. Middleditch, N.-J. Sung, A. Zlatkis, G. Settembre, Trace analysis of volatile polar organics by direct aqueous injection gas chromatography, *Chromatographia* 23 (1987) 273–278.
- [138] M. Wickramaarachchi, E. Premuzic, M. Lin, P. Snyder, Circular dichroism detection of optically active compounds in gas chromatography using vacuum ultraviolet synchrotron radiation, *J. Chromatogr. A* 390 (1987) 413–420.
- [139] K.A. Schug, I. Sawicki, D.D. Carlton Jr., F. Hui, H.M. McNair, J.P. Nimmo, P. Kroll, J. Smuts, P. Walsh, D. Harrison, Vacuum ultraviolet detector for gas chromatography, *Anal. Chem.* 86 (2014) 8329–8335.
- [140] J. Schenk, J.X. Mao, J. Smuts, P. Walsh, P. Kroll, K.A. Schug, Analysis and deconvolution of dimethylnaphthalene isomers using gas chromatography vacuum ultraviolet spectroscopy and theoretical computations, *Anal. Chim. Acta* 945 (2016) 1–8.
- [141] L. Bai, J. Smuts, P. Walsh, H. Fan, Z. Hildenbrand, D. Wong, D. Wetz, K.A. Schug, Permanent gas analysis using gas chromatography with vacuum ultraviolet detection, *J. Chromatogr. A* 1388 (2015) 244–250.
- [142] P. Walsh, M. Garbalena, K.A. Schug, Rapid analysis and time interval deconvolution for comprehensive fuel compound group classification and speciation using gas chromatography-vacuum ultraviolet spectroscopy, *Anal. Chem.* 88 (2016) 11130–11138.
- [143] L. Bai, J. Smuts, P. Walsh, C. Qiu, H.M. McNair, K.A. Schug, Pseudo-absolute quantitative analysis using gas chromatography – vacuum ultraviolet spectroscopy – a tutorial, *Anal. Chim. Acta* 953 (2017) 10–22.
- [144] A. Hulanicki, Absolute methods in analytical chemistry (Technical Report), *Pure Appl. Chem.* 67 (1995) 1905–1911.
- [145] C. Qiu, J. Smuts, K.A. Schug, Analysis of terpenes and turpentine using gas chromatography with vacuum ultraviolet detection, *J. Sep. Sci.* 40 (2017) 869–877.
- [146] H. Fan, J. Smuts, P. Walsh, D. Harrison, K.A. Schug, Gas chromatography–vacuum ultraviolet spectroscopy for multiclass pesticide identification, *J. Chromatogr. A* 1389 (2015) 120–127.
- [147] I.C. Santos, J. Smuts, K.A. Schug, Rapid profiling and authentication of Vanilla extracts using gas chromatography–vacuum ultraviolet spectroscopy, *Food Anal. Methods* 10 (2017) 4068–4078.
- [148] H. Fan, J. Smuts, L. Bai, P. Walsh, D.W. Armstrong, K.A. Schug, Gas chromatography–vacuum ultraviolet spectroscopy for analysis of fatty acid methyl esters, *Food Chem.* 194 (2016) 265–271.
- [149] B.M. Weber, P. Walsh, J.J. Harynuk, Determination of hydrocarbon group-type of diesel fuels by gas chromatography with vacuum ultraviolet detection, *Anal. Chem.* 88 (2016) 5809–5817.
- [150] C. Qiu, J. Cochran, J. Smuts, P. Walsh, K.A. Schug, Gas chromatography–vacuum ultraviolet detection for classification and speciation of polychlorinated biphenyls in industrial mixtures, *J. Chromatogr. A* 1490 (2017) 191–200.
- [151] L. Skultety, P. Frycak, C. Qiu, J. Smuts, L. Shear-Laude, K. Lemr, J.X. Mao, P. Kroll, K.A. Schug, A. Szwczak, C. Vaught, I. Lurie, V. Havlicek, Resolution of isomeric new designer stimulants using gas chromatography – vacuum ultraviolet spectroscopy and theoretical computations, *Anal. Chim. Acta* 971 (2017) 55–67.
- [152] T. Gröger, B. Gruber, D. Harrison, M. Saraji-Bozorgzad, M. Mthembu, A. Sutherland, R. Zimmermann, A vacuum ultraviolet absorption array spectrometer as a selective detector for comprehensive two-dimensional gas chromatography: concept and first results, *Anal. Chem.* 88 (2016) 3031–3039.
- [153] C.A. Weatherly, Y. Zhang, J.P. Smuts, H. Fan, C. Xu, K.A. Schug, J.C. Lang, D.W. Armstrong, Analysis of long-chain unsaturated fatty acids by ionic liquid gas chromatography, *J. Agric. Food Chem.* 64 (2016) 1422–1432.
- [154] S.V. Kala, E.D. Lykissa, R.M. Lebovitz, Detection and characterization of poly(dimethylsiloxane)s in biological tissues by GC/AED and GC/MS, *Anal. Chem.* 69 (1997) 1267–1272.
- [155] S. Brody, J. Chaney, Flame photometric detector: the application of a specific detector for phosphorus and for sulfur compounds – sensitive to subnanogram quantities, *J. Chromatogr. Sci.* 4 (1966) 42–46.
- [156] W.A. Aue, X.Y. Sun, B. Millier, Inter-elemental selectivity, spectra and computer-generated specificity of some main-group elements in the flame photometric detector, *J. Chromatogr. A* 606 (1992) 73–86.
- [157] X.-Y. Sun, W.A. Aue, Selective detection of volatile iron compounds by flame photometry, *J. Chromatogr. A* 467 (1989) 75–84.
- [158] G.-B. Jiang, Q.-F. Zhou, B. He, Speciation of organotin compounds, total tin, and major trace metal elements in poisoned human organs by gas chromatography-flame photometric detector and inductively coupled plasma-mass spectrometry, *Environ. Sci. Technol.* 34 (2000) 2697–2702.

- [159] S.O. Farwell, C.J. Barinaga, Sulfur-selective detection with the FPD: current enigmas, practical usage, and future directions, *J. Chromatogr. Sci.* 24 (1986) 483–494.
- [160] W. Wardenccki, B. Zygmunt, Gas chromatographic sulphur-sensitive detectors in environmental analysis, *Anal. Chim. Acta* 255 (1991) 1–13.
- [161] M.C. Bowman, M. Beroza, Gas chromatographic detector for simultaneous sensing of phosphorus- and sulfur-containing compounds by flame photometry, *Anal. Chem.* 40 (1968) 1448–1452.
- [162] P.L. Patterson, Dual-flame photometric detector for sulfur and phosphorus compounds in gas chromatograph effluents, *Anal. Chem.* 50 (1978) 339–344.
- [163] C.H. Burnett, D.F. Adams, S.O. Farwell, Relative FPD responses for a systematic group of sulfur-containing compounds, *J. Chromatogr. Sci.* 16 (1978) 68–73.
- [164] T. Sugiyama, Y. Suzuki, T. Takeuchi, Characteristics of S₂ emission intensity with a flame photometric detector, *J. Chromatogr. A* 77 (1973) 309–316.
- [165] M. Dressler, *Selective Gas Chromatographic Detectors*, Elsevier, New York, 1986.
- [166] C.G. Flinn, W.A. Aue, Geometric and chemical discrimination in a non-dispersive flame photometric detector, *J. Chromatogr. Sci.* 18 (1980) 136–138.
- [167] S. Kapila, C.R. Vogt, FPD: burner configurations and the response to heteroorganics, *J. Chromatogr. Sci.* 17 (1979) 327–332.
- [168] X.-Y. Sun, W.A. Aue, Constancy of spectral response ratios in the flame photometric detector, *J. Chromatogr. A* 667 (1994) 191–203.
- [169] W.A. Aue, X.-Y. Sun, Quenching in the flame photometric detector, *J. Chromatogr. A* 641 (1993) 291–299.
- [170] L. Kalontarov, H. Jing, A. Amirav, S. Cheskis, Mechanism of sulfur emission quenching in flame photometric detectors, *J. Chromatogr. A* 696 (1995) 245–256.
- [171] H. Jing, A. Amirav, Pulsed flame photometric detector – a step forward towards universal heteroatom selective detection, *J. Chromatogr. A* 805 (1998) 177–215.
- [172] S. Cheskis, E. Atar, A. Amirav, Pulsed-flame photometer: a novel gas chromatography detector, *Anal. Chem.* 65 (1993) 539–555.
- [173] N. Tzanani, A. Amirav, Combined pulsed flame photometric ionization detector, *Anal. Chem.* 67 (1995) 167–173.
- [174] S. Jang, K.T. Park, K. Lee, Y.S. Suh, An analytical system enabling consistent and long-term measurement of atmospheric dimethyl sulfide, *Atmos. Environ.* 134 (2016) 217–223.
- [175] K.B. Thurber, B.W. Cooke, W.A. Aue, Novel flame photometric detector for gas chromatography based on counter-current gas flows, *J. Chromatogr. A* 1029 (2004) 193–203.
- [176] K.B. Thurber, T.C. Hayward, Improved micro-flame detection method for gas chromatography, *Anal. Chim. Acta* 519 (2004) 121–128.
- [177] T.C. Hayward, K.B. Thurber, Characteristics of sulfur response in a micro-flame photometric detector, *J. Chromatogr. A* 1105 (2006) 66–70.
- [178] T.C. Hayward, K.B. Thurber, Quenching-resistant multiple micro-flame photometric detector for gas chromatography, *Anal. Chem.* 81 (2009) 8858–8867.
- [179] A.G. Clark, K.B. Thurber, Properties of a novel linear sulfur response mode in a multiple flame photometric detector, *J. Chromatogr. A* 1326 (2014) 103–109.
- [180] A.G. Clark, K.B. Thurber, An improved multiple flame photometric detector for gas chromatography, *J. Chromatogr. A* 1421 (2015) 154–161.
- [181] H. Singh, B. Millier, W. Aue, Time-integrated spectra from a flame photometric detector, *J. Chromatogr. A* 724 (1996) 255–264.
- [182] S.T. Chin, Z.Y. Wu, P.D. Morrison, P.J. Marriott, Observations on comprehensive two dimensional gas chromatography coupled with flame photometric detection for sulfur- and phosphorus-containing compounds, *Anal. Methods* 2 (2010) 243–253.
- [183] P. Korytár, H.-G. Janssen, E. Matisová, U.A.T. Brinkman, Practical fast gas chromatography: methods, instrumentation and applications, *Trends Anal. Chem.* 21 (2002) 558–572.
- [184] X. Du, Y.L. Ren, S.J. Beckett, An innovative rapid method for analysis of 10 organophosphorus pesticide residues in wheat by HS-SPME-GC-FPD/MSD, *J. AOAC Int.* 99 (2016) 520–526.
- [185] X. Zhao, W. Kong, J. Wei, M. Yang, Gas chromatography with flame photometric detection of 31 organophosphorus pesticide residues in *Alpinia oxyphylla* dried fruits, *Food Chem.* 162 (2014) 270–276.
- [186] S. Berijani, Y. Assadi, M. Anbia, M.-R. Milani Hosseini, E. Aghaee, Dispersive liquid–liquid microextraction combined with gas chromatography–flame photometric detection: very simple, rapid and sensitive method for the determination of organophosphorus pesticides in water, *J. Chromatogr. A* 1123 (2006) 1–9.
- [187] T. Otake, J. Yoshinaga, Y. Yanagisawa, Analysis of organic esters of plasticizer in indoor air by GC–MS and GC–FPD, *Environ. Sci. Technol.* 35 (2001) 3099–3102.
- [188] X. Lu, C. Fan, J. Shang, J. Deng, H. Yin, Headspace solid-phase microextraction for the determination of volatile sulfur compounds in odorous hypertrophic freshwater lakes using gas chromatography with flame photometric detection, *Microchem. J.* 104 (2012) 26–32.
- [189] V.P. Campos, A.S. Oliveira, L.P. Cruz, J. Borges, T.M. Tavares, Optimization of parameters of sampling and determination of reduced sulfur compounds using cryogenic capture and gas chromatography in tropical urban atmosphere, *Microchem. J.* 96 (2010) 283–289.
- [190] C.T. Yue, S.Y. Li, H. Song, Simulation experiments on the generation of organic sulfide in the Shengli crude oil, *Geochem. Int.* 53 (2015) 1052–1063.
- [191] N. Jantaraksa, P. Prasassarakich, P. Reubroycharoen, N. Hinchiranan, Cleaner alternative liquid fuels derived from the hydrosulfurization of waste tire pyrolysis oil, *Energy Convers. Manage.* 95 (2015) 424–434.
- [192] M.M. Rahman, J.-H. Choi, A.A. El-Aty, M.D. Abid, J.-H. Park, T.W. Na, Y.-D. Kim, J.-H. Shim, Pepper leaf matrix as a promising analyte protectant prior to the analysis of thermolabile terbufos and its metabolites in pepper using GC–FPD, *Food Chem.* 133 (2012) 604–610.
- [193] D.-Q. Ye, X.-T. Zheng, X.-Q. Xu, Y.-H. Wang, C.-Q. Duan, Y.-L. Liu, Evolutions of volatile sulfur compounds of Cabernet Sauvignon wines during aging in different oak barrels, *Food Chem.* 202 (2016) 236–246.
- [194] R. Yu, Q. Liu, J. Liu, Q. Wang, Y. Wang, Concentrations of organophosphorus pesticides in fresh vegetables and related human health risk assessment in Changchun, Northeast China, *Food Control* 60 (2016) 353–360.
- [195] W. Naksen, T. Prapamontol, A. Mangklabruks, S. Chantara, P. Thavornutikarn, M.G. Robson, P.B. Ryan, D.B. Barr, P. Panuwet, A single method for detecting 11 organophosphate pesticides in human plasma and breastmilk using GC-FPD, *J. Chromatogr. B* 1025 (2016) 92–104.
- [196] Q. Liu, W. Kong, F. Qiu, J. Wei, S. Yang, Y. Zheng, M. Yang, One-step extraction for gas chromatography with flame photometric detection of 18 organophosphorus pesticides in Chinese medicine health wines, *J. Chromatogr. B* 885–886 (2012) 90–96.
- [197] M. Zhang, L. Chen, Continuous underway measurements of dimethyl sulfide in seawater by purge and trap gas chromatography coupled with pulsed flame photometric detection, *Mar. Chem.* 174 (2015) 67–72.
- [198] J.P. Cao, Z.M. Zong, X.Y. Zhao, M. Zhou, X.X. Ma, G.J. Zhou, P. Wu, W. Zhao, B.M. Li, X.Y. Wei, Identification of octathioacane, organonitrogens, and organosulfurs in Tongchuan shale, *Energy Fuels* 21 (2007) 1193–1194.
- [199] X. Liu, D. Li, J. Li, G. Rose, P.J. Marriott, Organophosphorus pesticide and ester analysis by using comprehensive two-dimensional gas chromatography with flame photometric detection, *J. Hazard Mater.* 263 (Part 2) (2013) 761–767.
- [200] X. Liu, B. Mitrevski, D. Li, J. Li, P.J. Marriott, Comprehensive two-dimensional gas chromatography with flame photometric detection applied to organophosphorus pesticides in food matrices, *Microchem. J.* 111 (2013) 25–31.
- [201] C. Kulsing, P. Rawson, R.L. Webster, D.J. Evans, P.J. Marriott, Group-type analysis of hydrocarbons and sulfur compounds in thermally stressed Merox jet fuel samples, *Energy Fuels* 31 (2017) 8978–8984.
- [202] E. Engel, J. Ratel, P. Blinet, S.T. Chin, G. Rose, P.J. Marriott, Benchmarking of candidate detectors for multiresidue analysis of pesticides by comprehensive two-dimensional gas chromatography, *J. Chromatogr. A* 1311 (2013) 140–148.
- [203] B. Mitrevski, M.W. Amer, A.L. Chaffee, P.J. Marriott, Evaluation of comprehensive two-dimensional gas chromatography with flame photometric detection: potential application for sulfur speciation in shale oil, *Anal. Chim. Acta* 803 (2013) 174–180.
- [204] M. Clyne, B. Thrush, R. Wayne, Kinetics of the chemiluminescent reaction between nitric oxide and ozone, *Trans. Faraday Soc.* 60 (1964) 359–370.
- [205] A. Fontijn, A.J. Sabadell, R.J. Ronco, Homogeneous chemiluminescent measurement of nitric oxide with ozone, Implications for continuous selective monitoring of gaseous air pollutants, *Anal. Chem.* 42 (1970) 575–579.
- [206] X. Yan, Detection by ozone-induced chemiluminescence in chromatography, *J. Chromatogr. A* 842 (1999) 267–308.
- [207] X. Yan, Unique selective detectors for gas chromatography: nitrogen and sulfur chemiluminescence detectors, *J. Sep. Sci.* 29 (2006) 1931–1945.
- [208] *Selective Detectors, Environmental, Industrial, and Biomedical Applications*, John Wiley & Sons, New York, 1995.
- [209] X. Yan, Sulfur and nitrogen chemiluminescence detection in gas chromatographic analysis, *J. Chromatogr. A* 976 (2002) 3–10.
- [210] S.E. Eckert-Tilotta, S.B. Hawthorne, D.J. Miller, Comparison of commercially available atomic emission and chemiluminescence detectors for sulfur-selective gas chromatographic detection, *J. Chromatogr. A* 591 (1992) 313–323.
- [211] B.D. Quimby, D.A. Grudski, V. Giarrocco, Improved measurement of sulfur and nitrogen compounds in refinery liquids using gas chromatography–atomic emission detection, *J. Chromatogr. Sci.* 36 (1998) 435–443.
- [212] R.L. Shearer, E.B. Poole, J.B. Nowalk, Application of gas chromatography and flameless sulfur chemiluminescence detection to the analysis of petroleum products, *J. Chromatogr. Sci.* 31 (1993) 82–87.
- [213] B.M. Jones, C.G. Daughton, Chemiluminescence vs. Kjeldahl determination of nitrogen in oil shale retort waters and organonitrogen compounds, *Anal. Chem.* 57 (1985) 2320–2325.
- [214] J. Luong, R. Gras, M. Hawryluk, R. Shearer, A brief history and recent advances in ozone induced chemiluminescence detection for the determination of sulfur compounds by gas chromatography, *Anal. Methods* 8 (2016) 7014–7024.
- [215] J.K. Nelson, R.H. Getty, J.W. Birks, Fluorine induced chemiluminescence detector for reduced sulfur compounds, *Anal. Chem.* 55 (1983) 1767–1770.
- [216] R.J. Glinski, E.A. Mishalanie, J.W. Birks, Molecular emission spectra in the visible and near IR produced in the chemiluminescent reactions of molecular fluorine with organosulfur compounds, *J. Photochem.* 37 (1987) 217–231.
- [217] A.J. Hills, D.H. Lenschow, J.W. Birks, Dimethyl sulfide measurement by fluorine-induced chemiluminescence, *Anal. Chem.* 70 (1998) 1735–1742.

- [218] R.L. Benner, D.H. Stedman, Universal sulfur detection by chemiluminescence, *Anal. Chem.* 61 (1989) 1268–1271.
- [219] R.L. Shearer, Development of flameless sulfur chemiluminescence detection: application to gas chromatography, *Anal. Chem.* 64 (1992) 2192–2196.
- [220] T.B. Ryerson, R.M. Barkley, R.E. Sievers, Selective chemiluminescence detection of sulfur-containing compounds coupled with nitrogen–phosphorus detection for gas chromatography, *J. Chromatogr. A* 670 (1994) 117–126.
- [221] R. Gras, J. Luong, R. Mustacich, R. Shearer, DP-SCD and LTMGC for determination of low sulfur levels in hydrocarbons, *J. ASTM Int.* 2 (2005) 1–15.
- [222] H.R. Martin, R.J. Glinski, Chemiluminescence from sulfur compounds in novel flame and discharge systems: proof of sulfur dioxide as the emitter in the new sulfur chemiluminescence detector, *Appl. Spectrosc.* 46 (1992) 948–952.
- [223] S.A. Nyarady, R.M. Barkley, R.E. Sievers, Redox chemiluminescence detector: application to gas chromatography, *Anal. Chem.* 57 (1985) 2074–2079.
- [224] D. Fine, D. Lieb, F. Rufe, Principle of operation of the thermal energy analyzer for the trace analysis of volatile and non-volatile N-nitroso compounds, *J. Chromatogr. A* 107 (1975) 351–357.
- [225] R. Hua, Y. Li, W. Liu, J. Zheng, H. Wei, J. Wang, X. Lu, H. Kong, G. Xu, Determination of sulfur-containing compounds in diesel oils by comprehensive two-dimensional gas chromatography with a sulfur chemiluminescence detector, *J. Chromatogr. A* 1019 (2003) 101–109.
- [226] H.P. Tuan, H.-G.M. Janssen, C.A. Cramers, E.M. Kuiper-van Loo, H. Vlap, Evaluation of the performance of various universal and selective detectors for sulfur determination in natural gas, *J. High Resolut. Chromatogr.* 18 (1995) 333–342.
- [227] L.B. Jaycox, L.D. Olsen, Determination of total sulfur compounds and benzothiazole in asphalt fume samples by gas chromatography with sulfur chemiluminescence detection, *Appl. Occup. Environ. Hyg.* 15 (2000) 695–704.
- [228] S. Pandey, K.-H. Kim, A review of methods for the determination of reduced sulfur compounds (RSCs) in air, *Environ. Sci. Technol.* 43 (2009) 3020–3029.
- [229] R. Gras, J. Luong, R. Shearer, A unified approach for the measurement of individual or total volatile organic sulfur compounds in hydrocarbon matrices by dual-plasma chemiluminescence detector and low thermal mass gas chromatography, *J. Chromatogr. Sci.* 45 (2007) 671–676.
- [230] M.A.H. Khan, M.E. Whelan, R.C. Rhew, Analysis of low concentration reduced sulfur compounds (RSCs) in air: storage issues and measurement by gas chromatography with sulfur chemiluminescence detection, *Talanta* 88 (2012) 581–586.
- [231] D. Singh, A. Chopra, P.K. Mahendra, V. Kagdiyal, D. Saxena, Sulfur compounds in the fuel range fractions from different crude oils, *Pet. Sci. Technol.* 34 (2016) 1248–1254.
- [232] S. Tsuge, H. Yokoi, Y. Ishida, H. Ohtani, M.A. Becker, Photodegradative changes in chemical structures of silk studied by pyrolysis–gas chromatography with sulfur chemiluminescence detection, *Polym. Degrad. Stab.* 69 (2000) 223–227.
- [233] N. Ochial, K. Sasamoto, K. MacNamara, Characterization of sulfur compounds in whisky by full evaporation dynamic headspace and selectable one-dimensional/two-dimensional retention time locked gas chromatography–mass spectrometry with simultaneous element-specific detection, *J. Chromatogr. A* 1270 (2012) 296–304.
- [234] D. Rauhut, H. Kürbel, K. MacNamara, M. Grossmann, Headspace GC-SCD monitoring of low volatile sulfur compounds during fermentation and in wine, *Analyst* 26 (1998) 142–145.
- [235] M. Burmeister, C. Drummond, E. Pfisterer, D. Hysert, Y. Sin, K. Sime, D. Hawthorne, Measurement of volatile sulfur compounds in beer using gas chromatography with a sulfur chemiluminescence detector, *J. Am. Soc. Brew. Chem.* 50 (1992) 53–58.
- [236] J. Steely, K. Zeller, Molasses flavor investigations with sulfur chemiluminescence detection, in: T.H. Parment, M.J. Morello, R.J. McGorin (Editors), *Thermally Generated Flavors*, Maillard, Microwave, and Extrusion Processes, ACS Symposium Series, vol. 543, American Chemical Society, Washington, DC, 1994, pp. 80–94.
- [237] B. Wang, E.C. Sivret, G. Parcsi, R.M. Stuetz, Determination of VOSCs in sewer headspace air using TD-GC-SCD, *Talanta* 137 (2015) 71–79.
- [238] J. Sun, S. Hu, K.R. Sharma, B. Keller-Lehmann, Z. Yuan, An efficient method for measuring dissolved VOSCs in wastewater using GC-SCD with static headspace technique, *Water Res.* 52 (2014) 208–217.
- [239] V.V. Lobodin, W.K. Robbins, J. Lu, R.P. Rodgers, Separation and characterization of reactive and non-reactive sulfur in petroleum and its fractions, *Energy Fuels* 29 (2015) 6177–6186.
- [240] C.E. West, A.G. Scarlett, A. Tonkin, D. O'Carroll-Fitzpatrick, J. Pureveen, E. Tegelaar, R. Gieleciak, D. Hager, K. Petersen, K.-E. Tollefsen, Diaromatic sulphur-containing 'naphthenic' acids in process waters, *Water Res.* 51 (2014) 206–215.
- [241] C. Lorentz, D. Laurenti, J.L. Zotin, C. Geantet, Comprehensive GC×GC chromatography for the characterization of sulfur compound in fuels: a review, *Catal. Today* 292 (2017) 26–37.
- [242] H.E. Toraman, T. Dijkman, M.R. Djokic, K.M. Van Geem, G.B. Marin, Detailed compositional characterization of plastic waste pyrolysis oil by comprehensive two-dimensional gas-chromatography coupled to multiple detectors, *J. Chromatogr. A* 1359 (2014) 237–246.
- [243] M. Navas, A. Jiménez, Chemiluminescent methods in petroleum products analysis, *Crit. Rev. Anal. Chem.* 30 (2000) 153–162.
- [244] K.E. Edwards, K. Qian, F.C. Wang, M. Siskin, Quantitative analysis of conjugated dienes in hydrocarbon feeds and products, *Energy Fuels* 19 (2005) 2034–2040.
- [245] E.M. Fujinari, Pungent flavor profiles and components of spices by chromatography and chemiluminescent nitrogen detection, in: S.J. Risch, C.-T. Ho (Editors), *Spices. Flavor Chemistry and Antioxidant Properties*, ACS Symposium Series, vol. 660, American Chemical Society, Washington, DC, 1997, pp. 98–112.
- [246] B.A. Tomkins, W.H. Griest, C.E. Higgins, Determination of N-nitrosodimethylamine at part-per-trillion levels in drinking waters and contaminated groundwaters, *Anal. Chem.* 67 (1995) 4387–4395.
- [247] C.R. Bowerbank, P.A. Smith, D.D. Fetterolf, M.L. Lee, Solvating gas chromatography with chemiluminescence detection of nitroglycerine and other explosives, *J. Chromatogr. A* 902 (2000) 413–419.
- [248] F. Adam, F. Bertoncini, C. Dartiguelongue, K. Marchand, D. Thiébaud, M.C. Hennion, Comprehensive two-dimensional gas chromatography for basic and neutral nitrogen speciation in middle distillates, *Fuel* 88 (2009) 938–946.
- [249] M.Z. Ozel, F. Gogus, S. Yagci, J.F. Hamilton, A.C. Lewis, Determination of volatile nitrosamines in various meat products using comprehensive gas chromatography–nitrogen chemiluminescence detection, *Food Chem. Toxicol.* 48 (2010) 3268–3273.
- [250] Y. Weijun, Direct determination of acrylamide in food by gas chromatography with nitrogen chemiluminescence detection, *J. Sep. Sci.* 38 (2015) 2272–2277.
- [251] M.Z. Ozel, J.F. Hamilton, A.C. Lewis, New sensitive and quantitative analysis method for organic nitrogen compounds in urban aerosol samples, *Environ. Sci. Technol.* 45 (2011) 1497–1505.
- [252] K. Cai, Z. Xiang, J. Zhang, S. Zhou, Y. Feng, Z. Geng, Determination of eight tobacco alkaloids in flue-cured tobacco samples by gas chromatography with nitrogen chemiluminescence detection (NCD), *Anal. Methods* 4 (2012) 2095–2100.
- [253] N. Ramirez, L. Vallecillos, A.C. Lewis, F. Borrull, R.M. Marce, J.F. Hamilton, Comparative study of comprehensive gas chromatography–nitrogen chemiluminescence detection and gas chromatography–ion trap–tandem mass spectrometry for determining nicotine and carcinogenic organic nitrogen compounds in thirdhand tobacco smoke, *J. Chromatogr. A* 1426 (2015) 191–200.
- [254] T. Dijkman, M.R. Djokic, K.M. Van Geem, G.B. Marin, Comprehensive compositional analysis of sulfur and nitrogen containing compounds in shale oil using GC × GC–FID/SCD/NCD/TOF-MS, *Fuel* 140 (2015) 398–406.
- [255] O.Y. Al-Dirbashi, K. Nakashima, Hyphenated chromatographic methods for biomaterials, *Biomed. Chromatogr.* 14 (2000) 406–421.
- [256] I.D. Wilson, U.A.T. Brinkman, Hyphenation and hypernation: the practice and prospects of multiple hyphenation, *J. Chromatogr. A* 1000 (2003) 325–356.
- [257] M.J. Tomlinson, C.L. Wilkins, Evaluation of a semi-automated multidimensional gas chromatography–infrared–mass spectrometry system for irritant analysis, *J. High Resolut. Chromatogr.* 21 (1998) 347–354.
- [258] R. Navarro-González, P. Coll, R. Aliev, Pyrolysis of γ -irradiated bisphenol-A polycarbonate, *Polym. Bull.* 48 (2002) 43–51.
- [259] K.A. Krock, N. Ragunathan, C. Klawun, T. Sasaki, C.L. Wilkins, Multidimensional gas chromatography–infrared spectrometry–mass spectrometry, Plenary lecture, *Analyst* 119 (1994) 483–489.
- [260] G. Gachot, S. Grugeon, I. Jimenez-Gordon, G.G. Eshetu, S. Boyanov, A. Lecocq, G. Marlair, S. Pilard, S. Laruelle, Gas chromatography/Fourier transform infrared/mass spectrometry coupling: a tool for Li-ion battery safety field investigation, *Anal. Methods* 6 (2014) 6120–6124.
- [261] J. Taira, A. Tsuchiya, H. Furudate, Initial volatile aroma profiles of young and aged Awamori *Shochu* determined by GC/MS/pulsed FPD, *Food Sci. Technol. Res.* 18 (2012) 177–181.
- [262] L.L.P. Van Stee, P.E.G. Leonards, R.J.J. Vreuls, U.A.T. Brinkman, Identification of non-target compounds using gas chromatography with simultaneous atomic emission and mass spectrometric detection (GC-AED/MS): analysis of municipal wastewater, *Analyst* 124 (1999) 1547–1552.
- [263] T. Hankemeier, J. Rozenbrand, M. Abhadur, J.J. Vreuls, U.A.T. Brinkman, Data correlation in on-line solid-phase extraction–gas chromatography–atomic emission/mass spectrometric detection of unknown microcontaminants, *Chromatographia* 48 (1998) 273–283.
- [264] L.L.P. van Stee, J. Beens, R.J.J. Vreuls, U.A.T. Brinkman, Comprehensive two-dimensional gas chromatography with atomic emission detection and correlation with mass spectrometric detection: principles and application in petrochemical analysis, *J. Chromatogr. A* 1019 (2003) 89–99.
- [265] G.-B. Jiang, J.-Y. Liu, K.-W. Yang, Speciation analysis of butyltin compounds in Chinese seawater by capillary gas chromatography with flame photometric detection using in-situ hydride derivatization followed by headspace solid-phase microextraction, *Anal. Chim. Acta* 421 (2000) 67–74.